(19) Europäisches Patentamt
European Patent Office
Office européen des brevets

(11) EP 0 941 089 B1

(12) EUROPEAN PATENT SPECIFICATION

(45) Date of publication and mention of the grant of the patent:
16.05.2001 Bulletin 2001/20

(21) Application number: **97945697.7**

(22) Date of filing: **02.12.1997**

(51) Int Cl.[7]: **A61K 31/335**, A61K 31/22, A61K 31/425, A61K 31/36, A61K 31/70, A61K 33/08, A61K 33/16

(86) International application number:
PCT/CA97/00910

(87) International publication number:
WO 98/24427 (11.06.1998 Gazette 1998/23)

(54) USE OF ANTI-MICROTUBULE AGENTS FOR TREATING OR PREVENTING MULTIPLE SCLEROSIS

VERWENDUNG VON ANTI-MIKROTUBULI MITTELN ZUR BEHANDLUNG UND PROPHYLAXE DER MULTIPLEN SCLEROSE

UTILISATION DES AGENTS ANTI-MICROTUBULES POUR TRAITER OU PREVENIR LA SCLEROSE EN PLAQUES

(84) Designated Contracting States:
AT BE CH DE DK ES FI FR GB GR IE IT LI LU MC NL PT SE

(30) Priority: **02.12.1996 US 32215 P**
24.10.1997 US 63087 P

(43) Date of publication of application:
15.09.1999 Bulletin 1999/37

(60) Divisional application:
00123534.0 / 1 092 433
00123537.3 / 1 090 637
00123557.1 / 1 070 502

(73) Proprietor: **Angiotech Pharmaceuticals, Inc.**
Vancouver, British Columbia V6T 1Z4 (CA)

(72) Inventor: **HUNTER, William, L.**
Vancouver, British Columbia V5K 3L7 (CA)

(74) Representative:
Gowshall, Jonathan Vallance et al
FORRESTER & BOEHMERT
Franz-Joseph-Strasse 38
80801 München (DE)

(56) References cited:
EP-A- 0 038 567
EP-A- 0 262 681
EP-A- 0 288 794
EP-A- 0 717 041
WO-A-94/12158
WO-A-95/03795
WO-A-95/35095
US-A- 5 443 458
US-A- 5 565 439

- **DATABASE WPI Week 8619 Derwent Publications Ltd., London, GB; AN 86-123250 XP002062018 & JP 61 063 613 A (MITSUI TOATSU CHEM. INC.) , 1 April 1986**
- **YA MIN WANG ET AL.: "Preparation and characterization of poly(lactic-co-glycolic acid) microspheres for targeted delivery of a novel anticancer agent, taxol" CHEM. PHARM. BULL., vol. 44, no. 10, 1996, pages 1935-1940, XP000633466**

Printed by Jouve, 75001 PARIS (FR)

EP 0 941 089 B1

Description

TECHNICAL FIELD

[0001] The present invention relates to the use of an anti-microtubule agent for preparing a medicament for treating or preventing multiple sclerosis.

BACKGROUND OF THE INVENTION

[0002] Inflammatory diseases, whether of a chronic or acute nature, represent a substantial problem in the healthcare industry. Briefly, chronic inflammation is considered to be inflammation of a prolonged duration (weeks or months) in which active inflammation, tissue destruction and attempts at healing are proceeding simultaneously (*Robbins Pathological Basis of Disease* by R. S. Cotran, V. Kumar, and S. L. Robbins, W. B. Saunders Co., p. 75, 1989). Although chronic inflammation can follow an acute inflammatory episode, it can also begin as an insidious process that progresses with time, for example, as a result of a persistent infection (*e.g.*, tuberculosis, syphilis, fungal infection) which causes a delayed hypersensitivity reaction, prolonged exposure to endogenous *(e.g.,* elevated plasma lipids) or exogenous (*e.g.*, silica, asbestos, cigarette tar, surgical sutures) toxins, or, autoimmune reactions against the body's own tissues (e.g., rheumatoid arthritis, systemic lupus erythematosus, multiple sclerosis, psoriasis). Chronic inflammatory diseases therefore, include many common medical conditions such as rheumatoid arthritis, restenosis, psoriasis, multiple sclerosis, surgical adhesions, tuberculosis, and chronic inflammatory lung diseases (e.g., asthma, pneumoconiosis, chronic obstructive pulmonary disease, nasal polyps and pulmonary fibrosis).

MULTIPLE SCLEROSIS

[0003] Multiple sclerosis (MS), affecting 350,000 people (women:men = 2:1) in the United States, with 8,000 new cases reported each year, is the most common chronic inflammatory disease involving the nervous system. Typically, MS presents clinically as recurring episodes of adverse neurological deficits occurring over a period of several years. Roughly half of MS cases progress to a more chronic phase. Although the disease does not result in early death or impairment of cognitive functions, it cripples the patient by disturbing visual acuity; stimulating double vision; disturbing motor functions affecting walking and use of the hands; producing bowel and bladder incontinence; spasticity; and sensory deficits (touch, pain and temperature sensitivity).

[0004] The cause of MS is unknown, although there is considerable evidence that it is an autoimmune disease. Currently, there is no cure available for multiple sclerosis, and present therapeutic regimens have been only partially successful. For example, although chemotherapeutic agents such as methotrexate, cyclosporin and azathioprine, have been examined for the management of patients with treatment unresponsive progressive disease, minimal long-term beneficial effects have been demonstrated to date.

[0005] Other therapeutics which have been recently approved include interferon-β for use in ambulatory patients with relapsing-remitting MS (Paty et al., *Neurology 43*:662-667, 1993), specifically, Betaseron (recombinant interferon β-1β; human interferon beta substituted at position 17, Cys® Ser; Berlex/Chiron) or Avonex (recombinant interferon β-1α; glycosylated human interferon beta produced in mammalian cells; Biogen). Unfortunately, while Betaseron provides for an enhanced quality of life for MS patients, disease progression does not appear to be significantly improved. Adverse experiences associated with Betaseron therapy include: injection site reactions (inflammation, pain, hypersensitivity and necrosis), and a flu-like symptom complex (fever, chills, anxiety and confusion).

[0006] EP-A-0 288 794 discloses the use of certain chalcone derivatives to treat a variety of conditions including tumours, gout and multiple sclerosis.

SUMMARY OF THE INVENTION

[0007] Briefly stated, the present invention provides the use of an anti-microtubule agent for preparing a medicament for treating or preventing inflammatory diseases, comprising delivering to a site of inflammation an anti-microtubule agent, wherein the anti-microtubule agent is not a chalcone derivative of the structure:

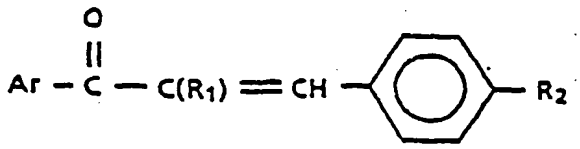

wherein

Ar is a 2,5-dimethoxyphenyl, 2,3,4-trimethoxyphenyl, or 3,4,5-trimethoxyphenyl group;
R_1 is a hydrogen, (C_1-C_4)alkyl, chloro, or bromo group; and
R_2 is a -$N(R)_2$ or -NHCOR wherein R is a (C_1-C_4)alkyl group

or a pharmaceutically acceptable salt thereof. Representative examples of such agents include taxanes (*e.g.*, paclitaxel and docetaxel), campothecin, eleutherobin, sarcodictyins, epothilones A and B, discodermolide, deuterium oxide (D_2O), hexylene glycol (2-methyl-2,4-pentanediol), tubercidin (7-deazaadenosine), LY290181 (2-amino-4-(3-pyridyl)-4H-naphtho(1,2-b)pyran-3-cardonitrile), aluminum fluoride, ethylene glycol bis-(succinimidylsuccinate), glycine ethyl ester, monoclonal anti-idiotypic antibodies, microtubule assembly promoting protein (taxol-like protein, TALP), cell swelling induced by hypotonic (190 mosmol/L) conditions, insulin (100 nmol/L) or glutamine (10 mmol/L), dynein binding, gibberelin, XCHO1 (kinesin-like protein), lysophosphatidic acid, lithium ion, plant cell wall components (*e.g.*, poly-L-lysine and extensin), glycerol buffers, Triton X-100 microtubule stabilizing buffer, microtubule associated proteins (*e.g.*, MAP2, MAP4, tau, big tau, ensconsin, elongation factor-1-alpha (EF-1α) and E-MAP-115), cellular entities (*e.g.*, histone H1, myelin basic protein and kinetochores), endogenous microtubular structures (*e.g.*, axonemal structures, plugs and GTP caps), stable tubule only polypeptide (*e.g.*, STOP145 and STOP220) and tension from mitotic forces, as well as any analogues and derivatives of any of the above. Within other embodiments, the anti-microtubule agent is formulated to further comprise a polymer.

[0008] Within certain embodiments of the invention, the anti-microtubule agents used for preparing a medicament may be formulated along with other compounds or compositions, such as, for example, an ointment, cream, lotion, gel, spray or the like. Within certain embodiments, the compound or composition may function as a carrier, which may be either polymeric, or non-polymeric. Representative examples of polymeric carriers include poly(ethylene-vinyl acetate), copolymers of lactic acid and glycolic acid, poly (caprolactone), poly (lactic acid), copolymers of poly (lactic acid) and poly (caprolactone), gelatin, hyaluronic acid, collagen matrices, and albumen. Representative examples of other suitable carriers include, but are not limited to ethanol; mixtures of ethanol and glycols (*e.g.*, ethylene glycol or propylene glycol); mixtures of ethanol and isopropyl myristate or ethanol, isopropyl myristate and water (*e.g.*, 55:5:40); mixtures of ethanol and eineol or D-limonene (with or without water); glycols (*e.g.*, ethylene glycol or propylene glycol) and mixtures of glycols such as propylene glycol and water, phosphatidyl glycerol, dioleoylphosphatidyl glycerol, Transcutol®, or terpinolene; mixtures of isopropyl myristate and 1-hexyl-2-pyrrolidone, N-dodecyl-2-piperidinone or 1-hexyl-2-pyrrolidone.

[0009] Within yet other aspects, the anti-microtubule agent may be formulated to be contained within, or, adapted to release by a surgical or medical device or implant, such as, for example, stents, sutures, indwelling catheters, prosthesis, and the like.

[0010] These and other disclosed aspects will become evident upon reference to the following detailed description and attached drawings. In addition, various references are set forth below which describe in more detail certain procedures, devices or compositions, and are therefore incorporated by reference in their entirety.

BRIEF DESCRIPTION OF THE DRAWINGS

[0011] Figure 1A is a graph which shows the chemiluminescence response of neutrophils ($5x10^6$ cells/ml) to plasma opsonized CPPD crystals (50 mg/ml). Effect of paclitaxel (also referred to as "taxol") at (o) no paclitaxel, (•) 4.5 μM, (Δ) 14 pM, (▲) 28 μM, (□) 46 μM; n = 3. Figure 1B is a graph which shows the time course concentration dependence of paclitaxel inhibition of plasma opsonized CPPD crystal-induced neutrophil chemiluminescence. Figure 1C is a graph which shows the effect of aluminum fluoride on opsonized zymozan-induced neutrophil activation as measured by chemiluminescence. Figure 1D is a graph which shows the effect of glycine ethyl ester on opsonized zymozan induced neutrophil activation as measured by chemiluminescence. Figure 1E is a graph which shows the effect of LY290181 on opsonized zymozan induced neutrophil chemiluminescence.

[0012] Figure 2 is a graph which shows lysozyme release from neutrophils ($5x10^6$/ml) in response to plasma opsonized CPPD crystals (50 mg/ml). Effect of paclitaxel at (o) no paclitaxel, (•) 28 μM, (Δ) Control (cells alone), (▲)

Control (cells and paclitaxel at 28 μM); n = 3.

[0013] Figure 3A is a graph which shows superoxide anion production by neutrophils ($5x10^6$ cells/ml) in response to plasma opsonized CPPD crystals (50 mg/ml). Effect of paclitaxel at (o) no paclitaxel, (•) 28 μM, (Δ) Control (cells alone); n = 3. Figure 3B is a graph which shows the time course concentration dependence of paclitaxel inhibition of plasma opsonized CPPD crystal-induced neutrophil superoxide anion production; n = 3. Figure 3C is a graph which depicts the effect of LY290181 on CPPD crystal induced neutrophil superoxide anion generation.

[0014] Figure 4A is a graph which shows the chemiluminescence response of neutrophils ($5x10^6$ cells/ml) in response to plasma opsonized zymosan (1 mg/ml). Effect of paclitaxel at (o) no paclitaxel, (•) 28 μM; n = 3. Figure 4B is a graph which shows plasma opsonized zymosan-induced neutrophil superoxide anion production. Effect of paclitaxel at (o) no paclitaxel, (•) 28 μM, (Δ) Control (cells alone); n = 3.

[0015] Figure 5A is a graph which shows myeloperoxidase release from neutrophils ($5x10^6$ cells/ml) in response to plasma opsonized CPPD crystals (50 mg/ml). Effect of paclitaxel at (o) no paclitaxel, (•) 28 μM, (Δ) Control (cells alone), (▲) Control (cells with paclitaxel at 28 μM); n = 3. Figure 5B is a graph which shows the concentration dependence of paclitaxel inhibition of myeloperoxidase release from neutrophils in response to plasma opsonized CPPD crystals; n = 3. Figures 5C and 5D are graphs which show that LY290181 decreases both lysozyme and myeoloperoxidase release in CPPD crystal-induced neutrophils.

[0016] Figure 6 is a graph which depicts proliferation of synoviocytes at various concentrations of paclitaxel.

[0017] Figure 7 is a graph which depicts the effects of paclitaxel on keratinocytes *in vitro.*

[0018] Figures 8A and 8B show the effect of paclitaxel on astrocyte morphology. Electron microscopic images revealed thick, well-organized filamentous processes in astrocytes of transgenic control animals, whereas transgenic animals treated with paclitaxel had morphologically altered astrocytes. Paclitaxel induced astrocyte cell rounding, thinned cellular processes and reduced cytoplasmic filaments relative to untreated animals.

[0019] Figure 9 is a graph which depicts the viability of EOMA cells treated with paclitaxel concentrations of greater than 10^{-8} M.

[0020] Figure 10 is a bar graph which depicts the percentage of apoptotic EOMA cells in culture treated with increasing concentrations of paclitaxel.

[0021] Figures 11A-11E are graphs which depict the effect of various anti-microtubule agents on synoviocytes after a period of 24 hours.

[0022] Figures 12A-12H are blots which show the effect of various anti-microtubule agents in inhibiting collagenase expression.

[0023] Figures 13A-13H are blots which show the effect of various anti-microtubule agents on proteoglycan expression.

[0024] Figures 14A and 14B are two photographs of a CAM having a tumor treated with control (unloaded) thermopaste. Briefly, in Figure 14A the central white mass is the tumor tissue. Note the abundance of blood vessels entering the tumor from the CAM in all directions. The tumor induces the ingrowth of the host vasculature through the production of "angiogenic factors." The tumor tissue expands distally along the blood vessels which supply it. Figure 14B is an underside view of the CAM shown in 15A. Briefly, this view demonstrates the radial appearance of the blood vessels which enter the tumor like the spokes of a wheel. Note that the blood vessel density is greater in the vicinity of the tumor than it is in the surrounding normal CAM tissue. Figures 14C and 14D are two photographs of a CAM having a tumor treated with 20% paclitaxel-loaded thermopaste. Briefly, in Figure 14C the central white mass is the tumor tissue. Note the paucity of blood vessels in the vicinity of the tumor tissue. The sustained release of the anti-microtubule agent is capable of overcoming the angiogenic stimulus produced by the tumor. The tumor itself is poorly vascularized and is progressively decreasing in size. Figure 14D is taken from the underside of the CAM shown in 14C, and demonstrates the disruption of blood flow into the tumor when compared to control tumor tissue. Note that the blood vessel density is reduced in the vicinity of the tumor and is sparser than that of the normal surrounding CAM tissue.

[0025] Figure 15A is a photograph which shows a shell-less egg culture on day 6. Figure 15B is a digitized computer-displayed image taken with a stereomicroscope of living, unstained capillaries (1040x). Figure 15C is a photograph of a corrosion casting which shows chorioallenteic membrane (CAM) microvasculature that are fed by larger, underlying vessels (arrows; 1300x). Figure 15D is a photograph which depicts a 0.5 mm thick plastic section cut transversely through the CAM, and recorded at the light microscope level. This photograph shows the composition of the CAM, including an outer double-layered ectoderm (Ec), a mesoderm (M) containing capillaries (arrows) and scattered adventitial cells, and a single layered endoderm (En) (400x). Figure 15E is a photograph at the electron microscope level (3500x) wherein typical capillary structure is presented showing thin-walled endothelial cells (arrowheads) and an associated pericyte.

[0026] Figures 16A, 16B, 16C and 16D are a series of digitized images of four different, unstained CAMs taken after a 48 hour exposure to 10 μg paclitaxel per 10 ml of methylcellulose. The transparent methylcellulose disk (*) containing paclitaxel is present on each CAM and is positioned over a singular avascular zone (A) with surrounding blood islands (Is). These avascular areas extend beyond the disk and typically have a diameter of approximately 6 mm. Fig. 16D

illustrates the typical "elbowing" effect (arrowheads) of both small and large vessels being redirected away from the periphery of the avascular zone.

[0027] Figure 17A is a photograph (= 400x) which shows that the capillaries (arrowheads) immediately peripheral to the avascular zone exhibit numerous endothelial cells arrested in mitosis. Ectoderm (Ec); Mesoderm (M); Endoderm (En). Figure 17B (= 400x) shows that within the avascular zone proper the typical capillary structure has been eliminated and there are numerous extravasated blood cells (arrowheads). Figure 17C (= 400x) shows that in the central area of the avascular zone, red blood cells are dispersed throughout the mesoderm.

[0028] Figure 18A (= 2,200x) shows a small capillary lying subjacent to the ectodermal layer (Ec) possessing three endothelial cells arrested in mitosis (*). Several other cell types in both the ectoderm and mesoderm are also arrested in mitosis. Figure 18B (= 2,800x) shows the early avascular phase contains extravasated blood cells subjacent to the ectoderm; these blood cells are intermixed with presumptive endothelial cells (*) and their processes. Degradative cellular vacuoles (arrowhead). Figure 18C (= 2,800x) shows that in response to paclitaxel, the ecto-mesodermal interface has become populated with cells in various stages of degradation containing dense vacuoles and granules (arrowheads).

[0029] Figure 19A schematically depicts the transcriptional regulation of matrix metalloproteinases. Figure 19B is a blot which demonstrates that IL-1 stimulates AP-1 transcriptional activity. Figure 19C is a graph which shows that IL-1 induced binding activity decreased in lysates from chondrocytes which were pretreated with paclitaxel.

[0030] Figure 20 is a blot which shows that IL-1 induction increases collagenase and stromelysin in RNA levels in chondrocytes, and that this induction can be inhibited by pretreatment with paclitaxel.

[0031] Figure 21 is a bar graph which depicts the effects of paclitaxel on viability of normal chondrocytes *in vitro*.

[0032] Figure 22 is a graph which plots the observed pseudo first order kinetic degradation of paclitaxel (20 $\mu g\ ml^{-1}$ in 10% HPβCD and 10% HPγCD solutions at 37°C and pH of 3.7 and 4.9, respectively.

[0033] Figure 23 is a graph which shows the phase solubility for cyclodextrins and paclitaxel in water at 37°C.

[0034] Figure 24 is a graph which shows second order plots of the complexation of paclitaxel and γCD, HPβCD or HPγCD at 37°C.

[0035] Figure 25 is a table which shows the melting temperature, enthalpy, molecular weight, polydispersity and intrinsic viscosity of a PDLLA-PEG-PDLLA composition.

[0036] Figure 26 is a graph which depicts DSC thermograms of PDLLA-PEG-PDLLA and PEG. The heating rate was 10°C/min. See Figure 30 for melting temperatures and enthalpies.

[0037] Figure 27 is a graph which depicts the cumulative release of paclitaxel from 20% paclitaxel loaded PDLLA-PEG-PDLLA cylinders into PBS albumin buffer at 37°C. The error bars represent the standard deviation of 4 samples. Cylinders of 40% PEG were discontinued at 4 days due to disintegration.

[0038] Figures 28A, 28B and 28C are graphs which depict the change in dimensions, length (A), diameter (B) and wet weight (C) of 20% paclitaxel loaded PDLLA-PEG-PDLLA cylinders during the *in vitro* release of paclitaxel at 37°C.

[0039] Figure 29 is a table which shows the mass loss and polymer composition change of PDLLA-PEG-PDLLA cylinders (loaded with 20% paclitaxel) during the release into PBS albumin buffer at 37°C.

[0040] Figure 30 is a graph which shows gel permeation chromatograms of PDLLA-PEG-PDLLA cylinders (20% PEG, 1 mm diameter) loaded with 20% paclitaxel during the release in PBS albumin buffer at 37°C.

[0041] Figures 31A, 31B, 31C and 31D are SEMs of dried PDLLA-PEG-PDLLA cylinders (loaded with 20% paclitaxel, 1 mm in diameter) before and during paclitaxel release. A: 20% PEG, day 0; B: 30% PEG, day 0; C: 20% PEG, day 69; D: 30% PEG, day 69.

[0042] Figure 32 is a graph which depicts the cumulative release of paclitaxel from 20% paclitaxel loaded PDLLA: PCL blends and PCL into PBS albumin buffer at 37°C. The error bars represent the standard deviations of 4 samples.

[0043] Figure 33 is a graph which depicts, over a time course, the release of paclitaxel from PCL pastes into PBS at 37°C. The PCL pastes contain microparticles of paclitaxel and various additives prepared using mesh #140. The error bars represent the standard deviation of 3 samples.

[0044] Figure 34 is a graph which depicts time courses of paclitaxel release from paclitaxel-gelatin-PCL pastes into PBS at 37°C. This graph shows the effects of gelatin concentration (mesh #140) and the size of paclitaxel-gelatin (1:1) microparticles prepared using mesh #140 or mesh #60. The error bars represent the standard deviation of 3 samples.

[0045] Figures 35A and 35B are graphs which depict the effect of additives (17A; mesh #140) and the size of microparticles (17B; mesh #140 or #60) and the proportion of the additive (mesh #140) on the swelling behavior of PCL pastes containing 20% paclitaxel following suspension in distilled water at 37°C. Measurements for the paste prepared with 270 μm microparticles in paclitaxel-gelatin and paste containing 30% gelatin were discontinued after 4 hours due to disintegration of the matrix. The error bars represent the standard deviation of 3 samples.

[0046] Figures 36A, 36B, 36C and 36D are representative scanning electron micrographs of paclitaxel-gelatin-PCL (20:20:60) pastes before (36A) and after (36B) suspending in distilled water at 37°C for 6 hours. Micrographs 36C and 36D are higher magnifications of 36B, showing intimate association of paclitaxel (rod shaped) and gelatin matrix.

[0047] Figures 37A and 37B are representative photomicrographs of CAMs treated with gelatin-PCL (37A) and pa-

clitaxel-gelatin-PCL (20:20:60; 37B) pastes showing zones of avascularity in the paclitaxel treated CAM.

[0048] Figure 38 is a graph which shows the phase solubility for cyclodextrins and paclitaxel in water at 37°C.

[0049] Figure 39 is a graph which shows second order plots of the complexation of paclitaxel and γCD, HPβCD or HPγCD at 37°C.

[0050] Figure 40 is a graph which shows the phase solubility for paclitaxel at 37°C and hydroxypropyl-β-cyclodextrin in 50:50 water:ethanol solutions.

[0051] Figure 41 is a graph which shows dissolution rate profiles of paclitaxel in 0, 5, 10 or 20% HPγCD solutions at 37°C.

[0052] Figure 42 is a graph which plots the observed pseudo first order kinetic degradation of paclitaxel (20 μg/ml) in 10% HPβCD and 10% HPγCD solutions at 37°C and pH of 3.7 and 4.9, respectively.

[0053] Figures 43A and 43B, respectively, are two graphs which show the release of paclitaxel from EVA films, and the percent paclitaxel remaining in those same films over time. Figure 43C is a graph which shows the swelling of EVA/F127 films with no paclitaxel over time. Figure 43D is a graph which shows the swelling of EVA/Span 80 films with no paclitaxel over time. Figure 43E is a graph which depicts a stress vs. strain curve for various EVA/F127 blends.

[0054] Figure 44 is a graph which shows the effect of plasma opsonization of polymeric microspheres on the chemiluminescence response of neutrophils (20 mg/ml microspheres in 0.5 ml of cells (conc. $5x10^6$ cells/ml)) to PCL microspheres.

[0055] Figure 45 is a graph which shows the effect of precoating plasma +/-2% Pluronic F127 on the chemiluminescence response of neutrophils ($5x10^6$ cells/ml) to PCL microspheres

[0056] Figure 46 is a graph which shows the effect of precoating plasma +/-2% Pluronic F127 on the chemiluminescence response of neutrophils ($5x10^6$ cells/ml) to PMMA microspheres

[0057] Figure 47 is a graph which shows the effect of precoating plasma +/-2% Pluronic F127 on the chemiluminescence response of neutrophils ($5x10^6$ cells/ml) to PLA microspheres

[0058] Figure 48 is a graph which shows the effect of precoating plasma +/-2% Pluronic F127 on the chemiluminescence response of neutrophils ($5x10^6$ cells/ml) to EVA:PLA microspheres

[0059] Figure 49 is a graph which shows the effect of precoating IgG (2 mg/ml), or 2% Pluronic F127 then IgG (2 mg/ml) on the chemiluminescence response of neutrophils to PCL microspheres.

[0060] Figure 50 is a graph which shows the effect of precoating IgG (2 mg/ml), or 2% Pluronic F127 then IgG (2 mg/ml) on the chemiluminescence response of neutrophils to PMMA microspheres.

[0061] Figure 51 is a graph which shows the effect of precoating IgG (2 mg/ml), or 2% Pluronic F127 then IgG (2mg/ml) on the chemiluminescence response of neutrophils to PVA microspheres.

[0062] Figure 52 is a graph which shows the effect of precoating IgG (2 mg/ml), or 2% Pluronic F127 then IgG (2 mg/ml) on the chemiluminescence response of neutrophils to EVA:PLA microspheres.

[0063] Figure 53A is a graph which shows release rate profiles from polycaprolactone microspheres containing 1%, 2%, 5% or 10% paclitaxel into phosphate buffered saline at 37°C. Figure 53B is a photograph which shows a CAM treated with control microspheres. Figure 53C is a photograph which shows a CAM treated with 5% paclitaxel loaded microspheres.

[0064] Figure 54 is a graph which depicts the range of particle sizes for control microspheres (PLLA:GA - 85:15).

[0065] Figure 55 is a graph which depicts the range of particle sizes for 20% paclitaxel loaded microspheres (PLLA:GA - 85:15).

[0066] Figure 56 is a graph which depicts the range of particle sizes for control microspheres (PLLA:GA - 85:15).

[0067] Figure 57 is a graph which depicts the range of particle sizes for 20% paclitaxel loaded microspheres (PLLA:GA - 85:15).

[0068] Figures 58A, 58B and 58C are graphs which show the release rate profiles of paclitaxel from varying ranges of microsphere size and various ratios of PLLA and GA.

[0069] Figures 59A and 59B are graphs which show the release rate profiles of paclitaxel from microspheres with various ratios of PLLA and GA.

[0070] Figures 60A and 60B are graphs which show the release rate profiles of paclitaxel from microspheres with various ratios of PLLA and GA.

[0071] Figures 61A, 61B and 61C are graphs which show the release rate profiles of paclitaxel from microspheres of varying size and various ratios of PLLA and GA.

[0072] Figure 62 is a graph which depicts paclitaxel release from paclitaxel-nylon microcapsules.

[0073] Figures 63A and 63B are photographs of fibronectin coated PLLA microspheres on bladder tissue (63A), and poly (L-lysine) microspheres on bladder tissue.

[0074] Figure 64 is a graph which shows that micellar paclitaxel improves the daily mean arthritis scores in the collagen-induced arthritis rat model.

[0075] Figures 65A-65D are a series of x-rays which show the effect of micellar paclitaxel in the collagen-induced arthritis rat model.

[0076] Figures 66A-66C are scanning electron micrographs of a rat ankle joint.

[0077] Figure 67 is a magnified view which shows the histopathology in the collagen-induced arthritis rat model.

[0078] Figures 68A and 68B are magnified views of the synovial vasculature in the collagen-induced arthritis rat model.

[0079] Figure 69 is a graph which depicts the induction of contact hypersensitivity reaction in mouse ears by oxazolone. Treatment with 1% paclitaxel gel or vehicle at the time of antigen challenge and then once daily. Skin inflammation was quantitated by measurements of ear swelling as compared to pre-challenge ear thickness. Data represent means values +/- SD (n=5). $^{**}p < 0.01$; $^{***}p < 0.001$.

[0080] Figure 70 is a graph which depicts the induction of contact hypersensitivity reaction in mouse ears by oxazolone. Initial treatment with 1% paclitaxel gel or vehicle at 24 hours after antigen challenge and thereafter once daily. Skin inflammation was quantitated by measurements of ear swelling as compared to pre-challenge ear thickness. Data represent mean values +/- SD (n=5). $^{*}p<0.05$; $^{**}p < 0.01$.

[0081] Figure 71 is a graph which depicts the induction of skin inflammation in mouse ears by topical application of PMA. Initial treatment with 1% paclitaxel gel or vehicle at 1 hour after PMA application and thereafter once daily. Skin inflammation was quantitated by measurements of ear swelling as compared to pre-challenge ear thickness. Data represent mean values +/- SD (n=5). $^{*}p<0.05$; $^{***}p< 0.001$.

[0082] Figure 72 is a graph which depicts the induction of skin inflammation in mouse ears by topical application of PMA. Initial treatment with 1% paclitaxel gel or vehicle at 24 hours after PMA application and thereafter once daily. Skin inflammation was quantitated by measurements of ear swelling as compared to pre-challenge ear thickness. Data represent mean values +/- SD (n=5). $^{**}p < 0.01$; $^{***}p< 0.001$.

[0083] Figure 73 illustrates induction of skin inflammation in mouse ears by topical application of PMA. Pre-treatment with 1% paclitaxel gel (right ear) or vehicle (left ear). Image was taken at 48 hours after PMA application. Note redness and dilated blood vessels of vehicle-treated left ears, as compared to paclitaxel-treated right ears. Similar results were obtained in a total of 5 mice.

[0084] Figure 74 is a graph which depicts the effect of paclitaxel on body weight of DM20 transgenic mice. Transgenic mice were treated with vehicle or paclitaxel (2.0 mg/kg) three times weekly for 24 days and then sacrificed on day 27. The results are for two animals treated with paclitaxel and one untreated animal. Paclitaxel treated animals demonstrated minimal weight loss, whereas control animals showed a 30% decrease in body weight, from 29g to 22g.

[0085] Figure 75 is a graph which depicts the effect of high dose interval paclitaxel therapy on the progression of clinical symptoms in transgenic mice. Transgenic mice were treated with 20 mg/kg paclitaxel once weekly for 4 weeks (week 0, 1, 2 and 3) and monitored for 10 weeks, every two days, with scores determined for each symptom. The data represents the average score (cumulative for all symptoms) for paclitaxel treated transgenic mice (n=5) and control mice (n=3). Paclitaxel treatment reduced the deterioration caused by overexpression of DM20 in transgenics, whereas control mice deteriorated very rapidly with 2 out of 3 animals not surviving to the end of the experimental protocol (as indicated).

[0086] Figures 76A and 76B show paclitaxel paste applied perivascularly (to the adventitia of the blood vessel) in the rat carotid artery model. The adventitial surface of the left common carotid artery was treated with 2.5 mg of either control paste (76A) or 20% paclitaxel-loaded paste (76B). Control arteries displayed an increase in the thickness of the arterial wall due to smooth muscle cell hyperproliferation, whereas the artery treated with paclitaxel-loaded paste did not show evidence of intimal thickening.

[0087] Figures 77A and 77B depict the proximity effect of perivascular paclitaxel paste in the rat carotid artery model. Paclitaxel-loaded paste applied immediately adjacent to the perivascular region of the vessel prevented restenosis; however, when the paste was not directly adjacent to the vascular wall neointimal hyperplasia was evident.

[0088] Figures 78A, 78B and 78C show the effect of paclitaxel on astrocyte GFAP staining. Brain sections from normal animals and transgenic animals (who develop a neurological disease similar to multiple sclerosis) treated with vehicle or paclitaxel were stained with GFAP (a marker for activated astrocytes) and examined histologically. In control transgenic mice there was an increase in the number of astrocytes and total GFAP levels compared to normal brain sections. However, the morphology of the cells was similar. Brain sections of paclitaxel treated transgenic mice show decreased numbers of astrocytes and GFAP levels compared to untreated transgenic animals. Histologically there is cell rounding and thinning of stellate processes in astrocytes.

[0089] Figures 79A and 79B are graphs which show that paclitaxel inhibits T-cell stimulation in response to myelin basic protein peptide (GP68-88) and ConA. A 48-hour culture of T-cell proliferation of RT-1 was performed with GP68-88 (A) or ConA (B) as stimulagens. Paclitaxel and its vehicle (micelles) were added at graded concentrations at the beginning of antigen stimulation or 24 hours later. Paclitaxel inhibited T-cell proliferation at concentrations as low as 0.02 μM, regardless of the stimulagen.

[0090] Figures 80A, 80B, 80C and 80D, are graphs which show that tubercidin and paclitaxel inhibit both IL-1- and TNF-induced NF-KB activity.

[0091] Figures 81A and 81B are graphs which show the effect of increasing concentrations of paclitaxel or camp-

tothecin on the cell growth of human prostate cancer cells (LNCaP) (2x103 cells/well) as measured by crystal violet (0.5%) staining and quantitation by absorbance at 492 nm. Percent growth is expressed as a % relative to controls and a mean of 8 results is given.

DETAILED DESCRIPTION OF THE INVENTION

[0092] Prior to setting forth the invention, it may be helpful to an understanding thereof to set forth definitions of certain terms that will be used hereinafter.

[0093] "Inflammatory Disease" as used herein refers to multiple sclerosis.

[0094] "Anti-microtubule Agents" should be understood to include any protein, peptide, chemical, or other molecule which impairs the function of microtubules, for example, through the prevention or stabilization of polymerization. A wide variety of methods may be utilized to determine the anti-microtubule activity of a particular compound, including for example, assays described by Smith et al. *(Cancer Lett* 79(2):213-219, 1994) and Mooberry et al., *(Cancer Lett. 96*(2):261-266, 1995).

[0095] As noted above, the use according to the invention is useful for treating or preventing inflammatory diseases, comprising the step of delivering to the site of inflammation an anti-microtubule agent. Briefly, a wide variety of agents may be delivered to a site of inflammation (or potential site of inflammation), either with or without a carrier (*e.g.*, a polymer or ointment), in order to treat or prevent an inflammatory disease. Representative examples of such agents include taxanes (*e.g.*, paclitaxel (discussed in more detail below) and docetaxel) (Schiff et al., *Nature* 277: 665-667, 1979; Long and Fairchild, *Cancer Research* 54: 4355-4361, 1994; Ringel and Horwitz, *J. Natl. Cancer Inst.* 83(4): 288-291, 1991; Pazdur et al., *Cancer Treat. Rev.* 19(4): 351-386, 1993), campothecin, elentherobin *(e.g.,* U.S. Patent No. 5,473,057), sarcodictyins (including sarcodictyin A), epothilones A and B (Bollag et al., *Cancer Research* 55: 2325-2333, 1995), discodermolide (ter Haar et al., *Biochemistry* 35: 243-250, 1996), deuterium oxide (D_2O) (James and Lefebvre, *Genetics* 130(2): 305-314, 1992; Sollott et al., *J. Clin. Invest.* 95: 1869-1876, 1995), hexylene glycol (2-methyl-2,4-pentanediol) (Oka et al., *Cell Struct. Funct.* 16(2): 125-134, 1991), tubercidin (7-deazaadenosine) (Mooberry et al., *Cancer Lett.* 96(2): 261-266, 1995), LY290181 (2-amino-4-(3-pyridyl)-4H-naphtho(1,2-b)pyran-3-cardonitrile) (Panda et al., *J. Biol. Chem.* 272(12): 7681-7687, 1997; Wood et al., *Mol. Pharmacol.* 52(3): 437-444, 1997), aluminum fluoride (Song et al., *J. Cell. Sci. Suppl.* 14: 147-150, 1991), ethylene glycol bis-(succinimidylsuccinate) (Caplow and Shanks, *J. Biol. Chem.* 265(15): 8935-8941, 1990), glycine ethyl ester (Mejillano et al., *Biochemistry* 31 (13): 3478-3483, 1992), monoclonal anti-idiotypic antibodies (Leu et al., *Proc. Natl. Acad. Sci. USA* 91(22): 10690-10694, 1994), microtubule assembly promoting protein (taxol-like protein, TALP) (Hwang et al., *Biochem. Biophys. Res. Commun.* 208(3): 1174-1180, 1995), cell swelling induced by hypotonic (190 mosmol/L) conditions, insulin (100 nmol/L) or glutamine (10 mmol/L) (Haussinger et al., *Biochem. Cell. Biol.* 72(1-2): 12-19, 1994), dynein binding (Ohba et al., *Biochim. Biophys. Acta* 1158(3): 323-332, 1993), gibberelin (Mita and Shibaoka, *Protoplasma* 119(1/2): 100-109, 1984), XCHO1 (kinesin-like protein) (Yonetani et al., *Mol. Biol. Cell* 7(suppl): 211A, 1996), lysophosphatidic acid (Cook et al., *Mol. Biol. Cell* 6(suppl): 260A, 1995), lithium ion (Bhattacharyya and Wolff, *Biochem. Biophys. Res. Commun.* 73(2): 383-390, 1976), plant cell wall components *(e.g.,* poly-L-lysine and extensin) (Akashi et al., *Planta* 182(3): 363-369, 1990), glycerol buffers (Schilstra et al., *Biochem. J.* 277(Pt. 3): 839-847, 1991; Farrell and Keates, *Biochem. Cell. Biol.* 68(11): 1256-1261, 1990; Lopez et al., *J. Cell. Biochem.* 43(3): 281-291, 1990), Triton X-100 microtubule stabilizing buffer (Brown et al., *J. Cell Sci.* 104(Pt. 2): 339-352, 1993; Safiejko-Mroczka and Bell, *J. Histochem. Cytochem.* 44(6): 641-656, 1996), microtubule associated proteins (*e.g.*, MAP2, MAP4, tau, big tau, ensconsin, elongation factor-1-alpha (EF-1α) and E-MAP-115) (Burgess et al., *Cell Motil. Cytoskeleton* 20(4): 289-300, 1991; Saoudi et al., *J. Cell. Sci.* 108(Pt. 1): 357-367, 1995; Bulinski and Bossler, J *Cell. Sci.* 107(Pt. 10): 2839-2849, 1994; Ookata et al., *J. Cell Biol.* 128(5): 849-862, 1995; Boyne et al., *J. Comp. Neurol.* 358(2): 279-293, 1995; Ferreira and Caceres, *J. Neurosci.* 11(2): 392-400, 1991; Thurston et al., *Chromosoma* 105(1): 20-30, 1996; Wang et al., *Brain Res. Mol. Brain Res.* 38(2): 200-208, 1996; Moore and Cyr, *Mol. Biol. Cell* 7(suppl): 221-A, 1996; Masson and Kreis, *J. Cell Biol.* 123(2), 357-371, 1993), cellular entities *(e.g.,* histone H1, myelin basic protein and kinetochores) (Saoudi et al., *J. Cell. Sci.* 108(Pt. 1): 357-367, 1995; Simerly et al., *J. Cell Biol.* 111(4): 1491-1504, 1990), endogenous microtubular structures *(e.g.,* axonemal structures, plugs and GTP caps) (Dye et al., *Cell Motil. Cytoskeleton* 21(3): 171-186, 1992; Azhar and Murphy, *Cell Motil. Cytoskeleton* 15(3): 156-161, 1990; Walker et al., *J. Cell Biol.* 114(1): 73-81, 1991; Drechsel and Kirschner, *Curr. Biol.* 4(12): 1053-1061, 1994), stable tubule only polypeptide *(e.g.,* STOP145 and STOP220) (Pirollet et al., *Biochim. Biophys. Acta* 1160(1): 113-119, 1992; Pirollet et al., *Biochemistry* 31(37): 8849-8855, 1992; Bosc et al., *Proc. Natl. Acad. Sci. USA* 93(5): 2125-2130, 1996; Margolis et al., *EMBO J.* 9(12): 4095-4102, 1990) and tension from mitotic forces (Nicklas and Ward, J *Cell Biol.* 126(5): 1241-1253, 1994), as well as any analogues and derivatives of any of the above. Such compounds can act by either depolymerizing microtubules *(e.g.,* colchicine and vinblastine), or by stabilizing microtubule formation *(e.g.,* paclitaxel).

[0096] Within one preferred embodiment of the invention, the therapeutic agent is paclitaxel, a compound which disrupts microtubule formation by binding to tubulin to form abnormal mitotic spindles. Briefly, paclitaxel is a highly

derivatized diterpenoid (Wani et al., *J. Am. Chem. Soc.* 93:2325, 1971) which has been obtained from the harvested and dried bark of *Taxus brevifolia* (Pacific Yew) and *Taxomyces Andreanae* and *Endophytic Fungus* of the Pacific Yew (Stierle et al., *Science 60*:214-216, 1993). "Paclitaxel" (which should be understood herein to include prodrugs, analogues and derivatives such as, for example, TAXOL® , TAXOTERE® , Docetaxel, 10-desacetyl analogues of paclitaxel and 3'N-desbenzoyl-3'N-t-butoxy carbonyl analogues of paclitaxel) may be readily prepared utilizing techniques known to those skilled in the art *(see e.g.,* Schiff et al., *Nature* 277:665-667, 1979; Long and Fairchild, *Cancer Research* 54: 4355-4361, 1994; Ringel and Horwitz, *J. Natl. Cancer Inst.* 83(4):288-291, 1991; Pazdur et al., *Cancer Treat. Rev. 19* (4):351-386, 1993; WO 94/07882; WO 94/07881; WO 94/07880; WO 94/07876; WO 93/23555; WO 93/10076; WO94/00156; WO 93/24476; EP 590267; WO 94/20089; U.S. Patent Nos. 5,294,637; 5,283,253; 5,279,949; 5,274,137; 5,202,448; 5,200,534; 5,229,529; 5,254,580; 5,412,092; 5,395,850; 5,380,751; 5,350,866; 4,857,653; 5,272,171; 5,411,984; 5,248,796; 5,248,796; 5,422,364; 5,300,638; 5,294,637; 5,362,831; 5,440,056; 4,814,470; 5,278,324; 5,352,805; 5,411,984; 5,059,699; 4,942,184; *Tetrahedron Letters 35*(52):9709-9712, 1994; *J. Med. Chem. 35*: 4230-4237. 1992; *J. Med. Chem. 34*:992-998, 1991; *J. Natural Prod. 57*(10):1404-1410, 1994; *J. Natural Prod. 57*(11): 1580-1583, 1994; *J. Am. Chem. Soc. 110*:6558-6560, 1988), or obtained from a variety of commercial sources, including for example, Sigma Chemical Co., St. Louis, Missouri (T7402 - from *Taxus brevifolia).*

[0097] Representative examples of such paclitaxel derivatives or analogues include 7-deoxy-docetaxol, 7,8-cyclopropataxanes, N-substituted 2-azetidones, 6,7-epoxy paclitaxels, 6,7-modified paclitaxels, 10-desacetoxytaxol, 10-deacetyltaxol (from 10-deacetylbaccatin III), phosphonooxy and carbonate derivatives of taxol, taxol 2',7-di(sodium 1,2-benzenedicarboxylate, 10-desacetoxy- 11,12-dihydrotaxol-10,12(18)-diene derivatives, 10-desacetoxytaxol, Protaxol (2'-and/or 7-O-ester derivatives), (2'-and/or 7-O-carbonate derivatives), asymmetric synthesis of taxol side chain, fluoro taxols, 9-deoxotaxane, (13-acetyl-9-deoxobaccatine III, 9-deoxotaxol, 7-deoxy-9-deoxotaxol, 10-desacetoxy-7-deoxy-9-deoxotaxol, Derivatives containing hydrogen or acetyl group and a hydroxy and tert-butoxycarbonylamino, sulfonated 2'-acryloyltaxol and sulfonated 2'-O-acyl acid taxol derivatives, succinyltaxol, 2'-γ-aminobutyryltaxol formate, 2'-acetyl taxol, 7-acetyl taxol, 7-glycine carbamate taxol, 2'-OH-7-PEG(5000) carbamate taxol, 2'-benzoyl and 2', 7-dibenzoyl taxol derivatives, other prodrugs (2'-acetyltaxol; 2',7-diacetyltaxol; 2'succinyltaxol; 2'-(beta-alanyl)-taxol); 2'gamma-aminobutyryltaxol formate; ethylene glycol derivatives of 2'-succinyltaxol; 2'-glutaryltaxol; 2'-(N,N-dimethylglycyl) taxol; 2'-(2-(N,N-dimethylamino)propionyl)taxol; 2'orthocarboxybenzoyl taxol; 2'aliphatic carboxylic acid derivatives of taxol, Prodrugs {2'(N,N-diethylaminopropionyl)taxol, 2'(N,N-dimethylglycyl)taxol, 7(N,N-dimethylglycyl)taxol, 2',7-di-(N,N-dimethylglycyl)taxol, 7(N,N-diethylaminopropionyl)taxol, 2',7-di(N,N-diethylaminopropionyl)taxol, 2'-(L-glycyl)taxol, 7-(L-glycyl)taxol, 2',7-di(L-glycyl)taxol, 2'-(L-alanyl)taxol, 7-(L-alanyl)taxol, 2',7-di(L-alanyl)taxol, 2'-(L-leucyl)taxol, 7-(L-leucyl)taxol, 2',7-di(L-leucyl)taxol, 2'-(L-isoleucyl)taxol, 7-(L-isoleucyl)taxol, 2',7-di(L-isoleucyl)taxol, 2'-(L-valyl)taxol, 7-(L-valyl)taxol, 2'7-di(L-valyl)taxol, 2'-(L-phenylalanyl)taxol, 7-(L-phenylalanyl)taxol, 2',7-di(L-phenylalanyl)taxol, 2'-(L-prolyl)taxol, 7-(L-prolyl)taxol, 2',7-di(L-prolyl)taxol, 2'-(L-lysyl)taxol, 7-(L-lysyl)taxol, 2',7-di(L-lysyl)taxol, 2'-(L-glutamyl)taxol, 7-(L-glutamyl)taxol, 2',7-di(L-glutamyl)taxol, 2'-(L-arginyl)taxol, 7-(L-arginyl)taxol, 2',7-di(L-arginyl)taxol}, Taxol analogs with modified phenylisoserine side chains, taxotere, (N-debenzoyl-N-tert-(butoxycaronyl)-10-deacetyltaxol, and taxanes *(e.g.,* baccatin III, cephalomannine, 10-deacetylbaccatin III, brevifoliol, yunantaxusin and taxusin).

[0098] Representative examples of microtubule depolymerizing (or destabilizing or disrupting) agents include Nocodazole (Ding et al., *J. Exp. Med. 171(3)*:715-727, 1990; Dotti et al., *J. Cell Sci. Suppl. 15:75-84,* 1991; Oka et al., *Cell Struct. Funct. 16(2)*: 125-134, 1991; Wiemer et al., *J. Cell. Biol. 136(1)*:71-80, 1997); Cytochalasin B (Illinger et al., *Biol. Cell 73(2-3)*:131-138, 1991); Vinblastine (Ding et al., *J. Exp. Med. 171(3)*:715-727, 1990; Dirk et al., *Neurochem. Res. 15(11)*:1135-1139, 1990; Illinger et al., *Biol. Cell 73(2-3)*:131-138, 1991; Wiemer et al., *J. Cell. Biol. 136(1)*:71-80, 1997); Vincristine (Dirk et al., *Neurochem. Res. 15(11)*:1135-1139, 1990; Ding et al., *J. Exp. Med. 171(3)*:715-727, 1990); Colchicine (Allen et al., *Am. J. Physiol. 261(4 Pt. 1)*:L315-L321, 1991; Ding et al., *J. Exp. Med. 171(3)*:715-727, 1990; Gonzalez et al., *Exp. Cell. Res. 192*(1):10-15, 1991; Stargell et al., *Mol. Cell. Biol.* 12(4):1443-1450, 1992); CI 980 (colchicine analogue) (Garcia et al., Anticancer Drugs *6(4)*:533-544, 1995); Colcemid (Barlow et al., *Cell. Motil. Cytoskeleton 19(1)*:9-17, 1991; Meschini et al., J *Microsc. 176(Pt. 3)*:204-210, 1994; Oka et al., *Cell Struct. Funct. 16 (2)*:125-134, 1991); Podophyllotoxin (Ding et al., *J. Exp. Med. 171(3)*:715-727, 1990); Benomyl (Hardwick et al., *J. Cell. Biol. 131(3)*:709-720, 1995; Shero et al., *Genes Dev. 5(4)*:549-560, 1991); Oryzalin (Stargell et al., *Mol. Cell. Biol. 12(4)*:1443-1450, 1992); Majusculamide C (Moore, *J. Ind. Microbiol. 16(2)*:134-143, 1996); Demecolcine (Van Dolah and Ramsdell, *J. Cell. Physiol. 166(1)*:49-56, 1996; Wiemer et al., *J. Cell. Biol. 136(1)*:71-80, 1997); and Methyl-2-benzimidazolecarbamate (MBC) (Brown et al., *J. Cell. Biol. 123(2)*:387-403, 1993).

FORMULATIONS

[0099] As noted above, therapeutic anti-microtubule agents described herein may be formulated in a variety of manners. and thus may additionally comprise a carrier. In this regard, a wide variety of carriers may be selected of either polymeric or non-polymeric origin.

[0100] For example, within one embodiment of the invention a wide variety of polymeric carriers may be utilized to contain and/or deliver one or more of the therapeutic agents discussed above, including for example both biodegradable and non-biodegradable compositions. Representative examples of biodegradable compositions include albumin, collagen, gelatin, hyaluronic acid, starch, cellulose (methylcellulose, hydroxypropylcellulose, hydroxypropylmethylcellulose, carboxymethylcellulose, cellulose acetate phthalate, cellulose acetate succinate, hydroxypropylmethylcellulose phthalate), casein, dextrans, polysaccharides, fibrinogen, poly(D,L lactide), poly(D,L-lactide-co-glycolide), poly(glycolide), poly(hydroxybutyrate), poly(alkylcarbonate) and poly(orthoesters), polyesters, poly(hydroxyvaleric acid). polydioxanone, poly(ethylene terephthalate), poly(malic acid), poly(tartronic acid), polyanhydrides, polyphosphazenes, poly (amino acids) and their copolymers *(see generally,* Illum, L., Davids, S.S. (eds.) "Polymers in Controlled Drug Delivery" Wright, Bristol, 1987; Arshady, J *Controlled Release 17*:1-22, 1991; Pitt, *Int. J. Phar. 59*:173-196, 1990; Holland et al., *J. Controlled Release 4*:155-0180, 1986). Representative examples of nondegradable polymers include poly(ethylene-vinyl acetate) ("EVA") copolymers, silicone rubber, acrylic polymers (polyacrylic acid, polymethylacrylic acid, polymethylmethacrylate, polyalkylcynoacrylate), polyethylene, polyproplene, polyamides (nylon 6,6), polyurethane, poly(ester urethanes), poly(ether urethanes), poly(ester-urea), polyethers (poly(ethylene oxide), poly(propylene oxide), Pluronics and poly(tetramethylene glycol)), silicone rubbers and vinyl polymers (polyvinylpyrrolidone, poly(vinyl alcohol), poly (vinyl acetate phthalate). Polymers may also be developed which are either anionic *(e.g.,* alginate, carrageenin, carboxymethyl cellulose and poly(acrylic acid), or cationic (e.g., chitosan, poly-L-lysine, polyethylenimine, and poly (allyl amine)) *(see generally,* Dunn et al., *J. Applied Polymer Sci. 50*:353-365, 1993; Cascone et al., *J. Materials Sci.: Materials in Medicine* 5:770-774, 1994; Shiraishi et al., *Biol. Pharm. Bull. 16*(11):1164-1168, 1993; Thacharodi and Rao, *Int'l J. Pharm. 120*:115-118, 1995; Miyazaki et al., *Int'l J. Pharm. 118*:257-263, 1995). Particularly preferred polymeric carriers include poly(ethylenevinyl acetate), poly (D,L-lactic acid) oligomers and polymers, poly (L-lactic acid) oligomers and polymers, poly (glycolic acid), copolymers of lactic acid and glycolic acid, poly (caprolactone), poly (valerolactone), polyanhydrides, copolymers of poly (caprolactone) or poly (lactic acid) with a polyethylene glycol (e.g., MePEG), and blends thereof.

[0101] Polymeric carriers can be fashioned in a variety of forms, with desired release characteristics and/or with specific desired properties. For example, polymeric carriers may be fashioned to release a therapeutic agent upon exposure to a specific triggering event such as pH *(see e.g.*, Heller et al., "Chemically Self-Regulated Drug Delivery Systems," in *Polymers in Medicine III*, Elsevier Science Publishers B.V., Amsterdam, 1988, pp. 175-188; Kang et al., *J. Applied Polymer Sci. 48*:343-354, 1993; Dong et al., *J. Controlled Release 19:171-178, 1992;* Dong and Hoffman, *J. Controlled Release 15*:141-152, 1991; Kim et al., *J. Controlled Release 28*:143-152, 1994; Cornejo-Bravo et al., *J. Controlled Release 33*:223-229, 1995; Wu and Lee, *Pharm. Res. 10*(10):1544-1547, 1993; Serres et al., *Pharm. Res. 13*(2):196-201, 1996; Peppas, "Fundamentals of pH- and Temperature-Sensitive Delivery Systems," in Gurny et al. (eds.), *Pulsatile Drug Delivery,* Wissenschaftliche Verlagsgesellschaft mbH, Stuttgart, 1993, pp. 41-55; Doelker, "Cellulose Derivatives," 1993, in Peppas and Langer (eds.), *Biopolymers I,* Springer-Verlag, Berlin). Representative examples of pH-sensitive polymers include poly(acrylic acid) and its derivatives (including for example, homopolymers such as poly(aminocarboxylic acid); poly(acrylic acid); poly(methyl acrylic acid), copolymers of such homopolymers, and copolymers of poly(acrylic acid) and acrylmonomers such as those discussed above. Other pH sensitive polymers include polysaccharides such as cellulose acetate phthalate; hydroxypropylmethylcellulose phthalate; hydroxypropylmethylcellulose acetate succinate; cellulose acetate trimellilate; and chitosan. Yet other pH sensitive polymers include any mixture of a pH sensitive polymer and a water soluble polymer.

[0102] Likewise, polymeric carriers can be fashioned which are temperature sensitive *(see e.g.,* Chen et al., "Novel Hydrogels of a Temperature-Sensitive Pluronic Grafted to a Bioadhesive Polyacrylic Acid Backbone for Vaginal Drug Delivery," in *Proceed. Intern. Symp. Control. Rel. Bioact. Mater. 22*:167-168, Controlled Release Society, Inc., 1995; Okano, "Molecular Design of Stimuli-Responsive Hydrogels for Temporal Controlled Drug Delivery," in *Proceed. Intern. Symp. Control. Rel. Bioact. Mater. 22*:111-112, Controlled Release Society, Inc., 1995; Johnston et al., *Pharm. Res.* 9 (3):425-433, 1992; Tung, *Int'l J. Pharm. 107*:85-90, 1994; Harsh and Gehrke, *J. Controlled Release 17*:175-186, 1991; Bae et al., *Pharm. Res. 8*(4):531-537, 1991; Dinarvand and D'Emanuele, *J Controlled Release* 36:221-227, 1995; Yu and Grainger, "Novel Thermo-sensitive Amphiphilic Gels: Poly N-isopropylacrylamide-co-sodium acrylate-co-n-N-alkylacrylamide Network Synthesis and Physicochemical Characterization," Dept. of Chemical & Biological Sci., Oregon Graduate Institute of Science & Technology, Beaverton, OR, pp. 820-821; Zhou and Smid, "Physical Hydrogels of Associative Star Polymers," Polymer Research Institute, Dept. of Chemistry, College of Environmental Science and Forestry, State Univ. of New York, Syracuse, NY, pp. 822-823; Hoffman et al., "Characterizing Pore Sizes and Water 'Structure' in Stimuli-Responsive Hydrogels," Center for Bioengineering, Univ. of Washington, Seattle, WA, p. 828; Yu and Grainger, "Thermo-sensitive Swelling Behavior in Crosslinked N-isopropylacrylamide Networks: Cationic, Anionic and Ampholytic Hydrogels," Dept. of Chemical & Biological Sci., Oregon Graduate Institute of Science & Technology, Beaverton, OR, pp. 829-830; Kim et al., *Pharm. Res.* 9(3):283-290, 1992; Bae et al., *Pharm. Res. 8*(5):624-628, 1991; Kono et al., *J. Controlled Release 30*:69-75, 1994; Yoshida et al., *J. Controlled Release 32*:97-102, 1994; Okano et al., *J. Controlled Release 36*:125-133, 1995; Chun and Kim, *J. Controlled Release 38*:39-47, 1996; D'Emanuele and

Dinarvand, *Int'l J. Pharm. 118*:237-242, 1995; Katono et al., *J. Controlled Release 16*:215-228, 1991; Hoffman, "Thermally Reversible Hydrogels Containing Biologically Active Species," in Migliaresi et al. (eds.), *Polymers in Medicine III*, Elsevier Science Publishers B.V., Amsterdam, 1988, pp. 161-167; Hoffman, "Applications of Thermally Reversible Polymers and Hydrogels in Therapeutics and Diagnostics," in *Third International Symposium on Recent Advances in Drug Delivery Systems,* Salt Lake City, UT, Feb. 24-27, 1987, pp. 297-305; Gutowska et al., *J. Controlled Release 22*: 95-104, 1992; Palasis and Gehrke, *J. Controlled Release 18*:1-12, 1992; Paavola et al., *Pharm. Res. 12*(12):1997-2002, 1995).

[0103] Representative examples of thermogelling polymers, and their gelatin temperature (LCST (°C)) include homopolymers such as poly(N-methyl-N-n-propylacrylamide), 19.8; poly(N-n-propylacrylamide), 21.5; poly(N-methyl-N-isopropylacrylamide), 22.3; poly(N-n-propylmethacrylarnide), 28.0; poly(N-isopropylacrylamide), 30.9; poly(N, n-diethylacrylamide), 32.0; poly(N-isopropylmethacrylamide), 44.0; poly(N-cyclopropylacrylamide), 45.5; poly(N-ethylmethyacrylamide), 50.0; poly(N-methyl-N-ethylacrylamide), 56.0; poly(N-cyclopropylmethacrylamide), 59.0; poly(N-ethylacrylamide), 72.0. Moreover thermogelling polymers may be made by preparing copolymers between (among) monomers of the above, or by combining such homopolymers with other water soluble polymers such as acrylmonomers (*e.g.*, acrylic acid and derivatives thereof such as methylacrylic acid, acrylate and derivatives thereof such as butyl methacrylate, acrylamide, and N-n-butyl acrylamide).

[0104] Other representative examples of thermogelling polymers include cellulose ether derivatives such as hydroxypropyl cellulose, 41°C; methyl cellulose, 55°C; hydroxypropylmethyl cellulose, 66°C; and ethylhydroxyethyl cellulose, and Pluronics such as F-127, 10 - 15°C; L-122, 19°C; L-92, 26°C; L-81, 20°C; and L-61, 24°C.

[0105] A wide variety of forms may be fashioned by the polymeric carriers of the present invention, including for example, rod-shaped devices, pellets, slabs, or capsules *(see e.g.,* Goodell et al., *Am. J. Hosp. Pharm. 43*:1454-1461, 1986; Langer et al., "Controlled release of macromolecules from polymers", in *Biomedical Polymers, Polymeric Materials and Pharmaceuticals for Biomsdical Use,* Goldberg, E.P., Nakagim, A. (eds.) Academic Press, pp. 113-137, 1980; Rhine et al., *J. Pharm. Sci. 69*:265-270, 1980; Brown et al., *J. Pharm. Sci.* 72:1181-1185, 1983; and Bawa et al., *J Controlled Release 1*:259-267, 1985). Therapeutic agents may be linked by occlusion in the matrices of the polymer, bound by covalent linkages, or encapsulated in microcapsules. Within certain preferred embodiments of the invention, therapeutic compositions are provided in non-capsular formulations such as microspheres (ranging from nanometers to micrometers in size), pastes, threads of various size, films and sprays.

[0106] Preferably, therapeutic compositions of the present invention are fashioned in a manner appropriate to the intended use. Within certain aspects of the present invention, the therapeutic composition should be biocompatible, and release one or more therapeutic agents over a period of several days to months. For example, "quick release" or "burst" therapeutic compositions are provided that release greater than 10%, 20%, or 25% (w/v) of a therapeutic agent (*e.g.*, paclitaxel) over a period of 7 to 10 days. Such "quick release" compositions should, within certain embodiments, be capable of releasing chemotherapeutic levels (where applicable) of a desired agent. Within other embodiments, "low release" therapeutic compositions are provided that release less than 1% (w/v) of a therapeutic agent over a period of 7 to 10 days. Further, therapeutic compositions of the present invention should preferably be stable for several months and capable of being produced and maintained under sterile conditions.

[0107] Within certain aspects of the present invention, therapeutic compositions may be fashioned in any size ranging from 50 nm to 500 μm, depending upon the particular use. Alternatively, such compositions may also be readily applied as a "spray", which solidifies into a film or coating. Such sprays may be prepared from microspheres of a wide array of sizes, including for example, from 0.1 μm to 3 μm, from 10 μm to 30 μm, and from 30 μm to 100 μm.

[0108] Therapeutic compositions of the present invention may also be prepared in a variety of "paste" or gel forms. For example, within one embodiment of the invention, therapeutic compositions are provided which are liquid at one temperature *(e.g.,* temperature greater than 37°C, such as 40°C, 45°C, 50°C, 55°C or 60°C), and solid or semi-solid at another temperature *(e.g.,* ambient body temperature, or any temperature lower than 37°C). Such "thermopastes" may be readily made given the disclosure provided herein.

[0109] Within yet other aspects of the invention, the therapeutic compositions of the present invention may be formed as a film. Preferably, such films are generally less than 5, 4, 3, 2, or 1 mm thick, more preferably less than 0.75 mm or 0.5 mm thick, and most preferably less than 500 μm to 100 μm thick. Such films are preferably flexible with a good tensile strength (*e.g.*, greater than 50, preferably greater than 100, and more preferably greater than 150 or 200 N/cm^2), good adhesive properties *(i.e.,* readily adheres to moist or wet surfaces), and have controlled permeability.

[0110] Within further aspects of the invention, the therapeutic compositions may be formulated for topical application. Representative examples include: ethanol; mixtures of ethanol and glycols *(e.g.,* ethylene glycol or propylene glycol); mixtures of ethanol and isopropyl myristate or ethanol, isopropyl myristate and water *(e.g.,* 55:5:40); mixtures of ethanol and eineol or D-limonene (with or without water); glycols *(e.g.,* ethylene glycol or propylene glycol) and mixtures of glycols such as propylene glycol and water, phosphatidyl glycerol, dioleoylphosphatidyl glycerol, Transcutol®, or terpinolene; mixtures of isopropyl myristate and 1-hexyl-2-pyrrolidone, N-dodecyl-2-piperidinone or 1-hexyl-2-pyrrolidone. Other excipients may also be added to the above, including for example, acids such as oleic acid and linoleic acid,

and soaps such as sodium lauryl sulfate. For a more detailed description of the above, *see generally,* Hoelgaard et al., *J. Contr. Rel.* 2:111, 1985; Liu et al., *Pharm. Res. 8*:938, 1991; Roy et al., *J. Pharm. Sci. 83:126,* 1991; Ogiso et al., *J. Pharm. Sci. 84*:482, 1995; Sasaki et al., *J. Pharm. Sci. 80*:533, 1991; Okabe et al., *J. Contr. Rel. 32*:243, 1994; Yokomizo et al., *J. Contr. Rel. 38:267,* 1996; Yokomizo et al., *J. Contr. Rel. 42*:37, 1996; Mond et al., *J. Contr. Rel. 33: 72,* 1994; Michniak et al., *J. Contr. Rel. 32*:147, 1994; Sasaki et al., J *Pharm. Sci. 80*:533, 1991; Baker & Hadgraft, *Pharm. Res. 12*:993, 1995; Jasti et al., *AAPS Proceedings,* 1996; Lee et al., *AAPS Proceedings,* 1996; Ritschel et al., *Skin Pharmacol. 4*:235, 1991; and McDaid & Deasy, *Int.* J. *Pharm. 133*:71, 1996.

[0111] Within certain embodiments of the invention, the therapeutic compositions may also comprise additional ingredients such as surfactants (*e.g.*, Pluronics such as F-127, L-122, L-92, L-81, and L-61).

[0112] Within further aspects of the present invention, polymeric carriers are provided which are adapted to contain and release a hydrophobic compound, the carrier containing the hydrophobic compound in combination with a carbohydrate, protein or polypeptide. Within certain embodiments, the polymeric carrier contains or comprises regions, pockets, or granules of one or more hydrophobic compounds. For example, within one embodiment of the invention, hydrophobic compounds may be incorporated within a matrix which contains the hydrophobic compound, followed by incorporation of the matrix within the polymeric carrier. A variety of matrices can be utilized in this regard, including for example, carbohydrates and polysaccharides such as starch, cellulose, dextran, methylcellulose, and hyaluronic acid, proteins or polypeptides such as albumin, collagen and gelatin. Within alternative embodiments, hydrophobic compounds may be contained within a hydrophobic core, and this core contained within a hydrophilic shell.

[0113] Other carriers that may likewise be utilized to contain and deliver the therapeutic agents described herein include: hydroxypropyl β cyclodextrin (Cserhati and Hollo, *Int. J. Pharm. 108:69-75,* 1994), liposomes *(see e.g.*, Sharma et al., *Cancer Res.* 53:5877-5881, 1993; Sharma and Straubinger, *Pharm. Res. 11*(60):889-896, 1994; WO 93/18751; U.S. Patent No. 5,242,073), liposome/gel (WO 94/26254), nanocapsules (Bartoli et al., *J. Microencapsulation* 7(2): 191-197, 1990), micelles (Alkan-Onyuksel et al., *Pharm. Res. 11*(2):206-212, 1994), implants (Jampel et al., *Invest. Ophthalm. Vis. Science 34*(11):3076-3083, 1993; Walter et al., *Cancer Res. 54*:22017-2212, 1994), nanoparticles (Violante and Lanzafame PAACR), nanoparticles - modified (U.S. Patent No. 5,145,684), nanoparticles (surface modified) (U.S. Patent No. 5,399,363), taxol emulsion/solution (U.S. Patent No. 5,407,683), micelle (surfactant) (U.S. Patent No. 5,403,858), synthetic phospholipid compounds (U.S. Patent No. 4,534,899), gas borne dispersion (U.S. Patent No. 5,301,664), liquid emulsions, foam, spray, gel, lotion, cream, ointment, dispersed vesicles, particles or droplets solid- or liquid- aerosols, microemulsions (U.S. Patent No. 5,330,756), polymeric shell (nano- and microcapsule) (U.S. Patent No. 5,439,686), taxoid-based compositions in a surface-active agent (U.S. Patent No. 5,438,072), emulsion (Tarr et al., *Pharm Res. 4:* 62-165, 1987), nanospheres (Hagan et al., *Proc. Intern. Symp. Control Rel. Bioact. Mater. 22*, 1995; Kwon et al., *Pharm Res. 12*(2):192-195; Kwon et al., *Pharm Res. 10*(7):970-974; Yokoyama et al., *J. Contr. Rel. 32*: 269-277, 1994; Gref et al., *Science 263*:1600-1603, 1994; Bazile et al., *J. Pharm. Sci. 84*:493-498, 1994) and implants (U.S. Patent No. 4,882,168).

[0114] As discussed in more detail below, therapeutic agents of the present invention, which are optionally incorporated within one of the carriers described herein to form a therapeutic composition, may be prepared and utilized to treat or prevent a wide variety of diseases.

TREATMENT OR PREVENTION OF INFLAMMATORY DISEASES

[0115] As noted above, the use according to the invention is useful for treating or preventing multiple sclerosis in a method comprising the step of administering to a patient an anti-microtubule agent.

1. *Multiple Sclerosis*

[0116] According to the use of the invention, anti-microtubule agents may be utilized to treat or prevent multiple sclerosis. Briefly, multiple sclerosis (MS) is a devastating demyelinating disease of the human central nervous system. Although its etiology and pathogenesis is not known, genetic, immunological and environmental factors are believed to play a role. In the course of the disease, there is a progressive demyelination in the brain of MS patients resulting in the loss of motor function. Although the exact mechanisms involved in the loss of myelin are not understood, there is an increase in astrocyte proliferation and accumulation in the areas of myelin destruction. At these sites, there is macrophage-like activity and increased protease activity which is at least partially responsible for degradation of the myelin sheath.

[0117] The anti-microtubule agent can be administered to the site of inflammation (or a potential site of inflammation), in order to treat or prevent the disease. Suitable anti-microtubule agents are discussed in detail above, and include for example, taxanes (*e.g.*, paclitaxel and docetaxel), campothecin, eleutherobin, sarcodictyins, epothilones A and B, discodermolide, deuterium oxide (D_2O), hexylene glycol (2-methyl-2,4-pentanediol), tubercidin (7-deazaadenosine), LY290181 (2-amino-4-(3-pyridyl)-4H-naphtho(1,2-b)pyran-3-cardonitrile), aluminum fluoride, ethylene glycol bis-(suc-

cinimidylsuccinate), glycine ethyl ester, monoclonal anti-idiotypic antibodies, microtubule assembly promoting protein (taxol-like protein, TALP), cell swelling induced by hypotonic (190 mosmol/L) conditions, insulin (100 nmol/L) or glutamine (10 mmol/L), dynein binding, gibberelin, XCHO1 (kinesin-like protein), lysophosphatidic acid, lithium ion, plant cell wall components (*e.g.*, poly-L-lysine and extensin), glycerol buffers, Triton X-100 microtubule stabilizing buffer, microtubule associated proteins (*e.g.*, MAP2, MAP4, tau, big tau, ensconsin, elongation factor-1-alpha (EF-1α) and E-MAP-115), cellular entities (*e.g.*, histone H1, myelin basic protein and kinetochores), endogenous microtubular structures (*e.g.*, axonemal structures, plugs and GTP caps), stable tubule only polypeptide (*e.g.*, STOP145 and STOP220) and tension from mitotic forces, as well as any analogues and derivatives of any of the above. Such agents may, within certain embodiments, be delivered as a composition along with a polymeric carrier, or in a liposome formulation as discussed in more detail both above and below. Within certain embodiments of the invention, the agents or compositions may be administered orally, intravenously, or by direct administration (preferably with ultrasound, CT, fluoroscopic, MRI or endoscopic guidance) to the disease site.

[0118] An effective anti-microtubule therapy for multiple sclerosis will accomplish one or more of the following: decrease the severity of symptoms; decrease the duration of disease exacerbations; increase the frequency and duration of disease remission/symptom-free periods; prevent fixed impairment and disability; and/or prevent/attenuate chronic progression of the disease. Clinically, this would result in improvement in visual symptoms (visual loss, diplopia), gait disorders (weakness, axial instability, sensory loss, spasticity, hyperreflexia, loss of dexterity), upper extremity dysfunction (weakness, spasticity, sensory loss), bladder dysfunction (urgency, incontinence, hesitancy, incomplete emptying), depression, emotional lability, and cognitive impairment. Pathologically the treatment reduces one or more of the following, such as myelin loss, breakdown of the blood-brain barrier, perivascular infiltration of mononuclear cells, immunologic abnormalities, gliotic scar formation and astrocyte proliferation, metalloproteinase production, and impaired conduction velocity.

[0119] The anti-microtubule agent can be administered in any manner to achieve the above endpoints. However, preferred methods of administration include intravenous, oral, or subcutaneous, intramuscular or intrathecal injection. The anti-microtubule agent can be administered as a chronic low dose therapy to prevent disease progression, prolong disease remission, or decrease symptoms in active disease. Alternatively, the therapeutic agent can be administered in higher doses as a "pulse" therapy to induce remission in acutely active disease. The minimum dose capable of achieving these endpoints can be used and can vary according to patient, severity of disease, formulation of the administered agent, and route of administration. For example, for paclitaxel, systemic chronic low dose therapy can be administered continuously at 10-50 mg/m^2 of paclitaxel every 1-4 weeks depending upon therapeutic response; systemic high dose "pulse" therapy can be administered at 50-250 mg/m^2 every 1-21 days for 1-6 cycles. Other anti-microtubule agents can be administered at equivalent doses adjusted for the potency and tolerability of the agent.

FORMULATION AND ADMINISTRATION

[0120] As noted above, anti-microtubule agents of the present invention may be formulated in a variety of forms (*e.g.*, microspheres, pastes, films, sprays, ointments, creams, gels and the like). Further, the compositions of the present invention may be formulated to contain more than one anti-microtubule agents, to contain a variety of additional compounds, to have certain physical properties *(e.g.,* elasticity, a particular melting point, or a specified release rate). Within certain embodiments of the invention, compositions may be combined in order to achieve a desired effect *(e.g.,* several preparations of microspheres may be combined in order to achieve both a quick and a slow or prolonged release of one or more anti-microtubule agents).

[0121] Anti-microtubule agents may be administered either alone, or in combination with pharmaceutically or physiologically acceptable carrier, excipients or diluents. Generally, such carriers should be nontoxic to recipients at the dosages and concentrations employed. Ordinarily, the preparation of such compositions entails combining the therapeutic agent with buffers, antioxidants such as ascorbic acid, low molecular weight (less than about 10 residues) polypeptides, proteins, amino acids, carbohydrates including glucose, sucrose or dextrins, chelating agents such as EDTA, glutathione and other stabilizers and excipients. Neutral buffered saline or saline mixed with nonspecific serum albumin are exemplary appropriate diluents.

[0122] As noted above, anti-microtubule agents, compositions, or pharmaceutical compositions provided herein may be prepared for administration by a variety of different routes, including for example, topically to a site of inflammation, orally, rectally, intracranially, intrathecally, intranasally, intraocularly, intravenously, subcutaneously, intraperitoneally, intramuscularly, sublingually and intravesically. Other representative routes of administration include direct administration (preferably with ultrasound, CT, fluoroscopic, MRI or endoscopic guidance) to the disease site.

[0123] The therapeutic agents, therapeutic compositions and pharmaceutical compositions provided herein may be placed within containers, along with packaging material which provides instructions regarding the use of such materials. Generally, such instructions include a tangible expression describing the reagent concentration, as well as within certain embodiments, relative amounts of excipient ingredients or diluents (*e.g.*, water, saline or PBS) which may be necessary

to reconstitute the anti-microtubule agent, anti-microtubule composition, or pharmaceutical composition.

[0124] The following examples are offered by way of illustration, and not by way of limitation.

EXAMPLES

[0125] As discussed above, chronic inflammation is a process characterized by tissue infiltration with white blood cells (macrophages, lymphocytes, neutrophils, and plasma cells), tissue destruction by inflammatory cells and cell products (reactive oxygen species, tissue degrading enzymes such as matrix metalloproteinases), and repeated attempts at repair by connective tissue replacement (angiogenesis and fibrosis).

[0126] In order to assess anti-microtubule agents for their ability to effect chronic inflammatory the following pathological/biological endpoints: (1) inhibition of the white blood cell response (macrophages, neutrophils and T cells) which initiates the inflammatory cascade; (2) inhibition of mesenchymal cell (fibroblasts, synoviocytes, etc.) hyperproliferation that leads to the development of fibrosis and loss of organ function; (3) inhibition of matrix metalloproteinase production/activity which causes tissue damage; (4) disruption of angiogenesis which may enhance the inflammatory response and provide the metabolic support necessary for the growth and development of the fibrous tissue; and (5) all of this must be achieved without substantial toxicity to normal parenchymal cells or impairing the normal synthesis of the matrix components (*e.g.*, collagen and proteoglycans).

[0127] As set forth in more detail below, the activity of agents which stabilize microtubules such as, for example, paclitaxel has been examined in several tissues and inflammatory disease states. These agents demonstrate an ability to alter many of the above disease parameters.

EXAMPLE 1

EFFECT OF ANTI-MICROTUBULE AGENTS ON NEUTROPHIL ACTIVITY

[0128] The example describes the effect of anti-microtubule agents on the response of neutrophils stimulated with opsonized CPPD crystals or opsonized zymosan. As shown by experiments set forth below, anti-microtubule agnets are strong inhibitors of particulate-induced neutrophil activation as measured by chemiluminescence, superoxide anion production and degranulation in response to plasma opsonized microcrystals or zymosan.

A. Materials and Methods

[0129] Hanks buffered saline solution (HBSS) pH 7.4 was used throughout this study. All chemicals were purchased from Sigma Chemical Co (St. Louis, MO) unless otherwise stated. All experiments were performed at 37°C unless otherwise stated.

1. PREPARATION AND CHARACTERIZATION OF CRYSTALS

[0130] CPPD (triclinic) crystals were prepared. The size distribution of the crystals was approximately 33% less than 10 μm, 58% between 10 and 20 μm and 9% greater than 20 μm. Crystals prepared under the above conditions are pyrogen-free and crystals produced under sterile, pyrogen-free conditions produced the same magnitude of neutrophil response as crystals prepared under normal, non-sterile laboratory conditions.

2. OPSONIZATION OF CRYSTALS AND ZYMOSAN

[0131] All experiments that studied neutrophil responses to crystals or zymosan in the presence of paclitaxel were performed using plasma opsonized CPPD or zymosan. Opsonization of crystals or zymosan was done with 50% heparinized plasma at a concentration of 75 mg of CPPD or 12 mg of zymosan per ml of 50% plasma. Crystals or zymosan were incubated with plasma for 30 minutes at 37°C and then washed in excess HBSS.

3. NEUTROPHIL PREPARATION

[0132] Neutrophils were prepared from freshly collected human citrated whole blood. Briefly, 400 ml of blood were mixed with 80 ml of 4% dextran T500 (Phamacia LKB, Biotechnology AB Uppsala, Sweden) in HBSS and allowed to settle for 1 hour. Plasma was collected continuously and 5 ml applied to 5 ml of Ficoll Paque (Pharmacia) in 15 ml polypropylene tubes (Corning, NY). Following centrifugation at 500 g for 30 minutes, the neutrophil pellets were washed free of erythrocytes by 20 seconds of hypotonic shock. Neutrophils were resuspended in HBSS, kept on ice and used for experiments within 3 hours. Neutrophil viability and purity was always greater than 90%.

4. INCUBATION OF NEUTROPHILS WITH ANTI-MICROTUBULE AGENTS

(a) Paclitaxel

[0133] A stock solution of paclitaxel at 12 mM in dimethylsulfoxide (DMSO) was freshly prepared before each experiment. This stock solution was diluted in DMSO to give solutions of paclitaxel in the 1 to 10 mM concentration range. Equal volumes of these diluted paclitaxel solutions was added to neutrophils at 5,000,000 cells per ml under mild vortexing to achieve concentrations of 0 to 50 μM with a final DMSO concentration of 0.5%. Cells were incubated for 20 minutes at 33°C then for 10 minutes at 37°C before addition to crystals or zymosan.

(b) Aluminum Fluoride

[0134] A stock solution of aluminum fluoride (AlF_3) at 1 M in HBSS was freshly prepared. This stock solution was diluted in HBSS to give solutions of AlF_3 in the 5 to 100 mM concentration range. Equal volumes (50 μl) of these diluted AlF_3 solutions was added to neutrophils at 5,000,000 cells per ml and incubated for 15 minutes at 37°C. Luminol (1 μM) was added and then 20 μl of opsonized zymosan (final concentration = 1 mg/ml) to activate the cells.

(c) Glycine Ethyl Ester

[0135] A stock solution of glycine ethyl ester at 100 mM in HBSS was freshly prepared. This stock solution was diluted in HBSS to give solutions of glycine ethyl ester in the 0.5 to 10 mM concentration range. Equal volumes (50 μl) of these diluted glycine ethyl ester solutions was added to neutrophils at 5,000,000 cells per ml and incubated for 15 minutes at 37°C. Luminol (1 μM) was added and then 20 μl of opsonized zymosan (final concentration = 1 mg/ml) to activate the cells.

(d) LY290181

[0136] A stock solution of LY290181 at 100 μM in HBSS was freshly prepared. This stock solution was diluted in HBSS to give solutions of LY290181 in the 0.5 to 50 μM concentration range. Equal volumes (50 μl) of these diluted LY290181 solutions was added to neutrophils at 5,000,000 cells per ml and incubated for 15 minutes at 37°C. Luminol (1 μM) was added and then 20 μl of opsonized zymosan (final concentration = 1 mg/ml) to activate the cells.

5. CHEMILUMINESCENCE ASSAY

[0137] All chemiluminescence studies were performed at a cell concentration of 5,000,000 cells/ml in HBSS with CPPD (50 mg/ml). In all experiments 0.5 ml of cells was added to 25 mg of CPPD or 0.5 mg of zymosan in 1.5 ml capped Eppendorf tubes. 10 μl of luminol dissolved in 25% DMSO in HBSS was added to a final concentration of 1 μM and the samples were mixed to initiate neutrophil activation by the crystals or zymosan. Chemiluminescence was monitored using an LKB Luminometer (Model 1250) at 37°C for 20 minutes with shaking immediately prior to measurements to resuspend the crystals or zymosan. Control tubes contained cells, drug and luminol (crystals absent).

6. SUPEROXIDE ANION GENERATION

[0138] Superoxide anion concentrations were measured using the superoxide dismutase inhibitable reduction of cytochrome C assay. Briefly, 25 mg of crystals or 0.5 mg of zymosan was placed in a 1.5 ml capped Eppendorf tube and warmed to 37°C. 0.5 ml of cells at 37°C were added together with ferricytochrome C (final concentration 1.2 mg/ml) and the cells were activated by shaking the capped tubes. At appropriate times tubes were centrifuged at 10,000g for 10 seconds and the supernatant collected for assay be measuring the absorbance of 550 nm. Control tubes were set up under the same conditions with the inclusion of superoxide dismutase at 600 units per ml.

7. NEUTROPHIL DEGRANULATION ASSAY

[0139] One and a half milliliter Eppendorf tubes containing either 25 mg of CPPD or I mg of zymosan were preheated to 37°C. 0.5 ml of cells at 37°C were added followed by vigorous shaking to initiate the reactions. At appropriate times, tubes were centrifuged at 10,000 g for 10 seconds and 0.4 ml of supernatant was stored at -20°C for later assay.

[0140] Lysozyme was measured by the decrease in absorbance at 450 nm of a *Micrococcus lysodeikticus* suspension. Briefly, *Micrococcus lysodeikticus* was suspended at 0.1 mg/ml in 65 mM potassium phosphate buffer, pH 6.2 and the absorbance at 450 nm was adjusted to 0.7 units by dilution. The crystal (or zymosan) and cell supernatant

(100 µl) was added to 2.5 ml of the *Micrococcus* suspension and the decrease in absorbance was monitored. Lysozyme standards (chicken egg white) in the 0 to 2000 units/ml range were prepared and a calibration graph of lyzozyme concentration against the rate of decrease in the absorbance at 450 nm was obtained.

[0141] Myeloperoxidase (MPO) activity was measured by the increase in absorbance at 450 nm that accompanies the oxidation of dianisidine. 7.8 mg of dianisidine was dissolved in 100 ml of 0.1 M citrate buffer, pH 5.5 at 3.2 mM by sonication. To a 1 ml cuvette, 0.89 mL of the dianisidine solution was added, followed by 50 µl of 1% Triton x 100, 10 µl of a 0.05% hydrogen peroxide in water solution and 50 µl of crystal-cell supernatant. MPO activity was determined from the change in absorbance (450 nm) per minute, Delta Å 450, using the following equation:

$$\text{Dianisidine oxidation (nmol/min)} = 50 \times \text{Delta Å } 450$$

8. NEUTROPHIL VIABILITY

[0142] To determine the effect of the anti-microtubule agents on neutrophil viability the release of the cytoplasmic marker enzyme, lactate dehydrogenase (LDH) was measured. Control tubes containing cells with drug (crystals absent) from degranulation experiments were also assayed for LDH.

B. Results

[0143] In all experiments statistical significance was determined using Students' t-test and significance was claimed at $p<0.05$. Where error bars are shown they describe one standard deviation about the mean value for the n number given.

1. NEUTROPHIL VIABILITY

(a) Paclitaxel

[0144] Neutrophils treated with paclitaxel at 46 µM for one hour at 37°C did not show any increased level of LDH release (always less than 5% of total) above controls indicating that paclitaxel did not cause cell death.

(b) Aluminum Fluoride

[0145] Neutrophils treated with aluminum fluoride at a 5 to 100 mM concentration range for 1 hour at 37°C did not show any increased level of LDH release above controls indicating that aluminum fluoride did not cause cell death.

(c) Glycine Ethyl Ester

[0146] Neutrophils treated with glycine ethyl ester at a 0.5 to 20 mM concentration range for 1 hour at 37°C did not show any increased level of LDH release above controls indicating that glycine ethyl ester did not cause cell death.

2. CHEMILUMINESCENCE

(a) Paclitaxel

[0147] Paclitaxel at 28 µM produced strong inhibition of both plasma opsonized CPPD and plasma opsonized zymosan-induced neutrophil chemiluminescence as shown in Figures 1A, 1B and 2A respectively. The inhibition of the peak chemiluminescence response was 52% (+/-12%) and 45% (+/-11%) for CPPD and zymosan respectively. The inhibition by paclitaxel at 28 µM of both plasma opsonized CPPD and plasma opsonized zymosan-induced chemiluminescence was significant at all times from 3 to 16 minutes (Figures 1 and 4A). Figures 1A and 1B show the concentration dependence of paclitaxel inhibition of plasma opsonized CPPD-induced neutrophil chemiluminescence. In all experiments control samples never produced chemiluminescence values of greater than 5 mV and the addition of paclitaxel at all concentrations used in this study had no effect on the chemiluminescence values of controls.

(b) Aluminum Fluoride

[0148] Aluminum fluoride at concentrations of 5 to 100 mM produced strong inhibition of plasma opsonized zymosan-induced neutrophil chemiluminescence as shown in Figure 1C. This figure shows the concentration dependence of

AlF_3 inhibition of plasma opsonized zymosan-induced neutrophil chemiluminescence. The addition of AlF_3 at all concentrations used in this study had no effect on the chemiluminescence values of controls.

(c) Glycine Ethyl Ester

[0149] Glycine ethyl ester at concentrations of 0.5 to 20 mM produced strong inhibition of plasma opsonized zymosan-induced neutrophil chemiluminescence as shown in Figure 1D. This figure shows the concentration dependence of glycine ethyl ester inhibition of plasma opsonized zymosan-induced neutrophil chemiluminescence. The addition of glycine ethyl ester at all concentrations used in this study had no effect on the chemiluminescence values of controls.

(d) LY290181

[0150] LY290181 at concentrations of 0.5 to 50 μM produced strong inhibition of plasma opsonized zymosan-induced neutrophil chemiluminescence as shown in Figure 1E. This figure shows the concentration dependence of LY290181 inhibition of plasma opsonized zymosan-induced neutrophil chemiluminescence. The addition of LY290181 at all concentrations used in this study had no effect on the chemiluminescence values of controls.

3. SUPEROXIDE GENERATION

[0151] The time course of plasma opsonized CPPD crystal-induced superoxide anion production, as measured by the superoxide dismutase (SOD) inhibitable reduction of cytochrome C, is shown in Figure 3. Treatment of the cells with paclitaxel at 28 μM produced a decrease in the amount of superoxide generated at all times. This decrease was significant at all times shown in Figure 3A. The concentration dependence of this inhibition is shown in Figure 3B. Stimulation of superoxide anion production by opsonised zymosan (Figure 4B) showed a similar time course to CPPD-induced activation. The inhibition of zymosan-induced superoxide anion production by paclitaxel at 28 μM was less dramatic than the inhibition of CPPD activation but was significant at all times shown in Figure 4B.

[0152] Treatment of CPPD crystal-induced neutrophils with LY290181 at 17 μ M also produced a decrease in the amount of superoxide generated (Figure 3C).

4. NEUTROPHIL DEGRANULATION

[0153] Neutrophil degranulation was monitored by the plasma opsonized CPPD crystal-induced release of myeloperoxidase and lysozyme or the plasma opsonized zymosan-induced release of myeloperoxidase. It has been shown that sufficient amounts of these two enzymes are released into the extracellular media when plasma coated CPPD crystals are used to stimulate neutrophils without the need for the addition of cytochalasin B to the cells. Figures 5 and 2 show the time course of the release of MPO and lysozyme respectively, from neutrophils stimulated by plasma-coated CPPD. Figure 5A shows that paclitaxel inhibits myeloperoxidase release from plasma opsonized CPPD activated neutrophils in the first 9 minutes of the crystal-cell incubation. Paclitaxel significantly inhibited CPPD-induced myeloperoxidase release at all times as shown in Figure 5A. Figure 5B shows the concentration dependence of paclitaxel inhibition of CPPD-induced myeloperoxidase release.

[0154] Paclitaxel at 28 μM reduced lysozyme release and this inhibition of degranulation was significant at all times as shown in Figure 2.

[0155] Only minor amounts of MPO and lysozyme were released when neutrophils were stimulated with opsonized zymosan. Despite these low levels it was possible to monitor 50% inhibition of MPO release after 9 minutes incubation in the presence of paclitaxel at 28 μM that was statistically significant ($p<0.05$) (data not shown).Treatment of CPPD crystal-induced neutrophils with LY290181 at 17 μM decreased both lysozyme and myeloperoxidase release from the cells (Figures SC and SD).

C. Discussion

[0156] These experiments demonstrate that paclitaxel and other anti-microtubule agents are strong inhibitors of crystal-induced neutrophil activation. In addition, by showing similar levels of inhibition in neutrophil responses to another form of particulate activator, opsonized zymosan, it is evident that the inhibitory activity of paclitaxel and other anti-microtubule agents are not limited to neutrophil responses to crystals. Paclitaxel, aluminum fluoride, glycine ethyl ester and LY290181 were also shown to be strong inhibitors of zymosan-induced neutrophil activation without causing cell death. LY290181 was shown to decrease superoxide anion production and degranulation of CPDD crystal-induced neutrophils.

EXAMPLE 2

T CELL RESPONSE TO ANTIGENIC STIMULUS

[0157] In order to determine whether paclitaxel affects T-cell activation in response to stimulagens, TR1 T-cell clones were stimulated with either the myelin basic protein peptide, GP68-88, or the lectin, conA, for 48 hours in the absence or presence of increasing concentrations of paclitaxel in a micellar formulation. Paclitaxel was added at the beginning of the experiment or 24 hours following the stimulation of cells with peptide or conA. Tritiated thymidine incorporation was determined as a measure of T-cell proliferation in response to peptide or conA stimulation.

[0158] The results demonstrated that T-cell stimulation increased in response to the peptide GP68-88 and conA. In the presence of control polymeric micelles, T-cell stimulation in response to both agonists was not altered. However, treatment with paclitaxel micelles, either at the beginning of the experiment or 24 hours following the stimulation, decreased T-cell response in a concentration dependent manner. Under both conditions, T-cell proliferation was completely inhibited by 0.02 μM paclitaxel (Figure 79).

[0159] These data indicate that paclitaxel is a potent inhibitor of T-cell proliferation in response to antigen-induced stimulation.

EXAMPLE 3

EFFECT OF PACLITAXEL ON SYNOVIOCYTE CELL PROLIFERATION *IN VITRO*

[0160] Two experiments were conducted in order to assess the effect of differing concentrations of paclitaxel on tritiated thymidine incorporation (a measurement of synoviocyte DNA synthesis) and cell proliferation *in vitro.*

A. Materials and Methods

1. ^{3}H-THYMIDINE INCORPORATION INTO SYNOVIOCYTES

[0161] Synoviocytes were incubated with different concentrations of paclitaxel (10^{-5} M, 10^{-6} M, 10^{-7} M, and 10^{-8} M) continuously for 6 or 24 hours *in vitro.* At these times, 1 x 10^{-6} cpm of ^{3}H-thymidine was added to the cell culture and incubated for 2 hours at 37°C. The cells were placed through a cell harvester, washed through a filter, the filters were cut, and the amount of radiation contained in the filter sections determined. Once the amount of thymidine incorporated into the cells was ascertained, it was used to determine the rate of cell proliferation. This experiment was repeated three times and the data collated.

2. SYNOVIOCYTE PROLIFERATION

[0162] Bovine synovial fibroblasts were grown in the presence and absence of differing concentrations (10^{-5} M, 10^{-6} M, 10^{-7} M, and 10^{-8} M) of paclitaxel for 24 hours. At the end of this time period the total number of viable synoviocyte cells was determined visually by dye exclusion counting using trypan blue staining. This experiment was conducted 4 times and the data collated.

B. Results

1. ^{3}H-THYMIDINE INCORPORATION INTO SYNOVIOCYTES

[0163] This study demonstrated that paclitaxel at low concentrations inhibits the incorporation of ^{3}H-thymidine (and by extension DNA synthesis) in synoviocytes at concentrations as low as 10^{-8} M. At six hours there was no significant difference between the degree of inhibition produced by the higher versus the lower concentrations of paclitaxel (Figure 8). However, by 24 hours some of the effect was lost at lower concentrations of the drug (10^{-8} M), but was still substantially lower than that seen in control animals.

2. SYNOVIOCYTE PROLIFERATION

[0164] This study demonstrated that paclitaxel was cytotoxic to proliferating synovial fibroblasts in a concentration dependent manner. Paclitaxel at concentrations as low as 10^{-7} M is capable of inhibiting proliferation of the synoviocytes (Figure 9). At higher concentrations of paclitaxel (10^{-6} M and 10^{-5} M) the drug was toxic to the synovial fibroblasts *in vitro.*

C. Discussion

[0165] The above study demonstrates that paclitaxel is capable of inhibiting the proliferation of fibroblasts derived from synovium at relatively low concentrations *in vitro*. Therefore, given the role of connective tissue in the development of chronic inflammation and their behavior during the pathogenesis of inflammatory disease, blocking cell proliferation will favorably affect the outcome of the disease *in vivo*.

EXAMPLE 4 (Reference example)

CHARACTERIZATION OF PACLITAXEL'S ACTIVITY ON HUMAN EPIDERMAL KERATINOCYTES *IN VITRO*

[0166] The time and dose-dependent effects of paclitaxel on actively proliferating normal human keratinocytes and HaCAT keratinocytes (spontaneously immortalized human epidermal keratinocytes) was investigated.

A. Materials and Methods

[0167] The effect of paclitaxel on keratinocytes was assessed by determining the cell number and ^{3}H-thymidine incorporation by the cells. For thymidine incorporation, keratinocytes plated at low density (in DMEM, supplemented with 10% FCS, glutamine, antibiotics) were treated with paclitaxel concentrations of 0 to 10^{-4} M for 6 hours during logarithmic growth. ^{3}H-thymidine was added to the cells and incubated for a further 6 hours. The cells were harvested and radioactivity determined. To determine the total cell numbers, keratinocytes were plated as described and incubated in the presence and absence of paclitaxel for 4 days. Following incubation, cells were collected and counted by the trypan blue exclusion assay.

B. Results

[0168] The number of viable cells as a percentage of untreated controls was determined. At a paclitaxel concentration of 10^{-9} M, cell viability was greater than 100% of untreated controls, while at 10^{-8} M viability was slightly less at 87% (Figure 7). There was a significant drop in cell viability at a paclitaxel concentration of 10^{-7} M or higher.

C. Discussion

[0169] Paclitaxel was extremely cytotoxic to human keratinocytes at concentrations as low as 10^{-7} M. In psoriasis, keratinocytes are abnormally proliferating cells and since paclitaxel stabilizes microtubules, its effect in this mitotically active system is expected. In other studies, paclitaxel was found to be cytotoxic to proliferating synoviocytes, but to have no effect on non-proliferating chondrocytes. Thus, paclitaxel may act on the hyperproliferating cells in psoriatic lesions, while being non-toxic to normal epidermal cells.

EXAMPLE 5

EFFECT OF PACLITAXEL ON ASTROCYTE PROLIFERATION

[0170] It is well established that there is an increase in the numbers of fibrous astrocytes in MS lesions, which are thought to be involved in the destruction of myelin through the production of cytokines and matrix metalloproteinases (Mastronardi et al., *J. Neurosci. Res. 36*:315-324, 1993; Chandler et al., *J. Neuroimmunol. 72*:155-161, 1997). Fibrous astrocytes have high levels of glial fibrillary acidic protein (GFAP) which serves as a biochemical marker for fibrous astrocyte proliferation. The ability of paclitaxel micelles to inhibit astrocyte proliferation was assessed in a transgenic mouse model of demyelinating disease (Mastronardi et al., *J. Neurosci. Res.* 36:315-324, 1993).

A. Materials and Methods

[0171] Subcutaneous administration of continuous paclitaxel therapy (2 mg/kg; 3x per week, total of 10 injections) was initiated at clinical onset of disease (approximately 4 months of age). Five animals received micellar paclitaxel, two mice were used as controls; one mouse was an untreated normal and one was an untreated transgenic littermate. Only one transgenic mouse was used as a control because the course of the disease has been well established in the laboratory. Four month old animals were injected with micellar paclitaxel, after the initial signs of neurological pathology of MS were evident.

[0172] Three days following the tenth injection, the experimental study was terminated and the brain tissues proc-

essed for histological analysis. For light microscopy, tissues were fixed in formalin and embedded in paraffin. Sections were stained with anti-GFAP antibody (DACO), washed and then reacted with secondary antibody conjugated with HPP. The sections were stained for HPP and counter-stained with haematoxylin. For electron microscopy, tissues were fixed in 2.5% glutaraldehyde and phosphate buffered saline (pH 7.2), and post-fixed with 1% osmium tetroxide. Sections were prepared and viewed with a JEOL 1200 EX II transmission EM.

B. Results

[0173] As the neurological pathology progresses, levels of GFAP are elevated in the transgenic mouse brains; this is thought to reflect an increase in the number of fibrous astrocytes present. In contrast, transgenic mice treated with paclitaxel have near normal levels of GFAP (Table 1). These data suggest that paclitaxel may inhibit astrocyte proliferation *in vivo* which may contribute to the prevention of demyelination in MS.

TABLE 1

Quantification of GFAP in Brain Homogenate		
Group	GFAP (ng)	GFAP (ng/µg homogenate protein)
Normal Mice	0.64 ± 0.02	12.8
Transgenic Mice	1.80 +/-0.10	36.0
Transgenic Mice Treated with Paclitaxel	0.69 +/-0.05	13.8

Further analysis of GFAP in brain tissue was assessed histologically. Figure 78 illustrates brain sections from normal mice, control transgenic mice not treated with paclitaxel and transgenic mice treated with paclitaxel.

[0174] Although control transgenic mice have higher numbers of fibrous astrocytes, the morphology of the astrocytes is similar to that seen in normal animals (thick stellate processes spreading from the cell body). However, in transgenic mice treated with paclitaxel the number of fibrous astrocytes decreased significantly. Further, two morphological changes are observed: the cell body of the fibrous astrocytes appears to round up (which has been shown to lead to apoptosis in culture) and the cellular processes become very thin around the cell body.

[0175] Further ultrastructural analysis using electron microscopy has shown that astrocytes of transgenic mice were characterized by densely stained astrocytic processes originating from the cell body. These broad processes contain a well-organized array of filaments indicating a viable, activated cell. However, the morphology of the astrocytes in transgenic animals treated with paclitaxel was characterized by cell rounding, thin filamentous processes and intracellular depletion and disorganization of filamentous proteins (Figure 80).

C. Conclusions

[0176] These data demonstrate that paclitaxel causes changes to fibrous astrocytes *in vivo,* the most proliferative cell type in MS lesions. It is likely that paclitaxel is also inhibiting the function of astrocytic processes and, thus, may alter cellular events involved in myelin destruction.

EXAMPLE 6

EFFECT OF PACLITAXEL ON ENDOTHELIAL CELL PROLIFERATION

[0177] In order to determine whether paclitaxel inhibits endothelial cell proliferation, EOMA cells (an endothelial cell line) were plated at low density and incubated in the absence and presence of increasing concentrations of paclitaxel for 48 hours. Following the incubation, the number of viable cells were determined using the trypan blue exclusion assay. The results (provided in Figure 9) show that paclitaxel at concentrations of 10^{-8}M inhibited endothelial cell proliferation by over 50% and concentrations of 10^{-7}M or greater completely inhibited cell proliferation. These data demonstrate that paclitaxel is a potent inhibitor of endothelial cell proliferation. All cell toxicity assays were performed three times, and each individual measurement was made in triplicate.

[0178] In order to determine the effect of paclitaxel on endothelial cell cycling and apoptosis, EOMA cells were incubated in the absence and presence of increasing concentrations of paclitaxel for 24 hours. The cells were fixed with 3.7% formaldehyde in phosphate buffered saline for 20 minutes, stained with DAPI (4'-6-diaminido-2-phenylindole), 1 ug/ml, and examined with a 40x objective under epifluorescent optics. Apoptotic cells were evaluated by scoring cells

for fragmented nuclei and condensed chromatin. The data show that concentrations of paclitaxel greater than 10^{-8}M induced endothelial cell apoptosis (Figure 10).

EXAMPLE 7

PROLIFERATION ASSAY PROTOCOL (MTT)

[0179] On day one, 5-10 x 10^4 synoviocytes were plated per well (96-well plate). Column # 1 was kept free of cells (blank). On day 2, the plate was flicked to discard the medium and 200 µl of medium containing various concentrations of drug was added. The cells were exposed for 6 hours, 24 hours or 4 days. There was no drug added to columns # 1 and # 2 (blank and untreated control, respectively). The medium containing the drug was discarded and 200 µl of fresh complete medium was added. The cells were then left to grow for an additional 3 to 4 days. On day five, 20 µl of dimethylthiazol diphenyltetrazoiium bromide salt (MTT) (5 mg/ml PBS) was added and allowed to incubate for 4 hours at 37°C. The medium was decanted and 200 µl of DMSO was added. The plate was agitated for 30 minutes and the absorbance read at 562 nm.

Results

[0180] The data were expressed as the % of survival which was obtained by dividing the number of cells remaining after treatment by the number of cells in the untreated control column #2 (the number of cells was obtained from a standard done prior to the assay). The IC_{50}, the concentration of drug that kills 50% of the population, can be interpolated from Figures 11A-E. For a 24-hour exposure, the LY290181 compound was found to be the most potent anti-microtubule agents to reduce and inhibit cell proliferation with an IC_{50} of less than 5 nM (Figure C). Paclitaxel, epothilone B and tubercidin were slightly less potent with IC_{50}s around 30 nM (Figure A), 45 nM (Figure F) and 45 nM (Figure B), respectively. Finally, the IC_{50}s for aluminum fluoride (AlF_3) and hexylene glycol were significantly higher with values around 32 µM (Figure E) and 64 mM (Figure D), respectively.

EXAMPLE 8

EFFECT OF PACLITAXEL AND OTHER ANTI-MICROTUBULE AGENTS ON MATRIX METALLOPROTEINASE PRODUCTION

A. Materials and Methods

1. IL-1 STIMULATED AP-1 TRANSCRIPTIONAL ACTIVITY IS INHIBITED BY PACLITAXEL

[0181] Chondrocytes were transfected with constructs containing an AP-1 driven CAT reporter gene, and stimulated with IL-1, IL-1 (50 ng/ml) was added and incubated for 24 hours in the absence and presence of paclitaxel at various concentrations. Paclitaxel treatment decreased CAT activity in a concentration dependent manner (mean ± SD). The data noted with an asterisk (*) have significance compared with IL-1-induced CAT activity according to a t-test, $P<0.05$. The results shown are representative of three independent experiments.

2. EFFECT OF PACLITAXEL ON IL-1 INDUCED AP-1 DNA BINDING ACTIVITY, AP-1 DNA

[0182] Binding activity was assayed with a radiolabeled human AP-1 sequence probe and gel mobility shift assay. Extracts from chondrocytes untreated or treated with various amounts of paclitaxel (10^{-7} to 10^{-5} M) followed by IL-1β (20 ng/ml) were incubated with excess probe on ice for 30 minutes, followed by non-denaturing gel electrophoresis. The "com" lane contains excess unlabeled AP-1 oligonucleotide. The results shown are representative of three independent experiments.

3. EFFECT OF PACLITAXEL ON IL-1 INDUCED MMP-1 AND MMP-3 MRNA EXPRESSION

[0183] Cells were treated with paclitaxel at various concentrations (10^{-7} to 10^{-5} M) for 24 hours. Then, treated with IL-1β (20 ng/ml) for additional 18 hours in the presence of paclitaxel. Total RNA was isolated, and the MMP-1 mRNA levels were determined by Northern blot analysis. The blots were subsequently stripped and reprobed with ^{32}P-radiolabeled rat GAPDH cDNA, which was used as a housekeeping gene. The results shown are representative of four independent experiments. Quantitation of collagenase-1 and stromelysin-expression mRNA levels. The MMP-1 and MMP-3 expression levels were normalized with GAPDH.

4. EFFECT OF OTHER ANTI-MICROTUBULES ON COLLAGENASE EXPRESSION

[0184] Primary chondrocyte cultures were freshly isolated from calf cartilage. The cells were plated at 2.5 x 10^6 per ml in 100 x 20 mm culture dishes and incubated in Ham's F12 medium containing 5% FBS overnight at 37°C. The cells were starved in serum-free medium overnight and then treated with anti-microtubule agents at various concentrations for 6 hours. IL-1 (20 ng/ml) was then added to each plate and the plates incubated for an additional 18 hours. Total RNA was isolated by the acidified guanidine isothiocyanate method and subjected to electrophoresis on a denatured gel. Denatured RNA samples (15 µg) were analyzed by gel electrophoresis in a 1% denatured gel, transferred to a nylon membrane and hydridized with the ^{32}P-labelled collagenase cDNA probe. ^{32}P-labelled glyceraldehyde phosphate dehydrase (GAPDH) cDNA as an internal standard to ensure roughly equal loading. The exposed films were scanned and quantitatively analyzed with ImageQuant.

B. Results

1. PROMOTERS ON THE FAMILY OF MATRIX METALLOPROTEINASES

[0185] Figure 19A shows that all matrix metalloproteinases contained the transcriptional elements AP-1 and PEA-3 with the exception of Gelatinase B. It has been well established that expression of matrix metalloproteinases such as collagenases and stromelysins are dependent on the activation of the transcription factors AP-1. Thus inhibitors of AP-1 would inhibit the expression of matrix metalloproteinases.

2. EFFECT OF PACLITAXEL ON AP- 1 TRANSCRIPTIONAL ACTIVITY

[0186] As demonstrated in Figure 19B, IL-1 stimulated AP-1 transcriptional activity 5-fold. Pretreatment of transiently transfected chondrocytes with paclitaxel reduced IL-1 induced AP-1 reporter gene CAT activity. Thus, IL-1 induced AP-1 activity was reduced in chondrocytes by paclitaxel in a concentration dependent manner (10^{-7} to 10^{-5} M). These data demonstrated that paclitaxel was a potent inhibitor of AP-1 activity in chondrocytes.

3. EFFECT OF PACLITAXEL ON AP-1 DNA BINDING ACTIVITY

[0187] To confirm that paclitaxel inhibition of AP-1 activity was not due to nonspecific effects, the effect of paclitaxel on IL-1 induced AP-1 binding to oligonucleotides using chondrocyte nuclear lysates was examined. As shown in Figure 19C, IL-1 induced binding activity decreased in lysates from chondrocyte which have been pretreated with paclitaxel at concentration 10^{-7} to 10^{-5} M for 24 hours. Paclitaxel inhibition of AP-1 transcriptional activity closely correlated with the decrease in AP-1 binding to DNA.

4. EFFECT OF PACLITAXEL ON COLLAGENASE AND STROMELYSIN EXPRESSION

[0188] Since paclitaxel was a potent inhibitor of AP-1 activity, the effect of paclitaxel or IL-1 induced collagenase and stromelysin expression, two important matrix metalloproteinases involved in inflammatory diseases was examined. Briefly, as shown in Figure 20, IL-1 induction increases collagenase and stromelysin mRNA levels in chondrocytes. Pretreatment of chondrocytes with paclitaxel for 24 hours significantly reduced the levels of collagenase and stromelysin mRNA. At 10^{-5} M paclitaxel, there was complete inhibition. The results show that paclitaxel completely inhibited the expression of two matrix metalloproteinases at concentrations similar to which it inhibits AP-1 activity.

5. EFFECT OF OTHER ANTI-MICROTUBULES ON COLLAGENASE EXPRESSION

[0189] Figures 12A-H demonstrate that anti-microtubule agents inhibited collagenase expression. Expression of collagenase was stimulated by the addition of IL-1 which is a proinflammatory cytokine. Pre-incubation of chondrocytes with various anti-microtubule agents, specifically LY290181, hexylene glycol, deuterium oxide, glycine ethyl ester, AlF_3, tubercidin epothilone, and ethylene glycol bis-(succinimidylsuccinate), all prevented IL-1-induced collagenase expression at concentrations as low as 1 x 10^{-7} M.

C. Discussion

[0190] Paclitaxel was capable of inhibiting collagenase and stromelysin expression *in vitro* at concentrations of 10^{-6} M. Since this inhibition can be explained by the inhibition of AP-1 activity, a required step in the induction of all matrix metalloproteinases with the exception of gelatinase B, it is expected that paclitaxel would inhibit other matrix metallo-

proteinases which are AP-1 dependent. The levels of these matrix metalloproteinases are elevated in all inflammatory diseases and play a principle role in matrix degradation, cellular migration and proliferation, and angiogenesis. Thus, paclitaxel inhibition of expression of matrix metalloproteinases such as collagenase and stromelysin will have a beneficial effect in inflammatory diseases.

EXAMPLE 9

EFFECT OF ANTI-MICROTUBULE AGENTS ON THE EXPRESSION OF PROTEOGLYCANS

[0191] Primary chondrocyte cultures were freshly isolated from calf cartilage. The cells were plated at 2.5 x 10^6 per ml in 100 x 20 mm culture dishes and incubated in Ham's F12 medium containing 5% FBS overnight at 37°C. The cells were starved in serum-free medium overnight and then treated with anti-microtubule agents at various concentrations (10^{-7} M, 10^{-6} M, 10^{-5} M and 10^{-4} M) for 6 hours. IL-1 (20 ng/ml) was then added to each plate and the plates incubated for an additional 18 hours. Total RNA was isolated by the acidified guanidine isothiocyanate method and subjected to electrophoresis on a denatured gel. Denatured RNA samples (15 µg) were analyzed by gel electrophoresis in a 1% denatured gel, transferred to a nylon membrane and hydridized with the ^{32}P-labelled proteoglycan (aggrecan) cDNA probe. ^{32}P-labelled glyceraldehyde phosphate dehydrase (GAPDH) cDNA as an internal standard to ensure roughly equal loading. The exposed films were scanned and quantitatively analyzed with ImageQuant.

Results

[0192] Figures 13A-H show that the anti-microtubule agents which had an inhibitory effect on collagenase expression (Example 8), specifically LY290181, hexylene glycol, deuterium oxide, glycine ethyl ester, AlF_3, tubercidin epothilone and ethylene glycol bis-(succinimidylsuccinate), did not affect the expression of aggrecan, a major component of cartilage matrix, at all concentrations evaluated.

EXAMPLE 10

NF-KB ACTIVITY (CELL-BASED) ASSAY

[0193] IL-1 and TNF were both identified as being proinflammatory cytokines that activate the transcription of genes driven by a transcription factor named NF-KB also involved in inflammatory processes. The inflammatory effect of IL-1 and TNF can therefore be indirectly assessed by means of a reporter gene assay (NF-κB) responding to IL-1 and TNF stimulation.

[0194] On day one, 5 x 10^4 NIH-3T3 (murine fibroblast), stably transfected with a NF-κB reporter construct (Luciferase, Promega Corp.), were plated per well (24-well plate). Once confluent (on day 3-4), cells were starved by replacing the complete medium with 1 ml of serum-free medium. Following a 24-hour starvation, cells were treated with various concentrations of anti-microtubule agents 6 hours prior to the addition of IL-1 (20 ng/ml) and TNF (20 ng/ml). Cells were exposed to IL-1 and TNF for 1 hour and 16 hours and NF-κB activity measured 24 hours later. On day five, the medium was discarded and the cells were rinsed once with PBS. Cells were then extracted for 15 minutes with 250 µl of lysis buffer (Promega Corp., Wisconsin). NF-KB transcriptional activity was assessed by adding 25 µl of luciferase substrate to a tube containing 2.5 µl of cell extract. The tube was immediately inserted in a luminometer (Turner Designs) and light emission measured for 10 seconds. The luciferase data were then normalized for protein concentration.

Results

[0195] The data were expressed by showing the interference that the anti-microtubule agents exhibited on NF-KB induction (fold induction). As shown in Figure 80A, 80B, 80C and 80D, tubercidin and paclitaxel inhibited both IL-1- and TNF-induced NF-κB activity. The inhibitory effect of tubercidin and paclitaxel for the 6-hour and 24-hour treatments were around 10 µM and 2 µM, respectively.

***

EXAMPLE 11 (Reference example)

INHIBITION OF TUMOR ANGIOGENESIS BY PACLITAXEL

[0196] Fertilized domestic chick embryos are incubated for 4 days prior to having their shells removed. The egg

contents are emptied by removing the shell located around the airspace, severing the interior shell membrane, perforating the opposite end of the shell and allowing the egg contents to gently slide out from the blunted end. The contents are emptied into round-bottom sterilized glass bowls, covered with petri dish covers and incubated at 90% relative humidity and 3% carbon dioxide.

[0197] MDAY-D2 cells (a murine lymphoid tumor) are injected into mice and allowed to grow into tumors weighing 0.5-1.0 g. The mice are sacrificed, the tumor sites wiped with alcohol, excised, placed in sterile tissue culture media, and diced into 1 mm pieces under a laminar flow hood. Prior to placing the dissected tumors onto the 9-day old chick embryos, CAM surfaces are gently scraped with a 30 gauge needle to ensure tumor implantation. The tumors are then placed on the CAMs after 8 days of incubation (4 days after deshelling), and allowed to grow on the CAM for four days to establish a vascular supply. Four embryos are prepared utilizing this method, each embryo receiving 3 tumors. On day 12, each of the 3 tumors on the embyros received either 20% paclitaxel-loaded thermopaste, unloaded thermopaste, or no treatment. The treatments were continued for two days before the results were recorded.

[0198] The explanted MDAY-D2 tumors secrete angiogenic factors which induce the ingrowth of capillaries (derived from the CAM) into the tumor mass and allow it to continue to grow in size. Since all the vessels of the tumor are derived from the CAM, while all the tumor cells are derived from the explant, it is possible to assess the effect of therapeutic interventions on these two processes independently. This assay has been used to determine the effectiveness of paclitaxel-loaded thermopaste on: (a) inhibiting the vascularization of the tumor and (b) inhibiting the growth of the tumor cells themselves.

[0199] Direct *in vivo* stereomicroscopic evaluation and histological examination of fixed tissues from this study demonstrated the following. In the tumors treated with 20% paclitaxel-loaded thermopaste, there was a reduction in the number of the blood vessels which supplied the tumor (Figures 14C and 14D), a reduction in the number of blood vessels within the tumor, and a reduction in the number of blood vessels in the periphery of the tumor (the area which is typically the most highly vascularized in a solid tumor) when compared to control tumors (Figures 14A and 14B). The tumors began to decrease in size and mass during the two days the study was conducted. Additionally, numerous endothelial cells were seen to be arrested in cell division indicating that endothelial cell proliferation had been affected. Tumor cells were also frequently seen arrested in mitosis. All 4 embryos showed a consistent pattern with the 20% paclitaxel-loaded thermopaste suppressing tumor vascularity while the unloaded thermopaste had no effect.

[0200] By comparison, in CAMs treated with unloaded thermopaste, the tumors were well vascularized with an increase in the number and density of vessels when compared to that of the normal surrounding tissue, and dramatically more vessels than were observed in the tumors treated with paclitaxel-loaded paste. The newly formed vessels entered the tumor from all angles appearing like spokes attached to the center of a wheel (Figures 14A and 14B). The control tumors continued to increase in size and mass during the course of the study. Histologically, numerous dilated thin-walled capillaries were seen in the periphery of the tumor and few endothelial cells were seen to be in cell division. The tumor tissue was well vascularized and viable throughout.

[0201] As an example, in two similarly-sized (initially, at the time of explantation) tumors placed on the same CAM the following data was obtained. For the tumor treated with 20% paclitaxel-loaded thermopaste the tumor measured 330 mm x 597 mm; the immediate periphery of the tumor has 14 blood vessels, while the tumor mass has only 3-4 small capillaries. For the tumor treated with unloaded thermopaste the tumor size was 623 mm x 678 mm; the immediate periphery of the tumor has 54 blood vessels, while the tumor mass has 12-14 small blood vessels. In addition, the surrounding CAM itself contained many more blood vessels as compared to the area surrounding the paclitaxel-treated tumor.

[0202] This study demonstrates that thermopaste releases sufficient quantities of paclitaxel to inhibit the pathological angiogenesis which accompanies tumor growth and development. Under these conditions angiogenesis is maximally stimulated by the tumor cells which produce angiogenic factors capable of inducing the ingrowth of capillaries from the surrounding tissue into the tumor mass. The 20% paclitaxel-loaded thermopaste is capable of blocking this process and limiting the ability of the tumor tissue to maintain an adequate blood supply. This results in a decrease in the tumor mass both through a cytotoxic effect of the drug on the tumor cells themselves and by depriving the tissue of the nutrients required for growth and expansion.

EXAMPLE 12

INHIBITION OF ANGIOGENESIS BY PACLITAXEL

A. Chick Chorioallantoic Membrane ("CAM") Assays

[0203] Fertilized, domestic chick embryos were incubated for 3 days prior to shell-less culturing. In this procedure, the egg contents were emptied by removing the shell located around the air space. The interior shell membrane was then severed and the opposite end of the shell was perforated to allow the contents of the egg to gently slide out from

the blunted end. The egg contents were emptied into round-bottom sterilized glass bowls and covered with petri dish covers. These were then placed into an incubator at 90% relative humidity and 3% CO_2 and incubated for 3 days.

[0204] Paclitaxel (Sigma, St. Louis, MI) was mixed at concentrations of 0.25, 0.5, 1, 5, 10, 30 µg per 10 ul aliquot of 0.5% aqueous methylcellulose. Since paclitaxel is insoluble in water, glass beads were used to produce fine particles. Ten microliter aliquots of this solution were dried on parafilm for 1 hour forming disks 2 mm in diameter. The dried disks containing paclitaxel were then carefully placed at the growing edge of each CAM at day 6 of incubation. Controls were obtained by placing paclitaxel-free methylcellulose disks on the CAMs over the same time course. After a 2 day exposure (day 8 of incubation) the vasculature was examined with the aid of a stereomicroscope. Liposyn II, a white opaque solution, was injected into the CAM to increase the visibility of the vascular details. The vasculature of unstained, living embryos were imaged using a Zeiss stereomicroscope which was interfaced with a video camera (Dage-MTI Inc., Michigan City, IN). These video signals were then displayed at 160x magnification and captured using an image analysis system (Vidas, Kontron; Etching, Germany). Image negatives were then made on a graphics recorder (Model 3000; Matrix Instruments, Orangeburg, NY).

[0205] The membranes of the 8 day-old shell-less embryo were flooded with 2% glutaraldehyde in 0.1M sodium cacodylate buffer; additional fixative was injected under the CAM. After 10 minutes *in situ*, the CAM was removed and placed into fresh fixative for 2 hours at room temperature. The tissue was then washed overnight in cacodylate buffer containing 6% sucrose. The areas of interest were postfixed in 1% osmium tetroxide for 1.5 hours at 4°C. The tissues were then dehydrated in a graded series of ethanols, solvent exchanged with propylene oxide, and embedded in Spurr resin. Thin sections were cut with a diamond knife, placed on copper grids, stained, and examined in a Joel 1200EX electron microscope. Similarly, 0.5 mm sections were cut and stained with toluene blue for light microscopy.

[0206] At day 11 of development, chick embryos were used for the corrosion casting technique. Mercox resin (Ted Pella, Inc., Redding, CA) was injected into the CAM vasculature using a 30-gauge hypodermic needle. The casting material consisted of 2.5 grams of Mercox CL-2B polymer and 0.05 grams of catalyst (55% benzoyl peroxide) having a 5 minute polymerization time. After injection, the plastic was allowed to sit *in situ* for an hour at room temperature and then overnight in an oven at 65°C. The CAM was then placed in 50% aqueous solution of sodium hydroxide to digest all organic components. The plastic casts were washed extensively in distilled water, air-dried, coated with gold/palladium, and viewed with the Philips 501B scanning electron microscope.

[0207] Results of the above experiments are shown in Figures 15-18. Briefly, the general features of the normal chick shell-less egg culture are shown in Figure 15A. At day 6 of incubation, the embryo is centrally positioned to a radially expanding network of blood vessels; the CAM develops adjacent to the embryo. These growing vessels lie close to the surface and are readily visible making this system an idealized model for the study of angiogenesis. Living, unstained capillary networks of the CAM can be imaged noninvasively with a stereomicroscope. Figure 15B illustrates such a vascular area in which the cellular blood elements within capillaries were recorded with the use of a video/computer interface. The 3-dimensional architecture of such CAM capillary networks is shown by the corrosion casting method and viewed in the scanning electron microscope (Figure 15C). These castings revealed underlying vessels which project toward the CAM surface where they form a single layer of anastomotic capillaries.

[0208] Transverse sections through the CAM show an outer ectoderm consisting of a double cell layer, a broader mesodermal layer containing capillaries which lie subjacent to the ectoderm, adventitial cells, and an inner, single endodermal cell layer (Figure 15D). At the electron microscopic level, the typical structural details of the CAM capillaries are demonstrated. Typically, these vessels lie in close association with the inner cell layer of ectoderm (Figure 15E).

[0209] After 48 hours exposure to paclitaxel at concentrations of 0.25, 0.5, 1, 5, 10, or 30 µg, each CAM was examined under living conditions with a stereomicroscope equipped with a video/computer interface in order to evaluate the effects on angiogenesis. This imaging setup was used at a magnification of 160x which permitted the direct visualization of blood cells within the capillaries; thereby blood flow in areas of interest could be easily assessed and recorded. For this study, the inhibition of angiogenesis was defined as an area of the CAM (measuring 2-6 mm in diameter) lacking a capillary network and vascular blood flow. Throughout the experiments, avascular zones were assessed on a 4 point avascular gradient (Table 1). This scale represents the degree of overall inhibition with maximal inhibition represented as a 3 on the avascular gradient scale. Paclitaxel was very consistent and induced a maximal avascular zone (6 mm in diameter or a 3 on the avascular gradient scale) within 48 hours depending on its concentration.

TABLE 1
AVASCULAR GRADIENT

0 -- normal vascularity
1 -- lacking some microvascular movement
2*-- small avascular zone approximately 2 mm in diameter
3*-- avascularity extending beyond the disk (6 mm in diameter)

* - indicates a positive antiangiogenesis response

[0210] The dose-dependent, experimental data of the effects of a various therapeutic agents at different concentrations are shown in Table 2.

TABLE 2

Agent	Delivery Vehicle	Concentration	Inhibition/n
paclitaxel	methylcellulose (10ul)	0.25 ug	2/11
	methylcellulose (10ul)	0.5 ug	6/11
	methylcellulose (10ul)	1 ug	6/15
	methylcellulose (10ul)	5 ug	20/27
	methylcellulose (10ul)	10 ug	16/21
	methylcellulose (10ul)	30 ug	31/31
	PCL paste (3mg)	0.05%	0/9
	PCL paste (3mg)	0.10%	1/8
	PCL paste (3mg)	0.25%	5/7
	PCL paste (3mg)	0.5%	4/4
	PCL paste (3mg)	1%	8/8
	PCL paste (3mg)	2%	10/10
	PCL paste (3mg)	5%	10/10
	PCL paste (3mg)	10%	9/9
	PCL paste (3mg)	20%	6/6
	20%gelatin:60%PCL paste (3mg)	20%	5/6
	gelatin (1mg)	20%	17/17
	opthalmic suspension (2x10ul)	0.3%	1/12
	ophthalmic suspension (2x15ul)	0.3%	3/3
	ophthalmic suspension (1x15ul)	0.3%	15/15
	ophth. microsphere suspension (15ul)	10%	4/4
	stent coating (~1mg)	2.5%	5/5
	stent coating (~1mg)	10%	1/1
	stent coating (~1mg)	33%	3/3
	cyclodextrin solution (10ul)	10%	5/5
	micellar formulation dry (1mg)	10%	too toxic
	micellar solution (10ul)	10%	too toxic
	micellar solution (10ul)	4ug	1/1 - too toxic
	Cremophor Taxol (10ul)	4ug	1/1 - too toxic
	4PCL:1MePEG flakes (1mg)	20%	10/13
	PCL:MePEG paste (3mg)	20%	6/9
	microspheres (mucoadhesive)	20%	7/7
	microspheres (EVA)	0.6%	2/2

TABLE 2 (continued)

Agent	Delivery Vehicle	Concentration	Inhibition/n
	microspheres (30-100um)-slow release	20%	11/11
	microspheres (30-100um)-slow release	10%	1/8
	microspheres (10-30um)-med release	20%	5/6
	microspheres (10-30um)-med release	10%	5/9
	microspheres (1-10um) -fast release	20%	8/11
	microspheres (1-10um) -fast release	10%	9/9
baccatin	paste (2mg)	2ug	2/3
	methylcellulose (5ul)	5ug	4/7
methotrexate	PCL paste (3mg)	1%	0/13
	PCL paste (3mg)	2%	0/3
	PCL paste (3mg)	20%	0/1
	PCL:MePEG paste (3mg)	2%	1/1
	95PCL:5MePEG paste (3mg)	1%	0/6
	95PCL:5MePEG paste (3mg)	10%	0/5
	methylcellulose (10ul)	2ug	0/8
prednisolone acetate	ophthalmic suspension (2x10ul)	1%	3/4
	ophthalmic suspension (2x15ul)	1%	1/1
pycnogenol (proanthocyanidin)	methylcellulose (10ul)	10ug	1/18
	PCL paste (3mg)	15%	1/2
	PCL paste (3mg)	30%	too toxic
verotoxin	methylcellulose (10ul)	long	0/8
	methylcellulose (10ul)	675ng	0/2
heparan sulphate fragment (1)	methylcellulose (10ul)	0.2ug	0/6
heparan sulphate fragment (2)	methylcellulose (10ul)	0.4ug	0/7
vanadate	microspheres (1mg)	5%	0/5
vanadyl sulphate	PCL paste (3mg)	2.5%	0/3
BMOV	PCL paste (3mg)	10%	too toxic
	PCL paste (3mg)	25%	too toxic
	PCL paste (3mg)	35%	too toxic
BEOV	PCL paste (3mg)	10%	too toxic
s-phosphonate	80%PLA:20%MePEG paste (1mg)	20%	too toxic
	PCL paste (1mg)	2%	2/7
	PCL paste (3mg)	1%	0/9
	PCL paste (3mg)	2%	0/6
	PCL paste (3mg)	4%	0/3
	PCL paste (3mg)	8%	1/9
tamoxifen shark cartilage powder	methylcellulose (10ul) N/A	5ug Img	0/2 0/5
estramustine sodium phosphate	PCL paste (3mg)	5%	0/6
	PCL paste (3mg)	10%	0/6
vinblastine	methylcellulose (10ul)	9ug	too toxic
	methylcellulose (10ul)	2ug	too toxic
	PCL paste (3mg)	0.25%	4/6
	PCL paste (3mg)	0.5%	0/4
	PCL paste (3mg)	1%	2/3

TABLE 2 (continued)

Agent	Delivery Vehicle	Concentration	Inhibition/n
	PCL paste (3mg)	2%	too toxic
vincristine	methylcellulose (10ul)	9ug	too toxic
	methylcellulose (10ul)	1ug	too toxic
	PCL paste (3mg)	0.05%	1/1 - too toxic
	PCL paste (3mg)	0.1 %	2/2 - too toxic
	PCL paste (3mg)	0.25%	1/1 - too toxic
	PCL paste (3mg)	0.5%	too toxic
	PCL paste (3mg)	1%	too toxic
	PCL paste (3mg)	2%	too toxic
diterpene -1	methylcellulose (10ul)	3ug	0/5
diterpene - 2	methylcellulose (10ul)	3ug	0/5
lavendustine-c	PCL paste (3mg)	10%	0/14
	PCL paste (3mg)	20%	0/10
MDHC (tyrosine inhibitor)	PCL paste (3mg)	20%	0/8
erbstatin	PCL paste (3mg)	20%	0/5 - too toxic
genistein	PCL paste (3mg)	10%	0/7
	PCL paste (3mg)	20%	0/4
herbimysin	PCL paste (3mg)	2%	3/4
	PCL paste (3mg)	0.5%	1/1
camptothecin	PCL paste (3mg)	0.25%	3/4
	PCL paste (3mg)	1%	2/3
	PCL paste (3mg)	5%	4/5
suramin and cortisone acetate	methylcellulose (10ul)	20ug/70ug	2/4
	methylcellulose (10ul)	50ug/40ug	5/14
	methylcellulose (10ul)	50ug/50ug	3/26
	methylcellulose (10ul)	20ug/50ug	0/24
	methylcellulose (10ul)	70ug/70ug	0/9
suramin and tetrahydo S	methylcellulose (10ul)	50ug/50ug	0/6
protamine sulphate	methylcellulose (10ul)	50ug	0/10
	methylcellulose (10ul)	100ug	1/10
TIMP	methylcellulose (10ul)	15ug	0/5
colchicine	methylcellulose (10ul)	3ug	1/1 - too toxic

[0211] Typical paclitaxel-treated CAMs are also shown with the transparent methylcellulose disk centrally positioned over the avascular zone measuring 6 mm in diameter.' At a slightly higher magnification, the periphery of such avascular zones is clearly evident (Figure 16C); the surrounding functional vessels were often redirected away from the source of paclitaxel (Figures 16C and 16D). Such angular redirecting of blood flow was never observed under normal conditions. Another feature of the effects of paclitaxel was the formation of blood islands within the avascular zone representing the aggregation of blood cells.

[0212] The associated morphological alterations of the paclitaxel-treated CAM are readily apparent at both the light and electron microscopic levels. For the convenience of presentation, three distinct phases of general transition from the normal to the avascular state are shown. Near the periphery of the avascular zone the CAM is hallmarked by an abundance of mitotic cells within all three germ layers (Figures 17A and 18A). This enhanced mitotic division was also a consistent observation for capillary endothelial cells. However, the endothelial cells remained junctionally intact with no extravasation of blood cells. With further degradation, the CAM is characterized by the breakdown and dissolution of capillaries (Figures 17B and 18B). The presumptive endothelial cells, typically arrested in mitosis, still maintain a close spatial relationship with blood cells and lie subjacent to the ectoderm; however, these cells are not junctionally linked. The most central portion of the avascular zone was characterized by a thickened ectodermal and endodermal layer (Figures 17C and 18C). Although these layers were thickened, the cellular junctions remained intact and the layers maintained their structural characteristics. Within the mesoderm, scattered mitotically arrested cells were abundant; these cells did not exhibit the endothelial cell polarization observed in the former phase. Also, throughout this

avascular region, degenerating cells were common as noted by the electron dense vacuoles and cellular debris (Figure 18C).

[0213] In summary, this study demonstrated that 48 hours after paclitaxel application to the CAM, angiogenesis was inhibited. The blood vessel inhibition formed an avascular zone which was represented by three transitional phases of paclitaxel's effect. The central, most affected area of the avascular zone contained disrupted capillaries with extravasated red blood cells; this indicated that intercellular junctions between endothelial cells were absent. The cells of the endoderm and ectoderm maintained their intercellular junctions and therefore these germ layers remained intact; however, they were slightly thickened. As the normal vascular area was approached, the blood vessels retained their junctional complexes and therefore also remained intact. At the periphery of the paclitaxel-treated zone, further blood vessel growth was inhibited which was evident by the typical redirecting or "elbowing" effect of the blood vessels (Figure 16D).

[0214] Paclitaxel-treated avascular zones also revealed an abundance of cells arrested in mitosis in all three germ layers of the CAM; this was unique to paclitaxel since no previous study has illustrated such an event. By being arrested in mitosis, endothelial cells could not undergo their normal metabolic functions involved in angiogenesis. In comparison, the avascular zone formed by suramin and cortisone acetate do not produce mitotically arrested cells in the CAM; they only prevented further blood vessel growth into the treated area. Therefore, even though these agents are anti-angiogenic, there are many points in which the angiogenesis process may be targeted.

[0215] The effects of paclitaxel over the 48 hour duration were also observed. During this period of observation it was noticed that inhibition of angiogenesis occurs as early as 9 hours after application. Histological sections revealed a similar morphology as seen in the first transition phase of the avascular zone at 48 hours illustrated in Figures 17A and 18A. Also, we observed in the revascularization process into the avascular zone previously observed. It has been found that the avascular zone formed by heparin and angiostatic steroids became revascularized 60 hours after application. In one study, paclitaxel-treated avascular zones did not revascularize for at least 7 days after application implying a more potent long-term effect.

EXAMPLE 13

EFFECT OF PACLITAXEL AND CAMPTOTHECIN ON LNCAP CELL PROLIFERATION

Materials and Methods

[0216] LNCaP cells were seeded at concentrations of 2x103 and $1x10^3$ cells/well respectively in 96 well plates. After 48 hours, different concentrations of paclitaxel or camptothecin (25µl) were added in each culture well and the plates were incubated at 37°C for 5 days. After incubation. the cells were fixed with 1% glutaraldehyde solution, and stained for 5 minutes with 0.5% crystal violet. The dye was successively eluted with 100 µl of buffer solution and the absorbance was read on a Titertek Multiskan microplate reader using a wavelength of 492 nm Absorbance. Cell growth was expressed as a percentage relative to control wells in the absence of the compound (set at 100%).

Results

[0217] Paclitaxel inhibited LNCaP cell growth with an EC_{50} of approximately 0.09 nM. Apoptosis experiments were performed on the cells in the wells after paclitaxel treatment using DNA fragmentation assays. Extensive apoptosis of cells was observed indicating that paclitaxel was cytotoxic by an apoptotic mechanism.

[0218] Camptothecin was extremely potent in its cytotoxic action against LNCaP cells. Concentrations as low as 0.001 nM were toxic to over 60% of cells. Therefore, the EC_{50} for this drug against LNCaP cells must lie in the femtomolar concentration range.

Table 1

N	Paclitaxel (nM)	492 nm Absorbance	% Growth
16	0.001	0.049±0.05	100
16	0.01	0.40±0.03	81
8	0.05	0.36+0.02	73
8	0.1	0.20±0.03	40
8	1	0.025±0.01	5
8	10	0.027±0.01	5
8	100	0.033±0.01	6

Table 1 (continued)

N	Paclitaxel (nM)	492 nm Absorbance	% Growth
492nm Absorbance of controls = 0.49±0.06			

Table 2

N	Camptothecin (nM)	492 nm Absorbance	% Growth
16	0.001	0.169±0.05	36
8	0.05	0.14±0.04	29
8	0.1	0.10±0.02	21
8	1	0.10±0.02	21
8	10	0.088±0.02	17
15	100	0.038±0.01	8
492nm Absorbance of controls = 0.47±0.05			

EXAMPLE 14

ANTI-ANGIOGENESIS ACTIVITY OF ADDITIONAL ANTI-MICROTUBULE AGENTS

[0219] In addition to paclitaxel, other anti-microtubule agents can likewise be incorporated within polymeric carriers. Representative examples which are provided below include campothecin and vinca alkaloids such as vinblastine and vincristine, and microtubule stabilizing agents such as tubercidin, aluminum fluoride and LY290181.

A. Incorporation of Agents into PCL

[0220] Agents were ground with a mortar and pestle to reduce the particle size to below 5 microns. This was then mixed as a dry powder with polycaprolactone (molecular wt. 18,000 Birmingham Polymers, AL USA). The mixture was heated to 65°C for 5 minutes and the molten polymer/agent mixture was stirred into a smooth paste for 5 minutes. The molten paste was then taken into a 1 ml syringe and extruded to form 3 mg pellets. These pellets were then placed onto the CAM on day 6 of gestation to assess their anti-angiogenic properties.

B. Effects of Camptothecin-loaded PCL Paste on the CAM

[0221] Camptothecin-loaded thermopaste was effective at inhibiting angiogenesis when compared to control PCL pellets. At 5% drug loading, 4/5 of the CAMs tested showed potent angiogenesis inhibition. In addition, at 1% and 0.25% loading, 2/3 and ¾ of the CAMs showed angiogenesis inhibition respectively. Therefore, it is evident from these results that camptothecin was sufficiently released from the PCL thermopaste and it has therapeutic anti-angiogenic efficacy.

C. Effects of Vinblastine - and Vincristine - loaded PCL Paste on the CAM

[0222] When testing the formulations on the CAM, it was evident that the agents were being released from the PCL pellet in sufficient amounts to induce a biological effect. Both vinblastine and vincristine induced anti-angiogenic effects in the CAM assay when compared to control PCL thermopaste pellets.

[0223] At concentrations of 0.5% and 0.1% drug loading, vincristine induced angiogenesis inhibition in all of the CAMs tested. When concentrations exceeding 2% were tested, toxic drug levels were achieved and unexpected embryonic death occurred.

[0224] Vinblastine was also effective in inhibiting angiogenesis on the CAM at concentrations of 0.25%, 0.5% and 1%. However, at concentrations exceeding 2%, vinblastine was toxic to the embryo.

D. Effects of Tubercidin-loaded PCL Paste on the CAM

[0225] Tubercidin-loaded paste was effective at inhibiting angiogenesis when compared to control pellets. At 1% drug loading, tubercidin induced angiogenesis inhibition in 1/3 CAMs tested. However, at greater drug concentrations of 5% drug loading, tubercidin potently inhibited angiogenesis in 2/3 CAMs. Therefore, it was evident frtom these results

that tubercidin was sufficiently released from the PCL paste and it has potent anti-angiogenic activity.

E. Effects of Aluminum Fluoride-loaded PCT Paste on the CAM

[0226] PCL pastes loaded with aluminum fluoride (AlF_3) were effective at inhibiting angiogenesis at a 20% drug loading when compared to control pellets. At 20% drug loading, 2/4 CAMs showed angiogenesis inhibition as evident by an avascular zone measuring between 2 to 6 mm in diameter. However, at lower drug loading, 1% and 5%, angiogenesis inhibition was not evident (0/6 and 0/5 CAMs, respectively). Therefore, aluminum fluoride was effective at inducing angiogenesis inhibition only at higher drug concentrations.

F. Effect of LY290181-loaded PCL Paste on the CAM

[0227] Assessment of PCL paste loaded with 5% LY290181 on the CAM, revealed that LY290181 induced angiogenesis inhibition in 1/3 CAMs tested. However, at 1% drug loading, LY290181 did not induce an anti-angiogenesis response (n=2).

EXAMPLE 15

EFFECT OF PACLITAXEL ON VIABILITY OF NON-PROLIFERATING CELLS

[0228] While it is important that a disease-modifying agent be capable of strongly inhibiting a variety of inappropriate cellular activities (proliferation, inflammation, proteolytic enzyme production) which occur in excess during the development of chronic inflammation, it must not be toxic to the normal tissues. It is particularly critical that normal cells not be damaged, as this would lead to progression of the disease. In this example, the effect of paclitaxel on normal non-dividing cell viability *in vitro* was examined, utilizing cultured chondrocytes grown to confluence.

[0229] Briefly, chondrocytes were incubated in the presence (10^{-5} M, 10^{-7} M, and 10^{-9} M) or absence (control) of paclitaxel for 72 hours. At the end of this time period, the total number of viable cells was determined visually by trypan blue dye exclusion. This experiment was conducted 4 times and the data collated.

[0230] Results of this experiment are shown in Figure 21. Briefly, as is evident from Figure 21, paclitaxel does not affect the viability of normal non-proliferating cells *in vitro* even at high concentrations (10^{-5} M) of paclitaxel. More specifically, even at drug concentrations sufficient to block the pathological processes described in the preceding examples, there is no cytotoxicity to normal chondrocytes.

EXAMPLE 16

SELECTION OF PERMEATION ENHANCER FOR TOPICAL PACLITAXEL FORMULATION

A. Paclitaxel solubility in various enhancers

[0231] The following permeation enhancers were examined: Transcutol®, ethanol, propylene glycol, isopropyl myristate, oleic acid and Transcutol:isopropyl myristate (9:1 v:v). One milliliter of each enhancer in glass vials was preheated to 37°C and excess paclitaxel was added. A sample of 0.5 ml of the fluid from each vial was centrifuged at 37°C and 13000 rpm for 2 minutes. Aliquots (0.1 ml) of supernatant from the centrifuge tubes were transferred to volumetric flasks and diluted with methanol. Paclitaxel content was assessed by high pressure liquid chromatography (HPLC).

B. Partition coefficient

[0232] A specific quantity of paclitaxel was dissolved in a volume of enhancer heated to 37°C. Aliquots (1 ml) of this solution were added to 1 ml of octanol in a 4 ml glass vial. Phosphate buffered saline (1 ml) (pH 7.4) was then added and the vials vortexed to create an emulsion. The vials were placed in a 37°C oven for 16 hours, after which 0.1 ml of octanol phase was removed from each vial and diluted with 9.9 ml methanol. For the water phases, 0.5 ml was sampled from the oleic acid and isopropyl myristate vials and 0.5 ml was sampled from the propylene glycol vials and diluted with 0.5 ml methanol. From the Transcutol vials, 0.1 ml was sampled and diluted with 9.9 ml 50:50 Transcutol:PBS and 0.1 ml from the ethanol vials was sampled and diluted with 50:50 ethanol:PBS. Paclitaxel content was determined by HPLC. Each determination was performed in triplicate.

C. Results

[0233] The solubility of paclitaxel in each enhancer at 37°C is listed in Table 1.

Table 1: Concentration of Paclitaxel at Saturation in Various Permeation Enhancers

	Paclitaxel concentration (mg/ml)	
Enhancer	*Average*	*Standard deviation*
Transcutol®	346.85	2.59
Ethanol	68.91	3.49
Propylene glycol	21.56	0.11
Isopropyl myristate	0.43	0.01
Oleic acid	0.31	0.01
Transcutol®:isopropyl myristate (9:1 v:v)	353.93	0.42

[0234] The octanol/water partition coefficients, $K_{o/w}$, are listed in Table 2.

Table 2:

Octanol/Water Partition Coefficient of Paclitaxel in Various Enhancer Solutions		
Enhancer	**$K_{o/w}$**	**Standard deviation**
Transcutol®	25.25	0.27
Ethanol	6.88	0.13
Propylene glycol	37.13	2.48
Isopropyl myristate	∞	-
Oleic acid	∞	-

[0235] To act effectively, paclitaxel must penetrate the skin to the lower strata of the viable epidermis. It has been established that for drugs to penetrate the viable epidermis, they must possess an octanol/water partition coefficient of close to 100 (Hadgraft J.H. and Walters K., Drug absorption enhancements, A.G. de Boers Ed., Harwood Publishers, 1994). Based on the results in Tables 1 and 2, propylene glycol and Transcutol show the best combination of solubilizing paclitaxel and enhancing its partitioning from an oil phase to an aqueous phase.

[0236] However, the $K_{o/w}$ produced by both Transcutol and propylene glycol may be somewhat low, therefore they were combined with isopropyl myristate which has an infinite $K_{o/w}$ in an attempt to increase the solubility of paclitaxel in the octanol phase. Isopropyl myristate and Transcutol were mixed in a 1:9 volume ratio. The isopropyl myristate dissolved readily at room temperature in the Transcutol. In order to form a homogeneous phase, the propylene glycol and isopropyl myristate were also mixed with ethanol in a ratio of 4:3.5:0.5 propylene glycol:ethanol:isopropyl myristate. The $K_{o/w}$ results are shown in Table 3.

Table 3:

Octanol/Water Partition Coefficients of Paclitaxel in Enhancer Combinations		
Enhancer	**$K_{o/w}$**	**Standard deviation**
Transcutol® :isopropyl myristate (9:1)	43.45	0.43
Propylene glycol:ethanol:isopropyl myristate (4.0:3.5:0.5)	42.39	1.66

[0237] The addition of isopropyl myristate to the Transcutol resulted in a significant increase in the partition coefficient. However, the propylene glycol:ethanol:isopropyl myristate solution did not result in a significant improvement in the partition coefficient over that of propylene glycol alone. This last result, and the fact that ethanol has been found to exacerbate the psoriatic condition, effectively eliminated this enhancer combination from further consideration. Furthermore, the addition of isopropyl myristate actually increased the solubility of paclitaxel over its solubility in Transcutol alone. The solubility of paclitaxel in Transcutol was 346.9 mg/ml whereas in Transcutol:isopropyl myristate combination

the solubility increased to 353.9 mg/ml. Therefore, this enhancer combination was chosen in the skin studies.

EXAMPLE 17

PREPARATION AND ANALYSIS OF TOPICAL PACLITAXEL FORMULATIONS

A. Preparation of paclitaxel ointment A

[0238] Transcutol (3.2 g), isopropyl myristate (0.3 g), labrasol (2.5 g), paclitaxel (0.01 g) and 0.5 mCi/ml ^{3}H-paclitaxel (0.3 ml) were combined in a 20 ml scintillation vial. In a separate scintillation vial, labrafil (2.5 g), arlacel 165 (1.2 g) and compritol (0.3 g) were combined and heated to 70°C until completely melted. The contents of the first scintillation vial are added to the melt, vortexed until homogeneous and allowed to cool.

B. Preparation of paclitaxel ointment B

[0239] Transcutol (2.5 g), isopropyl myristate (1.0 g), labrasol (2.5 g), paclitaxel (0.01 g) and 0.5 mCi/ml ^{3}H-paclitaxel (0.3 ml) were combined in a 20 ml scintillation vial. In a separate scintillation vial, labrafil (2.5 g), arlacel 165 (1.2 g) and compritol (0.3 g) were combined and heated to 70°C until completely melted. The contents of the first scintillation vial are added to the melt, vortexed until homogeneous and allowed to cool.

C. Skin preparation and penetration study

[0240] Frozen, excised Yucatan mini-pig skin was stored at -70°C until used. Skin samples were prepared using a no. 10 cork borer to punch disks from the frozen skin. Samples were rinsed with a streptomyocin-penicillin solution and placed into freezer bags and stored at -70°C.

[0241] Skin sections were mounted on Franz diffusion cells, stratum corneum side up. The bottom receptor solution was a 0.05% amoxicillin solution in R.O. water. A donor cell was clamped on to each skin surface. The paclitaxel ointment was heated until melted (40 to 50°C) and drawn into a syringe. While still molten, 0.1 ml was extruded onto each skin surface. The donor cells were covered with a glass disk and the assembly left for 24 hours.

[0242] After 24 hours, the cells were disassembled, excess ointment removed and stored in a scintillation vial. The skin surface was quickly washed with 3 ml dichloromethane (DCM) and dried. The wash DCM was stored in the same vial as the excess ointment. The skin sections and the receptor solution were placed into separate scintillation vials. The skin was cryotomed at -30°C into 30 µm sections and collected in separate vials. The initial shavings and remaining skin were also collected in separate glass vials. The sectioned skin samples were dissolved by adding 0.5 ml of tissue solubilizer to each vial. The samples were left overnight to dissolve at room temperature. The following day, 3 ml of scintillation cocktail was added to the vials. For the DCM wash solutions, 100 µl was transferred to 1 ml of acetonitrile and then 3 ml of scintillation cocktail was added. The radioactivity of all the solutions was measured using a beta counter.

[0243] Skin samples were mounted on the Franz diffusion cells and separated into three groups. Each sample was treated accordingly (no treatment or ointment B with or without paclitaxel). After 24 hours, the samples were removed and processed using standard histological techniques.

D. Results

[0244] From the histological sections, the stratum corneum section of untreated skin was found to be between 50 to 120 µm thick while the viable epidermis was between 400 to 700 µm thick. For the ointment which contained 3% w/w isopropyl myristate (ointment A), the concentration of paclitaxel in the skin was essentially constant at 1 µg/ml (1.2 x 10^{-6} M) in the stratum corneum and throughout the viable epidermis. For the ointment which contained 10% w/w isopropyl myristate (ointment B), the paclitaxel concentration was constant in the stratum corneum and the viable epidermis, but higher in the stratum corneum (6 µg/ml versus 2 µg/ml). There was no radioactivity in the receptor solution for each ointment investigation, indicating that paclitaxel did not pass completely through the skin section.

[0245] No gross differences were noted when the ointment containing paclitaxel was applied.

EXAMPLE 18 (Reference example)

DEVELOPMENT OF SYSTEMIC FORMULATIONS OF PACLITAXEL FOR THE TREATEMENT OF PSORIASIS

[0246] In severe cases of psoriasis, more aggressive treatments are deemed acceptable and therefore the toxicities associated with systemic treatment with paclitaxel may be acceptable.

[0247] The systemic formulation for paclitaxel is comprised of amphiphilic diblock copyolymers which in aqueous solutions form micelles consisting of a hydrophobic core and a hydrophilic shell in water. Diblock copolymers of poly (DL-lactide)-block-methoxy polyethylene glycol (PDLLA-MePEG), polycaprolactone-block methoxy polyethylene glycol (PCL-MePEG) and poly(DL-lactide-co-caprolactone)-block-methoxy polyethylene glycol (PDLLACL-MePEG) can be synthesized using a bulk melt polymerization procedure, or similar methods. Breifly, given amounts of monomers DL-lactide, caprolactone and methoxy polyethylene glycols with different molecular weights were heated (130°C) to melt under the bubbling of nitrogen and stirred. The catalyst stannous octoate (0.2% w/w) was added to the molten monomers. The polymerization was carried out for 4 hours. The molecular weights, critical micelle concentrations and the maximum paclitaxel loadings were measured with GPC, fluorescence, and solubilization testing, respectively (Figure 22). High paclitaxel carrying capacities were obtained. The ability of solubilizing paclitaxel depends on the compositions and concentrations of the copolymers (Figures 22 and 23). PDLLA-MePEG gave the most stable solubilized paclitaxel (Figures 23 and 24).

[0248] The strong association within the internal core of the polymeric micelles presents a high capacity environment for carrying hydrophobic drugs such as paclitaxel. The drugs can be covalently coupled to block copolymers to form a micellar structure or can be physically incorporated within the hydrophobic cores of the micelles. The mechanisms of drug release from the micelles include diffusion from the core and the exchange between the single polymer chains and the micelles. The small size of the micelles (nofrmally less than 100 nm) will eliminate the difficulties associated with injecting larger particles.

EXAMPLE 19

PROCEDURE FOR PRODUCING THERMOPASTE

[0249] Five grams of polycaprolactone mol. wt. 10,000 to 20,000; (Polysciences, Warrington Penn. USA) a 20 ml glass scintillation vial which was placed into a 600 ml beaker containing 50 ml of water weighed. The beaker was gently heated to 65°C and held at that temperature for 20 minutes until the polymer melted. A known weight of paclitaxel, or other angiogenesis inhibitor was thoroughly mixed into the melted polymer at 65°C. The melted polymer was poured into a prewarmed (60°C oven) mould and allowed to cool until the polymer solidified. The polymer was cut into small pieces (approximately 2 mm by 2 mm in size) and was placed into a 1 ml glass syringe.

[0250] The glass syringe was then placed upright (capped tip downwards) into a 500 ml glass beaker containing distilled water at 65°C (corning hot plate) until the polymer melted completely. The plunger was then inserted into the syringe to compress the melted polymer into a sticky mass at the tip end of the barrel. The syringe was capped and allowed to cool to room temperature.

[0251] For application, the syringe was reheated to 60°C and administered as a liquid which solidified when cooled to body temperature

EXAMPLE 20

MODIFICATION OF PACLITAXEL RELEASE FROM THERMOPASTE USING PDLLA-PEG-PDLLA AND LOW MOLECULAR WEIGHT POLY(D,L, LACTIC ACID)

A. Preparation of PDLLA-PEG-PDLLA and low molecular weight PDLLA

[0252] DL-lactide was purchased from Aldrich. Polyethylene glycol (PEG) with molecular weight 8,000, stannous octoate, and DL-lactic acid were obtained from Sigma. Poly-ε-caprolactone (PCL) with molecular weight 20,000 was obtained from Birmingham Polymers (Birmingham, AL). Paclitaxel was purchased from Hauser Chemicals (Boulder, CO). Polystyrene standards with narrow molecular weight distributions were purchased from Polysciences (Warrington, PA). Acetonitrile and methylene chloride were HPLC grade (Fisher Scientific).

[0253] The triblock copolymer of PDLLA-PEG-PDLLA was synthesized by a ring opening polymerization. Monomers of DL-lactide and PEG in different ratios were mixed and 0.5 wt% stannous octoate was added. The polymerization was carried out at 150°C for 3.5 hours. Low molecular weight PDLLA was synthesized through polycondensation of DL-lactic acid. The reaction was performed in a glass flask under the conditions of gentle nitrogen purge, mechanical stirring, and heating at 180°C for 1.5 hours. The PDLLA molecular weight was about 800 measured by titrating the carboxylic acid end groups.

B. Manufacture of paste formulations

[0254] Paclitaxel at loadings of 20% or 30% was thoroughly mixed into either the PDLLA-PEG-PDLLA copolymers

or blends of PDLLA:PCL 90:10, 80:20 and 70:30 melted at about 60°C. The paclitaxel-loaded pastes were weighed into 1 ml syringes and stored at 4°C.

C. Characterization of PDLLA-PEG-PDLLA and the paste blends

[0255] The molecular weights and distributions of the PDLLA-PEG-PDLLA copolymers were determined at ambient temperature by GPC using a Shimadzu LC-10AD HPLC pump and a Shimadzu RID-6A refractive index detector (Kyoto, Japan) coupled to a 10^4 Å Hewlett Packard PI gel column. The mobile phase was chloroform with a flow rate of 1 ml/minute. The injection volume of the sample was 20 µl at a polymer concentration of 0.2% (w/v). The molecular weights of the polymers were determined relative to polystyrene standards. The intrinsic viscosity of PDLLA-PEG-PDLLA in $CHCl_3$ at 25°C was measured with a Cannon-Fenske viscometer.

[0256] Thermal analysis of the copolymers was carried out by differential scanning calorimetry (DSC) using a TA Instruments 2000 controller and DuPont 910S DSC (Newcastle, Delaware). The heating rate was 10°C/min and the copolymer and paclitaxel/copolymer matrix samples were weighed (3 - 5 mg) into crimped open aluminum sample pans.

[0257] H nuclear magnetic resonance (NMR) was used to determine the chemical composition of the polymer. H NMR spectra of paclitaxel-loaded PDLLA-PEG-PDLLA were obtained in $CDCl_3$ using an NMR instrument (Bruker, AC-200E) at 200 MHz. The concentration of the polymer was 1 - 2%.

[0258] The morphology of the paclitaxel/PDLLA-PEG-PDLLA paste was investigated using scanning electron microscopy (SEM) (Hitachi F-2300). The sample was coated with 60% Au and 40% Pd (thickness 10 - 15 run) using a Hummer instrument (Technics, USA).

D. *In vitro* release of paclitaxel

[0259] A small pellet of 20% paclitaxel-loaded PDLLA:PCL paste (about 2 mg) or a cylinder (made by extruding molten paste through a syringe) of 20% paclitaxel-loaded PDLLA-PEG-PDLLA paste were placed into capped 14 ml glass tubes containing 10 ml phosphate buffered saline (pH 7.4) with 0.4 g/L albumin. The tube was incubated at 37°C with gentle rotational mixing. The supernatant was withdrawn periodically for paclitaxel analysis and replaced with fresh PBS/albumin buffer. The supernatant (10 ml) was extracted with 1 ml methylene chloride. The water phase was decanted and the methylene chloride phase was dried under a stream of nitrogen at 60°C. The dried residue was reconstituted in a 40:60 water:acetonitrile mixture and centrifuged at 10,000g for about 1 min. The amount of paclitaxel in the supernatant was then analyzed by HPLC. HPLC analysis was performed using a 110A pump and C-8 ultrasphere column (Beckman), and a SPD-6A UV detector set at 232 nm, a SIL-9A autoinjector and a C-R3A integrator (Shimadzu). The injection volume was 20 µl and the flow rate was 1 ml/minute. The mobile phase was 58% acetonitrile, 5% methanol, and 37% distilled water.

E. Results and Discussion

[0260] The molecular weight and molecular weight distribution of PDLLA-PEG-PDLLA, relative to polystyrene standards, were measured by GPC (Figure 30). The intrinsic viscosity of the copolymer in $CHCl_3$ at 25°C was determined using a Canon-Fenske viscometer. The molecular weight and intrinsic viscosity decreased with increasing PEG content. The polydispersities of PDLLA-PEG-PDLLA with PEG contents of 10% - 40% were from 2.4 to 3.5. However, the copolymer with 70% PEG had a narrow molecular weight distribution with a polydispersity of 1.21. This might be due to a high PEG content reducing the chance of side reactions such as transesterfication which results in a wide distribution of polymer molecular weights. Alternatively, a coiled structure of the hydrophobic-hydrophilic block copolymers may result in an artificial low polydispersity value.

[0261] DSC scans of pure PEG and PDLLA-PEG-PDLLA copolymers are given in Figures 25 and 26. The PEG and PDLLA-PEG-PDLLA with PEG contents of 70% and 40% showed endothermic peaks with decreasing enthalpy and temperature as the PEG content of the copolymer decreased. The endothermic peaks in the copolymers of 40% and 70% PEG were probably due to the melting of the PEG region, indicating the occurrence of phase separation. While pure PEG had a sharp melting peak, the copolymers of both 70% and 40% PEG showed broad peaks with a distinct shoulder in the case of 70% PEG. The broad melting peaks may have resulted from the interference of PDLLA with the crystallization of PEG. The shoulder in the case of 70% PEG might represent the glass transition of the PDLLA region. No thermal changes occurred in the copolymers with PEG contents of 10%, 20% and 30% in a temperature range of 10 - 250°C, indicating that no significant crystallization (therefore may be the phase separation) had occurred.

[0262] DSC thermograms of PDLLA:PCL (70:30, 80:20, 90:10) blends without paclitaxel or with 20% paclitaxel showed an endothermic peak at about 60°C, resulting from the melting of PCL. Due to the amorphous nature of the PDLLA and its low molecular weight (800), melting and glass transitions of PDLLA were not observed. No thermal changes due to the recrystallization or melting of paclitaxel was observed.

[0263] PDLLA-PEG-PDLLA copolymers of 20% and 30% PEG content were selected as optimum formulation materials for the paste for the following reasons: PDLLA-PEG-PDLLA of 10% PEG could not be melted at a temperature of about 60°C; the copolymers of 40% and 70% PEG were readily melted at 60°C, and the 20% and 30% PEG copolymer became a viscous liquid between 50°C to 60°C; and the swelling of 40% and 70% PEG copolymers in water was very high resulting in rapid dispersion of the pastes in water.

[0264] The *in vitro* release profiles of paclitaxel from PDLLA-PEG-PDLLA cylinders are shown in Figure 27. The experiment measuring release from the 40% PEG cylinders was terminated since the cylinders had a very high degree of swelling (about 200% water uptake within one day) and disintegrated in a few days. The released fraction of paclitaxel from the 30% PEG cylinders gradually increased over 70 days. The released fraction from the 20% PEG cylinders slowly increased up to 30 days and then abruptly increased, followed by another period of gradual increase. A significant difference existed in the extent to which each individual cylinder (20% PEG content) showed the abrupt change in paclitaxel release. Before the abrupt increase, the release fraction of paclitaxel was lower for copolymers of lower PEG content at the same cylinder diameter (1 mm). The 40% and 30% PEG cylinders showed much higher paclitaxel release rates than the 20% PEG cylinders. For example, the cylinder of 30% PEG released 17% paclitaxel in 30 days compared to a 2% release from the 20% PEG cylinder. The cylinders with smaller diameters resulted in faster release rates (*e. g.*, in 30 days the 30% PEG cylinders with 0.65 mm and 1 mm diameters released 26% and 17% paclitaxel, respectively (Figure 27)).

[0265] The above observations may be explained by the release mechanisms of paclitaxel from the cylinders. Paclitaxel was dispersed in the polymer as crystals as observed by optical microscopy. The crystals began dissolving in the copolymer matrix at 170°C and completely dissolved at 180°C as observed by hot stage microscopy DSC thermograms of 20% paclitaxel-loaded PDLLA-PEG-PDLLA (30% PEG) paste revealed a small recrystallization exotherm (16 J/g, 190°C) and a melting endotherm (6 J/g, 212°C) for paclitaxel (Figure 25) indicating the recrystallization of paclitaxel from the copolymer melt after 180°C. In this type of drug/polymer matrix, paclitaxel could be released via diffusion and/or polymer erosion.

[0266] In the diffusional controlled case, drug may be released by molecular diffusion in the polymer and/or through open channels formed by connected drug particles. Therefore at 20% loading, some particles of paclitaxel were isolated and paclitaxel may be released by dissolution in the copolymer followed by diffusion. Other particles of paclitaxel could form clusters connecting to the surface and be released through channel diffusion. In both cases, the cylinders with smaller dimension gave a faster drug release due to the shorter diffusion path (Figure 27).

[0267] The dimension changes and water uptake of the cylinders were recorded during the release (Figure 28). The changes in length, diameter and wet weight of the 30% PEG cylinders increased rapidly to a maximum within 2 days, remained unchanged for about 15 days, then decreased gradually. The initial diameter of the cylinder did not affect the swelling behavior. For the cylinder of 20% PEG, the length decreased by 10% in one day and leveled off, while the diameter and water uptake gradually increased over time. Since more PEG in the copolymer took up more water to facilitate the diffusion of paclitaxel, a faster release was observed (Figure 27).

[0268] The copolymer molecular weight degradation of PDLLA-PEG-PDLLA paste was monitored by GPC. For the 20% PEG cylinder, the elution volume at the peak position increased with time indicating a reduced polymer molecular weight during the course of the release experiment (Figure 30). A biphasic molecular weight distribution was observed at day 69. Polymer molecular weight was also decreased for 30% PEG cylinders (1 mm and 0.65 mm). However no biphasic distribution was observed.

[0269] NMR spectra revealed a PEG peak at 3.6 ppm and PDLLA peaks at 1.65 ppm and 5.1 ppm. The peak area of PEG relative to PDLLA in the copolymer decreased significantly after 69 days (Figure 29), indicating the dissolution of PEG after its dissociation from PDLLA. The dry mass loss of the cylinders was also recorded (Figure 29) and shows a degradation rate decreasing in the order 30% PEG-0.65mm > 30% PEG-1mm > 20% PEG-lmm.

[0270] The morphological changes of the dried cylinders before and during paclitaxel release were observed using SEM (Figure 31). Briefly, solid paclitaxel crystals and non-porous polymer matrices were seen before the release (Figures 31A and 31B). After 69 days of release, no paclitaxel crystals were observed and the matrices contained many pores due to polymer degradation and water uptake (Figures 31C and 31D).

[0271] The 30% PEG cylinders showed extensive swelling after only two days in water (Figure 28) and therefore the hindrance to diffusion of the detached water soluble PEG block and degraded PDLLA (*i.e.*, DL-lactic acid oligomers) was reduced. Since the mass loss and degradation of the 30% PEG cylinders was continuous, the contribution of erosion release gradually increased resulting in a sustained release of paclitaxel without any abrupt change (Figure 27). For the 20% PEG cylinders, the swelling was low initially (Figure 28) resulting in a slow diffusion of the degradation products. Therefore the degradation products in the interior region were primarily retained while there were fewer degradation products in the outer region due to the short diffusion path. The degradation products accelerated the degradation rate since the carboxylic acid end groups of the oligomers catalyzed the hydrolytic degradation. This resulted in a high molecular weight shell and a low molecular weight interior as indicated by the biphasic copolymer molecular weight distribution (Figure 30, day 69). Since the shell rupture was dependent on factors such as the strength,

thickness and defects of the shell and interior degradation products, the onset and the extent of the loss of interior degradation products were very variable. Because the shell rupture was not consistent and the drug in the polymer was not microscopically homogenous, the time point for the release burst and the extent of the burst were different for the 4 samples tested (Figure 27).

[0272] The release of paclitaxel from PDLLA and PCL blends and pure PCL are shown in Figure 32. Briefly, the released fraction increased with PDLLA content in the blend. For example, within 10 days, the released paclitaxel from 80:20, 70:30, and 0:100 PDLLA:PCL were 17%, 11%, and 6%, respectively. After an initial burst in one day, approximately constant release was obtained from 80:20 PDLLA:PCL paste. No significant degree of swelling was observed during the release. For the PDLLA:PCL blends, since PDLLA had a very low molecular weight of about 800, it was hydrolyzed rapidly into water soluble products without a long delay in mass loss. PCL served as the "holding" material to keep the paste from rapidly disintegrating. Therefore the release rate increased with PDLLA content in the blend due to the enhanced degradation. The continuous erosion of the PDLLA controlled the release of paclitaxel and resulted in a constant release. The release of paclitaxel from pure PCL was probably diffusion controlled due to the slow degradation rate (in 1-2 years) of PCL.

[0273] Difficulties were encountered in the release study for 20% paclitaxel loaded 90:10 PDLLA:PCL paste due to the disintegration of the paste pellet within 24 hours of incubation. Briefly, during the first 12 hours of incubation, samples were taken every hour in order to ensure sink conditions for paclitaxel release. The released paclitaxel from the 90:10 paste was 25-35% within 10 hours.

[0274] Paste of 90:10 PDLLA:PCL containing 30% paclitaxel released more paclitaxel than 90:10 PDLLA:PCL paste containing 20% paclitaxel. Thus, modulation of the release rate of paclitaxel, which was regulated by the properties of the polymer and chemotherapeutic agents as well as the site of administration, was important in the development of local therapy.

EXAMPLE 21

PREPARATION OF POLYMERIC COMPOSITIONS CONTAINING WATER SOLUBLE ADDITIVES AND PACLITAXEL

A. Preparation of polymeric compositions

[0275] Microparticles of co-precipitates of paclitaxel/additive were prepared and subsequently added to PCL to form pastes. Briefly, paclitaxel (100 mg) was dissolved in 0.5 ml of ethanol (95%) and mixed with the additive (100 mg) previously dissolved or dispersed in 1.0 ml of distilled water. The mixture was triturated until a smooth paste was formed. The paste was spread on a Petri dish and air-dried overnight at 37°C. The dried mass was pulverized using a mortar and pestle and passed through a mesh #140 (106 μm) sieve (Endecotts Test Sieves Ltd, London, England). The microparticles (40%) were then incorporated into molten PCL (60%) at 65°C corresponding to a 20% loading of paclitaxel. The additives used in the study were gelatin (Type B, 100 bloom, Fisher Scientific), methylcellulose, (British Drug Houses), dextran, T500 (Pharmacia, Sweden), albumin (Fisher Scientific), and sodium chloride (Fisher Scientific). Microparticles of paclitaxel and gelatin or albumin were prepared as described above but were passed through a mesh # 60 (270 μm) sieve (Endecotts Test Sieves Ltd, London, England) to evaluate the effect of microparticle size on the release of paclitaxel from the paste. Pastes were also prepared to contain 10, 20 or 30% gelatin and 20% paclitaxel in PCL to study the effect of the proportion of the additive on drug release. Unless otherwise specified, pastes containing 20% paclitaxel dispersed in PCL were prepared to serve as controls for the release rate studies.

B. Drug release studies

[0276] Approximately a 2.5 mg pellet of paclitaxel-loaded paste was suspended in 50 ml of 10 mM PBS (pH 7.4) in screw-capped tubes. The tubes were tumbled end-over-end at 37°C and at given time intervals 49.5 ml of supernatant was removed, filtered through a 0.45 μm membrane filter and retained for paclitaxel analysis. An equal volume of PBS was replaced in each tube to maintain sink conditions throughout the study. For analysis, the filtrates were extracted with 3 x 1 ml dichloromethane (DCM), the DCM extracts evaporated to dryness under a stream of nitrogen and redissolved in l ml acetonitrile. The analysis was by HPLC using a mobile phase of water:methanol:acetonitrile (37:5:58:) at a flow rate of 1 ml/minute (Beckman Isocratic Pump), a C18 reverse phase column (Beckman), and UV detection (Shimadzu SPD A) at 232 nm.

C. Swelling studies

[0277] Paclitaxel/additive/PCL pastes, prepared using paclitaxel-additive microparticles of mesh size # 140 (and #60 for gelatin only), were extruded to form cylinders, pieces were cut, weighed and the diameter and length of each piece

were measured using a micrometer (Mitutoyo Digimatic). The pieces were suspended in distilled water (10 ml) at 37°C and at predetermined intervals the water was discarded and the diameter and the length of the cylindrical pieces were measured and the samples weighed. The morphology of the samples (before and after suspending in water) was examined using scanning electron microscopy (SEM) (Hitachi F-2300). The samples were coated with 60% Au and 40% Pd (thickness 10 - 15 nm) using a Hummer Instrument (Technics, USA).

D. Chick embryo chorioallantoic membrane (CAM) studies

[0278] Fertilized, domestic chick embryos were incubated for 4 days prior to shell-less culturing. The egg contents were incubated at 90% relative humidity and 3% CO_2 and on day 6 of incubation, 1 mg pieces of the paclitaxel-loaded paste (containing 6% paclitaxel, 24% gelatin and 70% PCL) or control (30% gelatin in PCL) pastes were placed directly on the CAM surface. After a 2-day exposure the vasculature was examined using a stereomicroscope interfaced with a video camera; the video signals were then displayed on a computer and video printed.

E. Results and Discussion

[0279] Microparticles of co-precipitated paclitaxel and gelatin or albumin were hard and brittle and were readily incorporated into PCL, while the other additives produced soft particles which showed a tendency to break up during the preparation of the paste.

[0280] Figure 33 shows the time courses of paclitaxel release from pastes containing 20% paclitaxel in PCL or 20% paclitaxel, 20% additive and 60% PCL. The release of paclitaxel from PCL with or without additives followed a bi-phasic release pattern; initially, there was a faster drug release rate followed by a slower drug release of the drug. The initial period of faster release rate of paclitaxel from the pastes was thought to be due to dissolution of paclitaxel located on the surface or diffusion of paclitaxel from the superficial regions of the paste. The subsequent slower phase of the release profiles may be attributed to a decrease in the effective surface area of the drug particles in contact with the buffer, a slow ingress of the buffer into the polymer matrix or an increase in the mean diffusion paths of the drug through the polymer matrix.

[0281] Both phases of the release profiles of paclitaxel from PCL increased in the presence of the hydrophilic additives with gelatin, albumin and methylcellulose producing the greatest increase in drug release rates (Figure 33). There were further increases in the release of paclitaxel from the polymer matrix when larger paclitaxel-additive particles (270 μm) were used to prepare the paste compared with when the smaller paclitaxel-additive particles (106 μm) were used (Figure 34). Increases in the amount of the additive (*e.g.*, gelatin) produced a corresponding increase in drug release (Figure 34). Figure 35A shows the swelling behavior of pastes containing 20% paclitaxel, 20% additive and 60% PCL. The rate of swelling followed the order gelatin > albumin > methylcellulose > dextran > sodium chloride. In addition, the rate of swelling increased when a higher proportion of the water-soluble polymer was added to the paste (Figure 35B). The pastes containing gelatin or albumin swelled rapidly within the first 8 - 10 hours and subsequently the rate of swelling decreased when the change in the volume of the sample was greater than 40%. The paste prepared using the larger (270 μm) paclitaxel-gelatin particles swelled at a faster rate than those prepared with the smaller (106 μm) paclitaxel-gelatin particles. All pastes disintegrated when the volume increased greater than 50%. The SEM studies showed that the swelling of the pastes was accompanied by the cracking of the matrix (Figure 36). At high magnifications (Figures 36C and 36D) there was evidence of needle-or rod-shaped paclitaxel crystals on the surface of the paste and in close association with gelatin following swelling (Figures 36C and 36D).

[0282] Osmotic or swellable, hydrophilic agents embedded as discrete particles in the hydrophobic polymer resulted in drug release by a combination of matrix erosion, diffusion of drug through the polymer matrix, and/or diffusion and/or convective flow through pores created in the matrix by the dissolution of the water soluble additives. Osmotic agents and swellable polymers dispersed in a hydrophobic polymer would imbibe water (acting as wicking agents), dissolve or swell and exert a turgor pressure which could rupture the septa (the polymer layer) between adjacent particles, creating microchannels and thus facilitating the escape of the drug molecules into the surrounding media by diffusion or convective flow. The swelling and cracking of the paste matrix (Figure 36) likely resulted in the formation of microchannels throughout the interior of the matrix. The different rates and extent of swelling of the polymers (Figure 35) may account for the differences in the observed paclitaxel release rates (Figures 33 and 34).

[0283] Figure 37 shows CAMs treated with control gelatin-PCL paste (Figure 37A) and 20% paclitaxel-gelatin-PCL paste (Figure 37B). The paste on the surface of the CAMs are shown by the arrows in the figures. The CAM with the control paste shows a normal capillary network architecture. The CAMs treated with paclitaxel-PCL paste consistently showed vascular regression and zones which lacked a capillary network. Incorporation of additives in the paste markedly increased the diameter of the avascular zone (Figure 37).

[0284] This study showed that the *in vitro* release of paclitaxel from PCL could be increased by the incorporation of paclitaxel/hydrophilic polymer microparticles into PCL matrix. *In vivo* studies evaluating the efficacy of the formulation

in treating subcutaneous tumors in mice also showed that the paclitaxel/gelatin/PCL paste significantly reduced the tumor mass. Factors such as the type of water soluble agent, the microparticle size and the proportion of the additives were shown to influence the release characteristics of the drug.

EXAMPLE 22

PROCEDURE FOR PRODUCING NANOPASTE

[0285] Nanopaste is a suspension of microspheres in a hydrophilic gel. Within one aspect of the invention, the gel or paste can be smeared over tissue as a method of locating drug-loaded microspheres close to the target tissue. Being water based, the paste soon becomes diluted with bodily fluids causing a decrease in the stickiness of the paste and a tendency of the microspheres to be deposited on nearby tissue. A pool of microsphere encapsulated drug is thereby located close to the target tissue.

[0286] . Reagents and equipment which were utilized within these experiments include glass beakers, Carbopol 925 (pharmaceutical grade, Goodyear Chemical Co.), distilled water, sodium hydroxide (1 M) in water solution, sodium hydroxide solution (5 M) in water solution, microspheres in the 0.1 lm to 3 lm size range suspended in water at 20% w/v (see previous).

1. PREPARATION OF 5% W/V CARBOPOL GEL

[0287] A sufficient amount of carbopol was added to 1 M sodium hydroxide to achieve a 5% w/v solution. To dissolve the carbopol in the 1 M sodium hydroxide, the mixture was allowed to sit for approximately one hour. During this time period, the mixture was stirred and, after one hour, the pH was adjusted to 7.4 using 5 M sodium hydroxide until the carbopol was fully dissolved. Once a pH of 7.4 was achieved, the gel was covered and allowed to sit for 2 to 3 hours.

2. PROCEDURE FOR PRODUCING NANOPASTE

[0288] A sufficient amount of 0.1 μm to 3 μm microspheres was added to water to produce a 20% suspension of the microspheres. Carbopol gel (8 ml of the 5% w/v) was placed into a glass beaker and 2 ml of the 20% microsphere suspension was added. The mixture was stirred to thoroughly disperse the microspheres throughout the gel. This mixture was stored at 4°C.

EXAMPLE 23

COMPLEXATION OF PACLITAXEL WITH CYCLODEXTRINS

A. Materials

[0289] Paclitaxel was obtained from Hauser Chemicals Inc. (Boulder, Colorado). Disodium phosphate (Fisher), citric acid (British Drug Houses), hydroxypropyl-β-cyclodextrin (HPβCD), γ-cyclodextrin (γ-CD) and hydroxypropyl-γ-cyclodextrin (HPγCD) were obtained from American Maize-Products Company (Hammond, Indiana) and were used as received.

B. Methods

1. SOLUBILITY STUDIES

[0290] Excess amounts of paclitaxel (5 mg) were added to aqueous solutions containing various concentrations of γ-CD, HPγ-CD, or HPβ-CD and tumbled gently for about 24 hours at 37°C. After equilibration, aliquots of the suspension were filtered through a 0.45 μm membrane filter (Millipore), suitably diluted and analyzed using HPLC. The mobile phase was composed of a mixture of acetonitrile, methanol and water (58:5:37) at a flow rate of 1.0 ml/minute. The solubility of paclitaxel in a solvent composed of 50:50 water and ethanol (95%) containing various concentrations, up to 10%, of HPβ-CD was also investigated. In addition, dissolution rate profiles of paclitaxel were investigated by adding 2 mg of paclitaxel (as received) to 0, 5, 10 or 20% HPγ-CD solutions or 2 mg of previously hydrated paclitaxel (by suspending in water for 7 days) to pure water and tumbling gently at 37°C. Aliquots were taken at various time intervals and assayed for paclitaxel.

2. STABILITY STUDIES

[0291] The solutions containing 20% HPβCD or HPγCD had pH values of 3.9 and 5.2, respectively. The stability of paclitaxel in cyclodextrin solutions was investigated by assaying paclitaxel in solutions (20 µg ml) containing 10 or 20% HPγ-CD or HPβ-CD in either water or a 50:50 water-ethanol mixture at 37°C or 55°C at various time intervals. In addition, stability of paclitaxel in solutions (1 µg/ml) containing 1%, 2% or 5% HPβCD at 55°C were determined.

C. Results

1. SOLUBILITY STUDIES

[0292] The solubility of paclitaxel increased over the entire CD concentration range studied; HPβ-CD producing the greatest increase in the solubility of paclitaxel (Figure 38). The shape of the solubility curves suggests that the stoichiometries were of higher order than a 1:1 complex. Paclitaxel formed Type A_p curves with both HPβ-CD and HPγ-CD and Type AN curves with γ-CD. The solubility of paclitaxel in a 50% solution of HPβ-CD in water was 3.2 mg/ml at 37°C which was about a 2000-fold increase over the solubility of paclitaxel in water. The estimated stability constants (from Figure 39) for first order complexes of paclitaxel-cyclodextrins were 3.1, 5.8 and 7.2 M^{-1} for γ-CD, HPγ-CD and HPβ-CD and those for second order complexes were 0.785 x 10^3, 1.886 x 10^3 and 7.965 x 103 M^{-1} for γ-CD, HPγ-CD and HPβ-CD, respectively. The values of the observed stability constants suggested that the inclusion complexes formed by paclitaxel with cyclodextrins were predominantly second order complexes.

[0293] The solubility of paclitaxel in 50:50 water:ethanol mixture increased with an increase in the cyclodextrin concentration (Figure 40) as observed for complexation in pure water. The apparent stability constant for the complexation of paclitaxel and HPβ—CD in the presence of 50% ethanol (26.57 M^{-1}) was significantly lower (about 300 times) than the stability constant in the absence of ethanol. The lower stability constant may be attributed to a change in the dielectric constant or the polarity of the solvent in the presence of ethanol.

[0294] The dissolution profiles of paclitaxel in 0, 5, 10 and 20% γ-CD solutions (Figure 41) illustrates the formation of a metastable solution of paclitaxel in pure water or the cyclodextrin solutions; the amount of paclitaxel in solution gradually increased, reached a maximum and subsequently decreased. Dissolution studies using paclitaxel samples which were previously hydrated by suspending in water for 48 hours did not show the formation of the metastable solution. In addition, DSC analysis of the hydrated paclitaxel (dried in a vacuum oven at room temperature) showed two broad endothermic peaks between 60 and 110°C. These peaks were accompanied by about 4.5% weight loss (determined by thermogravimetric analysis) indicating the presence of hydrate(s). A loss in weight of about 2.1% would suggest the formation of a paclitaxel monohydrate. Therefore, the occurrence of the DSC peaks between 60°C and 110°C and the loss in weight of about 4.5% suggests the presence of a dihydrate. There was no evidence of endothermic peak(s) between 60°C and 110°C (DSC results) or a weight loss (TGA results) for paclitaxel samples as received. Therefore, (as received) paclitaxel was anhydrous and on suspension in water it dissolved to form a supersaturated solution which recrystallized as a hydrate of lower solubility (Figure 41).

2. STABILITY STUDIES

[0295] Paclitaxel degradation depended on the concentration of the cyclodextrin and followed pseudo-first order degradation kinetics (*e,g.*, Figure 42). The rate of degradation of paclitaxel in solutions (I µg/ml paclitaxel) containing 1% HPβ-CD at 55°C faster (k = 3.38 x 10^{-3} h^{-1}) than the rate at higher cyclodextrin concentrations. Degradation rate constants of 1.78 x 10^{-3} h^{-1} and 0.96 x 10^{-3} h^{-1} were observed for paclitaxel in 10% HPβ-CD and HPγ-CD, respectively. Paclitaxel solutions (1 µg/ml) containing 2, 4, 6 or 8% HPβ-CD did not show any significant difference in the rate of degradation from that obtained with the 10 or 20% HPβ-CD solutions (20 µg/ml). The presence of ethanol did not adversely affect the stability of paclitaxel in the cyclodextrin solutions.

D. Conclusion

[0296] This study showed that the solubility of paclitaxel could be increased by complexation with cyclodextrins. These aqueous-based cyclodextrin formulations may be utilized in the treatment of various inflammatory diseases.

EXAMPLE 24

POLYMERIC COMPOSITIONS WITH INCREASED CONCENTRATIONS OF PACLITAXEL

[0297] PDLLA-MePEG and PDLLA-PEG-PDLLA are block copolymers with hydrophobic (PDLLA) and hydrophilic

(PEG or MePEG) regions. At appropriate molecular weights and chemical composition, they may form tiny aggregates of hydrophobic PDLLA core and hydrophilic MePEG shell. Paclitaxel can be loaded into the hydrophobic core, thereby providing paclitaxel with an increased "solubility".

A. Materials

[0298] D,L-lactide was purchased from Aldrich, Stannous octoate, poly (ethylene glycol) (mol. wt. 8,000), MePEG (mol. wt. 2,000 and 5,000) were from Sigma. MePEG (mol. wt. 750) was from Union Carbide. The copolymers were synthesized by a ring opening polymerization procedure using stannous octoate as a catalyst (Deng et al, *J. Polym. Sci., Polym, Lett. 28*:411-416, 1990; Cohn et al, *J. Biomed, Mater. Res. 22*: 993-1009, 1988).

[0299] For synthesizing PDLLA-MePEG, a mixture of DL-lactide/MePEG/stannous octoate was added to a 10 milliliter glass ampoule. The ampoule was connected to a vacuum and sealed with flame. Polymerization was accomplished by incubating the ampoule in a 150°C oil bath for 3 hours. For synthesizing PDLLA-PEG-PDLLA, a mixture of D,L-lactide/PEG/stannous octoate was transferred into a glass flask, sealed with a rubber stopper, and heated for 3 hours in a 150°C oven. The starting compositions of the copolymers are given in Tables 1 and 2. In all the cases, the amount of stannous octoate was 0.5% - 0.7%.

B. Methods

[0300] The polymers were dissolved in acetonitrile and centrifuged at 10,000 g for 5 minutes to discard any non-dissolvable impurities. Paclitaxel acetonitrile solution was then added to each polymer solution to give a solution with paclitaxel (paclitaxel + polymer) of 10% wt. The solvent acetonitrile was then removed to obtain a clear paclitaxel/PDLLA-MePEG matrix, under a stream of nitrogen and 60°C warming. Distilled water, 0.9% NaCl saline, or 5% dextrose was added at four times weight of the matrix. The matrix was finally "dissolved" with the help of vortex mixing and periodic warming at 60°C. Clear solutions were obtained in all the cases. The particle sizes were all below 50 nm as determined by a submicron particle sizer (NICOMP Model 270). The formulations are given in Table 1.

Table 1.

Formulations of Paclitaxel/PDLLA-MePEG*		
PDLLA-MePEG	**Dissolving Media**	**Paclitaxel Loading (final paclitaxel concentrate)**
2000/50/50	water	10% (20 mg/ml)
2000/40/60	water	10% (20 mg/ml)
2000/50/50	0.9% saline	5% (10 mg/ml)
2000/50/50	0.9% saline	10% (20 mg/ml)
2000/50/50	5% dextrose	10% (10 mg/ml)
2000/50/50	5% dextrose	10% (20 mg/ml)

[0301] In the case of PDLLA-PEG-PDLLA (Table 2), since the copolymers cannot dissolve in water, paclitaxel and the polymer were co-dissolved in acetone. Water or a mixture of water/acetone was gradually added to this paclitaxel polymer solution to induce the formation of paclitaxel/polymer spheres.

Table 2.

Composition of PDLLA-PEG-PDLLA		
Copolymer Name	**Wt. of PEG (g)**	**Wt. of DL-lactide (g)**
PDLLA-PEG-PDLLA 90/10	1	9
PDLLA-PEG-PDLLA 80/20	2	8
PDLLA-PEG-PDLLA 70/30	3	7
PDLLA-PEG-PDLLA 60/40	4	6
PDLLA-PEG-PDLLA 30-/70	14	6
* PEG molecular weight. 8,000.		

C. Results

[0302] Many of the PDLLA-MePEG compositions form clear solutions in water, 0.9% saline, or 5% dextrose, indicating the formation of tiny aggregates in the range of nanometers. Paclitaxel was loaded into PDLLA-MePEG micelles successfully. For example, at % loading (this represents 10 mg paclitaxel in 1 ml paclitaxel/PDLLA-MePEG/aqueous system), a clear solution was obtained from 2000-50/50 and 2000-40/60. The particle size was about 60 nm.

EXAMPLE 25

PROCEDURE FOR PRODUCING FILM

[0303] The term film refers to a polymer formed into one of many geometric shapes. The film may be a thin, elastic sheet of polymer or a 2 mm thick disc of polymer, either of which may be applied to the tissue surface to prevent subsequent scarring and adhesion formation. This film was designed to be placed on exposed tissue so that any encapsulated drug can be released from the polymer over a long period of time at the tissue site. Films may be made by several processes, including for example, by casting, and by spraying.

[0304] In the casting technique, the polymer was either melted and poured into a shape or dissolved in dichloromethane and poured into a shape. The polymer then either solidified as it cooled or solidified as the solvent evaporated, respectively. In the spraying technique, the polymer was dissolved in solvent and sprayed onto glass, as the solvent evaporated the polymer solidified on the glass. Repeated spraying enabled a build up of polymer into a film that can be peeled from the glass.

[0305] Reagents and equipment which were utilized within these experiments include a small beaker, Corning hot plate stirrer, casting moulds (e.g., 50 ml centrifuge tube caps) and mould holding apparatus, 20 ml glass scintillation vial with cap (Plastic insert type), TLC atomizer, nitrogen gas tank, polycaprolactone ("PCL" - mol. wt. 10,000 to 20,000; Polysciences), paclitaxel (Sigma 95% purity), ethanol, "washed" (see previous) ethylene vinyl acetate ("EVA"), poly (DL)lactic acid ("PLA" - mol. wt. 15,000 to 25,000; Polysciences), DCM (HPLC grade; Fisher Scientific).

1. PROCEDURE FOR PRODUCING FILMS - MELT CASTING

[0306] A small glass beaker with a known weight of PCL was placed into a larger beaker containing water (to act as a water bath) and placed onto a hot plate at 70°C until the polymer was fully melted. A known weight of drug was added to the melted polymer and the mixture stirred thoroughly. The melted polymer was poured into a mould and allowed to cool.

2. PROCEDURE FOR PRODUCING FILMS - SOLVENT CASTING

[0307] A known weight of PCL was weighed directly into a 20 ml glass scintillation vial and sufficient DCM to achieve a 10% w/v solution was added. The solution was mixed followed by the addition of sufficient paclitaxel to achieve the desired final paclitaxel concentration. The solution was vortexed to dissolve the paclitaxel, allowed to sit for one hour (to diminish the presence of air bubbles) and then poured slowly into a mould. The mould was placed in the fume hood overnight allowing the DCM to evaporate.

3. PROCEDURE FOR PRODUCING FILMS - SPRAYED

[0308] A sufficient amount of polymer was weighed directly into a 20 ml glass scintillation vial and sufficient DCM added to achieve a 2% w/v solution. The solution was mixed to dissolve the polymer. Using an automatic pipette, a suitable volume (minimum 5 ml) of the 2% polymer solution was transferred to a separate 20 ml glass scintillation vial. Sufficient paclitaxel was added to the solution and dissolved by shaking the capped vial. To prepare for spraying, the cap of the vial was removed and the barrel of the TLC atomizer dipped into the polymer solution.

[0309] The nitrogen tank was connected to the gas inlet of the atomizer and the pressure gradually increased until atomization and spraying began. The moulds were sprayed using 5 second oscillating sprays with a 15 second dry time between sprays. Spraying was continued until a suitable thickness of polymer was deposited on the mould.

EXAMPLE 26

THERAPEUTIC AGENT-LOADED POLYMERIC FILMS COMPOSED OF ETHYLENE VINYL ACETATE AND A SURFACTANT

[0310] Two types of films were investigated within this example: pure EVA films loaded with paclitaxel and EVA/surfactant blend films loaded with paclitaxel.

[0311] The surfactants being examined are two hydrophobic surfactants (Span 80 and Pluronic L101) and one hydrophilic surfactant (Pluronic F127). The Pluronic surfactants were themselves polymers which was an attractive property since they can be blended with EVA to optimize various drug delivery properties. Span 80 is a smaller molecule which disperses in the polymer matrix, and does not form a blend.

[0312] Surfactants were useful in modulating the release rates of paclitaxel from films and optimizing certain physical parameters of the films. One aspect of the surfactant blend films which indicated that drug release rates can be controlled was the ability to vary the rate and extent to which the compound swelled in water. Diffusion of water into a polymer-drug matrix was critical to the release of drug from the carrier. Figures 43C and 43D shows the degree of swelling of the films as the level of surfactant in the blend was altered. Pure EVA films did not swell to any significant extent in over 2 months. However, by increasing the level of surfactant added to the EVA it was possible to increase the degree of swelling of the compound, and by increasing hydrophilicity swelling was increased.

[0313] Results of experiments with these films are shown below in Figures 43A-E. Briefly, Figure 43A shows paclitaxel release (in mg) over time from pure EVA films. Figure 43B shows the percentage of drug remaining for the same films. As can be seen from these two figures, as paclitaxel loading increased *(i.e.,* percentage of paclitaxel by weight increased), drug release rates increased, showing the expected concentration dependence. As paclitaxel loading was increased, the percent paclitaxel remaining in the film also increased, indicating that higher loading may be more attractive for long-term release formulations.

[0314] Physical strength and elasticity of the films was assessed and is presented in Figure 43E. Briefly, Figure 43E shows stress/strain curves for pure EVA and EVA/surfactant blend films. This crude measurement of stress demonstrated that the elasticity of films was increased with the addition of Pluronic F127, and that the tensile strength (stress on breaking) was increased in a concentration dependent manner with the addition of Pluronic F127. Elasticity and strength are important considerations in designing a film which must be manipulated for particular clinical applications without causing permanent deformation of the compound.

[0315] The above data demonstrates the ability of certain surfactant additives to control drug release rates and to alter the physical characteristics of the vehicle.

EXAMPLE 27

PROCEDURE FOR PRODUCING NANOSPRAY

[0316] Nanospray is a suspension of small microspheres in saline. If the microspheres are very small *(i.e.,* under 1 μm in diameter) they form a colloid so that the suspension will not sediment under gravity. As is described in more detail below, a suspension of 0.1 μm to 1 μm microparticles may be created suitable for aerosolized deposition onto tissue directly at the time of surgery *(e.g.,* for vascular adhesions), *via* laproscopic intervention, or through a finger pumped aerosol *(e.g.,* to be delivered topically). Equipment and materials which was utilized to produce nanospray include 200 ml water jacketed beaker (Kimax or Pyrex), Haake circulating water bath, overhead stirrer and controller with 2 inch diameter (4 blade, propeller type stainless steel stirrer; Fisher brand), 500 ml glass beaker, hot plate/stirrer (Corning brand), 4 x 50 ml polypropylene centrifuge tubes (Nalgene), glass scintillation vials with plastic insert caps, table top centrifuge (Beckman), high speed centrifuge - floor model (JS 21 Beckman), Mettler analytical balance (AJ 100, 0.1 mg), Mettler digital top loading balance (AE 163, 0.01 mg), automatic pipetter (Gilson), sterile pipette tips, pump action aerosol (Pfeiffer pharmaceuticals) 20 ml, laminar flow hood, PCL (mol. wt. 10,000 to 20,000; Polysciences, Warrington, Pennsylvania USA), "washed" (see previous) EVA, PLA (mol. wt. 15,000 to 25,000; polysciences), polyvinyl alcohol ("PVA" - mol. wt. 124,000 to 186,000; 99% hydrolyzed; Aldrich Chemical Co., Milwaukee, WI USA), DCM or "methylene chloride"; HPLC grade Fisher scientific), distilled water, sterile saline (Becton and Dickenson or equivalent)

1. PREPARATION OF 5% (W/V) POLYMER SOLUTIONS

[0317] Depending on the polymer solution being prepared, the following were weighed directly into a 20 ml glass scintillation vial: 1.00 g of PCL or PLA or 0.50 g each of PLA and washed EVA. Using a measuring cylinder, 20 ml of DCM was added and the vial tightly capped. The vial was allowed to sit at room temperature (25°C) until all the polymer had dissolved.

2. PREPARATION OF 3.5% (W/V) STOCK SOLUTION OF PVA

[0318] The solution was prepared by following the procedure given below, or by diluting the 5% (w/v) PVA stock solution prepared for production of microspheres (see Example 28). Briefly, 17.5 g of PVA was weighed directly into a 600 ml glass beaker, and 500 ml of distilled water added. The beaker was covered and placed into a 2000 ml glass beaker containing 300 ml of water. The PVA was stirred at 300 rpm at 85°C until fully dissolved.

3. PROCEDURE FOR PRODUCING NANOSPRAY

[0319] Briefly, 100 ml of the 3.5% PVA solution was placed in the 200 ml water jacketed beaker with a connected Haake water bath. The contents of the beaker were stirred at 3000 rpm and 10 ml of polymer solution (polymer solution used based on type of nanospray being produced) was dipped into the stirring PVA over a period of 2 minutes using a 5 ml automatic pipetter. After 3 minutes, the stir speed was adjusted to 2500 rpm (+/- 200 rpm) for 2.5 hours. After 2.5 hours, the stirring blade was removed from the nanospray preparation and rinsed with 10 ml of distilled water allowing the rinse solution to go into the nanospray preparation.

[0320] The microsphere preparation was poured into a 500 ml beaker. The jacketed water bath was washed with 70 ml of distilled water allowing the 70 ml rinse solution to go into the microsphere preparation. The 180 ml microsphere preparation was stirred with a glass rod and poured equally into four polypropylene 50 ml centrifuge tubes which were centrifuged at 10,000 g (+/- 1000 g) for 10 minutes. The PVA solution was drawn off of each microsphere pellet and discarded. Distilled water (5 ml) was added to each centrifuge tube and vortexed. The four microsphere suspensions were pooled into one centrifuge tube using 20 ml of distilled water and centrifuged for 10 minutes at 10,000 g (+/- 1000 g). The supernatant was drawn off of the microsphere pellet and 40 ml of distilled water was added and the microsphere preparation was vortexed (this process was repeated 3x). The microsphere preparation was then transferred into a preweighed glass scintillation vial.

[0321] The vial was allowed to sit for 1 hour at room temperature (25°C) to allow the 2 μm and 3 μm diameter microspherers to sediment out under gravity. After 1 hour, the top 9 ml of suspension was drawn off, placed into a sterile capped 50 ml centrifuge tube, and centrifuged at 10,000 g (+/- 1000 g) for 10 minutes. The supernatant was discarded and the pellet was resuspended in 20 ml of sterile saline by centrifuging the suspension at 10,000 g (+/- 1000 g) for 10 minutes. The supernatant was discarded and the pellet was resuspended in sterile saline. The quantity of saline used was dependent on the final required suspension concentration (usually 10% w/v). The nanospray suspension was added to the aerosol.

EXAMPLE 28

MANUFACTURE OF MICROSPHERES

[0322] The equipment used for the manufacture of microspheres include: 200 ml water jacketed beaker (Kimax or Pyrex), Haake circulating water bath, overhead stirrer and controller with 2 inch diameter (4 blade, propeller type stainless steel stirrer - Fisher brand), 500 ml glass beaker, hot plate/stirrer (Coming brand), 4 X 50 ml polypropylene centrifuge tubes (Nalgene), glass scintillation vials with plastic insert caps, table top centrifuge (GPR Beckman), high speed centrifuge- floor model (JS 21 Beckman), Mettler analytical balance (AJ 100, 0.1 mg), Mettler digital top loading balance (AE 163, 0.01 mg), automatic pipetter (Gilson). Reagents include PCL (mol. wt. 10,000 to 20,000; Polysciences, Warrington Pennsylvania, USA), "washed" (see later method of "washing") EVA, PLA (mol. wt. 15,000 to 25,000; Polysciences), polyvinyl alcohol ("PVA" - mol. wt. 124,000 to 186,000; 99% hydrolyzed; Aldrich Chemical Co., Milwaukee WI, USA), DCM or "methylene chloride"; HPLC grade Fisher scientific, and distilled water.

A. Preparation of 5% (w/v) Polymer Solutions

[0323] DCL (1.00 g) or PLA, or 0.50 g each of PLA and washed EVA was weighed directly into a 20 ml glass scintillation vial. Twenty milliliters of DCM was then added. The vial was capped and stored at room temperature (25°C) for one hour (occasional shaking may be used), or until all the polymer was dissolved. The solution may be stored at room temperature for at least two weeks.

B. Preparation of 5% (w/v) Stock Solution of PVA

[0324] Twenty-five grams of PVA was weighed directly into a 600 ml glass beaker and 500 ml of distilled water was added, along with a 3 inch Teflon coated stir bar. The beaker was covered with glass to decrease evaporation losses, and placed into a 2000 ml glass beaker containing 300 ml of water. The PVA was stirred at 300 rpm at 85°C (Corning

hot plate/stirrer) for 2 hours or until fully dissolved. Dissolution of the PVA was determined by a visual check; the solution should be clear. The solution was then transferred to a glass screw top storage container and stored at 4°C for a maximum of two months. The solution, however must be warmed to room temperature before use or dilution.

C. Procedure for Producing Microspheres

[0325] Based on the size of microspheres being made (see Table 1), 100 ml of the PVA solution (concentrations given in Table 1) was placed into the 200 ml water jacketed beaker. Haake circulating water bath was connected to this beaker and the contents were allowed to equilibrate at 27°C (+/-1°C) for 10 minutes. Based on the size of microspheres being made (see Table I), the start speed of the overhead stirrer was set, and the blade of the overhead stirrer placed half way down in the PVA solution. The stirrer was then started, and 10 ml of polymer solution (polymer solution used based on type of microspheres being produced) was then dripped into the stirring PVA over a period of 2 minutes using a 5 ml automatic pipetter. After 3 minutes the stir speed was adjusted (see Table 1), and the solution stirred for an additional 2.5 hours. The stirring blade was then removed from the microsphere preparation, and rinsed with 10 ml of distilled water so that the rinse solution drained into the microsphere preparation. The microsphere preparation was then poured into a 500 ml beaker, and the jacketed water bath washed with 70 ml of distilled water, which was also allowed to drain into the microsphere preparation. The 180 ml microsphere preparation was then stirred with a glass rod, and equal amounts were poured into four polypropylene 50 ml centrifuge tubes. The tubes were then capped, and centrifuged for 10 minutes (force given in Table 1). Forty-five millileters of the PVA solution was drawn off of each microsphere pellet.

TABLE 1

PVA concentrations, stir speeds, and centrifugal force requirements for each diameter range of microspheres.			
PRODUCTION STAGE	MICROSPHERE DIAMETER RANGES		
	30 µm to 100 µm	10 µm to 30 µm	0.1 µm to 3 µm
PVA concentration	2.5% (w/v) (*i.e.*,) dilute 5% stock with distilled water	5% (w/v) (*i.e.*, undiluted stock)	3.5% (w/v) (*i.e.*, dilute 5% stock with distilled water
Starting Stir Speed	500 rpm +/- 50 rpm	500 rpm +/- 50 rpm	3000 rpm +/- 200 rpm
Adjusted Stir Speed	500 rpm +/- 50 rpm	500 rpm +/- 50 rpm	2500 rpm +/- 200 rpm
Centrifuge Force	1000 g +/- 100 g (Table top model)	1000 g +/- 100 g (Table top model)	10 000 g +/- 1000 g (High speed model)

[0326] Five milliliters of distilled water was then added to each centrifuge tube and vortexed to resuspend the microspheres. The four microsphere suspensions were then pooled into one centrifuge tube along with 20 ml of distilled water, and centrifuged for another 10 minutes (force given in Table 1). This process was repeated two additional times for a total of three washes. The microspheres were then centrifuged a final time, and resuspended in 10 ml of distilled water. After the final wash, the microsphere preparation was transferred into a preweighed glass scintillation vial. The vial was capped, and left overnight at room temperature (25°C) in order to allow the microspheres to sediment out under gravity. Since microspheres which fall in the size range of 0.1 um to 3 um do not sediment out under gravity, they were left in the 10 ml suspension.

D. Drying of 10 µm to 30 µm or 30 µm to 100 µm Diameter Microspheres

[0327] After the microspheres sat at room temperature overnight, the supernatant was drawn off of the sedimented microspheres. The microspheres were allowed to dry in the uncapped vial in a drawer for a period of one week or until they were fully dry (vial at constant weight). Faster drying may be accomplished by leaving the uncapped vial under a slow stream of nitrogen gas (flow approx. 10 ml/minute.) in the fume hood. When fully dry (vial at constant weight), the vial was weighed and capped. The labeled, capped vial was stored at room temperature in a drawer. Microspheres were normally stored no longer than 3 months.

E. Determining the Concentration of 0.1 µm to 3 µm Diameter Microsphere Suspension

[0328] This size range of microspheres did not sediment out, so they were left in suspension at 4°C for a maximum

of four weeks. To determine the concentration of microspheres in the 10 ml suspension, a 200 µl sample of the suspension was pipetted into a 1.5 ml preweighed microfuge tube. The tube was then centrifuged at 10,000 g (Eppendorf table top microfuge), the supernatant removed, and the tube allowed to dry at 50°C overnight. The tube was then reweighed in order to determine the weight of dried microspheres within the tube.

F. Manufacture of Paclitaxel Loaded Microsphere

[0329] In order to prepare paclitaxel containing microspheres, an appropriate amount of weighed paclitaxel (based upon the percentage of paclitaxel to be encapsulated) was placed directly into a 20 ml glass scintillation vial. Ten milliliters of an appropriate polymer solution was then added to the vial containing the paclitaxel, which was then vortexed until the paclitaxel dissolved.

[0330] Microspheres containing paclitaxel may then be produced essentially as described above in steps (C) through (E).

EXAMPLE 29

SURFACTANT COATED MICROSPHERES

A. Materials and Methods

[0331] Microspheres were manufactured from poly (DL) lactic acid (PLA), poly methylmethacrylate (PMMA), polycaprolactone (PCL) and 50:50 Ethylene vinyl acetate (EVA):PLA essentially as described above. Size ranged from 10 to 100 um with a mean diameter 45um.

[0332] Human blood was obtained from healthy volunteers. Neutrophils (white blood cells) were separated from the blood using dextran sedimentation and Ficoll Hypaque centrifugation techniques. Neutrophils were suspended at 5 million cells per ml in HBSS.

[0333] Neutrophil activation levels were determined by the generation of reactive oxygen species as determined by chemiluminescence. In particular, chemiluminescence was determined by using an LKB luminometer with 1 uM luminol enhancer. Plasma precoating (or opsonization) of microspheres was performed by suspending 10 mg of microspheres in 0.5 ml of plasma and tumbling at 37°C for 30 minutes.

[0334] Microspheres were then washed in 1 ml of HBSS and the centrifuged microsphere pellet added to the neutrophil suspension at 37°C at time t=0. Microsphere surfaces were modified using a surfactant called Pluronic F127 (BASF) by suspending 10 mg of microspheres in 0.5 ml of 2% w/w solution of F127 in HBSS for 30 minutes at 37°C. Microspheres were then washed twice in 1 ml of HBSS before adding to neutrophils or to plasma for further precoating.

B. Results

[0335] Figure 44 shows that the untreated microspheres give chemiluminescence values less than 50 mV. These values represent low levels of neutrophil activation. By way of comparison, inflammatory microcrystals might give values close to 1000 mV, soluble chemical activators might give values close to 5000 mV. However, when the microspheres are precoated with plasma, all chemiluminescence values are amplified to the 100 to 300 mV range (Figure 44). These levels of neutrophil response or activation can be considered mildly inflammatory. PMMA gave the biggest response and could be regarded as the most inflammatory. PLA and PCL both become three to four times more potent in activating neutrophils after plasma pretreatment (or opsonization) but there is little difference between the two polymers in this regard. EVA:PLA is not likely to be used in angiogenesis formulations since the microspheres are difficult to dry and resuspend in aqueous buffer. This effect of plasma is termed opsonization and results from the adsorption of antibodies or complement molecules onto the surface. These adsorbed species interact with receptors on white blood cells and cause an amplified cell activation.

[0336] Figures 45-48 describe the effects of plasma precoating of PCL, PMMA, PLA and EVA:PLA respectively as well as showing the effect of Pluronic F127 precoating prior to plasma precoating of microspheres. These figures all show the same effect: (1) plasma precoating amplifies the response; (2) Pluronic F127 precoating has no effect on its own; (3) the amplified neutrophil response caused by plasma precoating can be strongly inhibited by pretreating the microsphere surface with 2% Pluronic F127.

[0337] The nature of the adsorbed protein species from plasma was also studied by electrophoresis. Using this method, it was shown that pretreating the polymeric surface with Pluronic F127 inhibited the adsorption of antibodies to the polymeric surface.

[0338] Figures 49-52 likewise show the effect of precoating PCL, PMMA, PLA or EVA:PLA microspheres (respectively) with either IgG (2 mg/ml) or 2% Pluronic F127 then IgG (2 mg/ml). As can be seen from these figures, the

amplified response caused by precoating microspheres with IgG can be inhibited by treatment with Pluronic F127.

[0339] This result shows that by pretreating the polymeric surface of all four types of microspheres with Pluronic F127, the "inflammatory" response of neutrophils to microspheres may be inhibited.

EXAMPLE 30

THERAPEUTIC AGENT ENCAPSULATION IN POLY(E-CAPROLACTONE) MICROSPHERES. INHIBITION OF ANGIOGENESIS ON THE CAM ASSAY BY PACLITAXEL-LOADED MICROSPHERES

[0340] This example evaluates the *in vitro* release rate profile of paclitaxel from biodegradable microspheres of poly (ε-caprolactone) (PCL) and demonstrates the *in vivo* anti-angiogenic activity of paclitaxel released from these microspheres when placed on the CAM.

[0341] Reagents which were utilized in these experiments include: PCL (molecular weight 35,000 - 45,000; purchased from Polysciences (Warrington, PA)); DCM from Fisher Scientific Co., Canada; polyvinyl alcohol (PVP) (molecular weight 12,000 - 18,000, 99% hydrolysed) from Aldrich Chemical Co. (Milwaukee, Wis.), and paclitaxel from Sigma Chemical Co. (St. Louis, MO). Unless otherwise stated all chemicals and reagents are used as supplied. Distilled water is used throughout.

A. Preparation of microspheres

[0342] Microspheres were prepared essentially as described in Example 28 utilizing the solvent evaporation method. Briefly, 5%w/w paclitaxel-loaded microspheres were prepared by dissolving 10 mg of paclitaxel and 190 mg of PCL in 2 ml of DCM, adding to 100 ml of 1% PVP aqueous solution and stirring at 1000 rpm at 25°C for 2 hours. The suspension of microspheres was centrifuged at 1000 x g for 10 minutes (Beckman GPR), the supernatant removed and the microspheres washed three times with water. The washed microspheres were air-dried overnight and stored at room temperature. Control microspheres (paclitaxel absent) were prepared as described above. Microspheres containing 1% and 2% paclitaxel were also prepared. Microspheres were sized using an optical microscope with a stage micrometer.

B. Encapsulation efficiency

[0343] A known weight of drug-loaded microspheres (about 5 mg) was dissolved in 8 ml of acetonitrile and 2 ml distilled water was added to precipitate the polymer. The mixture was centrifuged at 1000 g for 10 minutes and the amount of paclitaxel encapsulated was calculated from the absorbance of the supernatant measured in a UV spectrophotometer (Hewlett-Packard 8452A Diode Array Spectrophotometer) at 232 nm.

C. Drug release studies

[0344] About 10 mg of paclitaxel-loaded microspheres were suspended in 20 ml of 10 mM PBS (pH 7.4) in screw-capped tubes. The tubes were tumbled end-over-end at 37°C and at given time intervals 19.5 ml of supernatant was removed (after allowing the microspheres to settle at the bottom), filtered through a 0.45 μm membrane filter and retained for paclitaxel analysis. An equal volume of PBS was replaced in each tube to maintain sink conditions throughout the study. The filtrates were extracted with 3 x 1 ml DCM, the DCM extracts evaporated to dryness under a stream of nitrogen, redissolved in 1 ml acetonitrile and analyzed by HPLC using a mobile phase of water:methanol:acetonitrile (37:5:58) at a flow rate of 1 ml/minute (Beckman Isocratic Pump), a C8 reverse phase column (Beckman), and UV detection (Shimadzu SPD A) at 232 nm.

D. CAM studies

[0345] Fertilized, domestic chick embryos were incubated for 4 days prior to shell-less culturing. On day 6 of incubation, 1 mg aliquots of 5% paclitaxel-loaded or control (paclitaxel-free) microspheres were placed directly on the CAM surface. After a 2-day exposure the vasculature was examined using a stereomicroscope interfaced with a video camera; the video signals were then displayed on a computer and video printed.

E. Scanning electron microscopy

[0346] Microspheres were placed on sample holders, sputter-coated with gold and then placed in a Philips 501B SEM operating at 15 kV.

F. Results

[0347] The size range for the microsphere samples was between 30 - 100 µm, although there was evidence in all paclitaxel-loaded or control microsphere batches of some microspheres falling outside this range. The efficiency of loading PCL microspheres with paclitaxel was always greater than 95% for all drug loadings studied. Scanning electron microscopy demonstrated that the microspheres were all spherical and many showed a rough or pitted surface morphology. There appeared to be no evidence of solid drug on the surface of the microspheres.

[0348] The time courses of paclitaxel release from 1%, 2% and 5% loaded PCL microspheres are shown in Figure 53A. The release rate profiles were biphasic. There was an initial rapid release of paclitaxel or "burst phase" at all drug loadings. The burst phase occurred over 1-2 days at 1% and 2% paclitaxel loading and over 3-4 days for 5% loaded microspheres. The initial phase of rapid release was followed by a phase of significantly slower drug release. For microspheres containing 1% or 2% paclitaxel there was no further drug release after 21 days. At 5% paclitaxel loading, the microspheres had released about 20% of the total drug content after 21 days.

[0349] Figure 53B shows CAMs treated with control PCL microspheres, and Figure 53C shows treatment with 5% paclitaxel loaded microspheres. The CAM with the control microspheres showed a normal capillary network architecture. The CAM treated with paclitaxel-PCL microspheres showed marked vascular regression and zones which were devoid of a capillary network.

G. Discussion

[0350] The solvent evaporation method of manufacturing paclitaxel-loaded microspheres produced very high paclitaxel encapsulation efficiencies of between 95-100%. This was due to the poor water solubility of paclitaxel and its hydrophobic nature favoring partitioning in the organic solvent phase containing the polymer.

[0351] The biphasic release profile for paclitaxel was typical of the release pattern for many drugs from biodegradable polymer matrices. Poly(ε-caprolactone) is an aliphatic polyester which can be degraded by hydrolysis under physiological conditions and it is non-toxic and tissue compatible. The degradation of PCL is significantly slower than that of the extensively investigated polymers and copolymers of lactic and glycolic acids and is therefore suitable for the design of long-term drug delivery systems. The initial rapid or burst phase of paclitaxel release was thought to be due to diffusional release of the drug from the superficial region of the microspheres (close to the microsphere surface). Release of paclitaxel in the second (slower) phase of the release profiles was not likely due to degradation or erosion of PCL because studies have shown that under *in vitro* conditions in water there was no significant weight loss or surface erosion of PCL over a 7.5-week period. The slower phase of paclitaxel release was probably due to dissolution of the drug within fluid-filled pores in the polymer matrix and diffusion through the pores. The greater release rate at higher paclitaxel loading was probably a result of a more extensive pore network within the polymer matrix.

[0352] Paclitaxel microspheres with 5% loading have been shown to release sufficient drug to produce extensive inhibition of angiogenesis when placed on the CAM. The inhibition of blood vessel growth resulted in an avascular zone as shown in Figure 53C.

EXAMPLE 31

MANUFACTURE OF PLGA MICROSPHERES

[0353] Microspheres were manufactured from lactic acid-glycolic acid copolymers (PLGA).

A. Method

[0354] Microspheres were manufactured in the size ranges 0.5 to 10 µm, 10-20 µm and 30-100 µm using standard methods (polymer was dissolved in dichloromethane and emulsified in a polyvinyl alcohol solution with stirring as previously described in PCL or PDLLA microspheres manufacture methods). Various ratios of PLLA to GA were used as the polymers with different molecular weights (given as Intrinsic Viscosity (I.V.))

B. Result

[0355] Microspheres were manufactured successfully from the following starting polymers:

PLLA	GA	I.V.
50	50	0.74

(continued)

50	50	0.78
50	50	1.06
65	35	0.55
75	25	0.55
85	15	0.56

[0356] Paclitaxel at 10% or 20% loadings was successfully incorporated into all these microspheres. Examples of size distributions for one starting polymer (85:15, IV=0.56) are given in Figures 54-57. Paclitaxel release experiments were performed using microspheres of various sizes and various compositions. Release rates are shown in Figures 58-61.

EXAMPLE 32

ENCAPSULATION OF PACLITAXEL IN NYLON MICROCAPSULES

[0357] Therapeutic agents may also be encapsulated in a wide variety of carriers which may be formed into a selected form or device. For example, as described in more detail below, paclitaxel may be incorporated into nylon microcapsules which may be formulated into artificial heart valves, vascular grafts, surgical meshes, or sutures.

A. Preparation of paclitaxel-loaded microcapsules

[0358] Paclitaxel was encapsulated into nylon microcapsules using the interfacial polymerization techniques. Briefly, 100 mg of paclitaxel and 100 mg of Pluronic F-127 was dissolved in 1 ml of DCM and 0.4 ml (about 500 mg) of adipoyl chloride (ADC) was added. This solution was homogenized into 2% PVA solution using the Polytron homogenizer (1 setting) for 15 seconds. A solution of 1,6-hexanediamine (HMD) in 5 ml of distilled water was added dropwise while homogenizing. The mixture was homogenized for a further 10 seconds after the addition of HMD solution. The mixture was transferred to a beaker and stirred with a magnetic stirrer for 3 hours. The mixture was centrifuged, collected and resuspended in 1 ml distilled water.

B. Encapsulation efficiency/paclitaxel-loading

[0359] About 0.5 ml of the suspension was filtered and the microspheres were dried. About 2.5 mg of the microcapsules was weighed and suspended in 10 ml of acetonitrile for 24 hours. The supernatant analyzed for paclitaxel and the result was expressed as a percentage of paclitaxel. Preliminary studies have shown that paclitaxel could be encapsulated in nylon microcapsules at a high loading (up to 60%) and high encapsulation efficiency (greater than 80%).

C. Paclitaxel release studies

[0360] About 2.5 mg of the paclitaxel-nylon microspheres were suspended in 50 ml water containing 1 M each of sodium chloride and urea and analyzed periodically. Release of paclitaxel from the microcapsule was fast with more than 95% of the drug released after 72 hours (Figure 62).

EXAMPLE 33

BIOADHESIVE MICROSPHERES

A. Preparation of bioadhesive microspheres

[0361] Microspheres were made from 100k g/mol PLLA with a particle diameter range of 10-60 μm. The microspheres were incubated in a sodium hydroxide solution to produce carboxylic acid groups on the surface by hydrolysis of the polyester. The reaction was characterized with respect to sodium hydroxide concentration and incubation time by measuring surface charge. The reaction reached completion after 45 minutes of incubation in 0.1 M sodium hydroxide. Following base treatment, the microspheres were coated with dimethylaminoproylcarbodiimide (DEC), a crosslinking agent, by suspending the microspheres in an alcoholic solution of DEC and allowing the mixture to dry into a dispersible powder. The weight ratio of microspheres to DEC was 9:1. After the microspheres were dried, they were dispersed

with stirring into a 2% w/v solution of poly (acrylic acid) (PAA) and the DEC allowed to react with PAA to produce a water insoluble network of cross-linked PAA on the microspheres surface. Scanning electron microscopy was used to confirm the presence of PAA on the surface of the microspheres.

[0362] Differential scanning calorimetry of the microspheres before and after treatment with base revealed that no changes in bulk thermal properties (Tg, melting, and degree of crystallinity) were observed by SEM.

B. *In vitro* paclitaxel release rates

[0363] Paclitaxel-loaded microspheres (10% and 30% w/w loadings) with the same particle diameter size range were manufactured and *in vitro* release profiles for 10 days release in PBS. Release was proportional to drug loading, with 400 µg of paclitaxel released from 5 mg of 30% loaded microspheres in 10 days and 150 µg released from 10% loaded microspheres in the same period. The efficiency of encapsulation was about 80%. The paclitaxel-loaded microspheres were incubated in 0.1 M sodium hydroxide for 45 minutes and the zeta potential measured before and after incubation in sodium hydroxide. The surface charge of paclitaxel-loaded microspheres was lower than microspheres with no paclitaxel both before and after treatment with base.

C. Preparation and *in vitro* evaluation of PLLA coated with either poly-lysine or fibronectin

[0364] PLLA microspheres were prepared containing 1% sudan black (to color the microspheres). These spheres were suspended in a 2% (w/volume) solution of either poly-lysine (Sigma chemicals - Hydrobromell form) or fibronectin (Sigma) for 10 minutes. The microspheres were washed in buffer once and placed on the inner surface of freshly prepared bladders from rats. The bladder were left for 10 minutes then washed three times in buffer. Residual (bound) microspheres were present on the bladder wall after the process therefore showing bioadhesion had occurred (Figures 63A and 63B) for both fibronectin-and poly-1-lysine-coated microspheres.

EXAMPLE 34 (Reference example)

PREVENTION OF ARTHRITIS ONSET BY PACLITAXEL IN THE CIA RAT MODEL

A. Materials and Methods

[0365] Syngeneic female Louvain rats weighing 120 to 150 grams were injected intradermally with 0.5 mg of native chick collagen II (Genzyme, Boston, MA) solubilized in 0.1 M acetic acid and emulsified in FIA (Difco, Detroit, MI). Approximately 9 days after immunization, animals developed a polyarthritis with histologic changes of pannus formation and bone/cartilage erosions. A total of 45 rats in 4 protocols were used: a control group (n=17) that received vehicle alone and 3 paclitaxel treatment groups consisting of a prevention and 2 suppression protocols. In order to evaluate the effect of paclitaxel, paclitaxel (solubilized in 1:1 dilution of ethanol and Cremophor E.L.® (Sigma) and added to saline for a final concentration of 4.8 mg/ml paclitaxel in 5% w/v ethanol and Cremophor E.L.) was administered intra-peritoneally (i.p.) beginning on day 2 after immunization (prevention protocol) or at arthritis onset on day 9 (suppression protocol). For the prevention protocol (n=8), paclitaxel was given at a concentration of 1 mg/kg body weight starting on day 2 with 5 subsequent doses on days 5, 7, 9, 12 and 14. For the high dose suppression protocol (n=10), paclitaxel (1 mg/kg body weight) was given on alternate days starting on day 9. In the low dose suppression protocol (n=10), paclitaxel was given at 1 mg/kg body weight on days 9, 11 and 13 and then at 75% of this does level (0.75 mg/kg body weight) on alternate days through to day 21. The control and experimental animals were evaluated for disease severity both clinically and radiographically by individuals blinded to treatment groups.

[0366] The severity of inflammation for each limb was evaluated daily and scored based on standardized levels of swelling and periarticular erythema (0 being normal and 4 severe). Animals were evaluated radiographically on day 28 of the experiment. The radiographs of both hind limbs were graded by the degree of soft tissue swelling, joint space narrowing, bone destruction, and periosteal new bone formation. A scale of 0-3 was used to quantify each limb (0 = normal, 1 = soft tissue swelling, 2 = early erosions of bone, 3 = severe bone destruction and/or ankylosis). Histological assessment of the joints was completed at the conclusion of the experiment.

[0367] Delayed-type hypersensitivity (DTH) to CII was determined by a radiometric ear assay completed on day 28. Radiometric ear indices ≥ 1.4 represent a significant response to CII. The presence of anti-CII IgG antibodies was determined by enzyme-linked immunosorbent assay (ELISA). Serum samples obtained on day 26 were diluted to 1: 2,560, and the results were expressed as the mean optical density at 490 nm, in quadruplicate aliquots. Background levels in normal rat serum at this dilution are 0 and are readily distinguishable from collagen-immunized rat serum.

B. Results

[0368] In this model, paclitaxel treatment instituted prior to arthritis onset completely precluded development of the disease in all rats treated (even after the discontinuation of paclitaxel treatment) compared with the vehicle control group.

[0369] In control animals there was a progressive increase in clinical symptoms of disease until deformity and loss of joint function occurred. Animals that received both low- and high-dose paclitaxel after the onset of arthritis demonstrated significant clinical improvement. On average, the clinical scores were equivalent to those seen at the initiation of treatment, indicating an ability of paclitaxel to prevent clinical progression of the disease.

[0370] Animals receiving paclitaxel were able to weight bear and ambulate and demonstrated few, if any toxic effects of the treatment. Wound healing and hair regrowth at the vaccination site was observed in treated animals. Paclitaxel-treated animals gained weight relative to controls.

[0371] None of the rats in the paclitaxel arthritis prevention protocol manifested any radiographic changes or clinical arthritis. Both the high- and low-dose paclitaxel groups had significantly less radiographic disease compared with control group. Further histological assessment revealed that control group rats demonstrated marked pannus, with bone and cartilage erosions, however, paclitaxel-treated rats had minimal if any pannus, with preservation of articular cartilage.

[0372] Using an ELISA assay, IgG antibodies to type II collagen were significantly lower in paclitaxel-treated rats as compared to control group; rats in the prevention protocol had significantly lower IgG antibodies when compared to the rats in the high and low paclitaxel dose suppression protocols.

C. Discussion

[0373] Paclitaxel is a viable treatment for arthritis and potentially other types of autoimmune disease since it blocks the disease process when administered after immunization but prior to arthritis onset. The results indicate that paclitaxel could completely abrogate arthritis onset if initiated 2 days after CII immunization. With paclitaxel treatment in the suppression protocol, the severity of arthritis continued to decrease throughout the duration of paclitaxel administration but began to rise within 4 days after the cessation of treatment in both suppression protocols. However, early intervention with paclitaxel appeared to attenuate the need for continuous therapy.

EXAMPLE 35 (Reference example)

REGRESSION OF COLLAGEN-INDUCED ARTHRITIS WITH PACLITAXEL

[0374] Paclitaxel demonstrated disease-modifying effects in the CIA model when administered systemically in a micellar formulation. In order to evaluate the potential disease-modifying effect of paclitaxel, micellar (Cremophor-free) paclitaxel was administered intraperitoneally (i.p.), every four days (q.o.d.) at 5 mg/kg (group 1) or 10 mg/kg (group 2) to immunized animals at the onset of clinically detectable arthritis (day 9). Paclitaxel was administered throughout the evaluation period. As a comparison with standard therapy, a third group received methotrexate at 0.3 mg/kg i.p. (human equivalent dose) on days 0, 5 and 10 post-arthritis onset. A fourth group received methotrexate (0.3 mg/kg) and micellar paclitaxel (10 mg/kg) combination therapy. The control (group 5) and experimental animals were evaluated for disease severity both clinically and radiographically by individuals blinded to treatment groups.

[0375] The severity of inflammation for each limb was evaluated daily and scored based on standardized levels of swelling and periarticular erythema (0 being normal and 4 severe). Animals were evaluated radiographically on day 28 of the experiment. The radiographs of both hind limbs were graded by the degree of soft tissue swelling, joint space narrowing, bone destruction and periosteal new bone formation; a scale of 0 to 3 was used to quantify each hind limb (0 = normal, 1 = soft tissue swelling, 2 = early erosions of bone, 3 = severe bone destruction and/or ankylosis) (Brahn et al., *Arthritis Rheum.* 37: 839-845, 1994; Oliver et al., *Cell. Immunol.*, 157: 291-299, 1994). Histological assessment of the joints was completed at the conclusion of the experiment.

[0376] In this model, micellar paclitaxel treatment instituted prior to arthritis onset completely precluded development of the disease even after the discontinuance of paclitaxel treatment. In control animals, there was a progressive increase in clinical symptoms of disease (Figure 64) until deformity and loss of joint function occurred. Animals receiving methotrexate therapy were not statistically improved as compared to controls (Figure 64 & Table 1). Animals that received low dose micellar paclitaxel (5 mg/kg) after the onset of arthritis demonstrated some improvement, but animals that received doses of micellar paclitaxel at 10 mg/kg demonstrated a highly significant (p=0.0002) clinical improvement (Figure 64). On average, the clinical scores were equivalent to those seen at the initiation of treatment, indicating an ability of micellar paclitaxel to prevent clinical progression of the disease (Table 1).

TABLE 1

Micellar Paclitaxel Improves Clinical Indices in the Collagen-Induced Arthritis Rat Model			
	Arthritic Index on Day 10	Maximum Mean Arthritis Score	Antibody to Collagenase II
Arthritic Controls (n=11)	6.1 ± 0.6	6.4 ± 0.5	0.199 ± 0.0042
Methotrexate (0.3 mg/kg) (n=5)	5.4 ± 0.6 (P = NS)	5.7 ± 0.6 (p = NS)	0.182 ± 0.0034 (p < 0.03)
Micellar Paclitaxel (5 mg/kg) (n=4)	4.3 ± 1.8 (P = NS)	4.3 ± 1.8 (p = NS)	0.176 ± 0.0042 (p < 0.01)
Micellar Paclitaxel (10 mg/kg) (n=5)	2.0 ± 0.7 (p = 0.0002)	3.8 ± 0.7 (p = 0.0002)	0.162 ± 0.0194 (p < 0.02)
Micellar Paclitaxel (10 mg/kg)/ Methotrexate (0.3 mg/kg) Combo (n=7)	1.1 ± 0.5 (p=0.0001)	3.6 ± 0 9 (p≤0.0001)	0.164 ± 0.0090 (p<0.001)

• The arthritic index quantified levels of swelling and periarticular erythema, with 0 representing normal and 4 representing severe, and maximum possible score of 8 for the sum of the hind limbs. T-tests compared drug-treated rats to control collagen-induced arthritis rats at day 10 post-arthritis onset.

• Clinical scores of the paclitaxel-treated animals were significantly lower than control animals and were equivalent to those seen at the initiation of treatment, indicating an ability to prevent progression of disease.

• NS = not significant.

[0377] Animals receiving micellar paclitaxel were able to bear weight and ambulate and did not show any toxic effects of the treatment. Wound healing and hair regrowth at the vaccination site was observed in treated animals. Micellar paclitaxel-treated animals gained weight relative to untreated controls. Animals receiving both micellar paclitaxel and methotrexate tolerated the therapy well and showed impressive clinical improvement ($p \leq 0.0001$), relative to controls (Figure 64). Using an enzyme linked immunosorbant antibody (ELISA) assay, IgG antibodies to type II collagen were lower in paclitaxel and combination (MTX/paclitaxel)-treated rats as compared to controls.

[0378] Radiographic studies also demonstrated a significant improvement with paclitaxel therapy. While control and methotrexate-treated animals displayed radiographic evidence of soft tissue swelling, joint space narrowing, bone destruction and periosteal new bone formation, paclitaxel-treated animals had almost normal joint features on x-ray (Figure 65).

[0379] In fact, only a small percentage (17 to 18%) of animals receiving micellar paclitaxel alone (10 mg/kg) or in combination with methotrexate developed cartilage erosions. Cartilage erosions, an important indicator of disease progression/outcome, occur four times more frequently in control animals (72%) or those receiving methotrexate alone than in animals receiving micellar paclitaxel therapy (Table 2).

TABLE 2

Micellar Paclitaxel Improves Radiographic Indices in Collagen-Induced Arthritis Rats		
	Percentage of Animals with Erosions	Radiographic Score
Arthritic Controls (n = 32)	72%	4.31 ± 0.45
Methotrexate (0.3 mg/kg) (n = 17)	76% (p = NS)	4.25 ± 0.64 (p = NS)
Micellar Paclitaxel (5 mg/kg) (n = B)	50% (p = NS)	3.25 ± 1.60 (p = NS)
Micellar Paclitaxel (10 mg/kg) (n=18)	17% (p=0.0005)	1.78 ± 0.60 (p <0.003)
Micellar Paclitaxel (10 mg/kg)/ Methotrexate (0.3 mg/kg) Combo (n = 22)	18% (p=0.0003)	1.45 ± 0.39 (P <0.0001)

• Radiographs of both hind limbs, of collagen-induced arthritis (CIA) rats, were graded by the degree of soft tissue swelling, Joint space narrowing, bone destruction and periosteal new bone formation. An integer scale of 0 to 3 was used to quantify each limb, with a maximum possible score of 6 from the sum of both limbs.

TABLE 2 (continued)

Micellar Paclitaxel Improves Radiographic Indices in Collagen-Induced Arthritis Rats		
	Percentage of Animals with Erosions	Radiographic Score
• The presence of cartilage erosions, an important indicator of disease progression/outcome, occurs four times more frequently in control animals (72%) than in animals receiving micellar paclitaxel therapy (18%).		

[0380] Scanning electron micrographs illustrate the chondroprotective effects of paclitaxel therapy *in vivo*. The normal articular surface is characterized by a smooth intact cartilage matrix surrounded by a thin synovial lining (Figure 66A). In CIA, the cartilage surface is eroded by MMP produced by pannus tissue and an inflamed synovium (Figure 66B). The superficial cartilage matrix is digested, exposing chondrocytes or the empty lacunae they once occupied (Figure 66B inset). In animals with CIA that received paclitaxel treatment after the onset of clinical arthritis, the joint surface remained intact (Figure 66C) and the cartilage matrix appeared largely normal, even at high magnification (Figure 66C inset). Pannus tissue formation and synovial hypertrophy was not seen in paclitaxel-treated groups.

[0381] Histologically, CIA is characterized by marked synovial hypertrophy, inflammatory cell infiltration of the synovium and cartilage destruction (Figure 67A). In paclitaxel-treated animals, the synovium appeared normal, with only 1-2 layers of synoviocytes and no inflammatory cell infiltrate (Figure 67B).

[0382] Corrosion casts were also evaluated to determine if paclitaxel was capable of blocking angiogenesis in the synovium of animals with CIA. Mercox polymer was infused into the femoral artery of sacrificed animals at a pressure of 100 mmHg, allowed to solidify *in situ* and the tissues subsequently digested to produce a cast of the lower limb vasculature. Scanning electron micrographs of casts of the synovial vasculature in animals with CIA revealed blind-ended capillary sprouts projecting inwards towards the joint space (Figure 68A). These vessels appeared morphologically similar to growing angiogenic vessels described in solid tumors and other angiogenic conditions (Figure 68A inset). In contrast, the synovial vessels of paclitaxel-treated animals were arranged in capillary loops (Figure 68B) with no evidence of neovascular sprouts.

[0383] There was involution of vessel proliferation and morphologic vascular structures in paclitaxel/MTX recipients similar to that found in naive controls. These studies suggest that micellar paclitaxel and combination paclitaxel/methotrexate therapy, can regress neovascularization, inhibit inflammatory processes, involute established synovitis and prevent joint destruction.

[0384] It has been demonstrated that systemic administration of paclitaxel is a viable treatment for arthritis. The natural course of the disease is to flare and remit, with each successive flare resulting in additive damage which ultimately leads to joint destruction. The potential exists for short-term, higher dose, systemic therapy to be used to induce remission of the disease or sustained low dose therapy to maintain disease control. Alternative methods of delivering paclitaxel include direct intra-articular injection of the drug into afflicted joints in patients with 1 or 2 joint predominant disease.

EXAMPLE 36 (Reference example)

EVALUATION OF PACLITAXEL FORMULATIONS IN ANIMAL MODELS OF PSORIASIS

A. Skin Angiogenesis Model

[0385] A novel animal model is used to investigate skin-specific angiogenesis. Immunodeficient SCID mice are used as recipients for surface transplants of human keratinocyte lines transfected with vascular endothelial growth factor (VEGF) in sense or antisense orientation. Keratinocytes are transplanted *via* use of modified silicone transplantation chamber assay onto the skin of recipient mice. Keratinocytes are allowed to differentiate and to induce skin angiogenesis. Paclitaxel is then given either systemically or topically (cream, ointment, lotion, gel), and morphometric measurements of vessel numbers and sizes are performed in untreated and treated groups.

B. Mouse model for cutaneous delayed-type hypersensitivity reactions

[0386] The mouse model for cutaneous delayed type hypersensitivity reactions was used to investigate the effects of paclitaxel on induced skin inflammation. Briefly, mice were sensitized to oxazolone by topical application of the compound onto the skin. Five days later, mice were challenged with oxazolone by topical application onto the ear skin (left ear: oxazolone, right ear: vehicle alone), resulting in a cutaneous inflammatory, "delayed-type hypersensitivity" reaction. The extent of inflammation was quantified by measurements of the resulting ear swelling over a period of 48

hours (see Figures 69 and 70). Epon-embedded, Giesma-stained, 1 μm tissue sections were evaluated for the presence of inflammatory cells, for the presence of tissue mast cells and their state of activation, and for the degree of epidermal hyperplasia. Paclitaxel was given either systemically or topically to quantitate its effect on the cutaneous inflammatory reaction in this *in vivo* model.

C. Results

[0387] These studies have shown that topical administration of 1% paclitaxel versus vehicle alone in the treatment of experimentally-induced skin inflammation in mice revealed that paclitaxel exerts inhibitory effects on skin inflammation. In experimentally-induced delayed-type hypersensitivity reactions, there was a significant decrease in ear swelling in the ears treated topically with 1% paclitaxel versus vehicle alone. Topical application of 1% paclitaxel formulation significantly inhibited ear swelling and skin erythema (redness) induced by topical application of PMA (phorbol 12-myristol 13-acetate) (see Figures 71 and 72). As illustrated in Figure 73, the paclitaxel treated ear (right ear) was normal in appearance when compared to controls (left ear). Similar results were obtained in a total of 5 mice.

[0388] To assess the skin irritation of 1% paclitaxel versus vehicle alone, application of these two formulations werer applied daily at 20 μl to each side of the ears for 8 days. After 8 days, there was no detection of skin irritation after application of either vehicle alone or 1% paclitaxel formulation onto normal or inflamed mouse ear skin.

EXAMPLE 37 (Reference example)

EVALUATION OF CHRONIC REJECTION IN AN ANIMAL MODEL

[0389] An accelerated form of atherosclerosis develops in the majority of cardiac transplant recipients and limits long-term graft survival. The Lewis-F344 heterotopic rat cardiac transplantation model of chronic rejection is a useful experimental model because it produces atherosclerotic lesions in stages, in medium and long-term surviving allografts. The advantages of the Lewis-F344 model are that:
(i) the incidence and severity of atherosclerotic lesions in long-surviving grafts is quite high; and (ii) an inflammatory stage of lesion development is easily recognized since this system does not require immunosuppression.

[0390] Adult male Lewis rats serve as donors and F-344 rats as recipients. Twenty heterotopic abdominal cardiac allografts are transplanted by making a long midline abdominal incision in anesthetized recipients to expose the aorta and inferior vena cava. The two vessels are separated from each other and from the surrounding connective tissue and small clamps are placed on the vessels. Longitudinal incisions (2 to 3 mm) are made in each vessel at the site of anastomosis.

[0391] The abdomen of anesthetized donor rat is opened for injection of 300 units of aqueous heparin into the inferior vena cava. The chest wall is opened to expose the heart. Venae cavae are ligated, followed by the transection of the ascending aorta and main pulmonary artery, with vessel origins 2 to 3 mm in length left attached to the heart. Venae cavae distal to the ligatures are divided and the ligature placed around the mass of the left atrium and pulmonary veins. Vessels on the lung side of the ligatures are divided and the heart is removed.

[0392] The donor heart is placed in the abdominal cavity of the recipient and the aortae are sutured together at the site of incision on the recipient vessel. Similarly, the pulmonary artery is connected to the incision site on the inferior vena cava in a similar manner. Vessel clamps are released (proximal vena cava, distal cava and aorta, and proximal aorta) to minimize bleeding from the needle holes.

[0393] Following transplantation, paclitaxel (33%) in polycaprolactone (PCL) paste (n=10) or PCL paste alone (n=10) is injected through the epicardium over a length of the outer surface of a coronary artery in 10 rats, such that the artery area embedded in the myocardium remains untreated.

[0394] All recipients receive a single intramuscular injection of penicillin G (100,000 units) at the time of grafting. Allografts are followed by daily palpation and their function assessed on a scale of 1 to 4, with 4 representing a normal heartbeat and 0 the absence of mechanical activity. Five rats from each group are sacrificed at 14 days and the final five at 28 days. The rats are observed for weight loss and other signs of systemic illness. After 14 or 28 days, the animals are anesthetized and the heart exposed in the manner of the initial experiment. Coated and uncoated coronary arteries are isolated, fixed in 10% buffered formaldehyde and examined for histology.

[0395] The initial experiment can be modified for the use of paclitaxel/EVA film or coated stents in the coronary arteries following transplantation. The EVA film is applied to the extraluminal surface of the coronary artery in a similar manner as above, while the coated stent is placed intraluminally.

[0396] In addition, these investigations can be further extended to include other organ transplants as well as graft transplants (*e.g.*, vein, skin).

EXAMPLE 38

EFFECTS OF PACLITAXEL IN AN ANIMAL MODEL OF MS

[0397] The ability of paclitaxel micelles to inhibit the progression of MS symptoms and pathogenesis in a demyelinating transgenic mouse model (Mastronardi et al., *J Neurosci. Res.* 36:315-324, 1993) was examined. These transgenic mice contain 70 copies of the transgene DM20, a myelin proteolipid. Clinically, the animals appear normal up to 3 months of age. After 3 months, evidence of neurological pathology, such as seizures, shaking, hind limb mobility, unsteadiness of gait, limp tail, wobbly gait and reduction in the degree of activity, appear and progressively increase in severity until the animals die between 6 and 8 months of age. Clinical signs correlate histologically with demyelination and increased fibrous astrocyte proliferation in the brain (Mastronardi et al., *J. Neurosci. Res. 36*:315-324, 1993).

A. Materials and Methods

[0398] Two animal studies were carried out using subcutaneous administration of either a low dose continuous therapy paclitaxel protocol (2.0 mg/kg; 3x per week, total of 10 injections) or a high dose "pulse" therapy paclitaxel protocol (20 mg/kg; four times, once weekly) initiated at the clinical onset of disease (approximately 4 months of age). For the low dose protocol, 5 animals received micellar paclitaxel, two mice were used as controls; one mouse was an untreated normal and one was an untreated transgenic littermate. Only one transgenic mcuse was used as a control because the course of the disease has been well established in the laboratory. Four month old animals were injected with micellar paclitaxel, after the initial signs of MS had reached a score of 1+ for the symptom categories described above The course of treatment was for 24 days (2.0 mg/kg paclitaxel, 3x per week, x 10 doses). The body weight and clinical signs were determined on each injection day.

B. Results

[0399] The 5 animals that received paclitaxel did not demonstrate a significant weight loss. However, the untreated transgenic mouse showed a 30% decrease in body weight, from 29 g to 22 g (Figure 74), as is normally associated with progression of the disease.

[0400] The clinical indicators of MS, such as shaking, hind limb mobility, seizures, head tremors, unsteadiness of gait, limp tail and degree of activity, were monitored daily. At the onset of treatment, animals had a score of 1+ in the major symptom categories. Untreated animals progressed from a 1+ to a 4+ scoring over the next 27 days in a number of symptoms; 3+ was characterized with poor balance, one of the major features of the disease. In the paclitaxel treated group, all five animals remained at 1+ scoring over the same period in all of the symptoms monitored (Table 1).

TABLE 1

Effect of Low Dose Continuous Paclitaxel on the Progression of Multiple Sclerosis Symptoms in Transgenic Mice

Mice	Age (Months)	Seizures	Shaking	Hind Limb Paralysis	Head tremors	Decreased Wt. (%)
Transgenic Animals (untreated)	3	1+	1+	1+	1+	0
	6	2+ - 3+	2+ - 3+	2+ - 4+	3+	30%
Transgenic Animals (paclitaxel-treated)	3	1+	1+	1+	1+	0
	6	1+	1+	1+	1+	5-10%
Control Animals (paclitaxel-treated)	3	0	0	0	0	0
	6	0	0	0	0	0-5%

TABLE 1 (continued)

Effect of Low Dose Continuous Paclitaxel on the Progression of Multiple Sclerosis Symptoms in Transgenic Mice						
Mice	Age (Months)	Seizures	Shaking	Hind Limb Paralysis	Head tremors	Decreased Wt. (%)
• Untreated transgenic animals had a progression of severe symptoms over 27 days whereas paclitaxel-treated animals had minimal neurological symptoms over the same time period. • A score of 1 + means definite but minimal signs; 4+ is moribund.						

[0401] For the high-dose protocol, mice were treated with 20 mg/kg of paclitaxel once weekly for 4 weeks to mimic interval pulse chemotherapy (given monthly for breast and ovarian cancer) as is used in oncology patients. The animals were monitored for 10 weeks, every two days and scores were determined for each symptom. In 3 untreated animals, neurological symptoms progressed rapidly and two of the animals died (on week 5 and week 9) during the course of the experiment; the third surviving animal had severe clinical symptoms. In the 5 transgenic animals receiving paclitaxel treatment initiated after symptoms onset, there was a reduction in MS scores relative to controls after the first week of monitoring and, thereafter, further neurological deterioration was not observed. In these animals, disease progression was not observed and the animals remained clinically in remission both during therapy (weeks 0 to 3) and subsequent to cessation of drug treatment (weeks 4 to 10) (Figure 75).

C. Conclusions

[0402] Paclitaxel prevented the rapid progression of neurological symptoms observed in this animal model of MS with both low and high dosing. These data suggest that paclitaxel may be a potential therapeutic agent of demyelinating disease.

EXAMPLE 39 (Reference example)

EVALUATION OF PACLITAXEL AND OTHER MICROTUBULE STABILIZING AGENTS FOR THE TREATMENT OF NASAL POLYPS

[0403] Epithelial cell cultures and/or nasal polyp tissue cultures are used to evaluate the efficacy of formulations containing paclitaxel or other agents in the treatment of nasal polyps. This approach is based on the premise that epithelial cells release cytokines and contribute to chronic inflammation detected in nasal polyposis as well as in rhinitis and asthma and that a prolonged release medication will prevent eosinophilia and inhibit cytokine gene expression.

[0404] Paclitaxel formulations including solutions (the use of cyclodextrins) or suspensions containing paclitaxel encapsulated into mucoadhesive polymers for use as nasal sprays, and/or micro-encapsulated paclitaxel in mucoadhesive polymers are used as insufflations. These formulations are used in the studies detailed below.

A. Effect of Paclitaxel *in vitro*

[0405] Tissue handling - Normal nasal mucosal (NM) specimens are obtained from patients with no clinical evidence of rhinitis and negative skin-prick test during nasal reconstructive surgery. Nasal polyp (NP) specimens are obtained from patients with positive and negative skin-prick test undergoing nasal polypectomy. The nasal specimens are placed in Ham's F12 medium supplemented with 100 UI/ml penicillin, 100 µg/ml streptomycin and 2 µg/ml amphotericin B and immediately transported to the laboratory.

[0406] Epithelial cell culture - Nasal epithelial cells from NM and NP are isolated by protease digestion as follows. Tissue specimens are rinsed 2-3 times with Ham's F12 supplemented with 100 UI/ml penicillin, 100 µg/ml streptomycin and 2 µg/ml amphotericin B and then incubated in a 0.1% protease type XIV in Ham's F12 at 4°C overnight. After incubation, 10% FBS is added to neutralize protease activity and epithelial cells are detached by gentle agitation. Cell suspensions are filtered through a 60 mesh cell dissociation sieve and centrifuged at 500g for 10 minutes at room temperature. The cell pellet is then resuspended in hormonally defined Ham's F12 culture medium (Ham's HD) containing the following reagents: 100 UI/ml penicillin, 100 µg/ml streptomycin, 2 µg/ml amphotericin B, 150 µg/ml glutamine, 5 µg/ml transferin, 5 µg/ml insulin, 25ng/ml epidermal growth factor, 15 µg/ml endothelial cell growth supplement, 200 pM triiodothryonine and 100 nM hydrocortisone. Cell suspensions (10^5 cells/well) are then plated on collagen coated wells in 2 ml of Ham's HD and cultured in a 5% CO_2 humidified atmosphere at 37°C. Culture medium is changed at day and subsequently every other day. Monolayer cell confluence is achieved after 6-10 days of culture.

[0407] Human epithelial conditioned media (HECM) generation - When epithelial cell cultures reached confluence, Ham's HD is switched to RPMI 1640 medium (Irvin, Scotland) supplemented with 100 UI/ml penicillin, 100 µg/ml streptomycin, 2 µg/ml amphotericin B, 150 µg/ml glutamine and 25 mM Hepes buffer (RPMI 10%). HECM which is generated after 48 hours of incubation with RPMI (10%) is harvested from cultures, centrifuged at 400g for 10 minutes at room temperature (RT), sterilized by filtration through 0.22 µm filters and stored at -70°C until used.

[0408] Eosinophil survival and effect of paclitaxel — Eosinophils are isolated from the peripheral blood and the effect of HECM from both NM and NP on eosinophil survival is determined in two different ways: time-course and dose response analyses. In time-course experiments, eosinophils at a concentration of approximately 250,000/ml are incubated in six well tissue cultures with or without (negative control) 50% HECM and survival index assessed at days 2,4, 6 and 8. Other experiments are conducted with 1 to 50% HECM. In experiments where the effect of drugs (e.g., paclitaxel) on HECM-induced eosinophil survival is tested, the drug (paclitaxel) from 0.1 nM to 10 µM is incubated with eosinophils at 37°C over 1 hour before the addition of HECM. In each experiment, negative control (culture media only) and positive control (culture media with HECM) wells are always assessed. To investigate whether the drugs have any toxic effect, the viability of eosinophils incubated with the drug (various concentrations) are compared with eosinophils cultured with RPMI 10% alone over 24 hour period.

B. Effect of paclitaxel on cytokine gene expression and release from epithelial cells

[0409] Epithelial cells obtained from nasal polyps and normal nasal mucosa are cultured to confluence, human epithelial cell conditioned media generated with or with paclitaxel (or other agents) and supernatants are measured by ELISA. Cytokine gene expression is investigated by reverse transcription-polymerase chain reaction (RT-PCR) as described by Mullol et al., *Clinical and Experimental Allergy* 25:607-615, 1995.

[0410] The results show whether paclitaxel modulates cytokine gene expression as a means of inhibiting eosinophil survival. The main disadvantage of using primary cell cultures is that it takes 10 days for the cells to reach confluence, dissociating cellular functions from local melieu as well as systemic effects, which would have led to the disease in the first place. However, this is an excellent *in vitro/ex vivo* model to study the growth factors regulating the function and proliferation of structural cells (*e.g.*, epithelial cells) and thereby elucidate some aspects of mucosal inflammation.

C. Immunologic release of chemical mediators from human nasal polyps

[0411] Mediation by paclitaxel and other agents - Polyps are obtained at the time of resection and are washed 5 times with Tyrode's buffer and fragmented with fine scissors into replicates about 200 mg in wet weight. The replicates are suspended in 3 ml buffer containing various concentrations of paclitaxel at 37°C and challenged (5 minutes later) with 0.2 µg/ml of antigen E. After 15 minutes incubation with the antigen, the diffusates are removed and the tissues boiled in fresh buffer for 10 minutes to extract the residual histamine. The histamine and SRS-A released are assayed using HPLC.

EXAMPLE 40

PERIVASCULAR ADMINISTRATION OF AGENTS THAT DISRUPT MICROTUBULE FUNCTION

[0412] Studies have been conducted to evaluate the efficacy of paclitaxelcamptothecin loaded surgical paste (PCL) and/or an EVA film as a perivascular treatment for restenosis.

A. Materials and Methods

[0413] WISTAR rats weighing 250 to 300 g were anesthetized by the intramuscular injection of Innovar (0.33 ml/kg). Once sedated they were then placed under Halothane anesthesia. After general anesthesia was established, fur over the neck region was shaved, the skin clamped and swabbed with betadine. A vertical incision was made over the left carotid artery and the external carotid artery exposed. Two ligatures were placed around the external carotid artery and a transverse arteriotomy was made. A number 2 French Fogarty balloon catheter was then introduced into the carotid artery and passed into the left common carotid artery and the balloon inflated with saline. The endothelium was denuded by passing the inflated balloon up and down the carotid artery three times. The catheter was then removed and the ligature tied off on the left external carotid artery.

[0414] Rats were randomized into groups of 10 to receive no treatment, polymer alone (EVA film or PCL paste), or polymer plus 20% paclitaxel. The polymer mixture (2.5 mg) was placed in a circumferential manner around the carotid artery. The wound was then closed. Five rats from each group were sacrificed at 14 and the final five at 28 days. In the interim, the rats were observed for weight loss or other signs of system illness. After 14 or 28 days, the animals

were anesthetized and the left carotid artery was isolated, fixed with 10% buffered formaldehyde and examined histologically.

[0415] As a preliminary study, two rats were treated with 10% camptothecin-loaded EVA film for 14 days to assess camptothecin's efficacy in this disease model.

B. Results

[0416] Results from these studies revealed that paclitaxel-loaded (20%) polymers completely prevented restenosis whereas the control animals and the animals receiving polymer alone developed between 28% and 55% luminal compromise at 14 and 28 days post-balloon injury (Figures 76A and 76B).

[0417] There was an absolute inhibition of intimal hyperplasia where paclitaxel was in contact with the vessel wall. However, the effect was very local as evidenced by the uneven effect of paclitaxel where there was an inability to maintain the drug adjacent to the vessel wall (Figures 77A and 77B).

[0418] Preliminary data has shown that camptothecin-loaded EVA film was efficacious in preventing a restenotic response in this animal model of disease. Camptothecin completely inhibited intimal hyperplasia in the two animals tested.

EXAMPLE 41 (Reference example)

EFFECTS OF PACLITAXEL IN AN ANIMAL MODEL OF SURGICAL ADHESIONS

[0419] The use of a paclitaxel-loaded EVA film to reduce adhesion formation is examined in the rabbit uterine horn model.

[0420] New Zealand female white rabbits are anesthetized and a laparotomy is performed through a midline incision. The uterine horns are exposed and a 5 cm long segment of each is abraded using a scalpel blade. This abrasion is sufficient to remove the serosa, resulting in punctate bleeding. Rabbits are randomly assigned to the control or paclitaxel treated groups and to post-operative evaluation periods of two, four and eight weeks. In the paclitaxel treated group, each uterine horn is completely wrapped with paclitaxel-loaded EVA film following abrasion. The musculoperitoneal layer is closed with sutures and the cutaneous layer with skin staples.

[0421] Animals are evaluated for adhesion formation two, four or eight weeks after surgery. The animals are euthanized humanely and necropsies performed. The uterine horns are examined grossly and histologically using standard microscopic techniques. Grossly, the adhesions are graded using a standard scoring system which is based on the fact that 5 cm of the uterine horn is traumatized; thus, the extent of adhesion formation is determined by measuring the length of the area containing adhesions. The following grading system is used: 0 = no adhesions, 1 = adhesion on 25% of the area, 2 = adhesions on 50% of the area and 3 = total adhesion involvement. The severity of the adhesions is measured as follows: 0 = no resistance to separation, 0.5 = some resistance (moderate force needed), and 1 = sharp dissection required. The total grade is additive, with an adhesion score range of 0 - 4 which represents both extent and severity.

EXAMPLE 42 (Reference example)

MICELLAR PACLITAXEL IN THE TREATMENT OF INFLAMMATORY BOWEL DISEASE (IBD)

[0422] Inflammatory bowel disease (IBD), namely Crohn's disease and ulcerative colitis, is characterized by periods of relapse and remission. The best available model of IBD is produced in the rat by the intracolonic injection of 2,4,6-trinitrobenzene sulphonic acid (TNB) in a solution of ethanol and saline (Morris et al., *Gastroenterology,* 96: 795-803, 1989). A single administration initiates an acute and chronic inflammation that persists for several weeks. However, pharmacologically, the rabbit colon has been shown to resemble the human colon more so than does the rat (*Gastroenterology,* 99: 13424-1332, 1990).

[0423] Female New Zealand white rabbits are used in all experiments. The animals are anesthetized intravenously (i.v.) with pentobarbitol. An infants' feeding tube is inserted rectally, so that the tip is 20 cm proximal to the anus, for injection of the TNB (0.6 ml; 40 mg in 25% ethanol in saline). One week following TNB administration, the rabbits are randomized into 3 treatment groups. At this time, the animals receive either no treatment, micelles alone (i.v.) or micellar paclitaxel (i.v.). This is repeated every 4 days for a total of 4 treatments.

[0424] During the course of the study, rabbits are examined weekly by endoscopy using a pediatric bronchoscope under general anesthesia, induced as above. Damage is scored by an endoscopist (blinded) according to the following scale: 0, no abnormality; 1, inflammation, but no ulceration; 2, inflammation and ulceration at 1 site (< 1 cm); 3, two or more sites of inflammation and ulceration or one major site of inflammation and ulceration (> 1 cm) along the length

of the colon.

[0425] Following the last treatment, the rabbits are sacrificed with Euthanol at 24 hours and 1, 2, 4 and 6 weeks. The entire colon is isolated, resected and opened along the anti-mesenteric border, washed with saline and placed in Hank's balanced salt solution containing antibiotics. The colon is examined with a stereomicroscope and scored according to the same criteria as at endoscopy. As well, specimens of colon are selected at autopsy, both from obviously inflamed and ulcerated regions and from normal colon throughout the entire length from anus to ascending colon. The tissues are fixed in 10% formaldehyde and processed for embedding in paraffin; 5 (m sections are cut and stained with hemotoxylin and eosin. The slides are examined for the presense or absence of IBD histopathology.

[0426] The initial experiment can be modified for the use of oral paclitaxel following induction of colitis in rabbits by the intracolonic injection of TNB. The animals are randomized into 3 groups receiving no treatment, vehicle alone or orally formulated paclitaxel.

EXAMPLE 43 (Reference example)

EFFECT OF PACLITAXEL IN AN ANIMAL MODEL OF SYSTEMIC LUPUS ERYTHEMATOSUS

[0427] Paclitaxel's efficacy in systemic lupus erythematosus is determined by treating female NZB/NZW F_1 mice (B/W) with micellar paclitaxel. This strain of mice develops disease similar to human SLE. At one month of age, these mice have an elevated level of spleen B-cells spontaneously secreting immunoglobulin compared to normal mice. High levels of anti-ssDNA antibody occurs at 2 months of age. At five months of age, immunoglobulin accumulates along glomerular capillary walls. Severe glomerulonephritis evolves and by 9 months of age, 50% of B/W mice are dead.

A. Materials and Methods

[0428] Female B/W mice are purchased from The Jackson Laboratory (Bar Harbor, ME, USA). Five-month-old female B/W mice are randomly assigned into treatment and control groups. Treatment groups receive either a low dose continuous micellar paclitaxel (2.0 mg/kg; 3 times per week, total of 10 injections) or a high dose "pulse" micellar paclitaxel (20 mg/kg; four times, once weekly). The control group receives control micelles.

[0429] At predetermined time intervals, paclitaxel treated and untreated control B/W mice of comparable age are sacrificed, their spleens removed aseptically and single cell suspensions are prepared for lymphocyte counts. To identify spleen lymphocyte subpopulations, fluorescence analysis is conducted. The number of cells/million spleen B-cells spontaneously secreting immunoglobulin (IgG, IgM, total immunoglobulin) or anti-ssDNA antibody is determined using ELISA.

Claims

1. Use of an anti-microtubule agent for the manufacture of a medicament for treating multiple sclerosis, wherein the medicament is suitable for administration to a patient in a therapeutically effective amount of said anti-microtubule agent such that said multiple sclerosis is treated, wherein the agent is not a chalcone derivative of the structure:

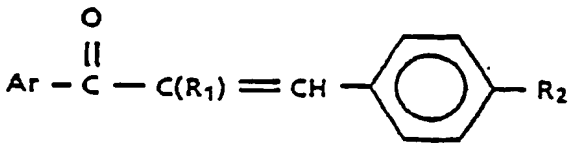

wherein

Ar is a 2,5-dimethoxyphenyl, 2,3,4-trimethoxyphenyl, or 3,4,5-trimethoxyphenyl group;
R_1 is a hydrogen, (C_1-C_4)alkyl, chloro, or bromo group; and
R_2 is a -N(R)$_2$ or -NHCOR wherein R is a (C_1-C_4)alkyl group

or a pharmaceutically acceptable salt thereof.

2. The use according to Claim 1 wherein said anti-microtubule agent is selected from the group consisting of epothi-

lone A or B, discodermolide, deuterium oxide (D_2O), hexylene glycol, tubercidin, LY290181, aluminium fluoride, ethylene glycol bis-(succinimidylsuccinate), glycine ethyl ester, as well as analogues or derivatives thereof.

3. The use according to Claim 1 wherein said anti-microtubule agent is paclitaxel, or an analogue or derivative thereof.

4. The use according to Claim 1, 2, or 3 wherein said anti-microtubule agent is suitable for subcutaneous or intramuscular addministration.

5. The use according to Claim 1, 2, or 3 wherein said anti-microtubule agent is suitable for oral or intravenous administration.

6. The use according to Claim 3, wherein said paclitaxel is suitable for administration at a dosage of 10 to 50 mg/m2 once every one to four weeks.

7. The use according to Claim 3, wherein said paclitaxel is suitable for administration at a dosage of 50 to 250 mg/m2 every 1 - 21 days for 1 - 6 cycles.

8. The use according to Claim 1, 2 or 3 wherein said agent further comprises a polymer.

9. The use according to Claim 8 wherein said polymer is formed into microspheres having an average size of between 0.5 and 200µm.

10. The use according to Claim 8 wherein said polymer is copolymer of lactic acid and glycolic acid.

11. The use according to Claim 8 wherein said polymer comprises poly (caprolactone).

12. The use according to Claim 8 wherein said polymer comprises poly (lactic acid).

13. The use according to Claim 8 wherein said polymer is a copolymer of poly (lactic acid) and polyethyleneglycol.

14. The use according to Claim 8 wherein said polymer is a copolymer of poly (caprolactone) and polyethyleneglycol.

15. The use according to Claim 8 wherein said polymer comprises ethylene vinyl acetate.

16. The use according to Claim 8 wherein said polymer comprises isopropyl myristate.

17. The use according to Claim 8 wherein said polymer is a diblock or triblock copolymer.

Patentansprüche

1. Verwendung eines anti-Mikrotubuli-Mittels zur Herstellung eines Medikaments zur Behandlung Multipler Sklerose, wobei das Medikament zur Verabreichung an einen Patienten in einer therapeutisch effektiven Menge des anti-Mikrotubuli-Mittels, so daß die Multiple Sklerose behandelt wird, geeignet ist, wobei das Mittel nicht ein Chalkonderivat der Struktur

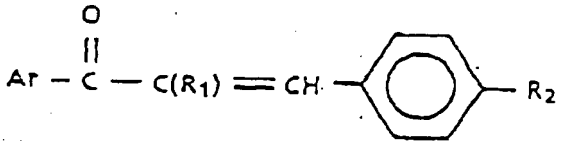

ist, worin

Ar eine 2,5-Dimethoxyphenyl-, 2, 3, 4-Trimethoxyphenyl- oder 3, 4, 5-Trimcthoxyphenylgruppe ist;
R_1 Wasserstoff, eine (C_1-C_4)-Alkyl, Chlor oder Bromgruppe ist; und

R_2 ein -$N(R)_2$ oder -NHCOR ist, worin R eine (C_1-C_4)-Alkylgruppe darstellt,

oder ein pharmazeutisch annehmbares Salz davon.

2. Verwendung nach Anspruch 1, wobei das anti-Mikrotubuli-Mittel ausgewählt ist aus der Gruppe bestehend aus Epothilon A oder B, Diskodermolid, Deuteriumoxid (D_2O), Hexylenglykol, Tubercidin, LY290181, Aluminiumfluorid, Ethylenglykol-bis-(succinimidylsuccinat), Glyzinethylester, sowie Analoga oder Derivate davon.

3. Verwendung nach Anspruch 1, wobei das anti-Mikrotubulin-Mittel Paklitaxel oder ein Analog oder Derivat davon ist.

4. Verwendung nach Anspruch 1, 2 oder 3, wobei das anti-Mikrotubuli-Mittel zur subcutanen oder intramuskulären Verabreichung geeignet ist.

5. Verwendung nach Anspruch 1, 2 oder 3, wobei das anti-Mikrotubuli-Mittel zur oralen oder intravenösen Verabreichung geeignet ist.

6. Verwendung nach Anspruch 3, wobei das Paklitaxel für eine Verabreichung in einer Dosis von 10 bis 50 mg/m2 einmal jede erste bis vierte Woche geeignet ist,

7. Verwendung nach Anspruch 3, wobei das Paklitaxel zur Verabreichung in einer Dosis von 50 bis 250 mg/m2 jede 1 - 21 Tage für 1 -6 Zyklen geeignet ist.

8. Verwendung nach Anspruch 1, 2 oder 3, wobei das Mittel weiterhin ein Polymer umfaßt.

9. Verwendung nach Anspruch 8, wobei das Polymer in Mikrosphären geformt ist, die eine durchschnittliche Größe von zwischen 0,5 und 200 µm aufweisen.

10. Verwendung nach Anspruch 8, wobei das Polymer ein Copolymer von Milchsäure und Glykolsäure ist.

11. Verwendung nach Anspruch 8, wobei das Polymer Poly(caprolacton) umfaßt.

12. Verwendung nach Anspruch 8, wobei das Polymer Poly(milchsäure) umfaßt.

13. Verwendung nach Anspruch 8, wobei das Polymer ein Copolymer von Poly(milchsäure) und Polyethylenglykol ist.

14. Verwendung nach Anspruch 8, wobei das Polymer ein Copolymer von Poly(caprolacton) und Polyethylenglykol ist.

15. Verwendung nach Anspruch 8, wobei das Polymer Ethylenvinylacetat umfaßt.

16. Verwendung nach Anspruch 8, wobei das Polymer Isopropylmyristat umfaßt.

17. Verwendung nach Anspruch 8, wobei das Polymer ein Diblock- oder Triblockcopolymer ist.

Revendications

1. Utilisation d'un agent anti-microtubules pour la production d'un médicament destiné au traitement de la sclérose en plaques, dans laquelle le médicament est apte à l'administration à un patient en une quantité thérapeutiquement efficace dudit agent anti-microtubules de manière à traiter ladite sclérose en plaques, l'agent n'étant pas un dérivé de chalcone de structure :

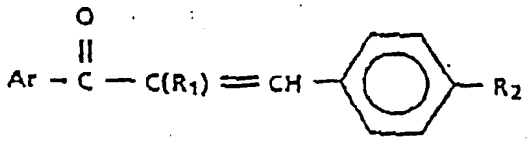

dans laquelle

Ar représente un groupe 2,5-diméthoxyphényle, 2,3,4-triméthoxyphényle ou 3,4,5-triméthoxyphényle ;
R_1 représente un atome d'hydrogène, un groupe alkyle en C_1 à C_4, chloro ou bromo ; et
R_2 représente un groupe $-N(R)_2$ ou -NHCOR dans lequel R représente un groupe alkyle en C_1 à C_4

ou un de ses sels pharmaceutiquement acceptables.

2. Utilisation suivant la revendication 1, dans laquelle l'agent anti-microtubules est choisi dans le groupe consistant en l'épothilone A ou B, le descodermolide, l'oxyde de deutérium (D_2O), l'hexylène-glycol, la tubercidine, le LY290181, le fluorure d'aluminium, le bis-(succinimidylsuccinate) d'éthylène-glycol, l'ester éthylique de glycine, ainsi que leurs analogues ou dérivés.

3. Utilisation suivant la revendication 1, dans laquelle l'agent anti-microtubules est le paclitaxel ou un de ses analogues ou dérivés.

4. Utilisation suivant la revendication 1, 2 ou 3, dans laquelle l'agent anti-microtubules est apte à l'administration sous-cutanée ou intramusculaire.

5. Utilisation suivant la revendication 1, 2 ou 3, dans laquelle l'agent anti-microtubules est apte à l'administration par voie orale ou intraveineuse.

6. Utilisation suivant la revendication 3, dans laquelle le paclitaxel est apte à l'administration à une dose de 10 à 50 mg/m^2 une fois par semaine à une fois toutes les quatre semaines.

7. Utilisation suivant la revendication 3, dans laquelle le paclitaxel est apte à l'administration à une dose de 50 à 250 mg/m^2 1 fois par jour à une fois tous les 21 jours pendant 1 à 6 cycles.

8. Utilisation suivant la revendication 1, 2 ou 3, dans laquelle l'agent comprend en outre un polymère.

9. Utilisation suivant la revendication 8, dans laquelle le polymère est mis sous forme de microsphères ayant un diamètre moyen de 0,5 à 200 µm.

10. Utilisation suivant la revendication 8, dans laquelle le polymère est un copolymère d'acide lactique et d'acide glycolique.

11. Utilisation suivant la revendication 8, dans laquelle le polymère comprend la poly(caprolactone).

12. Utilisation suivant la revendication 8, dans laquelle le polymère comprend le poly(acide lactique).

13. Utilisation suivant la revendication 8, dans laquelle le polymère est un copolymère de poly(acide lactique) et de polyéthylène-glycol.

14. Utilisation suivant la revendication 8, dans laquelle le polymère est un copolymère de poly-(caprolactone) et de polyéthylène-glycol.

15. Utilisation suivant la revendication 8, dans laquelle le polymère comprend un polymère éthylène-acétate de vinyle.

16. Utilisation suivant la revendication 8, dans laquelle le polymère comprend le myristate d'isopropyle.

17. Utilisation suivant la revendication 8, dans laquelle le polymère est un copolymère diséquencé ou triséquencé.

FIGURE 1A-1B

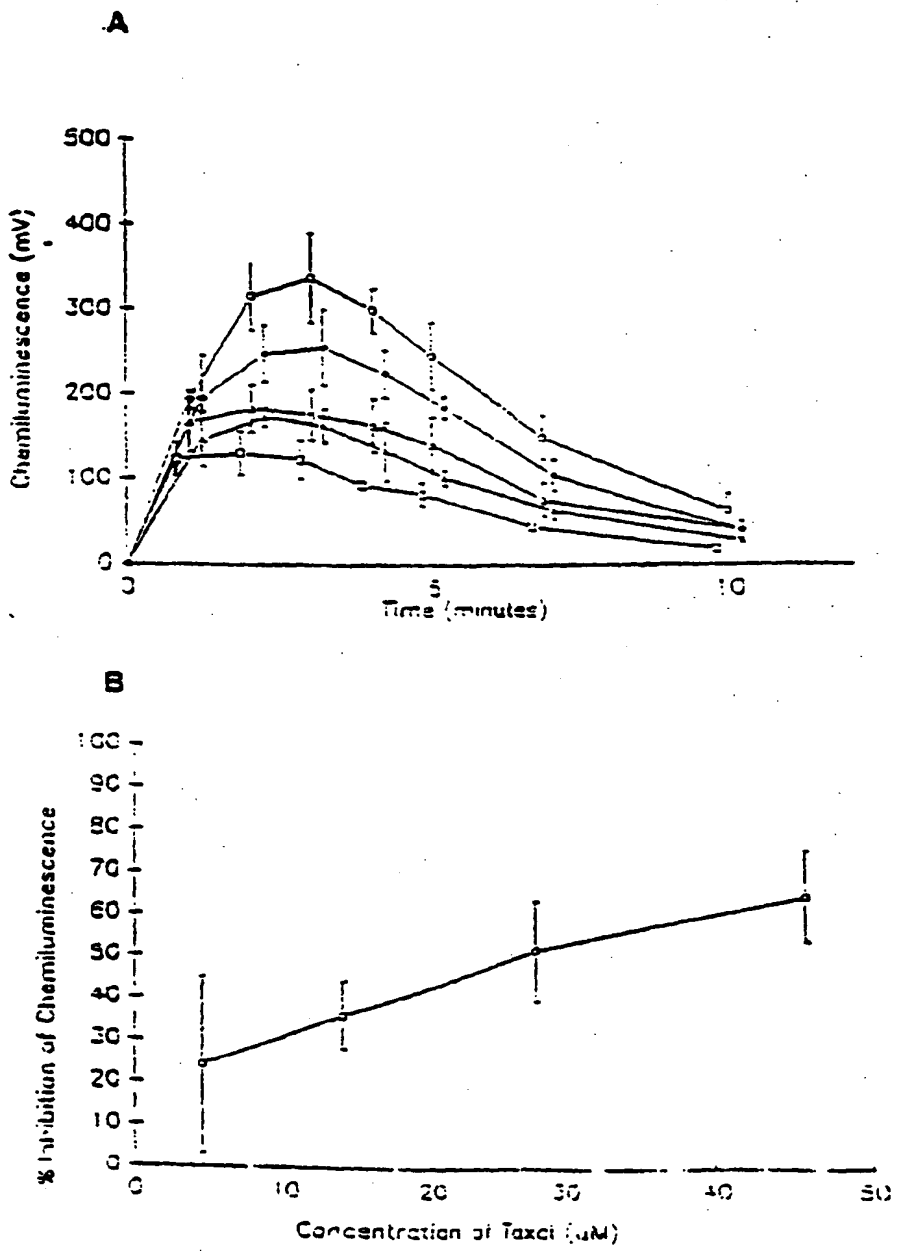
A
500
400
300
200
100
0
Chemiluminescence (mV)
0
5
10
Time (minutes)
B
100
90
80
70
60
50
40
30
20
10
0
% Inhibition of Chemiluminescence
0
10
20
30
40
50
Concentration of Taxol (uM)

FIGURE 1

C.

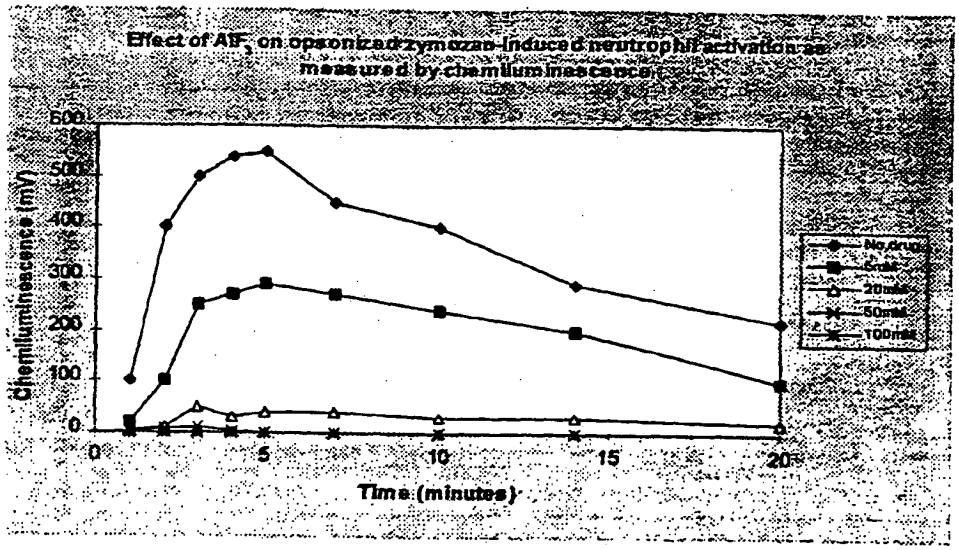
Effect of AlF3 on opsonized zymozan-induced neutrophil activation as measured by chemiluminescence
Chemiluminescence (mV)
Time (minutes)
No drug
2mM
20mM
50mM
100mM

D.

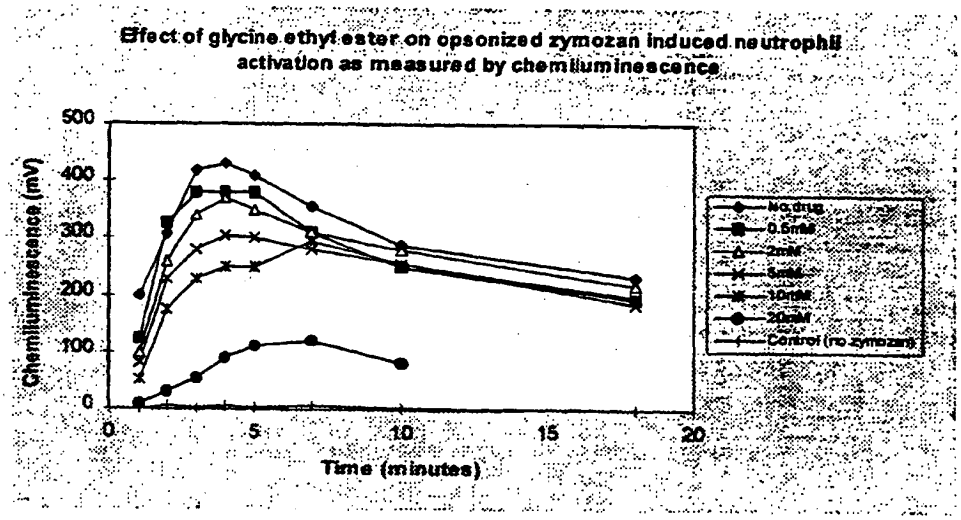
Effect of glycine ethyl ester on opsonized zymozan induced neutrophil activation as measured by chemiluminescence
Chemiluminescence (mV)
Time (minutes)
No drug
0.5mM
2mM
5mM
10mM
20mM
Control (no zymozan)

FIGURE 1E

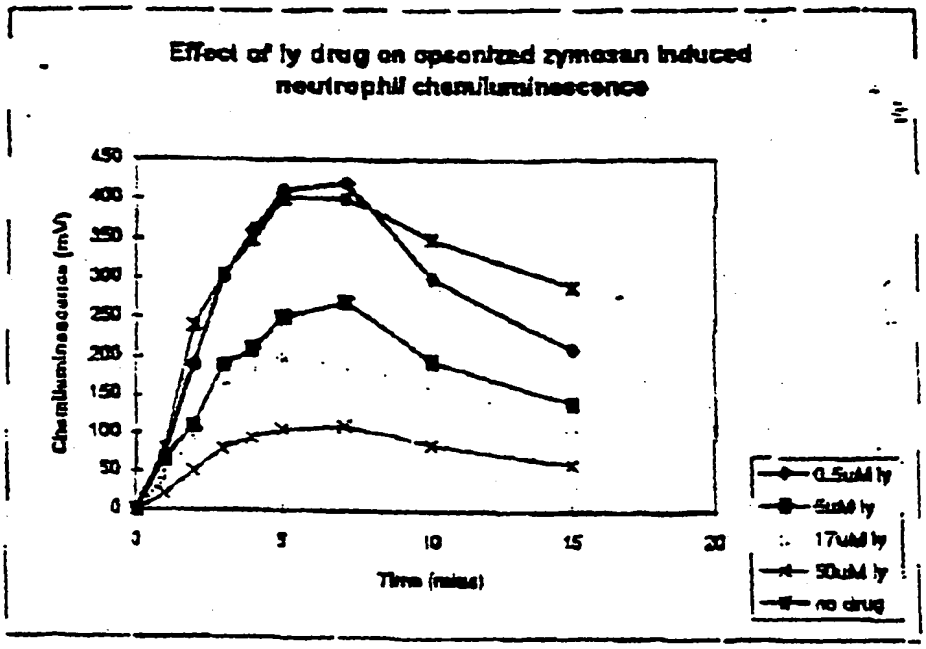
Effect of ly drug on opsonized zymosan induced neutrophil chemiluminescence
Chemiluminescence (mV)
450
400
350
300
250
200
150
100
50
0
3
5
10
15
20
Time (mins)
0.5uM ly
5uM ly
17uM ly
50uM ly
no drug

FIGURE 2

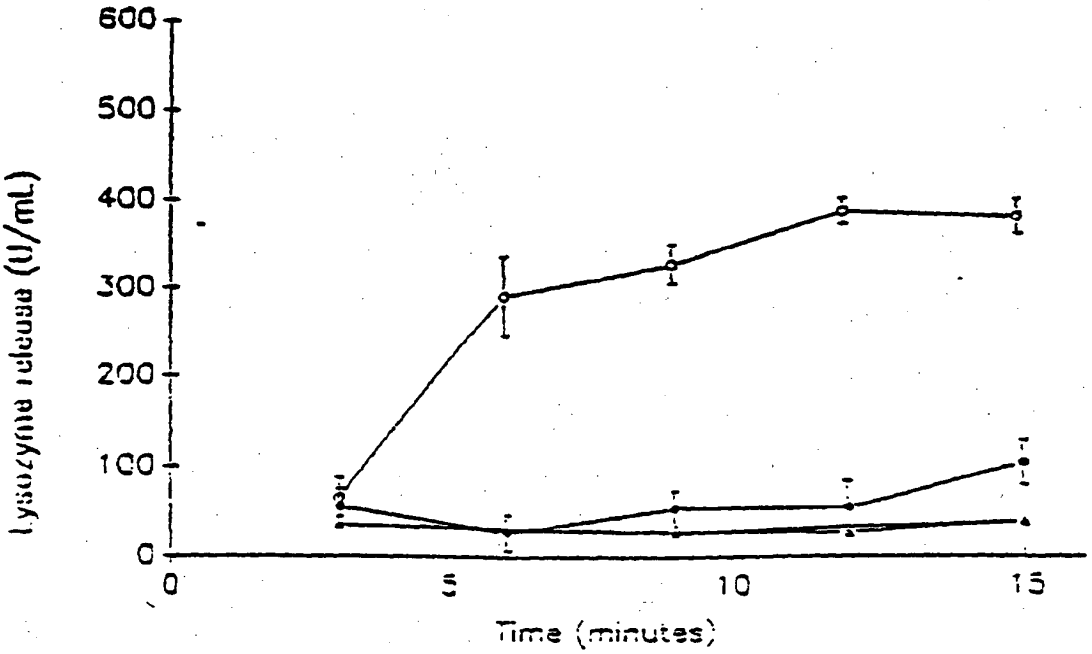

FIGURE 3A-3B

A

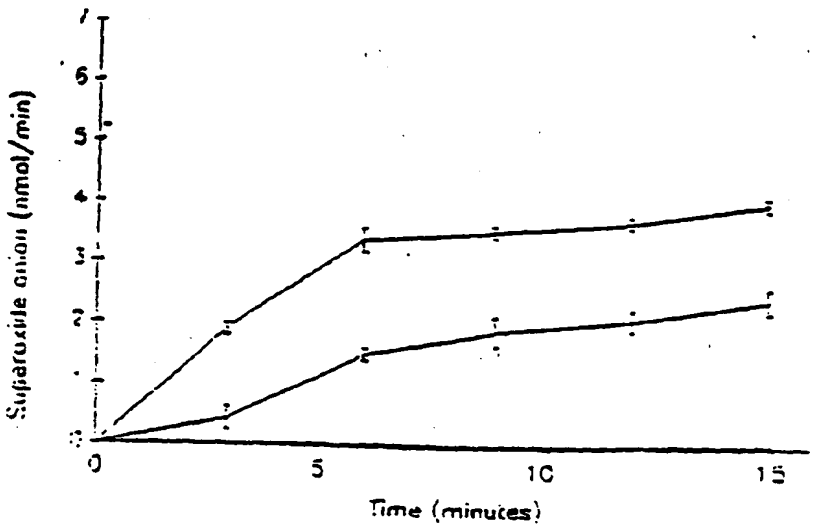

B

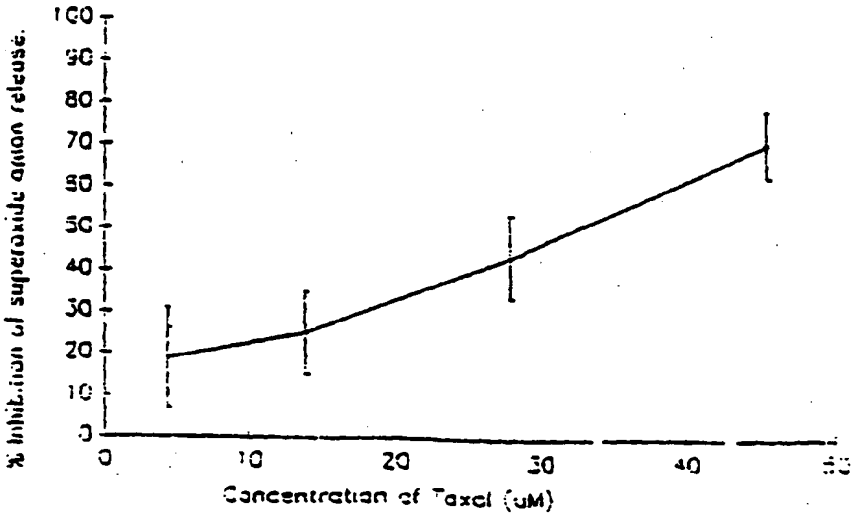

FIGURE 3C

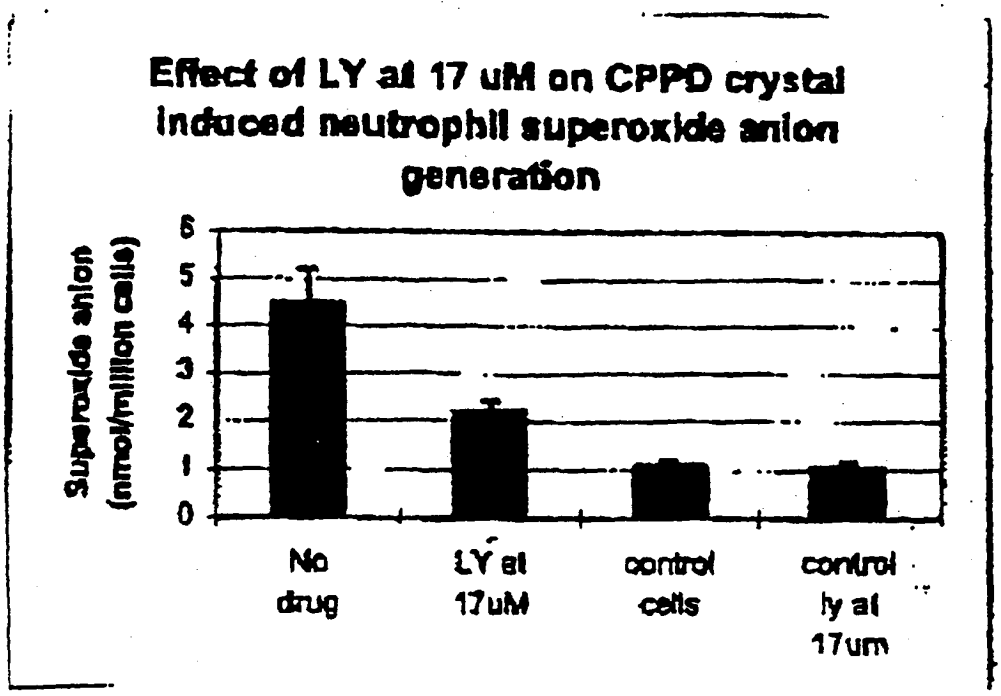
Effect of LY at 17 uM on CPPD crystal induced neutrophil superoxide anion generation
Superoxide anion (nmol/million cells)
6
5
4
3
2
1
0
No drug
LY at 17uM
control cells
control ly at 17um

FIGURE 4A-4B

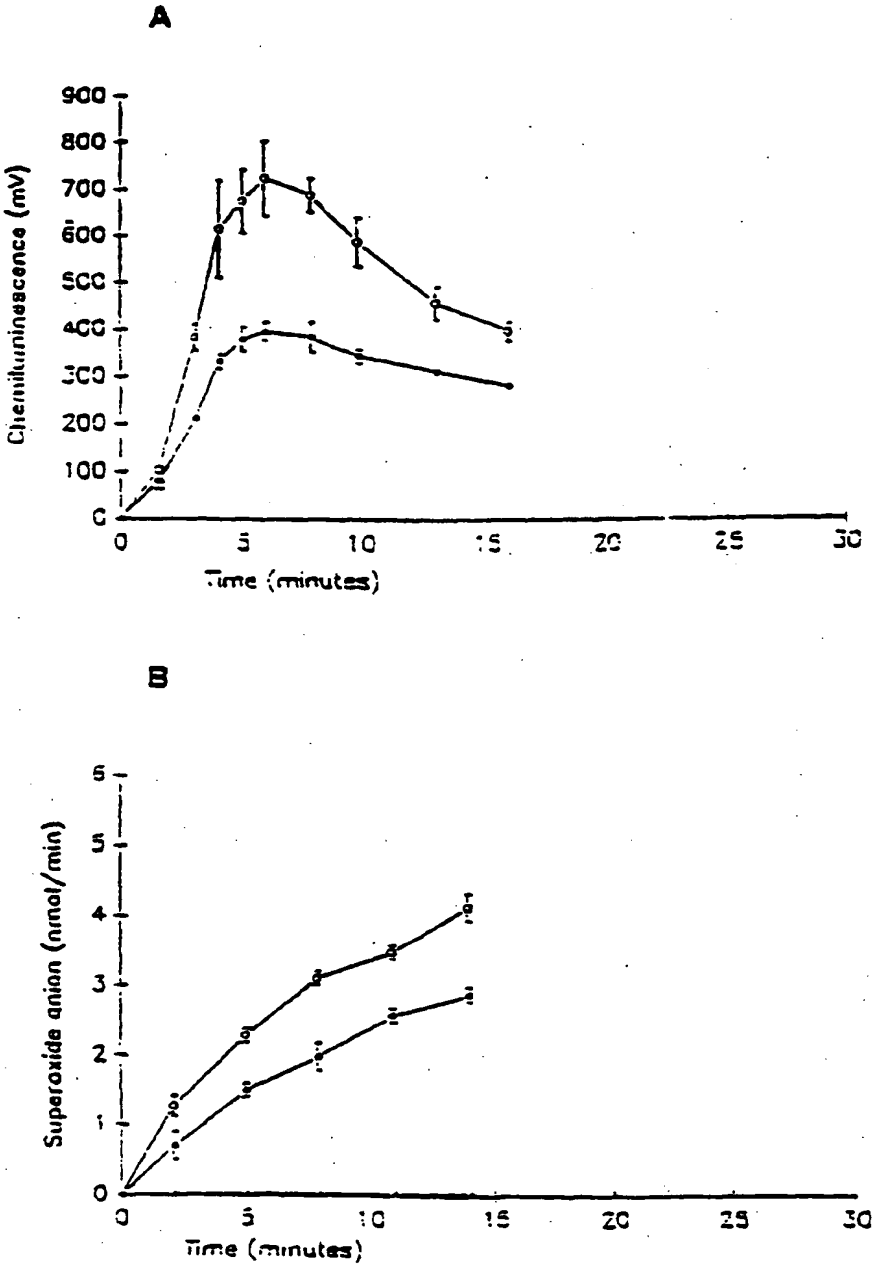
A
Chemiluminescence (mV)
900
800
700
600
500
400
300
200
100
0
0
5
10
15
20
25
30
Time (minutes)
B
Superoxide anion (nmol/min)
6
5
4
3
2
1
0
0
5
10
15
20
25
30
Time (minutes)

FIGURE 5A-5B

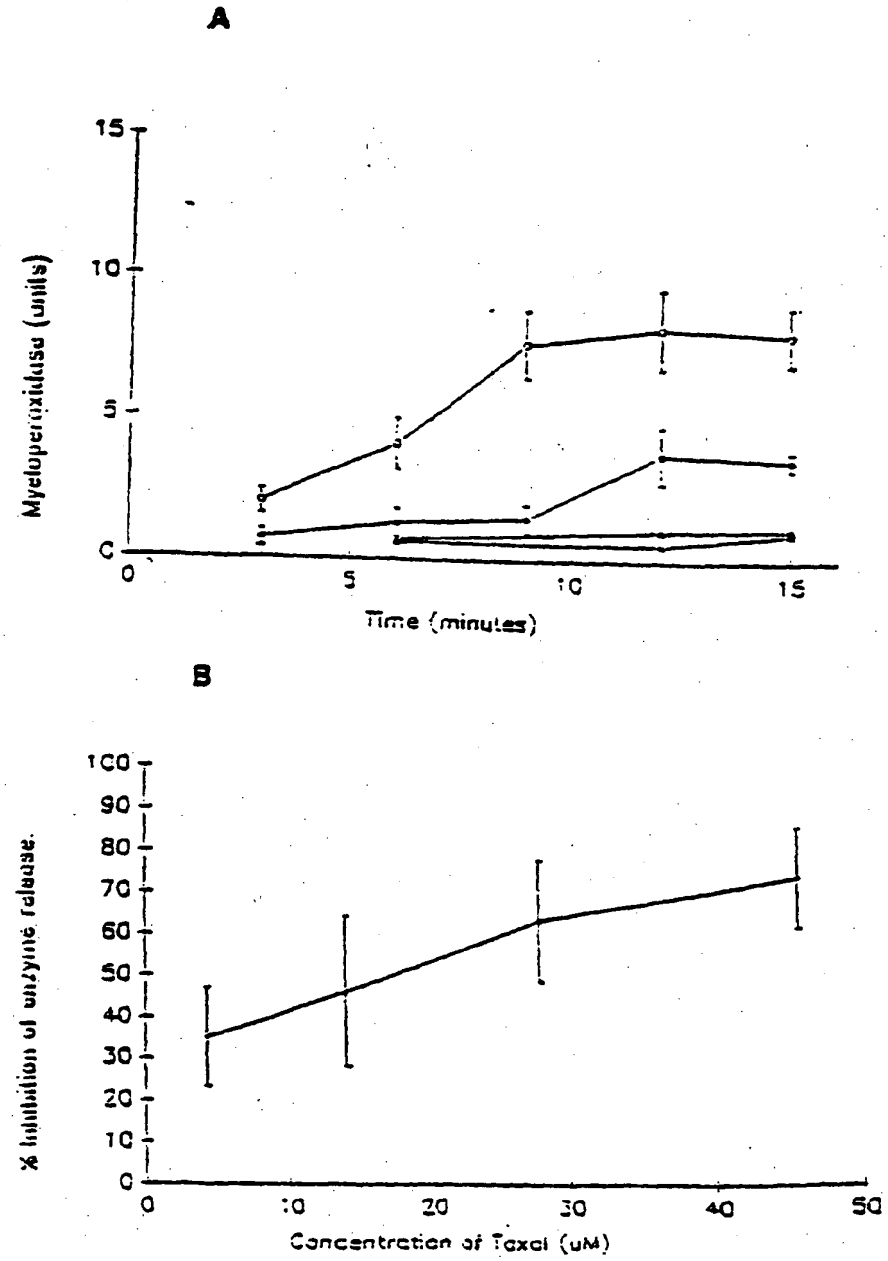
A
15
10
5
0
0
5
10
15
Time (minutes)
B
100
90
80
70
60
50
40
30
20
10
0
0
10
20
30
40
50
Concentration of Taxol (uM)

FIGURE 5C

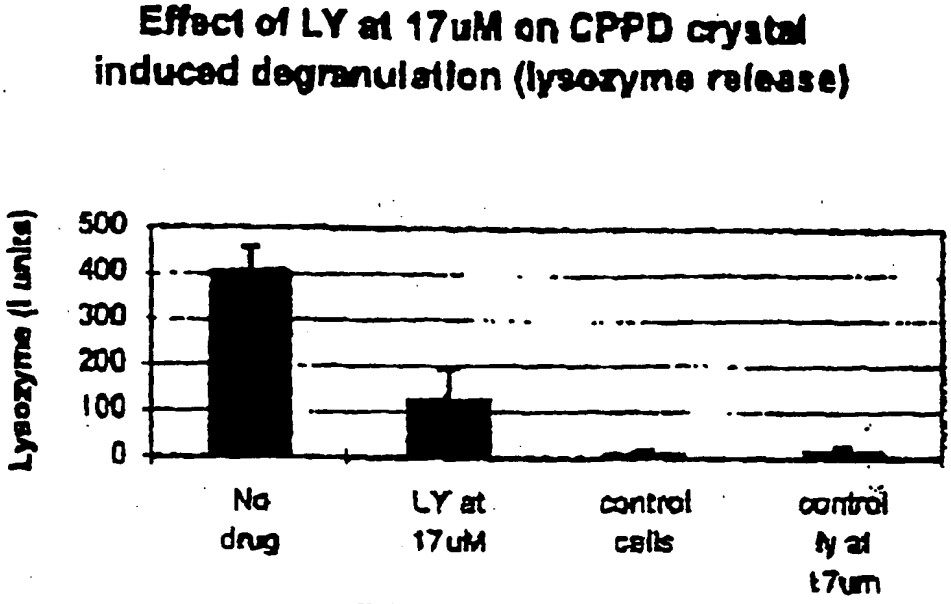

FIGURE 5D

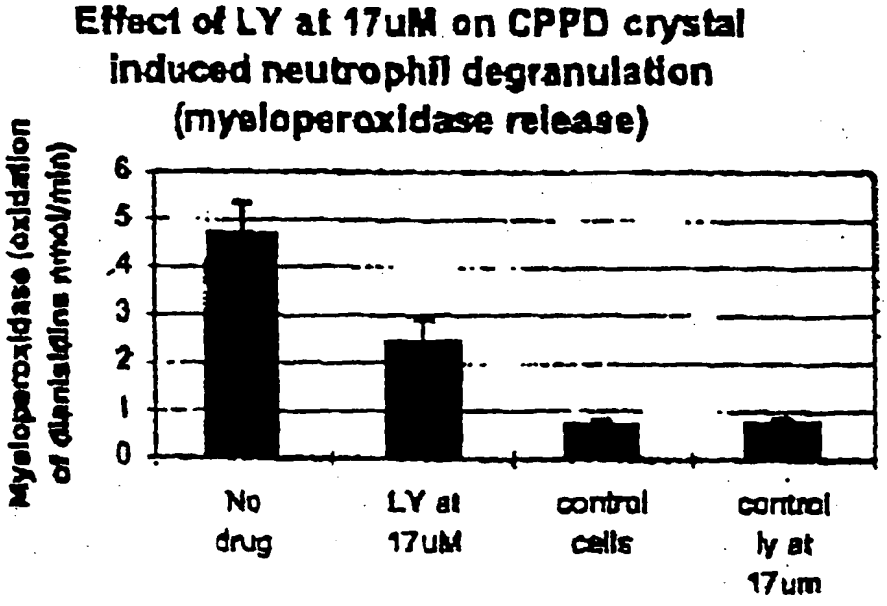

FIGURE 6

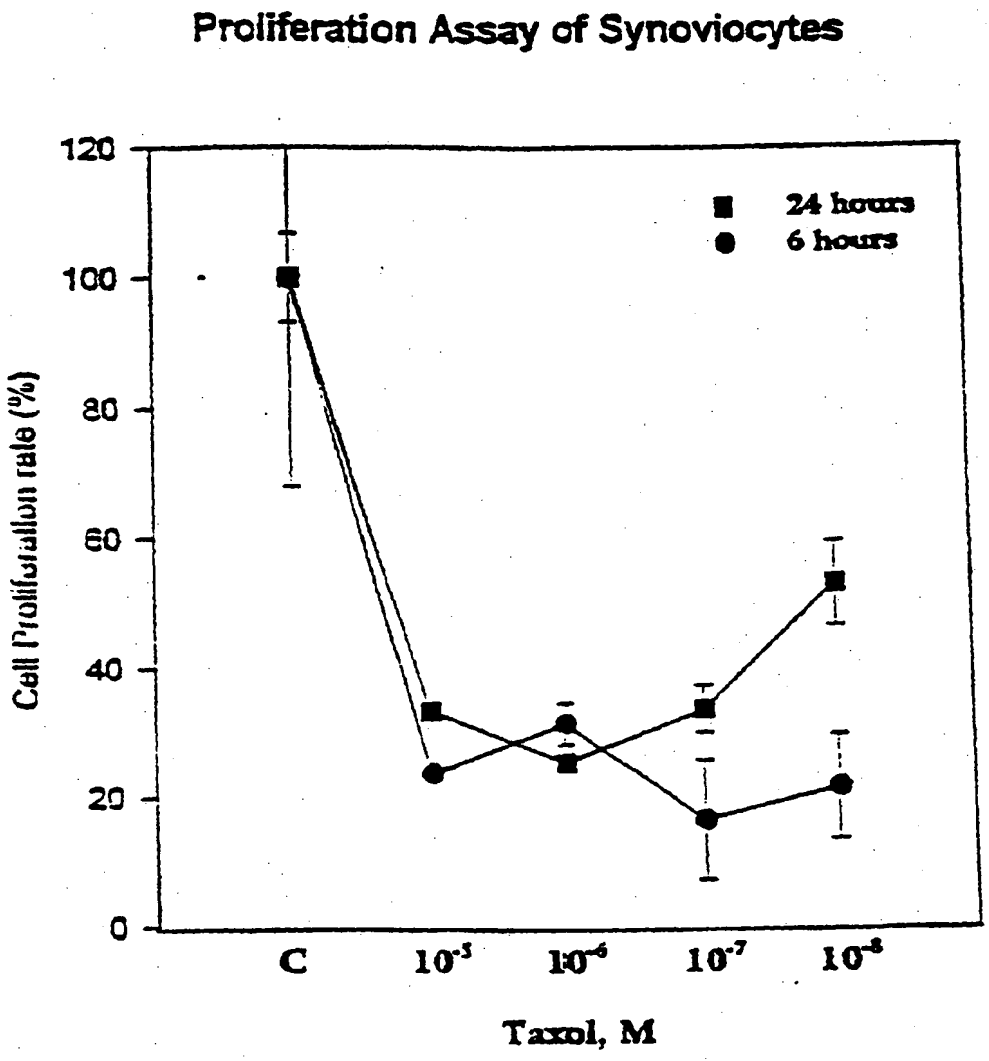
Proliferation Assay of Synoviocytes
120
100
80
60
40
20
0
Cell Proliferation rate (%)
24 hours
6 hours
C
10-5
10-6
10-7
10-8
Taxol, M

FIGURE 7

Effect of Paclitaxel on Keratinocytes *(in vitro)*

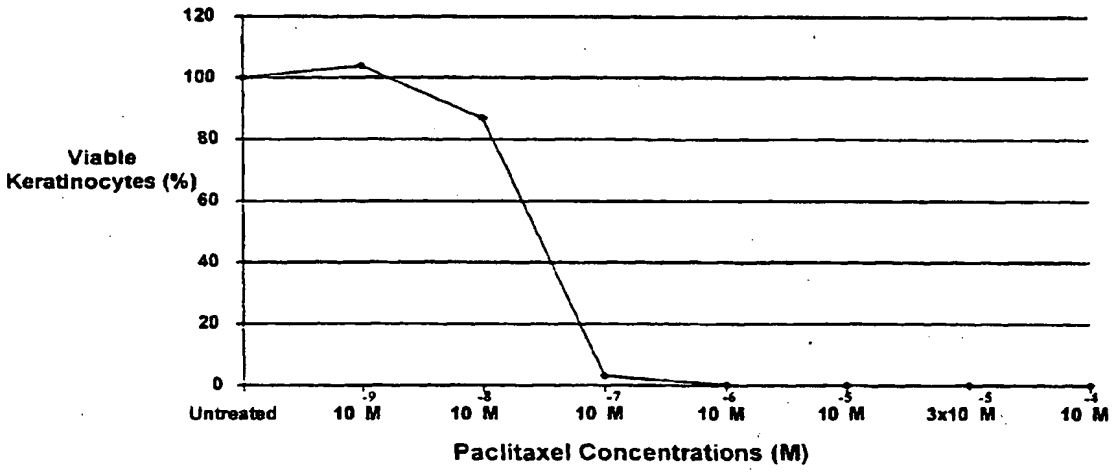

FIGURE 8

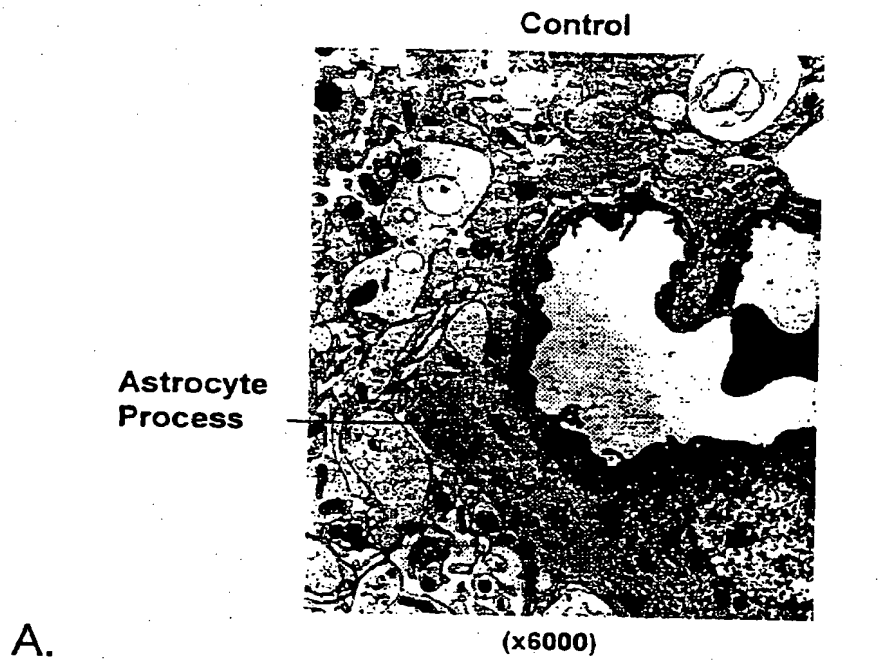
Control
Astrocyte Process
A.
(x6000)
Paclitaxel Treated
Loss of Filaments
Nucleus
B.
(x5000)

FIGURE 9

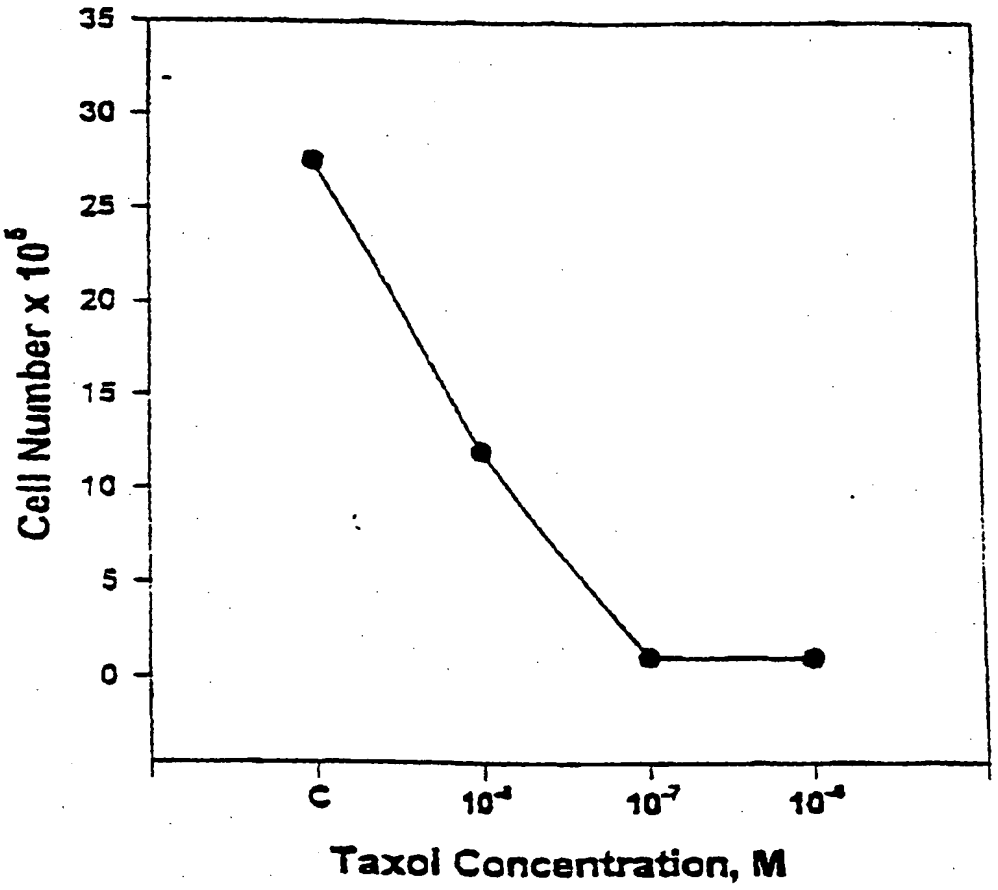
35
30
25
20
15
10
5
0
Cell Number x 10^5
C
10^-8
10^-7
10^-6
Taxol Concentration, M

FIGURE 10

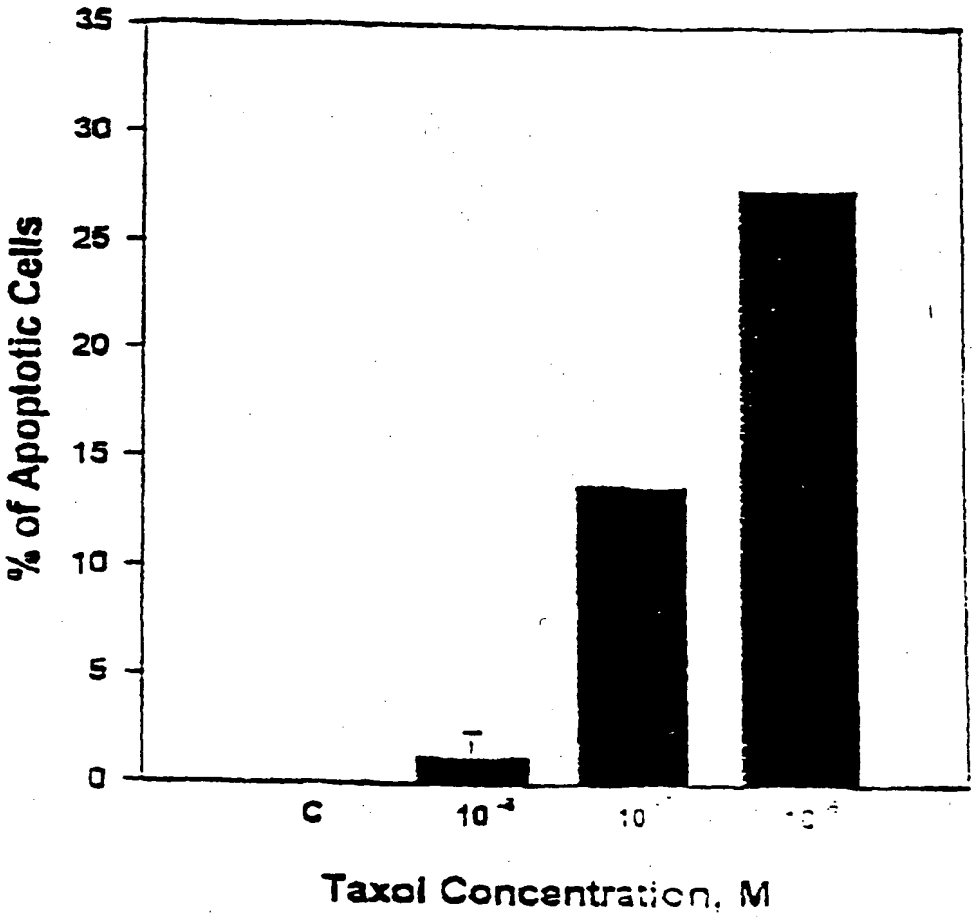
35
30
25
20
15
10
5
0
% of Apoptotic Cells
C
Taxol Concentration, M

FIGURE 11

A.

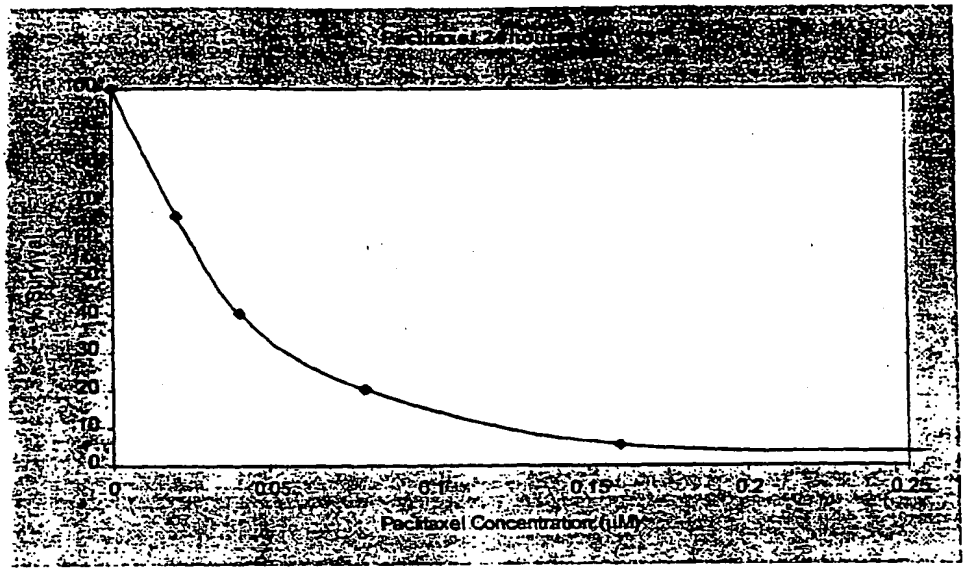
Paclitaxel 24 hours
% Survival
100
90
80
70
60
50
40
30
20
10
0
0
0.05
0.1
0.15
0.2
0.25
Paclitaxel Concentration (μM)

B.

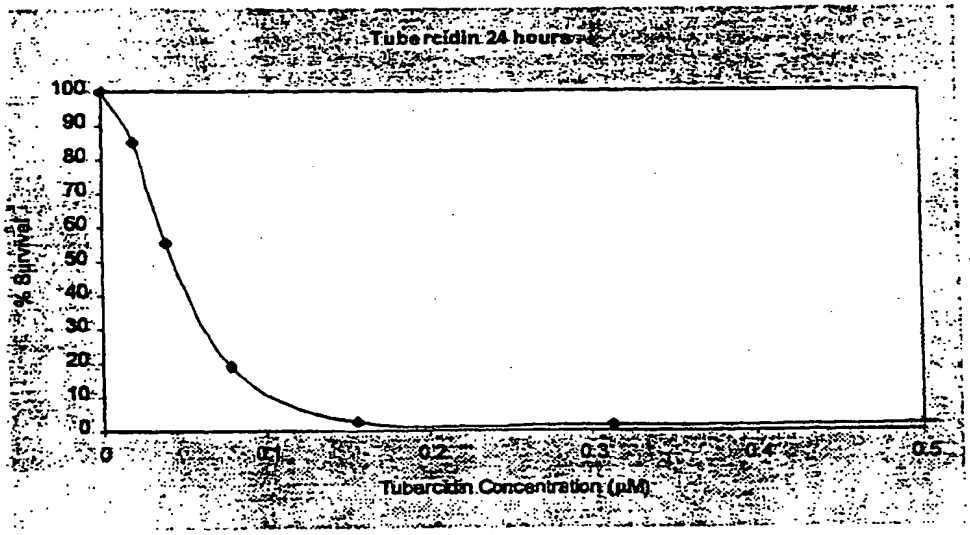
Tubercidin 24 hours
% Survival
100
90
80
70
60
50
40
30
20
10
0
0
0.1
0.2
0.3
0.4
0.5
Tubercidin Concentration (μM)

FIGURE 11

C.

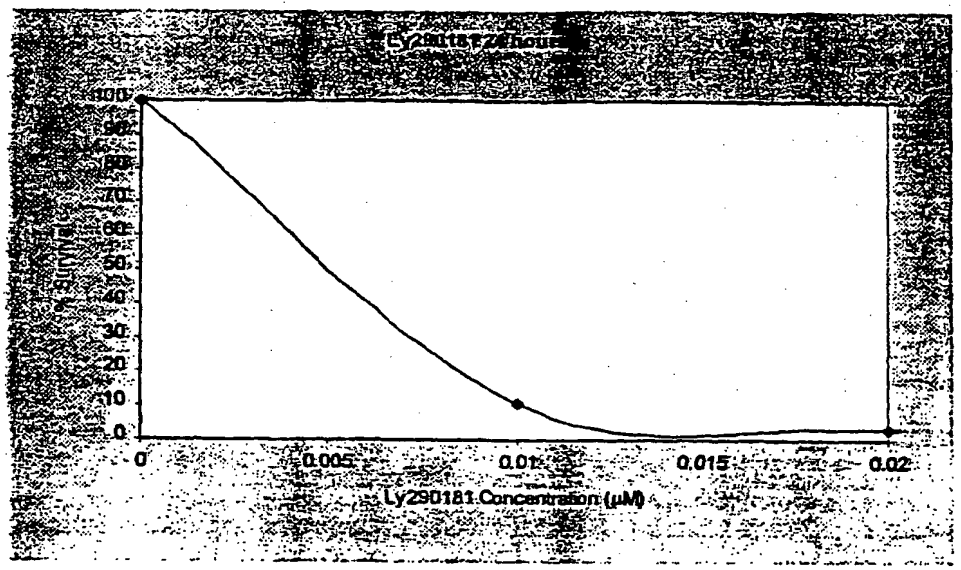
Cyclohexane 24 hours
% Survival
100
90
80
70
60
50
40
30
20
10
0
0
0.005
0.01
0.015
0.02
Ly290181 Concentration (µM)

D.

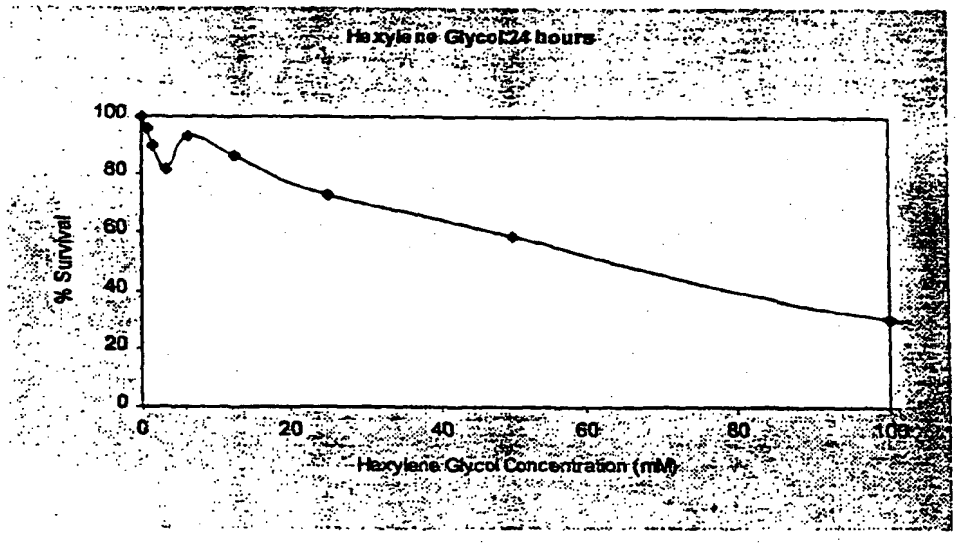
Hexylene Glycol 24 hours
% Survival
100
80
60
40
20
0
0
20
40
60
80
100
Hexylene Glycol Concentration (mM)

FIGURE 11

E.

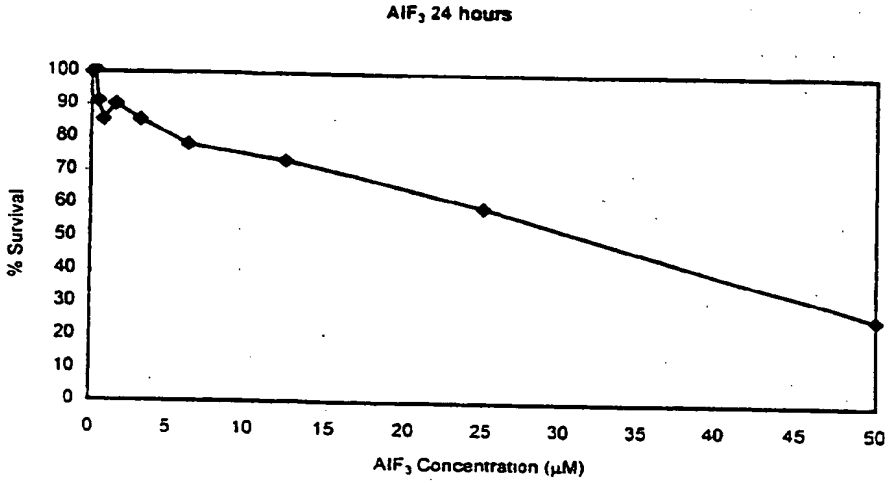
AlF3 24 hours
% Survival
100
90
80
70
60
50
40
30
20
10
0
0
5
10
15
20
25
30
35
40
45
50
AlF3 Concentration (µM)

F.

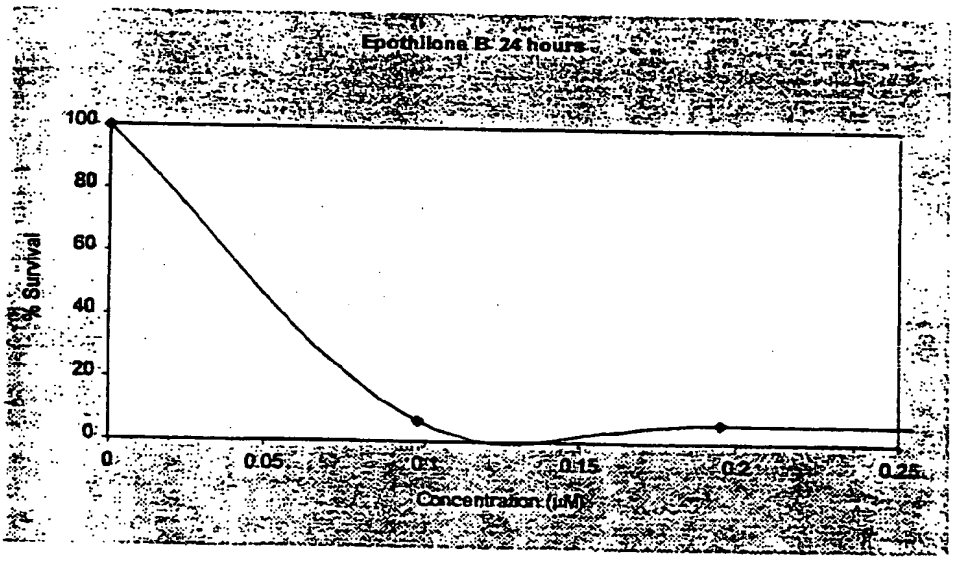
Epothilone B 24 hours
% Survival
100
80
60
40
20
0
0
0.05
0.1
0.15
0.2
0.25
Concentration (µM)

FIGURE 12A

Ly 290181

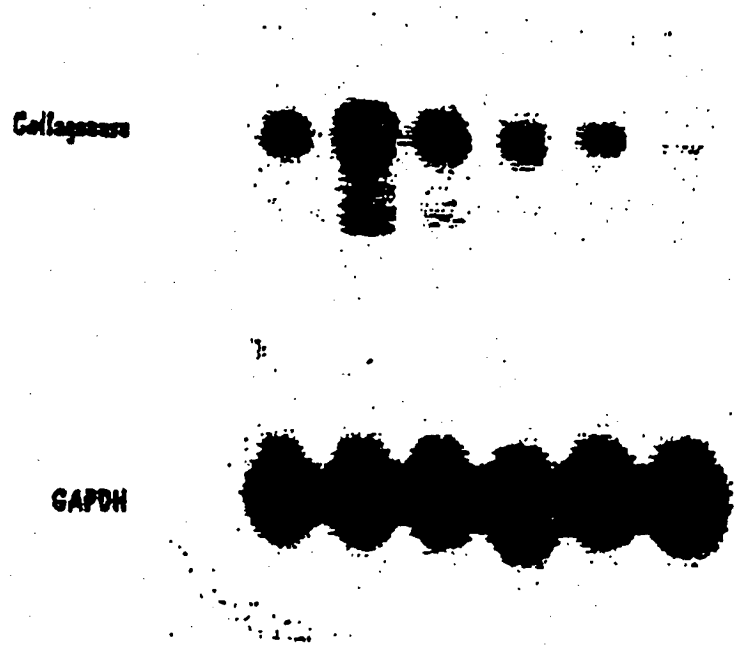

FIGURE 12B

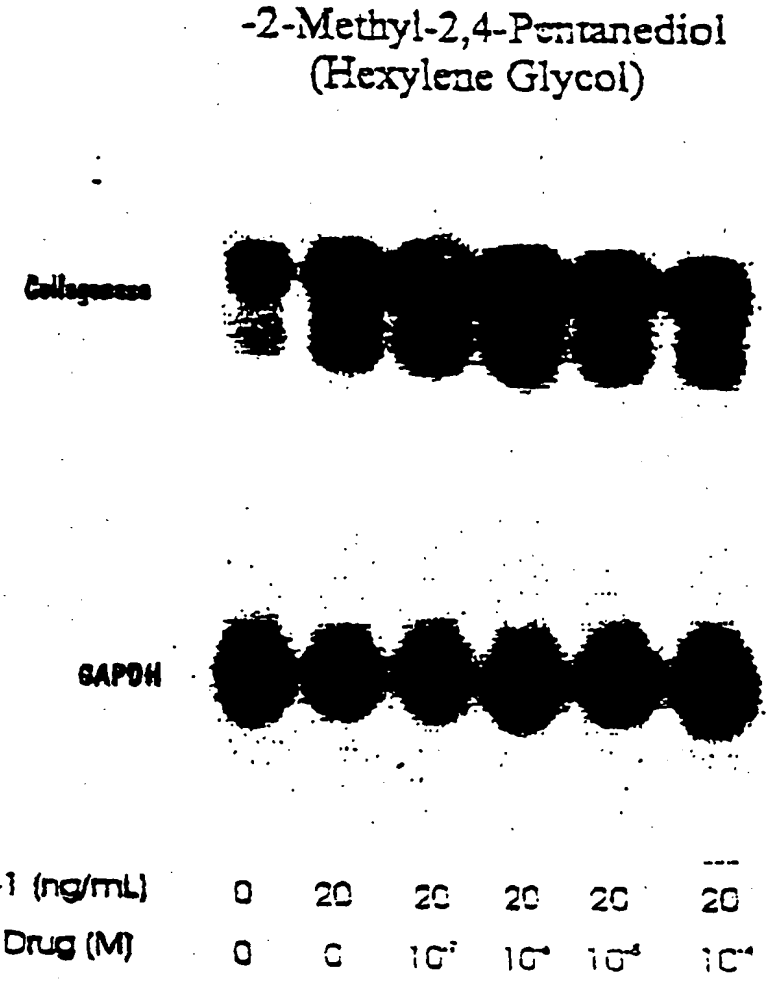
-2-Methyl-2,4-Pentanediol
(Hexylene Glycol)
Collagenase
GAPDH
IL-1 (ng/mL) 0 20 20 20 20 20
Drug (M) 0 0 10⁻⁷ 10⁻⁶ 10⁻⁵ 10⁻⁴

FIGURE 12C

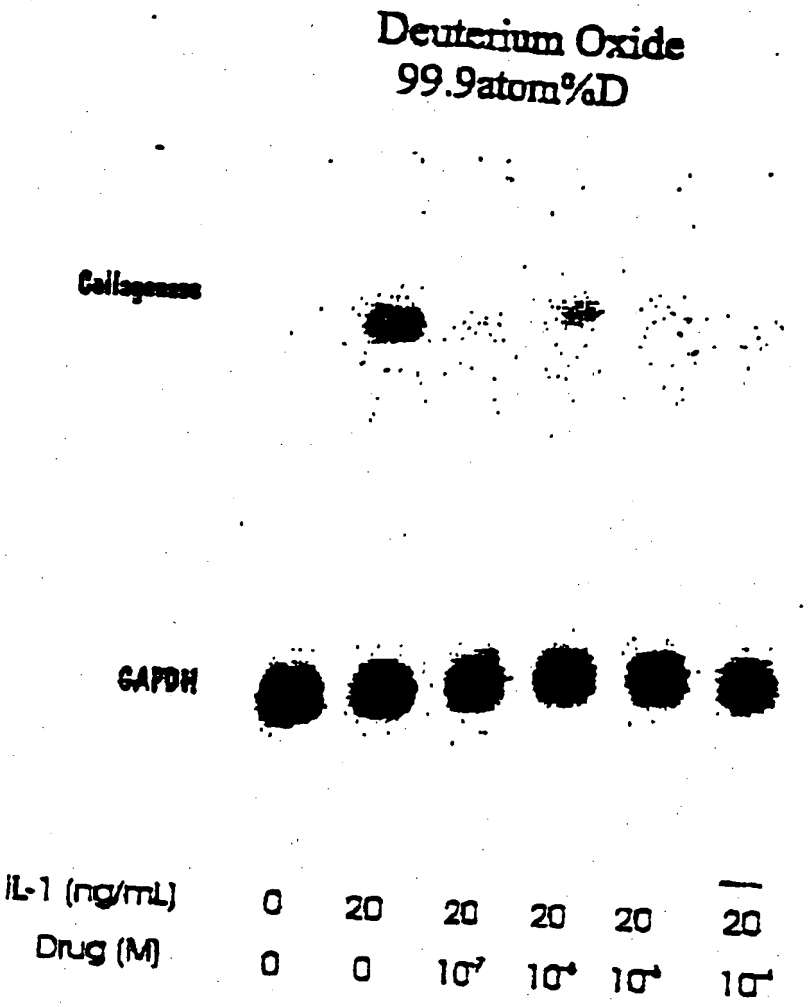
Deuterium Oxide
99.9atom%D
Collagenase
GAPDH
IL-1 (ng/mL) 0 20 20 20 20 20
Drug (M) 0 0 10⁻⁷ 10⁻⁶ 10⁻⁵ 10⁻⁴

FIGURE 12D

Glycine Ethyl Ester

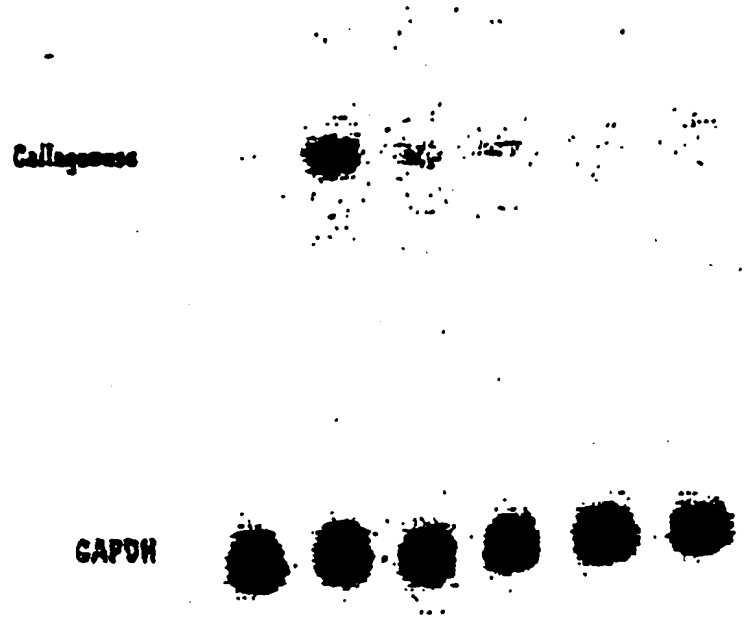

FIGURE 12E

Ethylene Glycol Bis-
(succinimidylsuccinate)

FIGURE 12F

Tubercidin

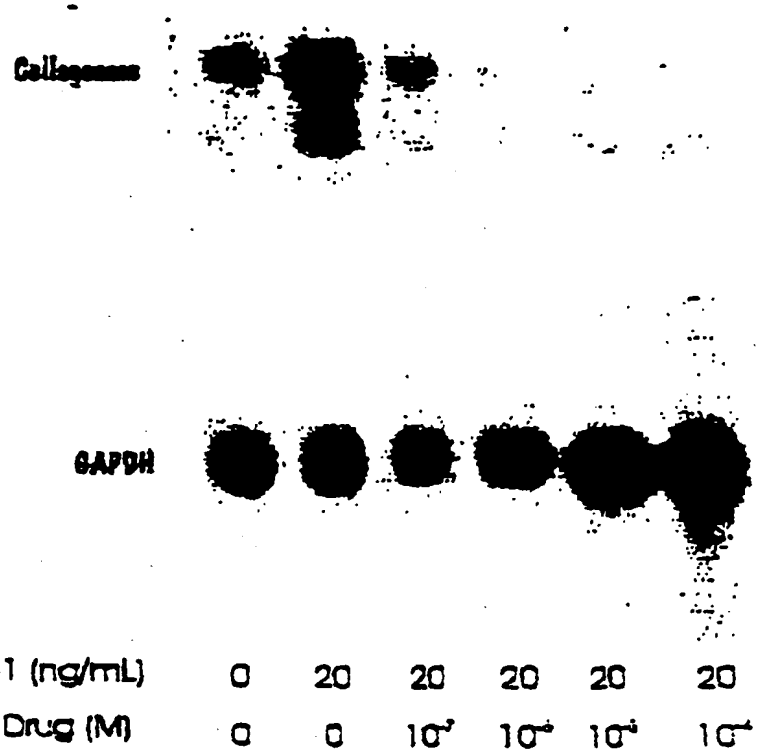

FIGURE 12G

Aluminum Fluoride

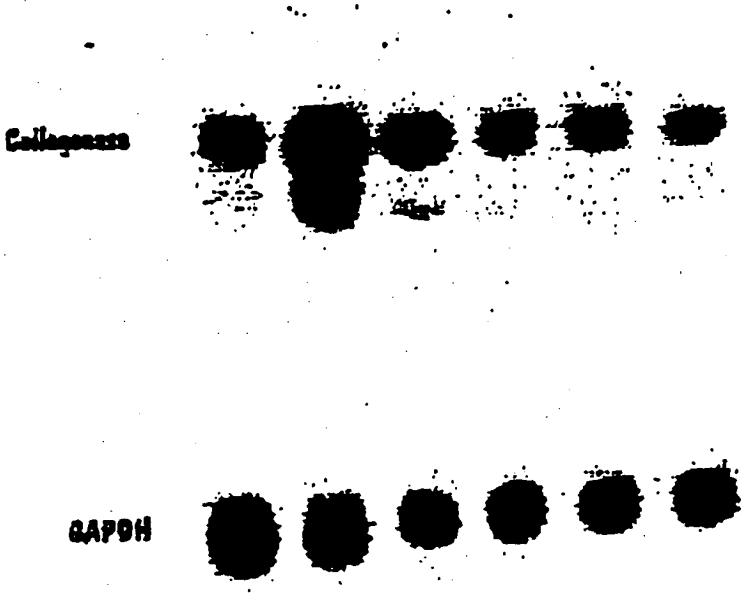

FIGURE 12H

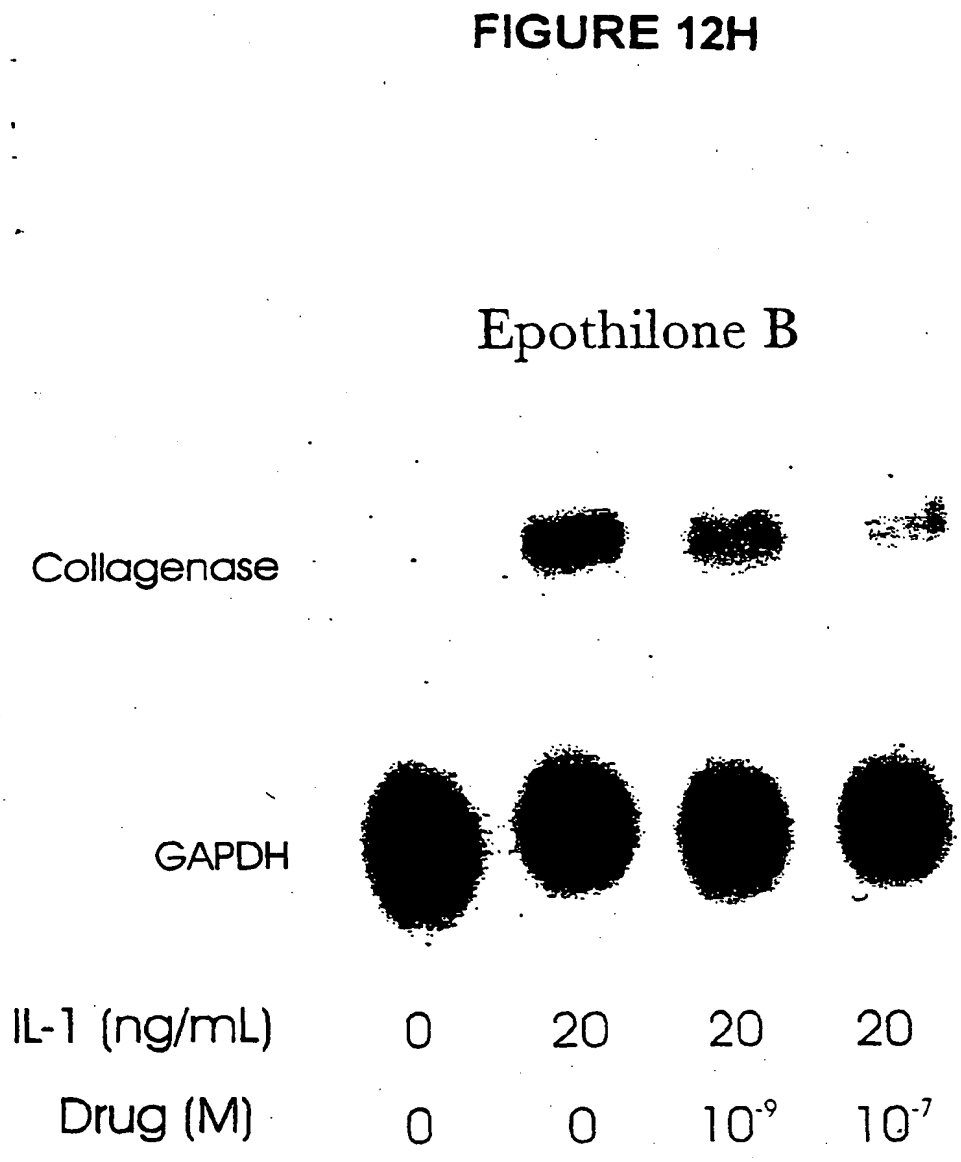
Epothilone B
Collagenase
GAPDH
IL-1 (ng/mL) 0 20 20 20
Drug (M) 0 0 10-9 10-7

FIGURE 13A

Ly 290181

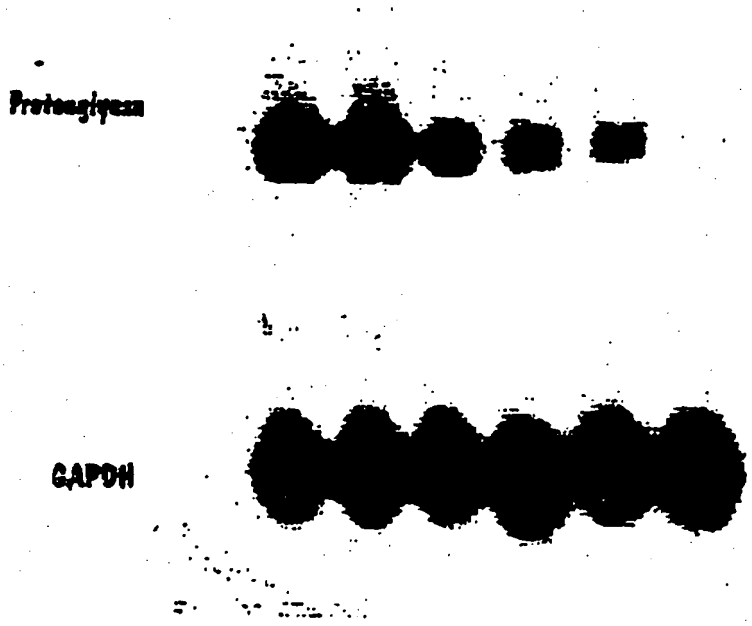

FIGURE 13B

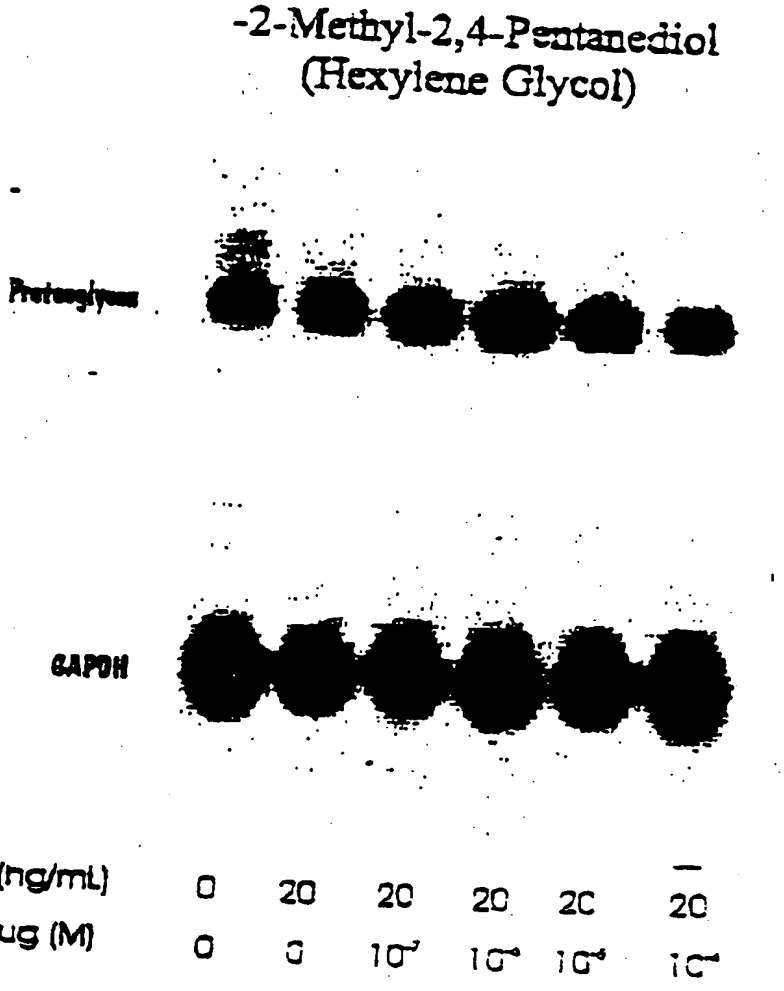
-2-Methyl-2,4-Pentanediol
(Hexylene Glycol)
Proteoglycan
GAPDH
IL-1 (ng/mL) 0 20 20 20 20 20
Drug (M) 0 0 10⁻⁷ 10⁻⁶ 10⁻⁵ 10⁻⁴

FIGURE 13C

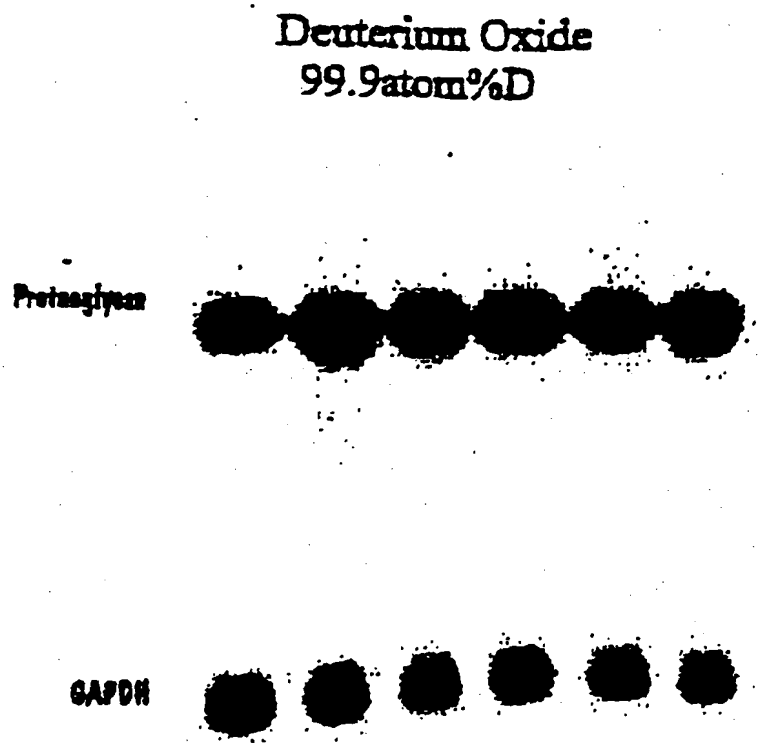
Deuterium Oxide
99.9atom%D
Prolargiyase
GAPDH
IL-1 (ng/mL) 0 20 20 20 20 20
Drug (M) 0 0 10⁻⁷ 10⁻⁶ 10⁻⁵ 10⁻⁴

FIGURE 13D

Glycine Ethyl Ester

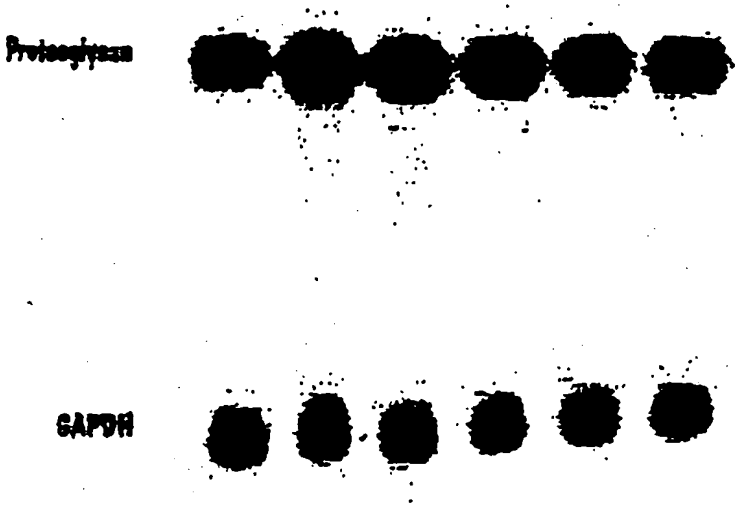

FIGURE 13E

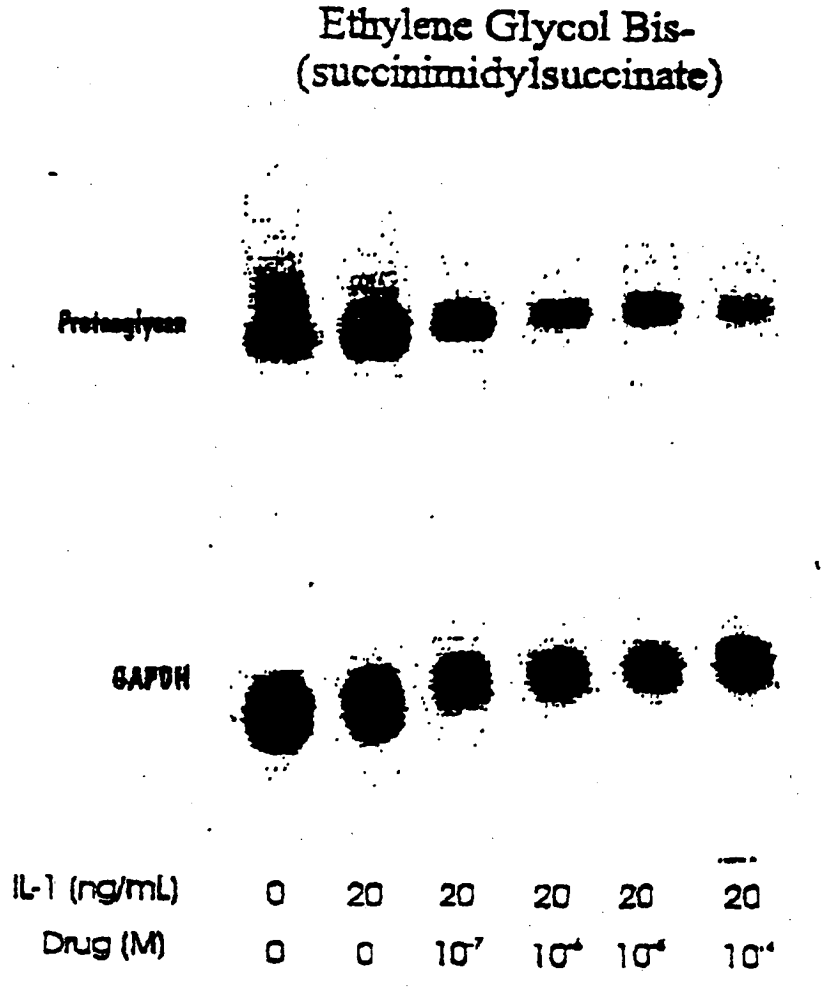
Ethylene Glycol Bis-
(succinimidylsuccinate)
Proteoglycan
GAPDH
IL-1 (ng/mL) 0 20 20 20 20 20
Drug (M) 0 0 10⁻⁷ 10⁻⁶ 10⁻⁵ 10⁻⁴

FIGURE 13F

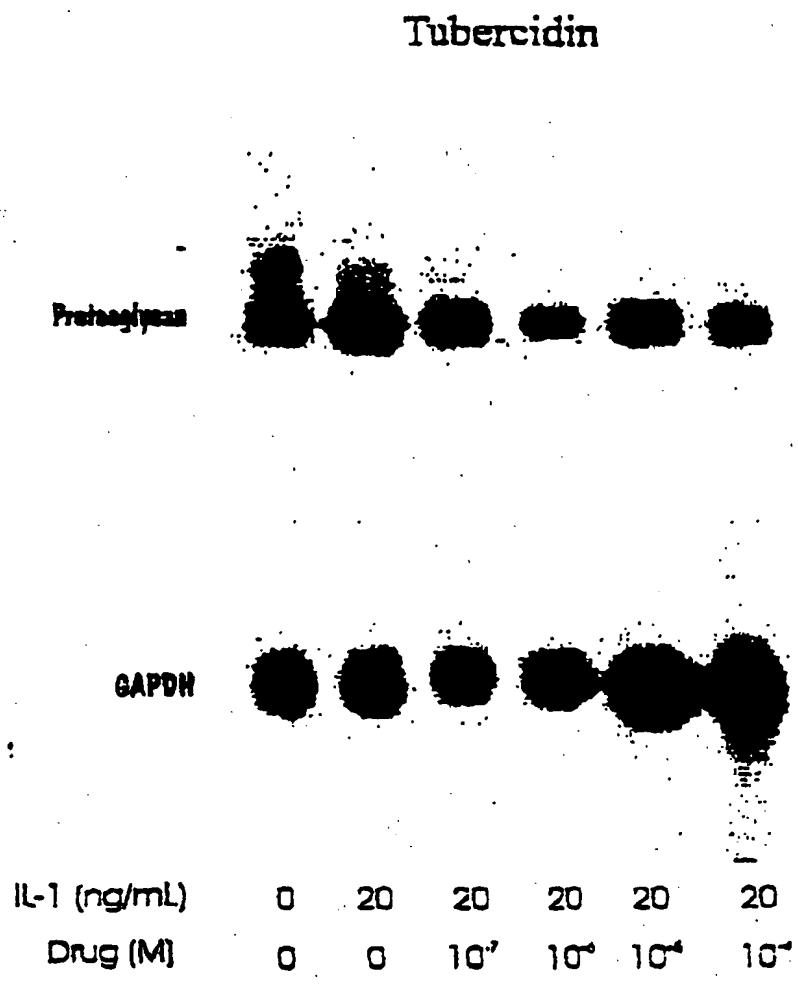
Tubercidin
Proteoglycan
GAPDH
IL-1 (ng/mL) 0 20 20 20 20 20
Drug (M) 0 0 10⁻⁷ 10⁻⁶ 10⁻⁵ 10⁻⁴

FIGURE 13G

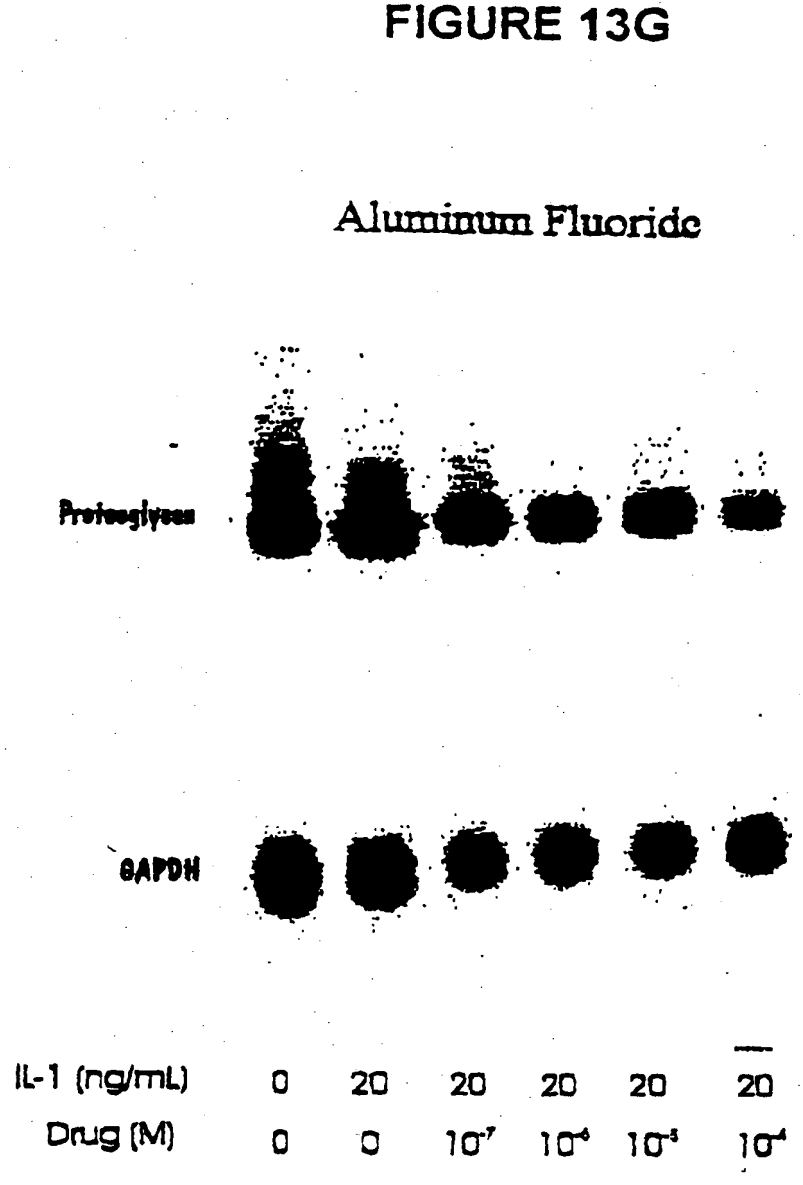
Aluminum Fluoride
Proteoglycan
GAPDH
IL-1 (ng/mL) 0 20 20 20 20 20
Drug (M) 0 0 10⁻⁷ 10⁻⁶ 10⁻⁵ 10⁻⁴

FIGURE 13H

Epothilone B

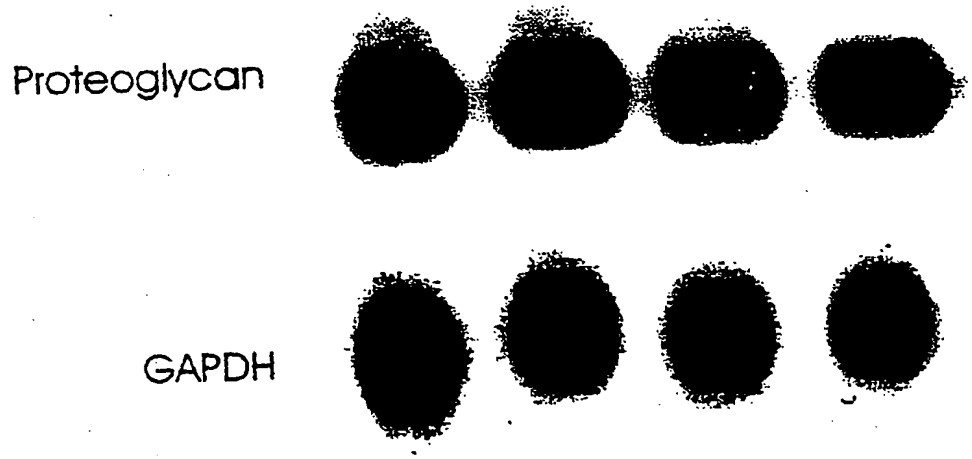

FIGURE 14A

FIGURE 14B

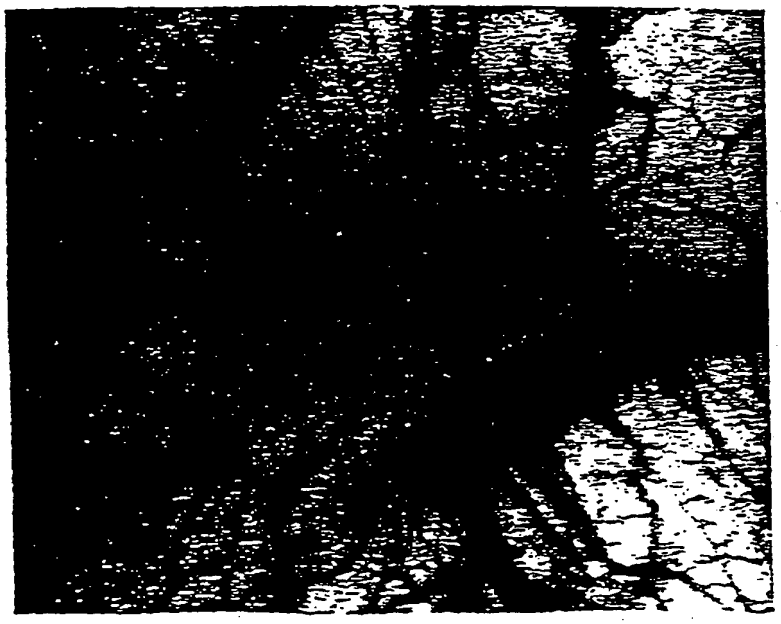

FIGURE 14C

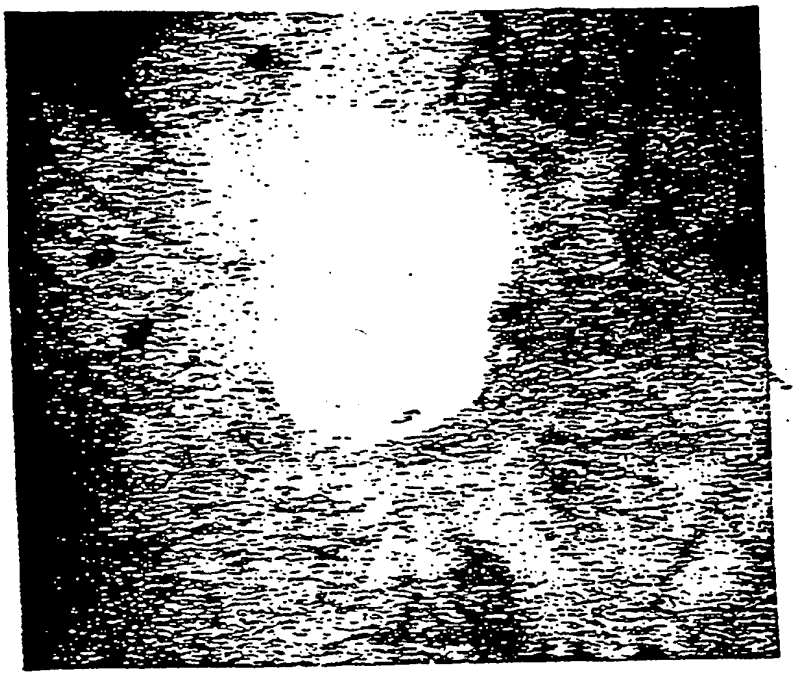

FIGURE 14D

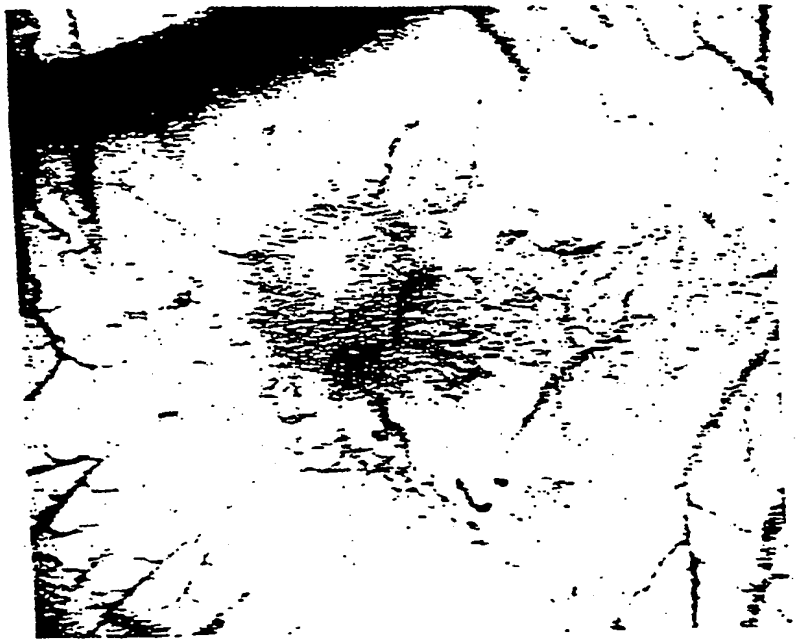

FIGURE 15A-15E

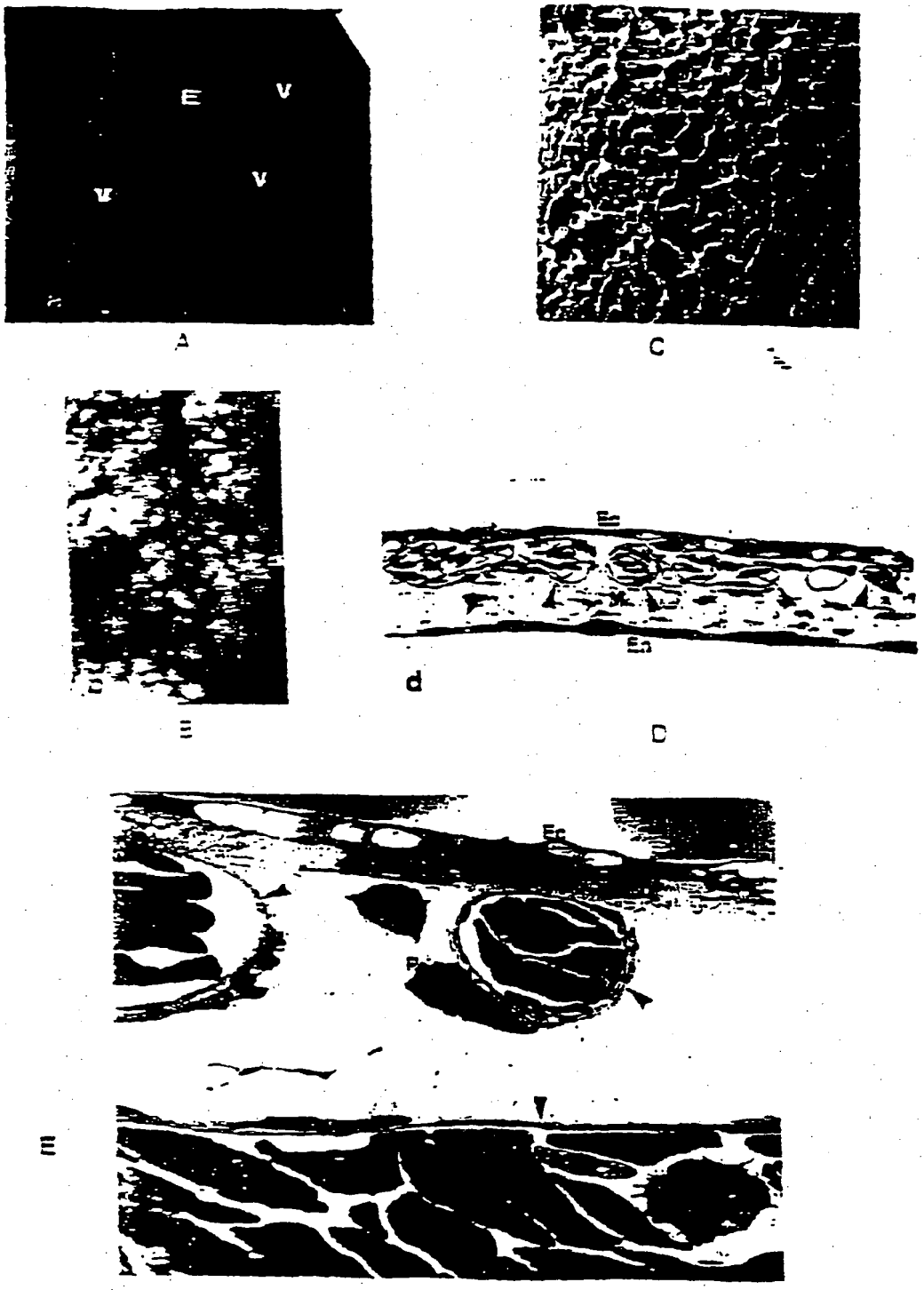

FIGURE 16A-16D

A

B

C

D

FIGURE 17A-17C

FIGURE 18A-18C

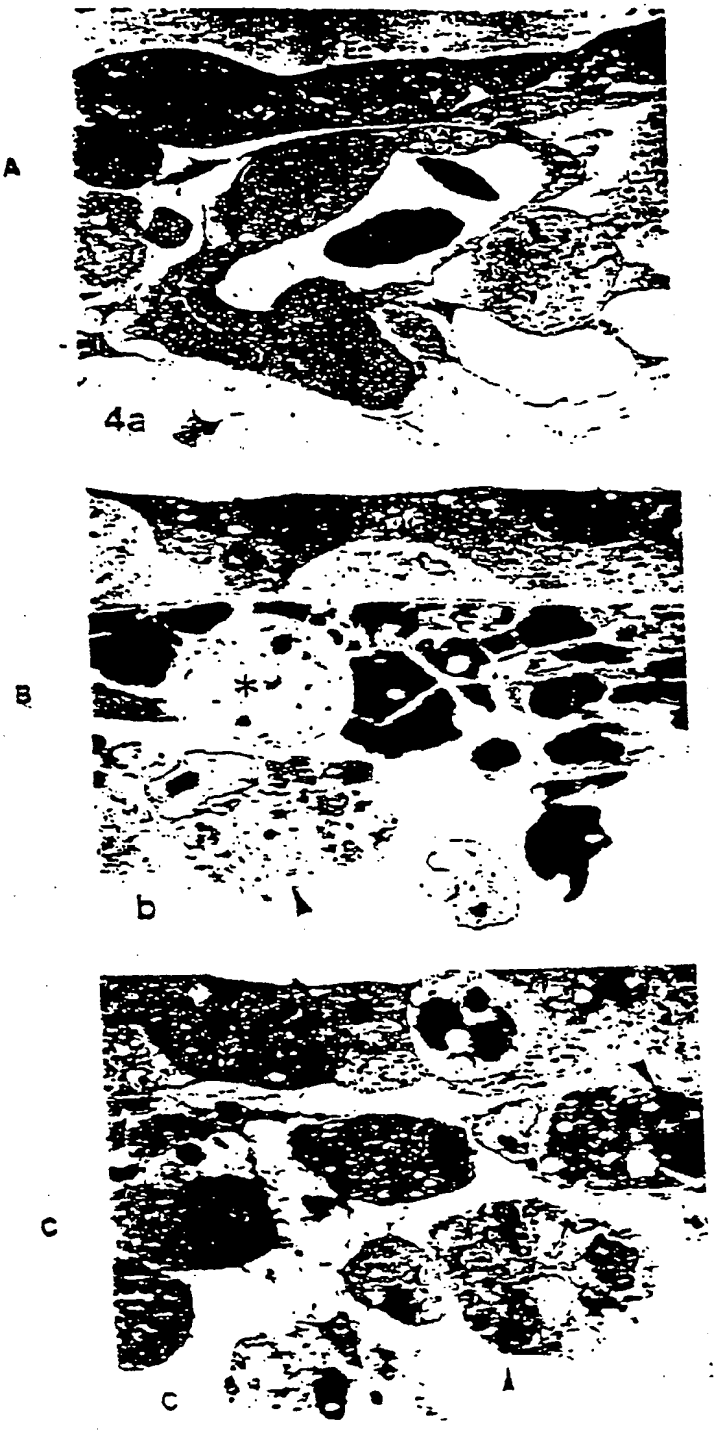

Transcriptional Regulation of MMPs

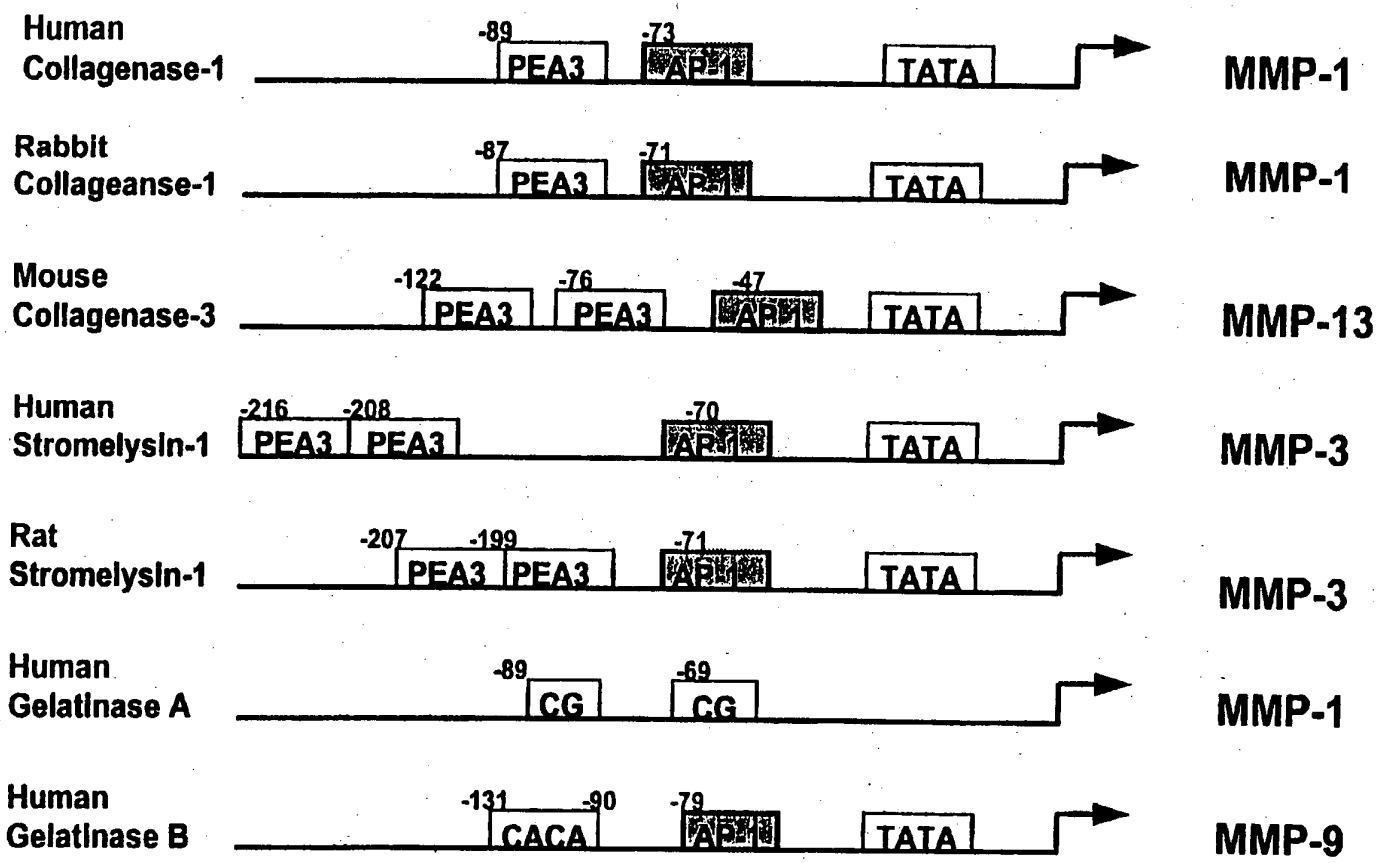

FIGURE 19A

EP 0 941 089 B1

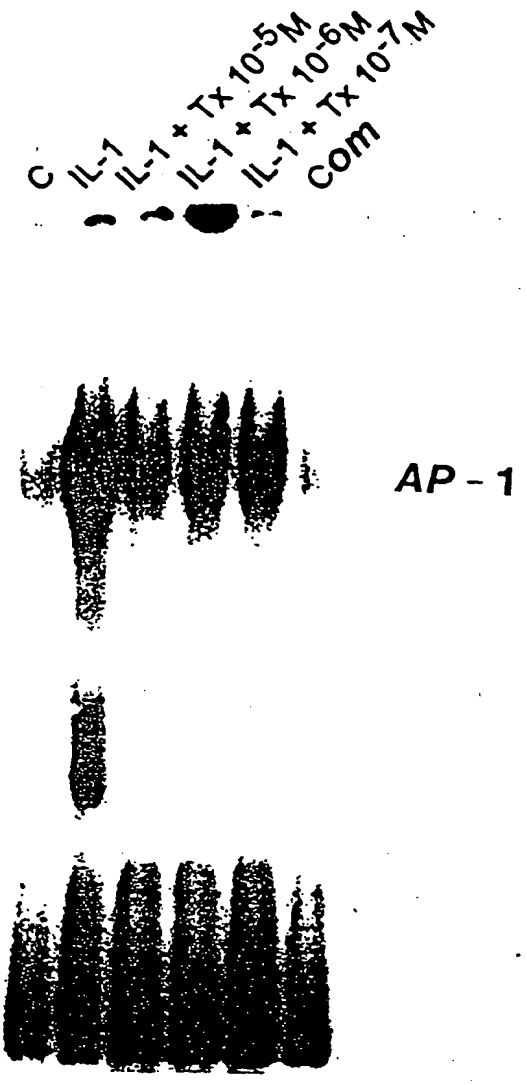

FIGURE 19B

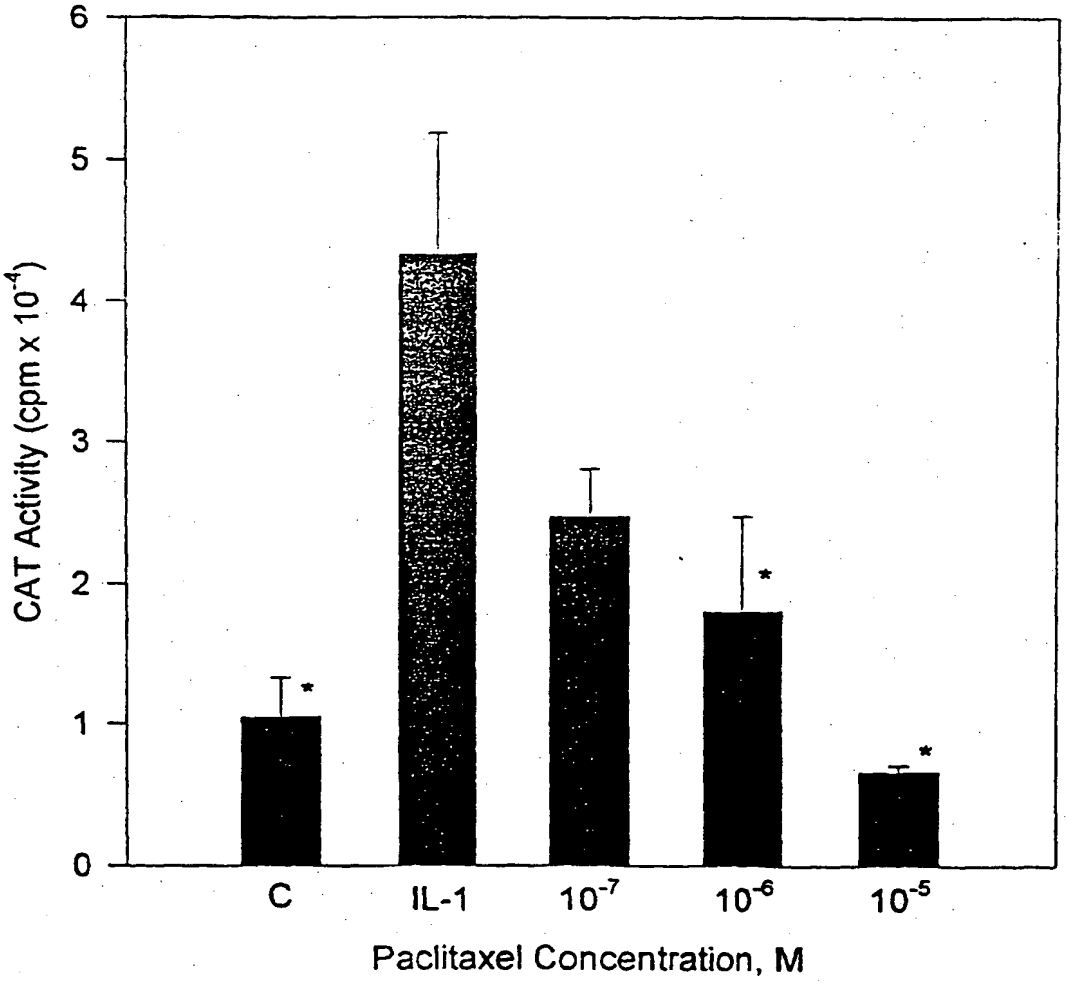
6
5
4
3
2
1
0
CAT Activity (cpm x 10^{-4})
*
*
*
C
IL-1
10^{-7}
10^{-6}
10^{-5}
Paclitaxel Concentration, M

FIGURE 19C

FIGURE 20

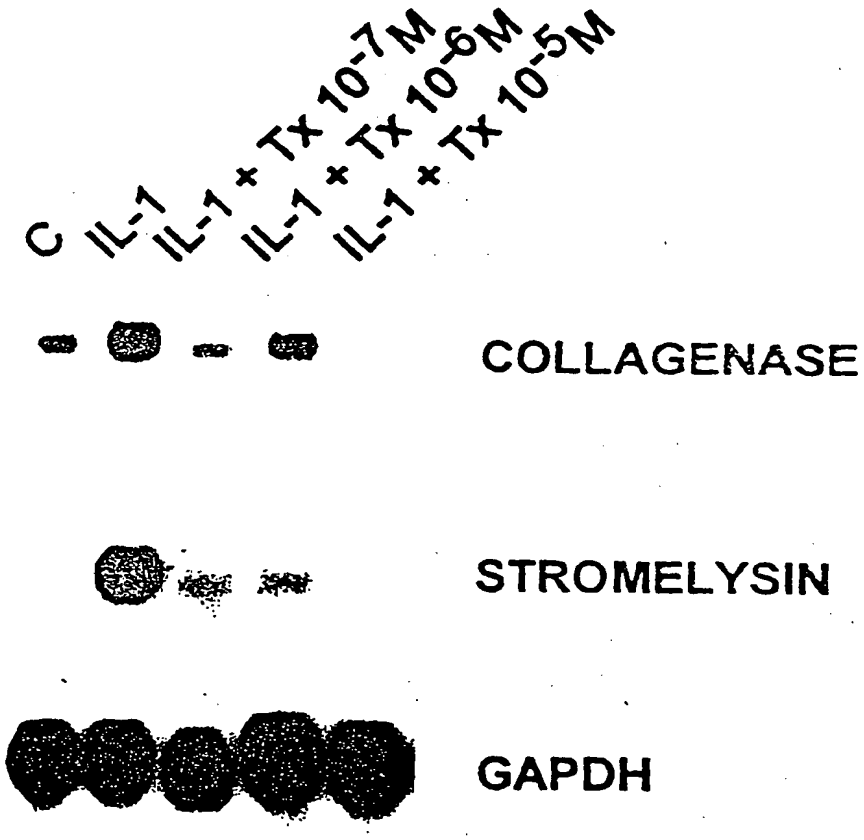
C
IL-1
IL-1 + TX 10-7M
IL-1 + TX 10-6M
IL-1 + TX 10-5M
COLLAGENASE
STROMELYSIN
GAPDH

FIGURE 21

Effect of Taxol on Viability of Normal Chondrocytes *In Vitro*

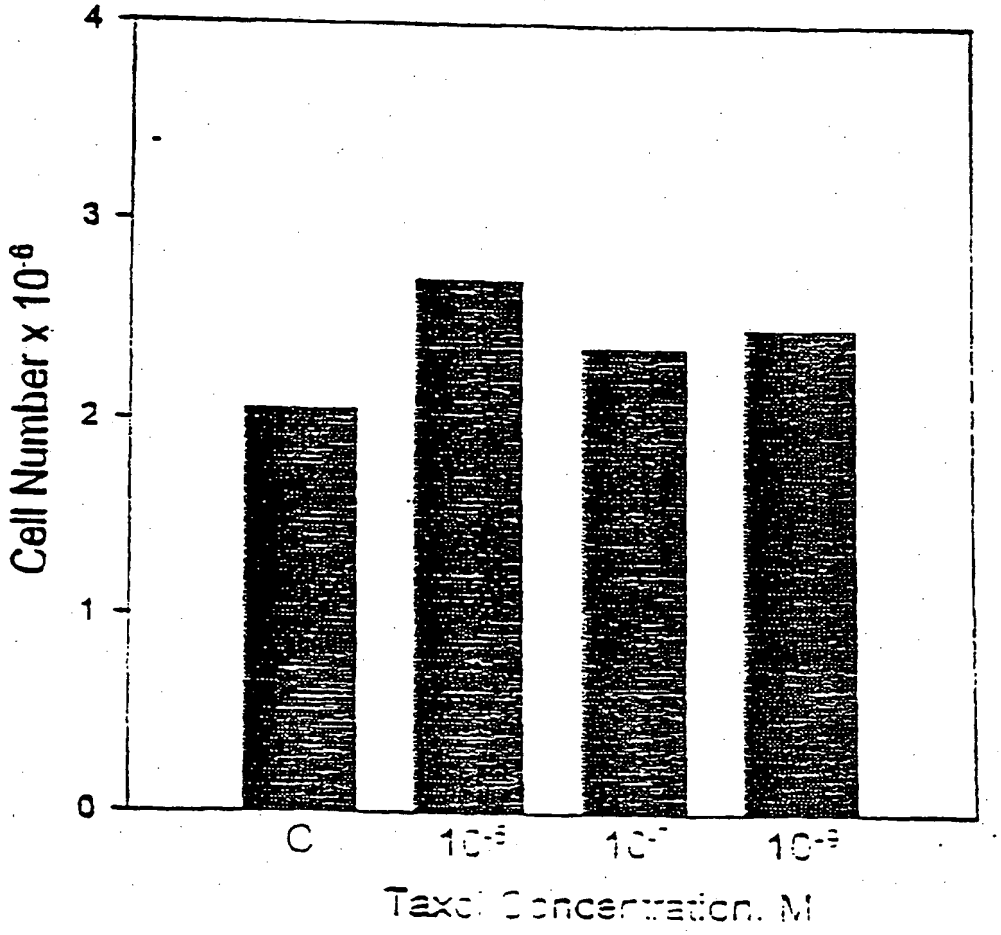

FIGURE 22

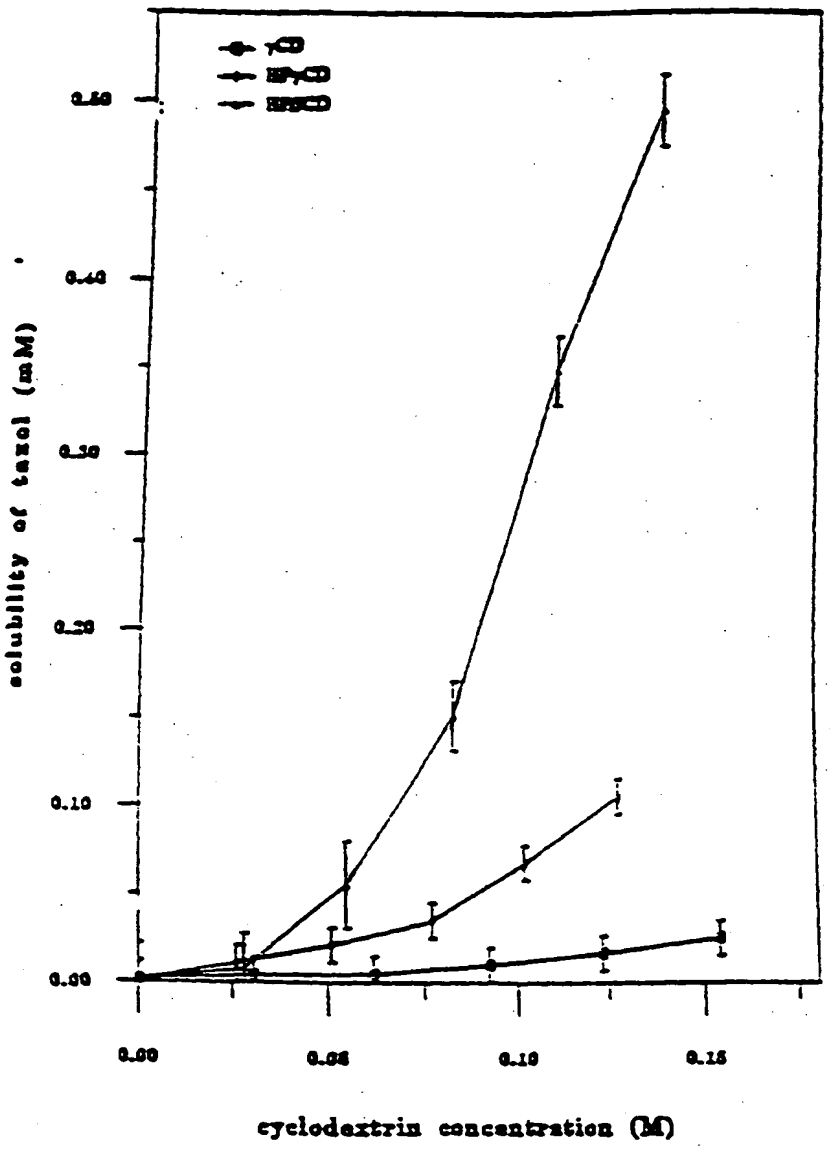
solubility of taxol (mM)
0.00
0.10
0.20
0.40
0.00
0.05
0.10
0.15
cyclodextrin concentration (M)

FIGURE 23

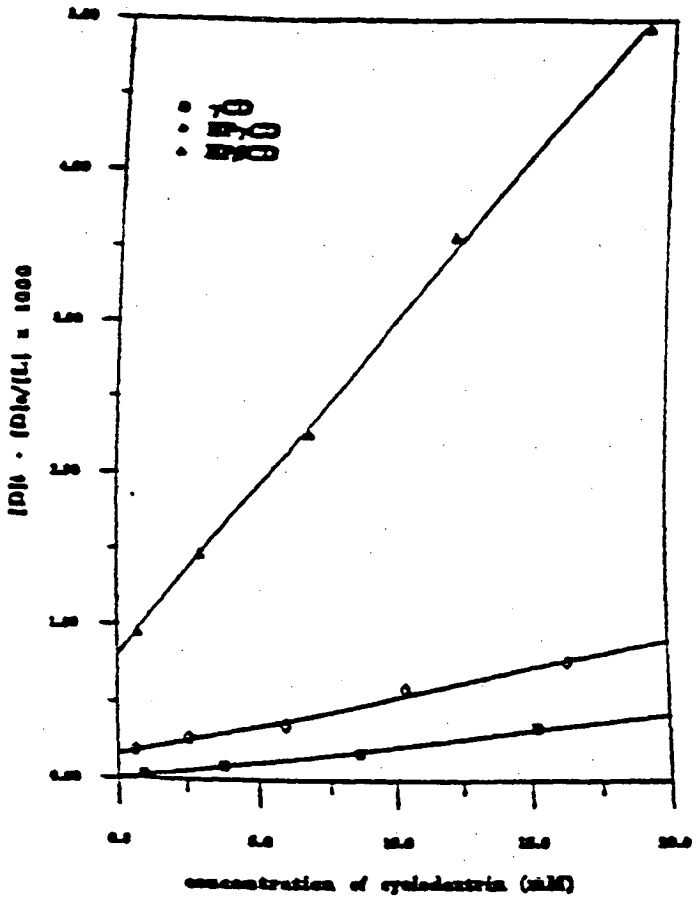

FIGURE 24

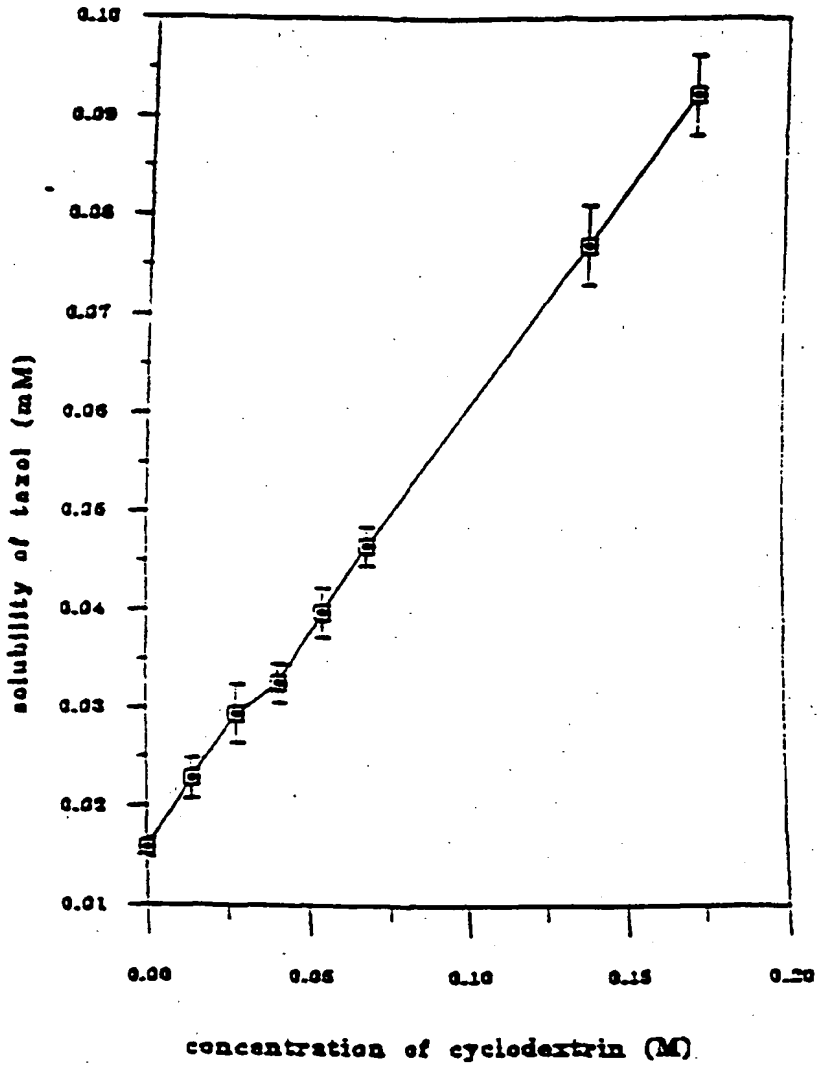
solubility of taxol (mM)
0.01
0.02
0.03
0.04
0.05
0.06
0.07
0.08
0.09
0.10
0.00
0.05
0.10
0.15
0.20
concentration of cyclodextrin (M)

FIGURE 25

Melting temperature, enthalpy, molecular weight (M_n), polydispersity (M_w/M_n), and intrinsic viscosity ([η]) of PDLLA-PEG-PDLLA

PDLLA-PEG-PDLLA PEG content	Melting Temp.[a], °C	ΔH[a], J/g	M_n[b], x10^{-4}	M_w/M_n[b]	[η][c], dl/g
100%	61.8	184.8	0.8[d]	–	–
70%	50.2	72.2	2.1	1.21	0.27
40%	46.3	42.3	4.5	3.5	0.29
30%	None	None	5.9	2.95	1.0
20%	None	None	5.1	2.96	1.45
10%	None	None	11	2.38	1.5
taxol	212	59.3	–	–	–
20% taxol loaded copolymer (30%PEG)	212.1	5.6	–	–	–

a: measured by DSC.

b: measured by GPC, relative to polystyrene standard.

c: in $CHCl_3$ at 25°C

d: data supplied by manufacturer

FIGURE 26

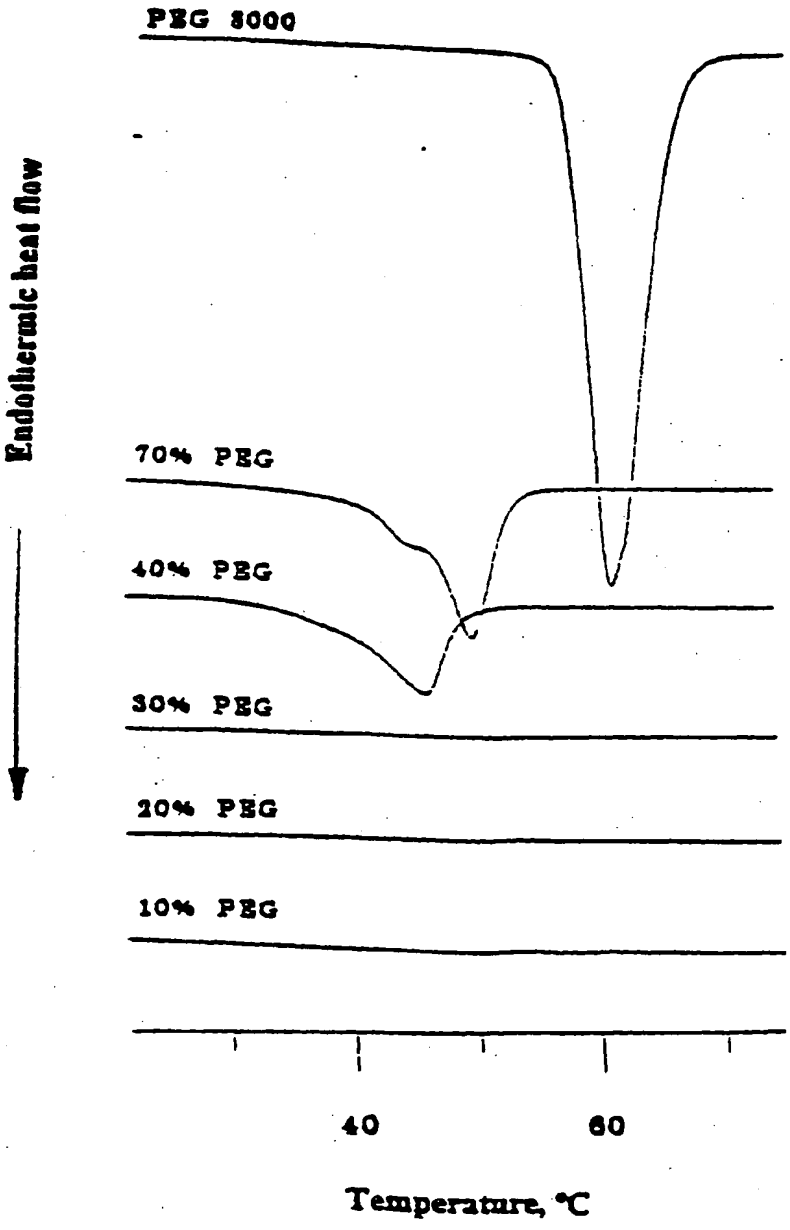
PEG 8000
70% PEG
40% PEG
30% PEG
20% PEG
10% PEG
Endothermic heat flow
40
60
Temperature, °C

FIGURE 27

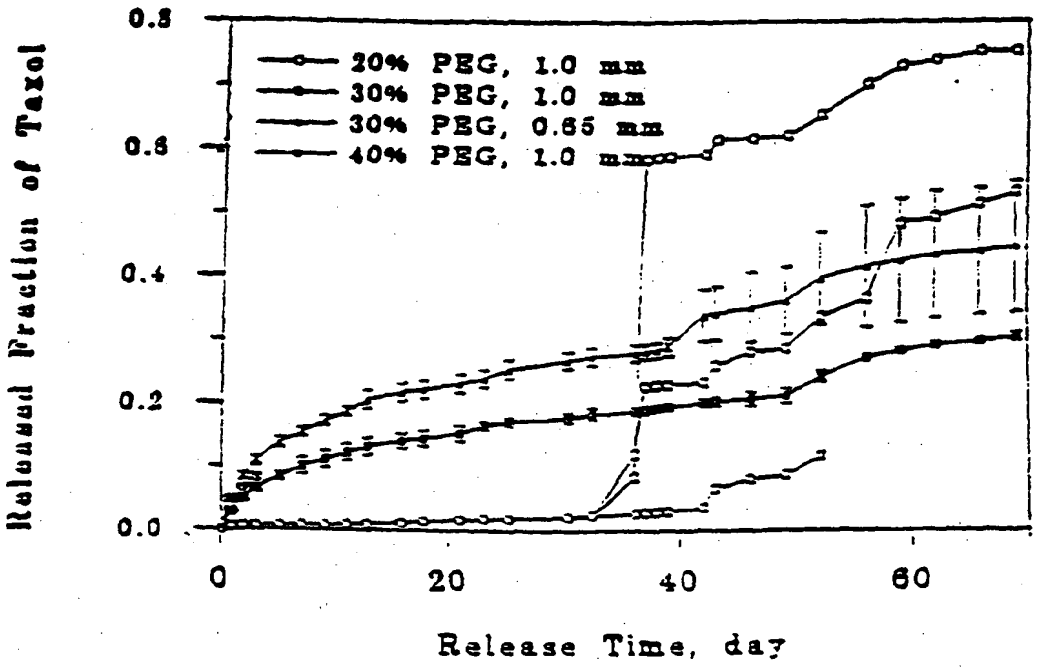
0.8
0.6
0.4
0.2
0.0
0
20
40
60
Released Fraction of Taxol
Release Time, day
20% PEG, 1.0 mm
30% PEG, 1.0 mm
30% PEG, 0.65 mm
40% PEG, 1.0 mm

FIGURE 28A-28C

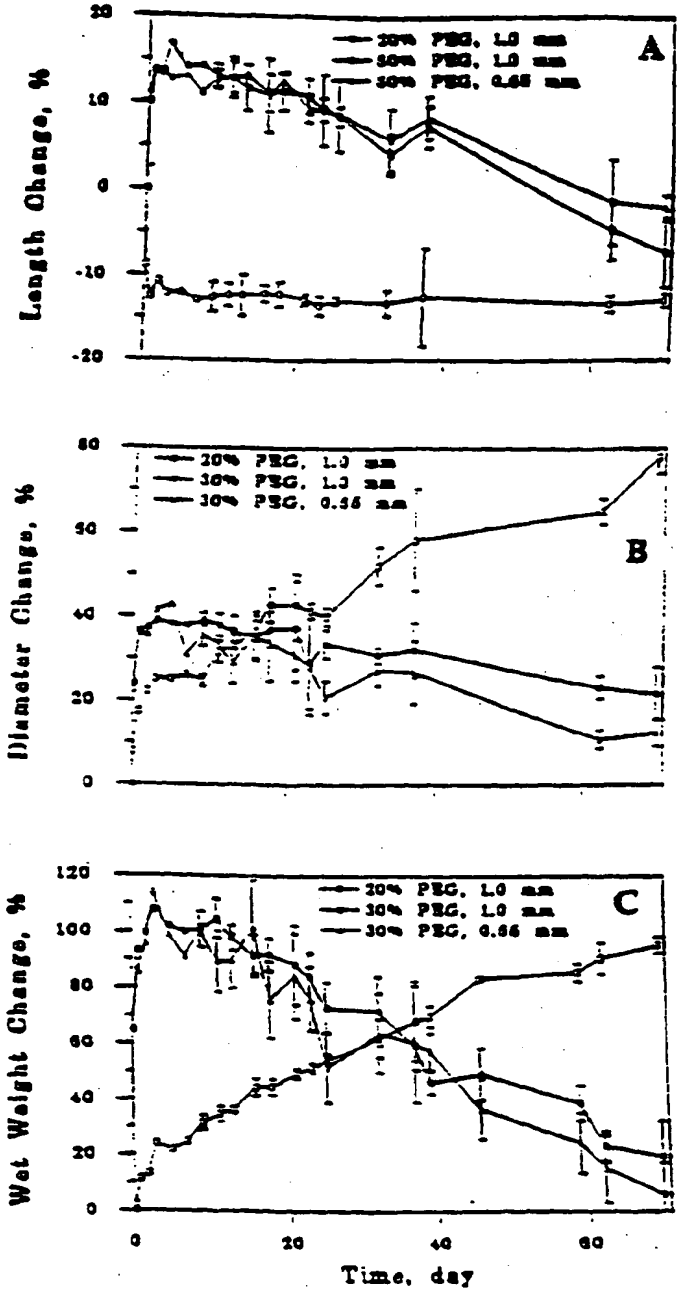

FIGURE 29

Mass loss and polymer composition change of PDLLA-PEG-PDLLA cylinders (loaded with 20% taxol) during the release into PBS albumin buffer at 37°C

°C

Sample[a]	Time, day	Dry wt loss, %	1.65/5.1[b]	3.6/5.1[b]
20% PEG-1mm	0	0	3.51	1.65
20% PEG-1mm	32	7.9	–	–
20% PEG-1mm	69	19.2	3.63	0.68
30% PEG-1mm	0	0	3.39	3.91
30% PEG-1mm	32	28.9	–	–
30% PEG-1mm	69	45.5	4.3	0.56
30% PEG-0.65mm	0	0	3.39	3.91
30% PEG-0.65mm	32	26.7	–	–
30% PEG-0.65mm	69	57.5	5.8	0.21

a: PDLLA-PEG-PDLLA copolymer cylinders showing PEG content and diameter of cylinder.

b: measured by ^{1}H-NMR in $CDCl_3$; 1.65/5.1 represents the ratio of peak areas at 1.65ppm (due to $-CHCH_3^*-$ in PDLLA) and 5.1ppm (due to $-CH^*CH_3-$ in PDLLA); 3.6/5.1 represents the ratio of peak areas at 3.6ppm (due to $-CH_2^*CH_2^*-$ in PEG) and 5.1ppm.

FIGURE 30

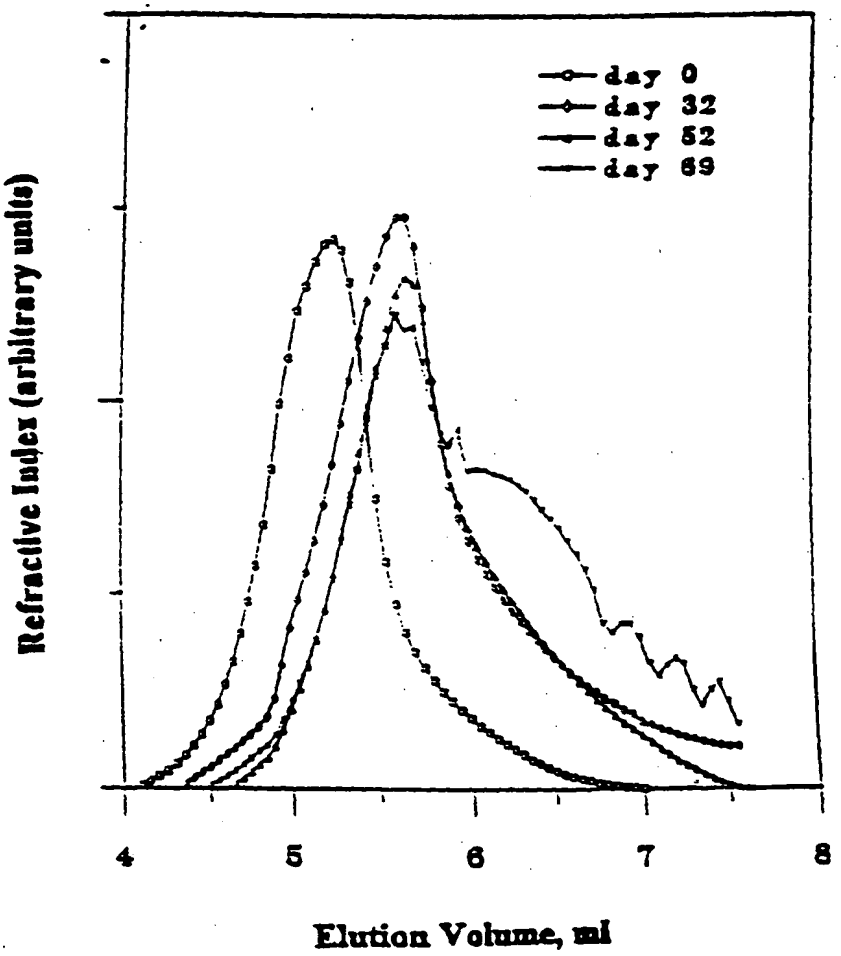
day 0
day 32
day 52
day 69
Refractive Index (arbitrary units)
4
5
6
7
8
Elution Volume, ml

FIGURE 31

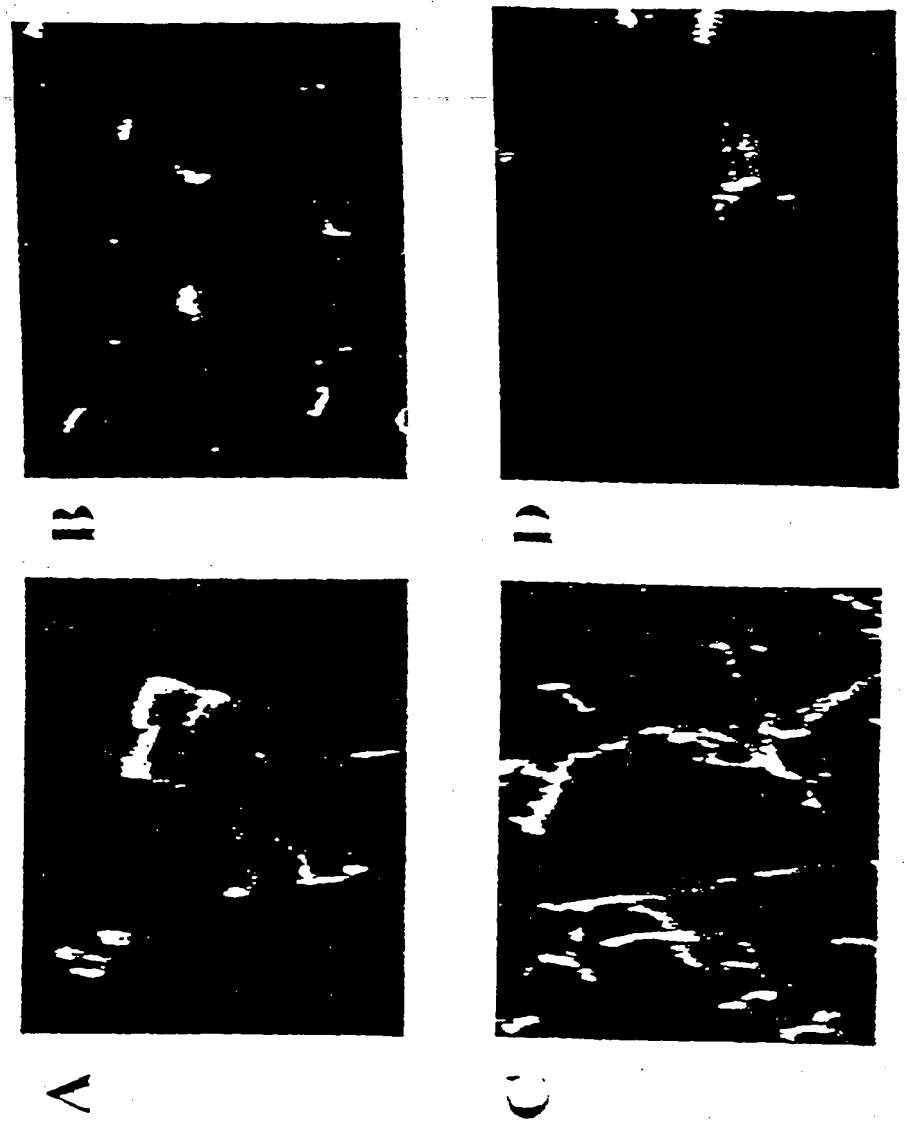

FIGURE 32

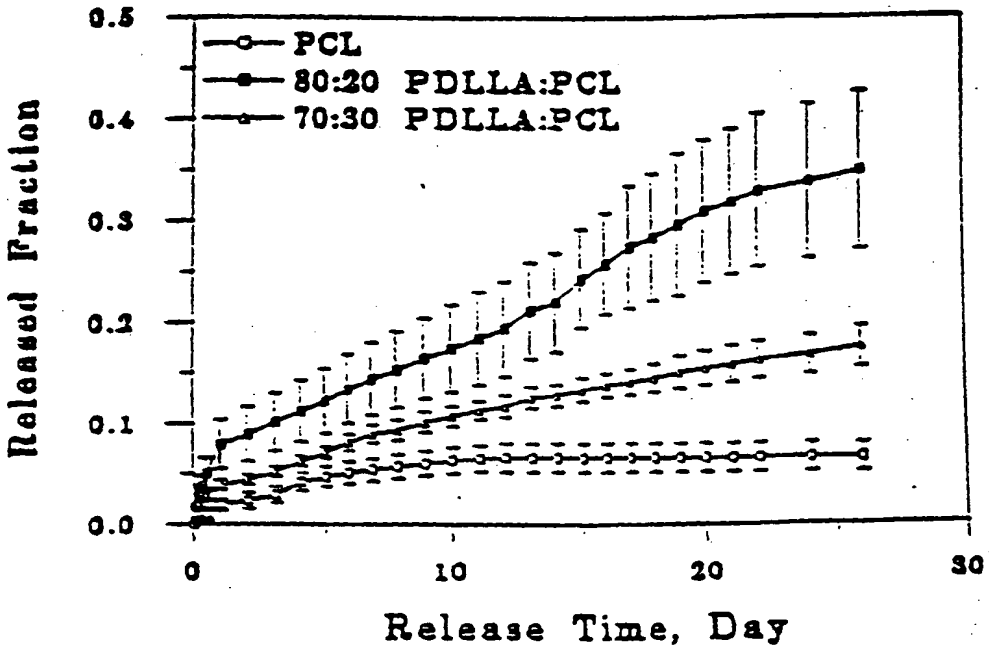
PCL
80:20 PDLLA:PCL
70:30 PDLLA:PCL
Released Fraction
0.0
0.1
0.2
0.3
0.4
0.5
0
10
20
30
Release Time, Day

FIGURE 33

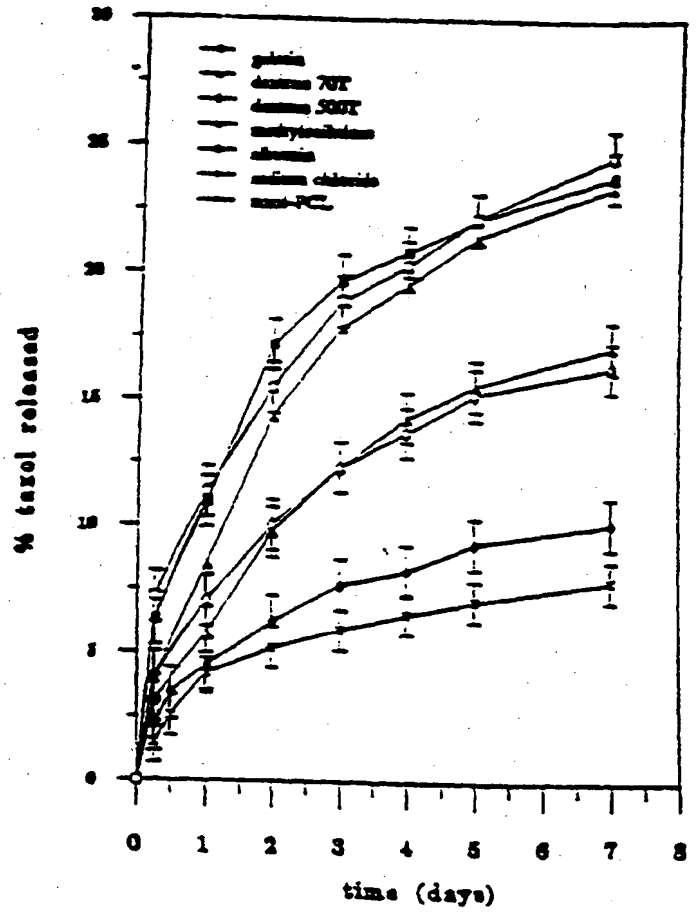

FIGURE 34

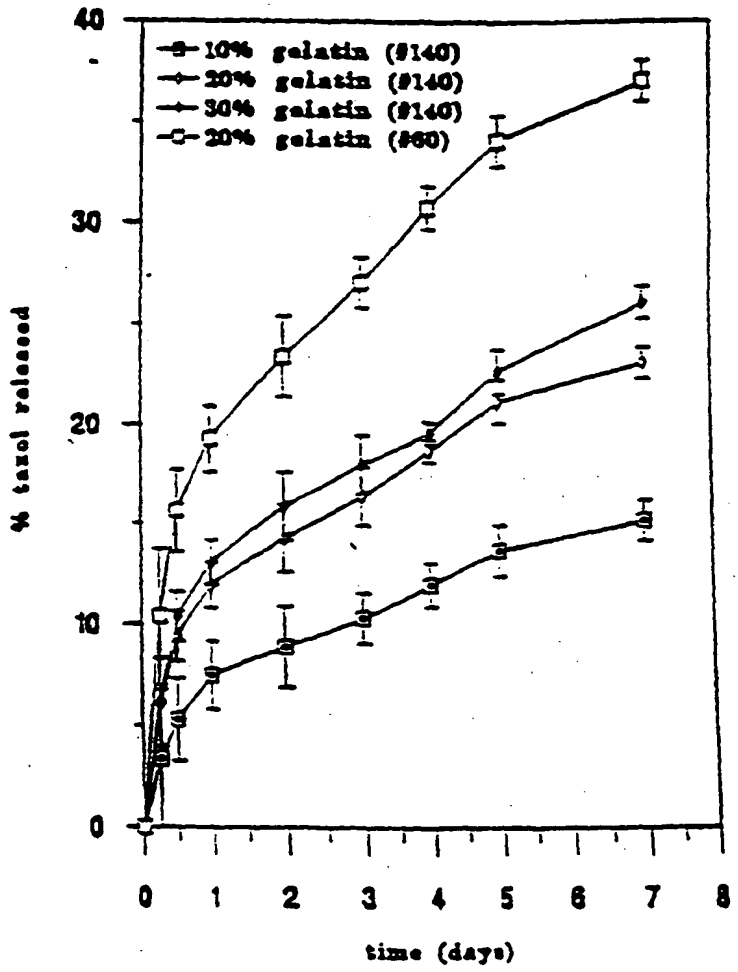
10% gelatin (#140)
20% gelatin (#140)
30% gelatin (#140)
20% gelatin (#60)
% taxol released
time (days)
0
10
20
30
40
0
1
2
3
4
5
6
7
8

FIGURE 35

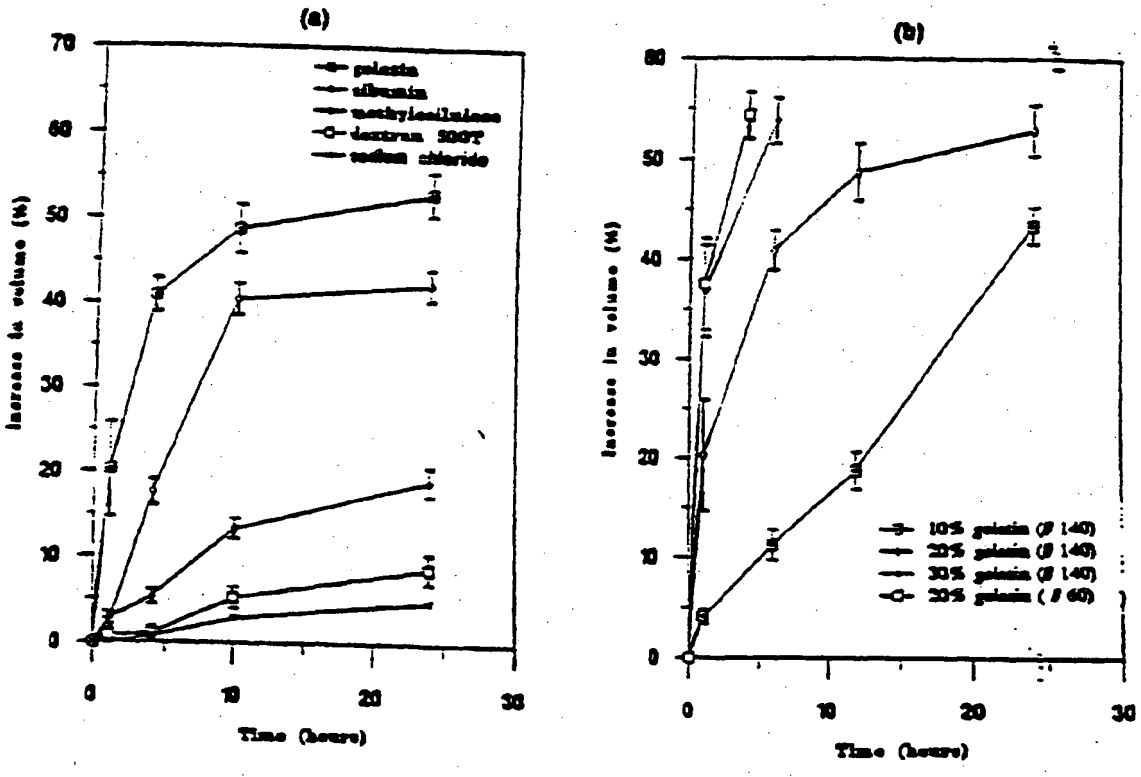
(a)
gelatin
albumin
methylcellulose
dextran 500T
sodium chloride
Increase in volume (%)
Time (hours)
(b)
10% gelatin (# 140)
20% gelatin (# 140)
30% gelatin (# 140)
20% gelatin (# 60)
Increase in volume (%)
Time (hours)

FIGURE 36A-36D

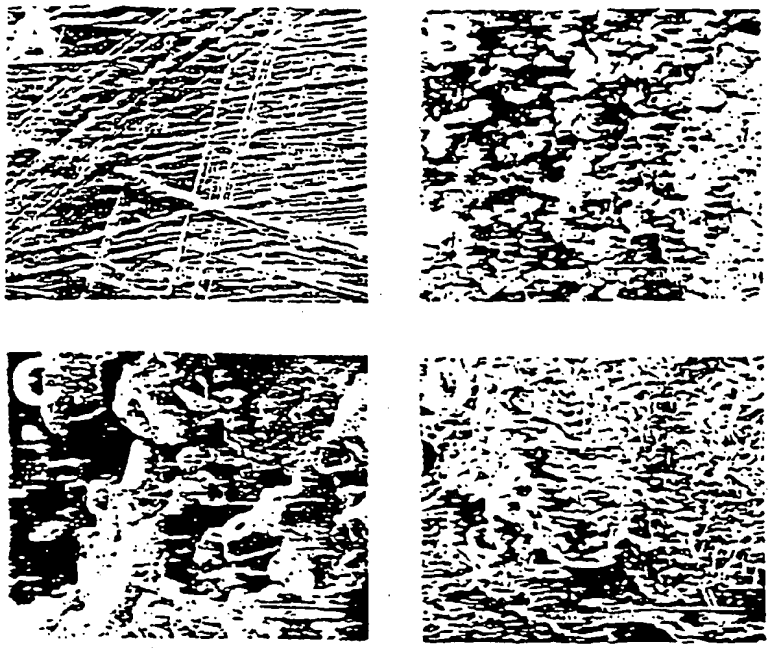

FIGURE 37A-37B

FIGURE 38

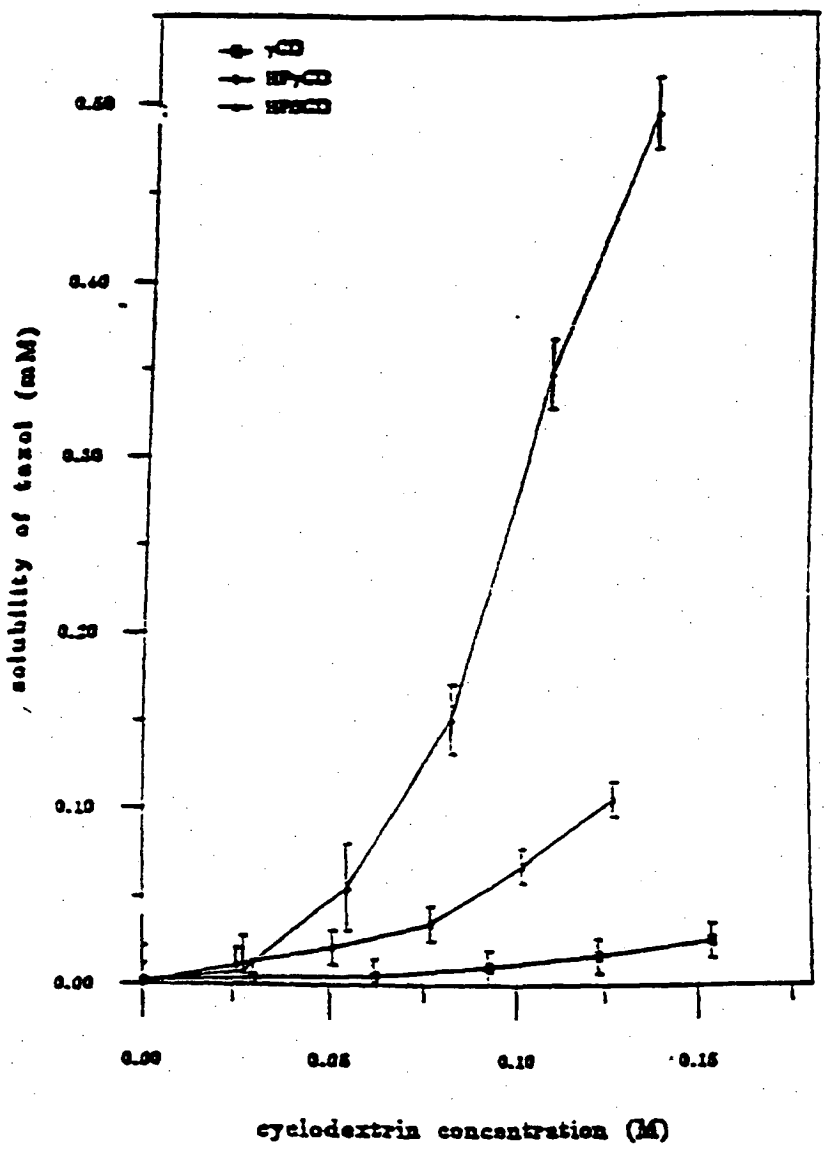
γCD
solubility of taxol (mM)
0.00
0.05
0.10
0.15
cyclodextrin concentration (M)

FIGURE 39

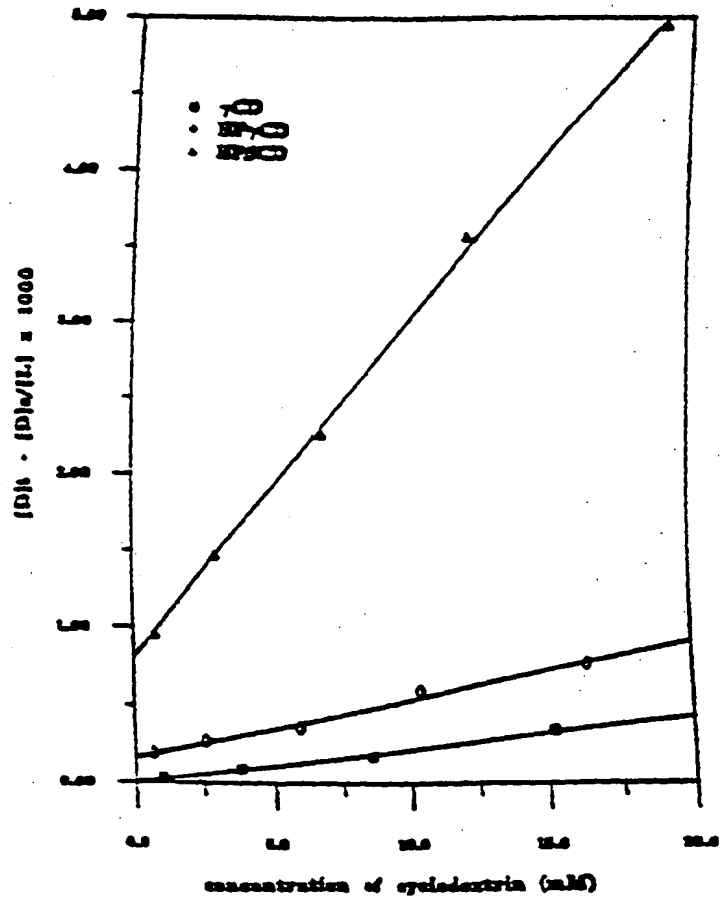

FIGURE 40

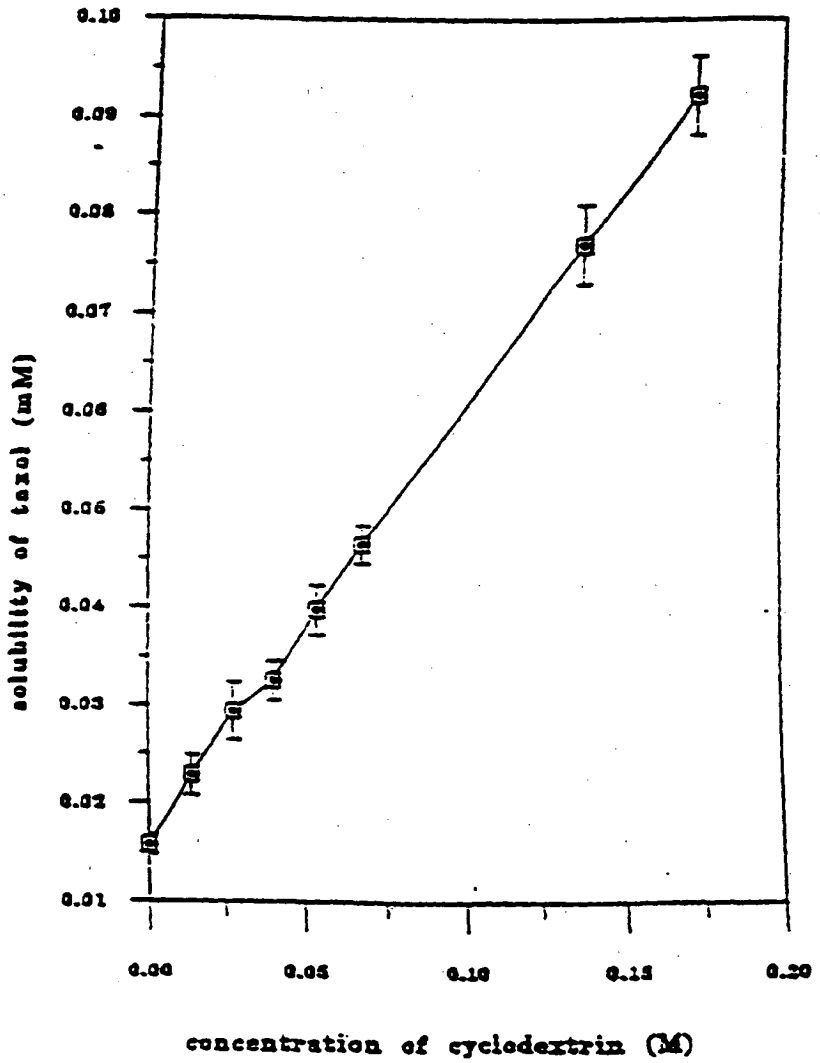
0.10
0.09
0.08
0.07
0.06
0.05
0.04
0.03
0.02
0.01
solubility of taxol (mM)
0.00
0.05
0.10
0.15
0.20
concentration of cyclodextrin (M)

FIGURE 41

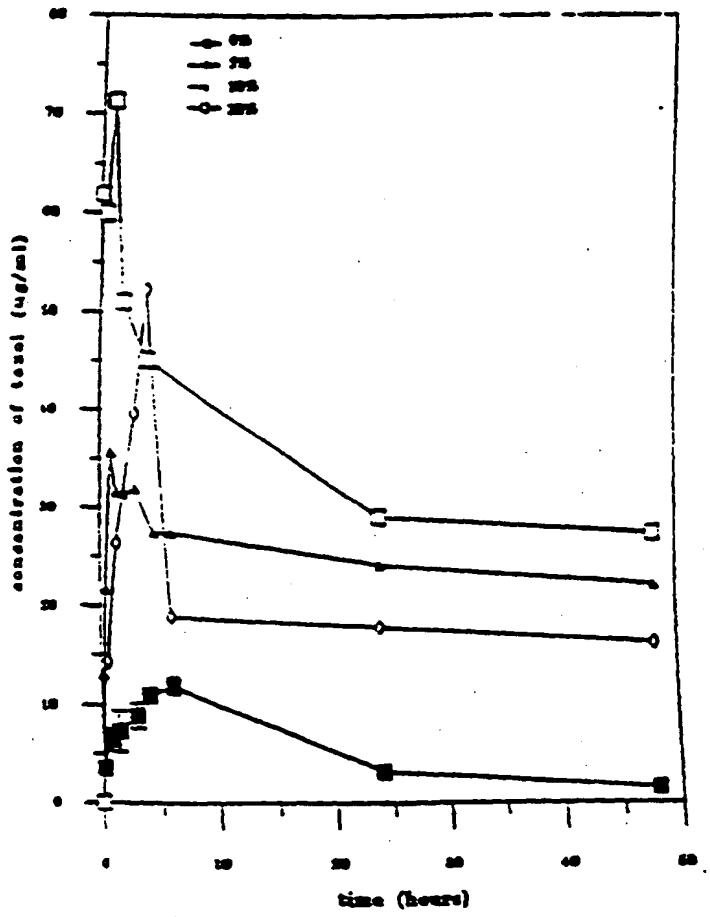

FIGURE 42

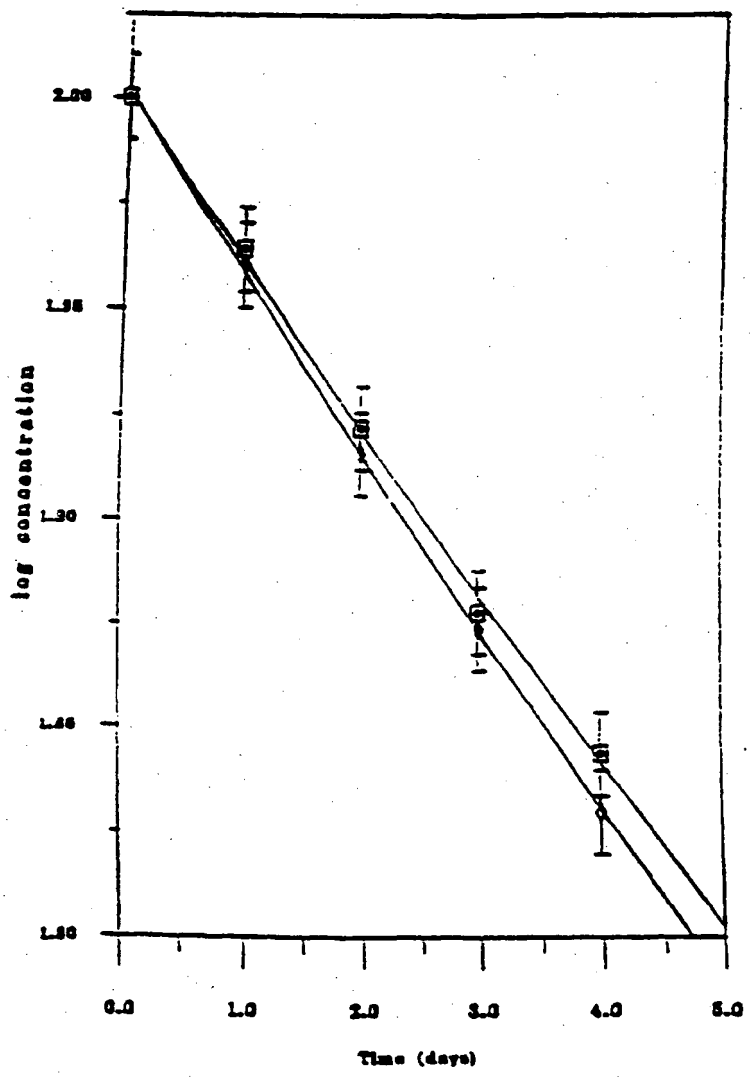

FIGURE 43A

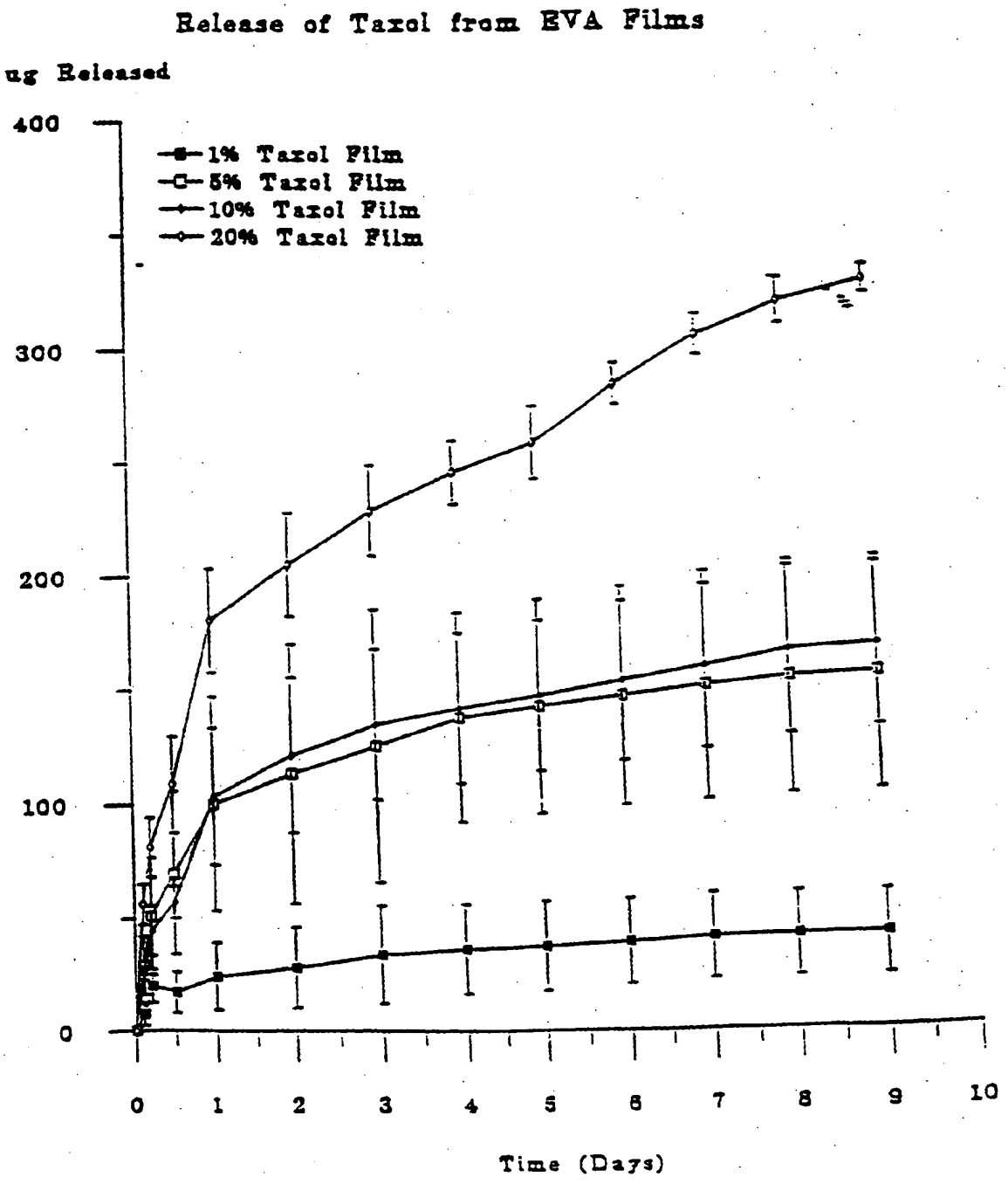
Release of Taxol from EVA Films
ug Released
400
300
200
100
0
1% Taxol Film
5% Taxol Film
10% Taxol Film
20% Taxol Film
0
1
2
3
4
5
6
7
8
9
10
Time (Days)

FIGURE 43B

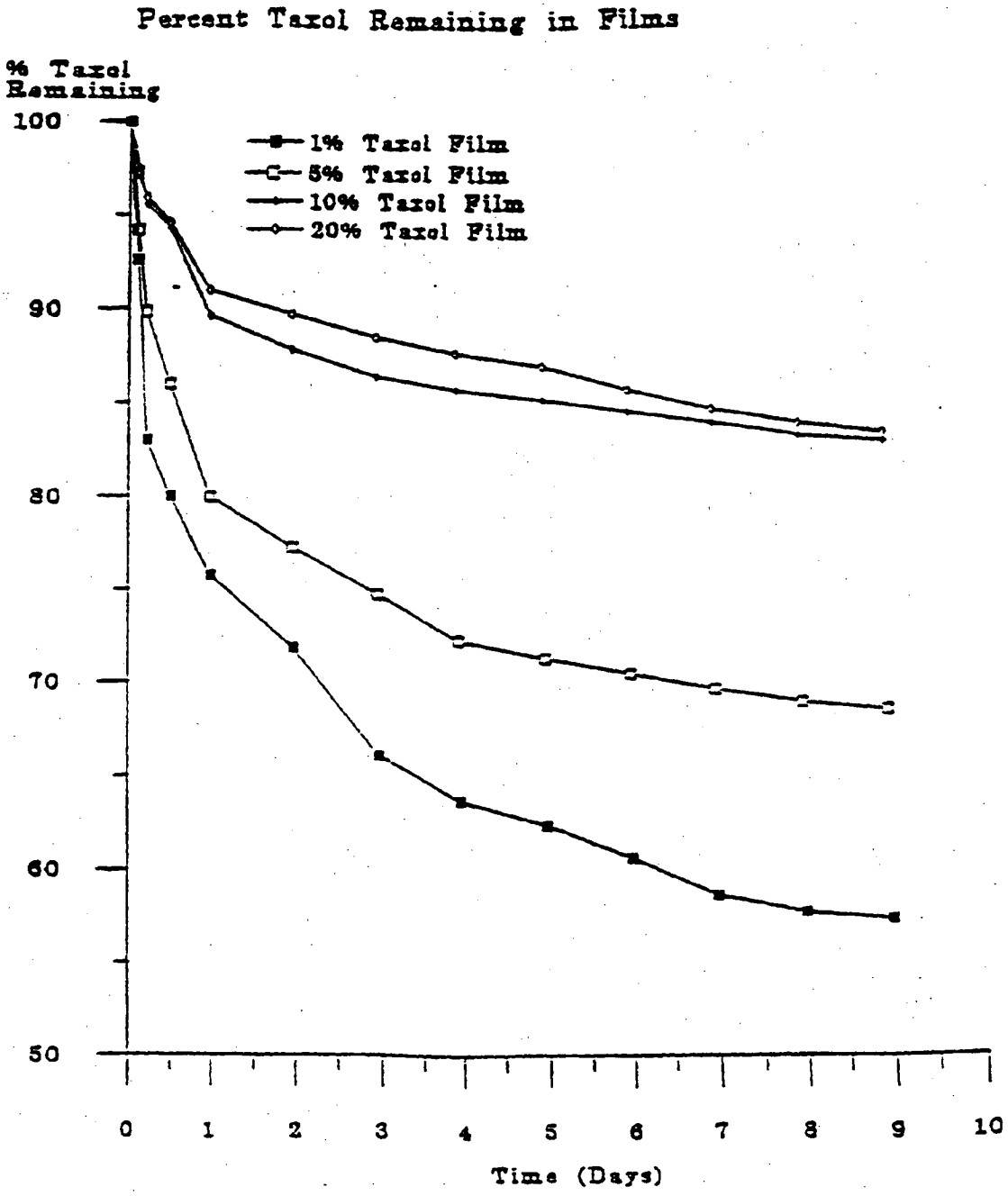
Percent Taxol Remaining in Films
% Taxol Remaining
100
90
80
70
60
50
1% Taxol Film
5% Taxol Film
10% Taxol Film
20% Taxol Film
0
1
2
3
4
5
6
7
8
9
10
Time (Days)

FIGURE 43C

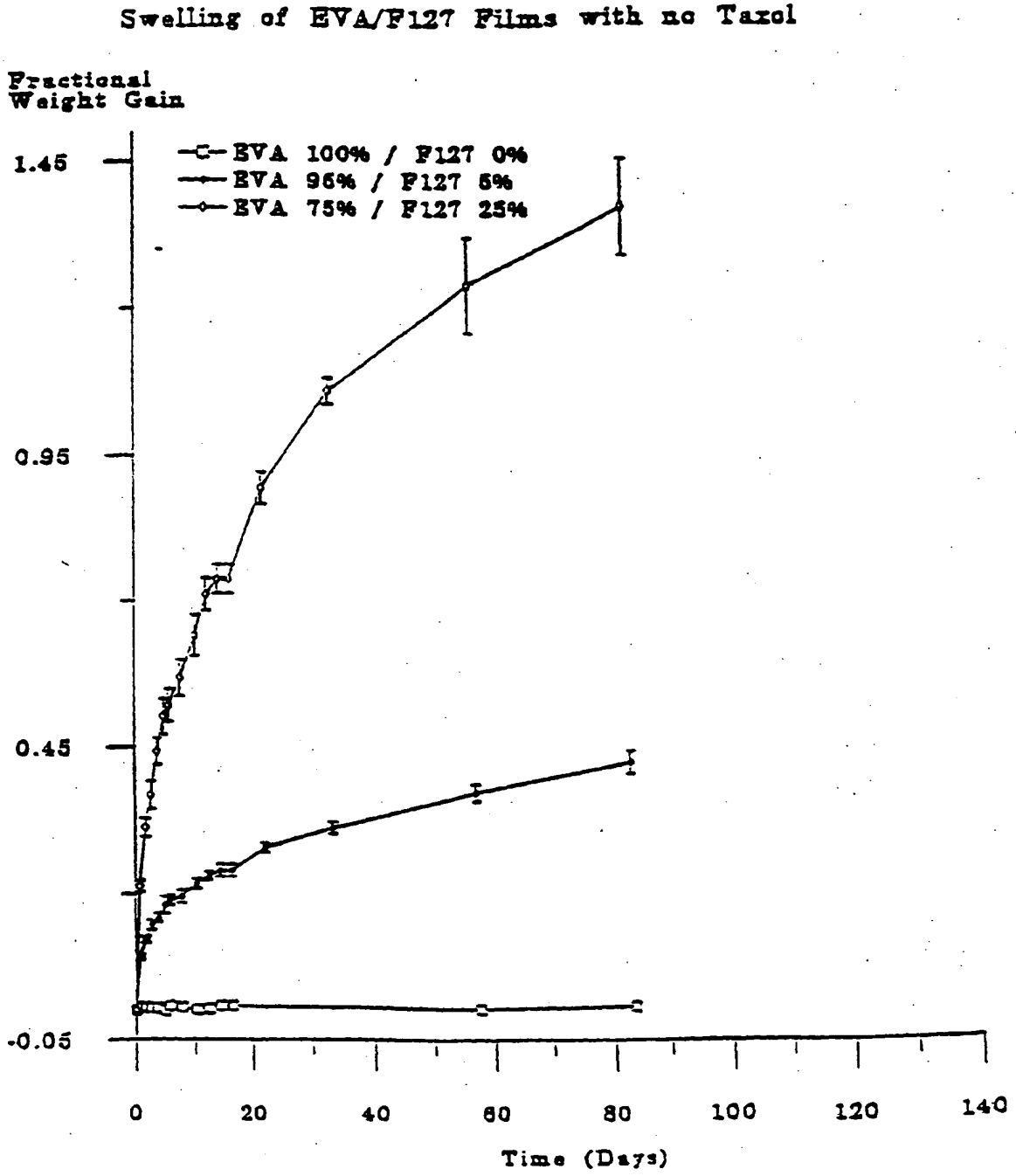
Swelling of EVA/F127 Films with no Taxol
Fractional Weight Gain
EVA 100% / F127 0%
EVA 95% / F127 5%
EVA 75% / F127 25%
1.45
0.95
0.45
-0.05
0
20
40
60
80
100
120
140
Time (Days)

FIGURE 43D

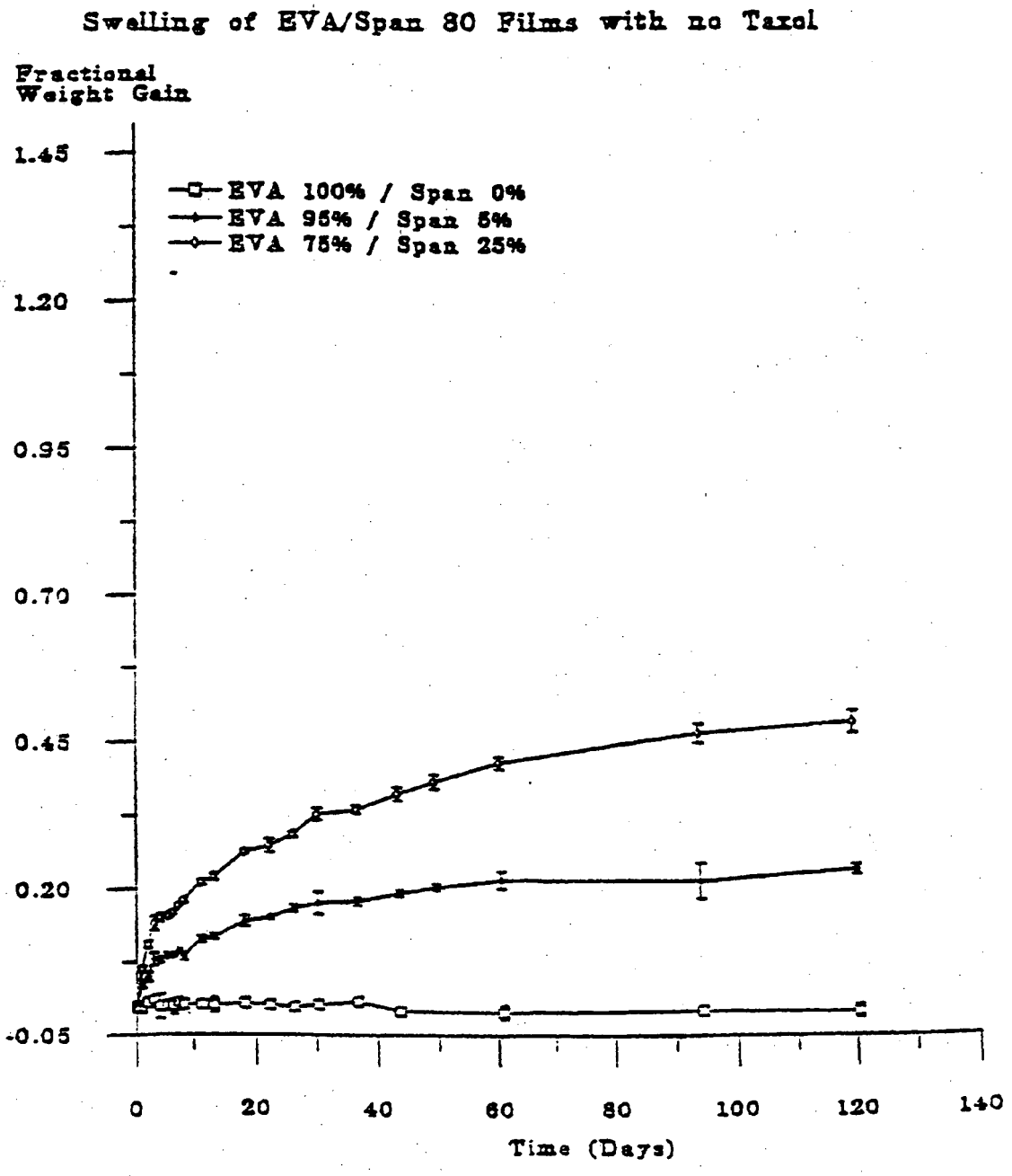
Swelling of EVA/Span 80 Films with no Taxol
Fractional Weight Gain
1.45
1.20
0.95
0.70
0.45
0.20
-0.05
EVA 100% / Span 0%
EVA 95% / Span 5%
EVA 75% / Span 25%
0
20
40
60
80
100
120
140
Time (Days)

FIGURE 43E

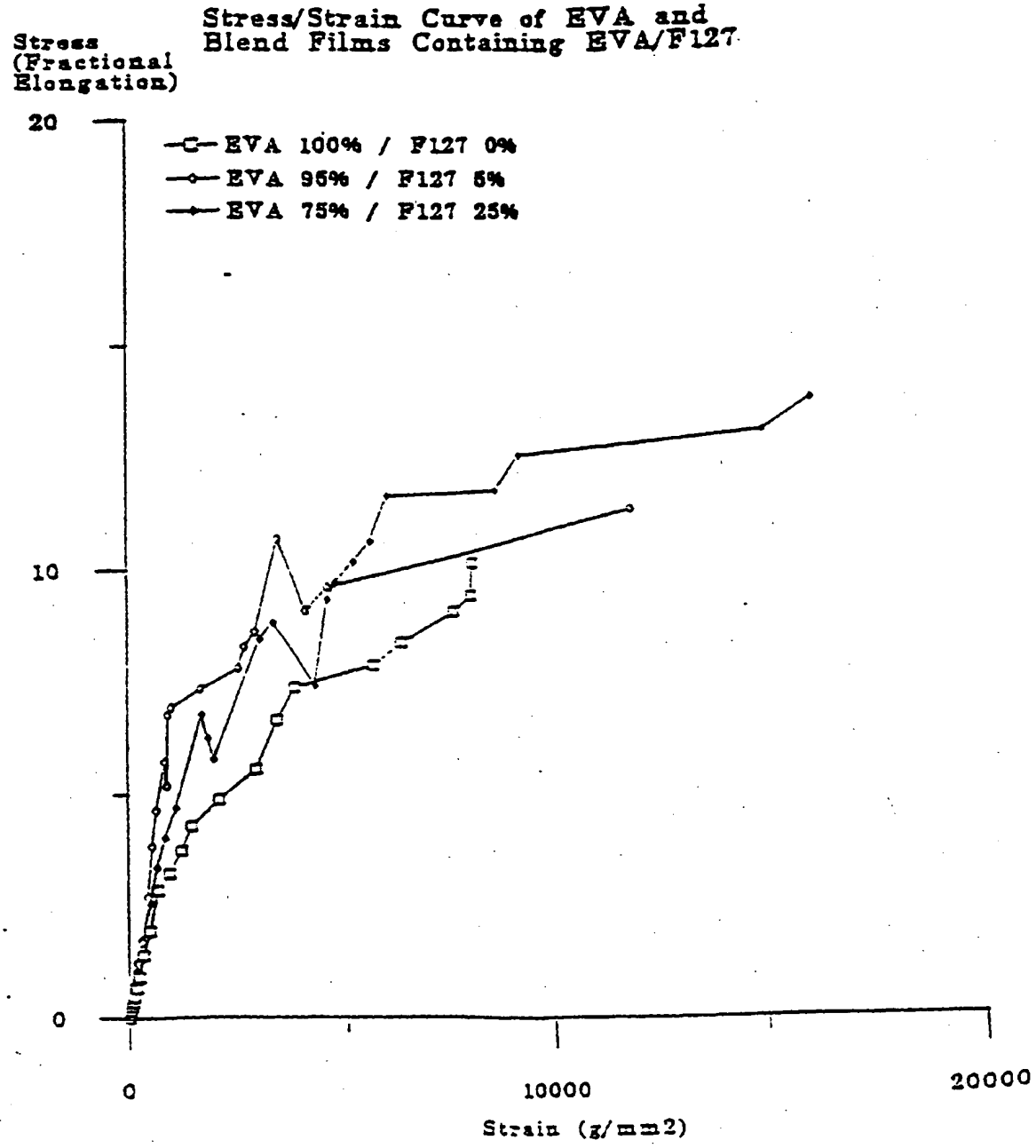
Stress/Strain Curve of EVA and Blend Films Containing EVA/F127
Stress (Fractional Elongation)
20
10
0
EVA 100% / F127 0%
EVA 95% / F127 5%
EVA 75% / F127 25%
0
10000
20000
Strain (g/mm2)

FIGURE 44

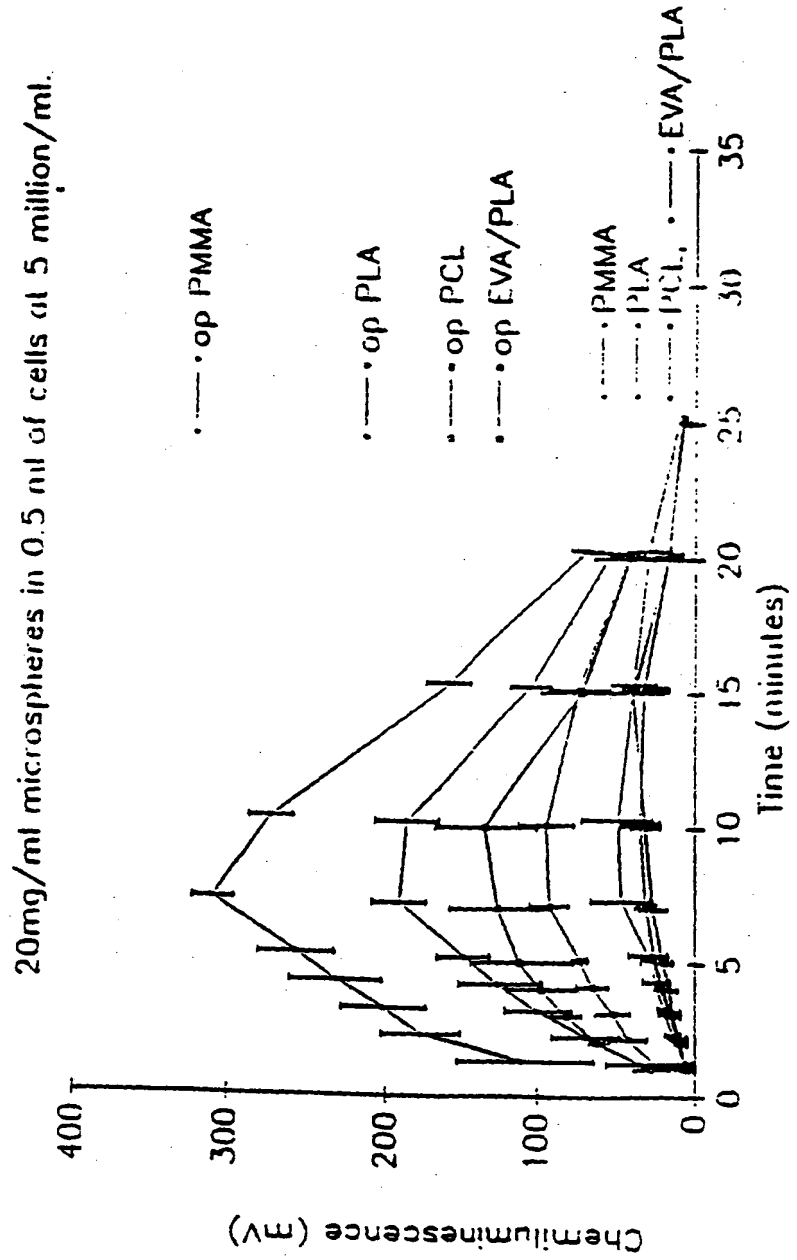
20mg/ml microspheres in 0.5 ml of cells at 5 million/ml.
op PMMA
op PLA
op PCL
op EVA/PLA
PMMA
PLA
PCL
EVA/PLA
Chemiluminescence (mV)
400
300
200
100
0
0
5
10
15
20
25
30
35
Time (minutes)

FIGURE 45

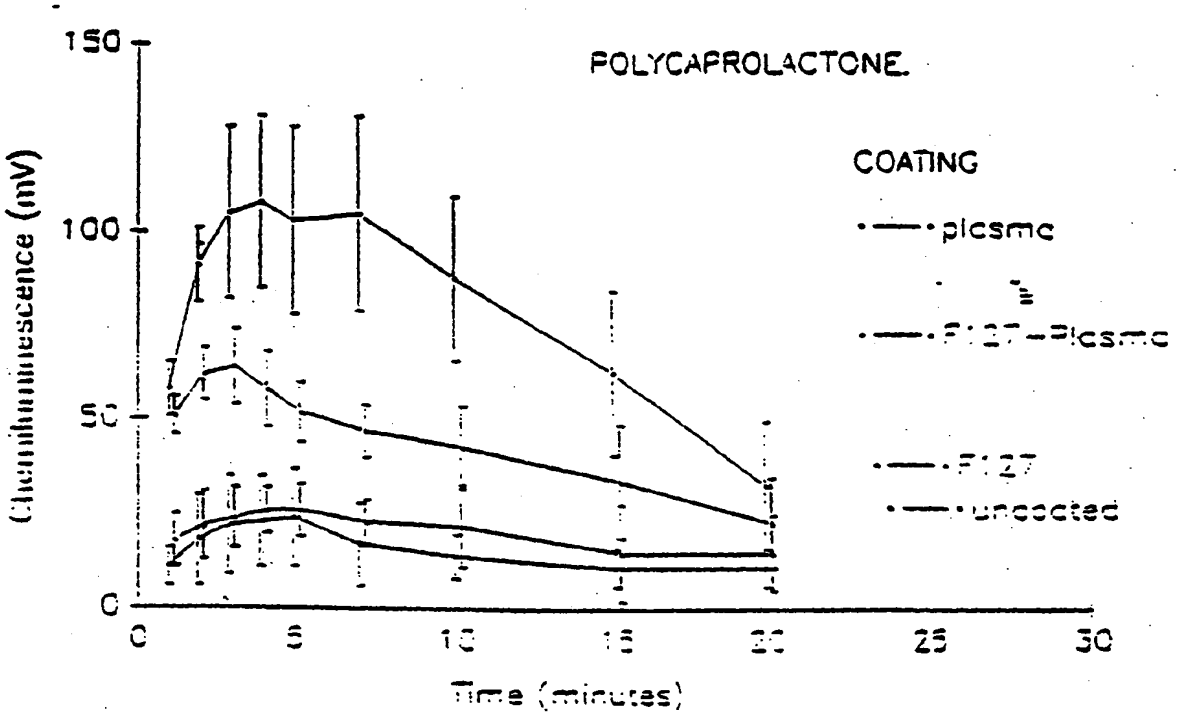
POLYCAPROLACTONE
COATING
plcsmc
F127-Plcsmc
F127
uncoated
Chemiluminescence (mV)
150
100
50
0
0
5
10
15
20
25
30
Time (minutes)

FIGURE 46

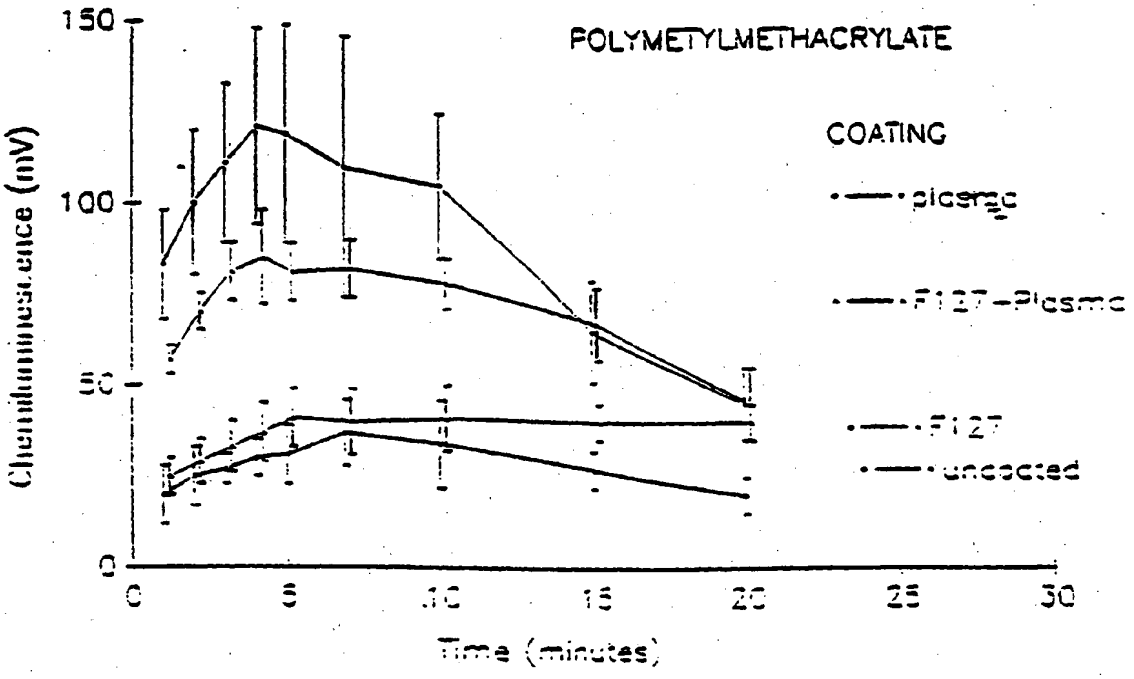
POLYMETYLMETHACRYLATE
COATING
F127-Plasma
F127
uncoated
Chemiluminescence (mV)
150
100
50
0
0
5
10
15
20
25
30
Time (minutes)

FIGURE 47

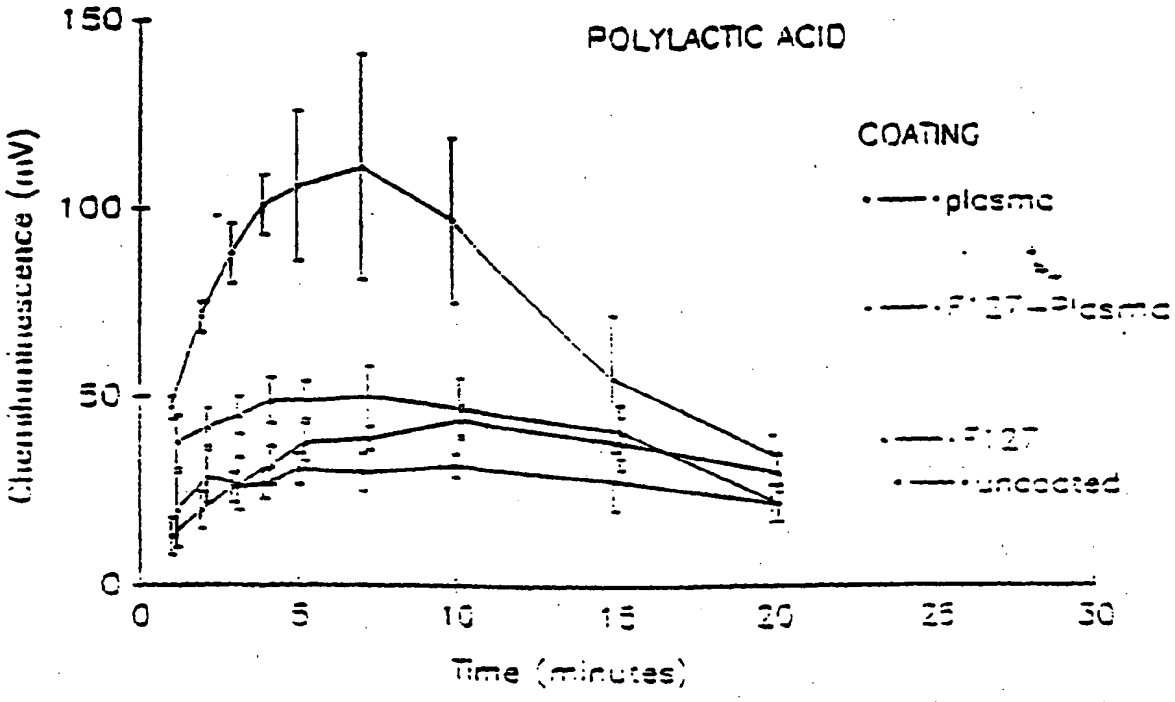
POLYLACTIC ACID
COATING
plasma
F127-Plasma
F127
uncoated
Chemiluminescence (mV)
150
100
50
0
0
5
10
15
20
25
30
Time (minutes)

FIGURE 48

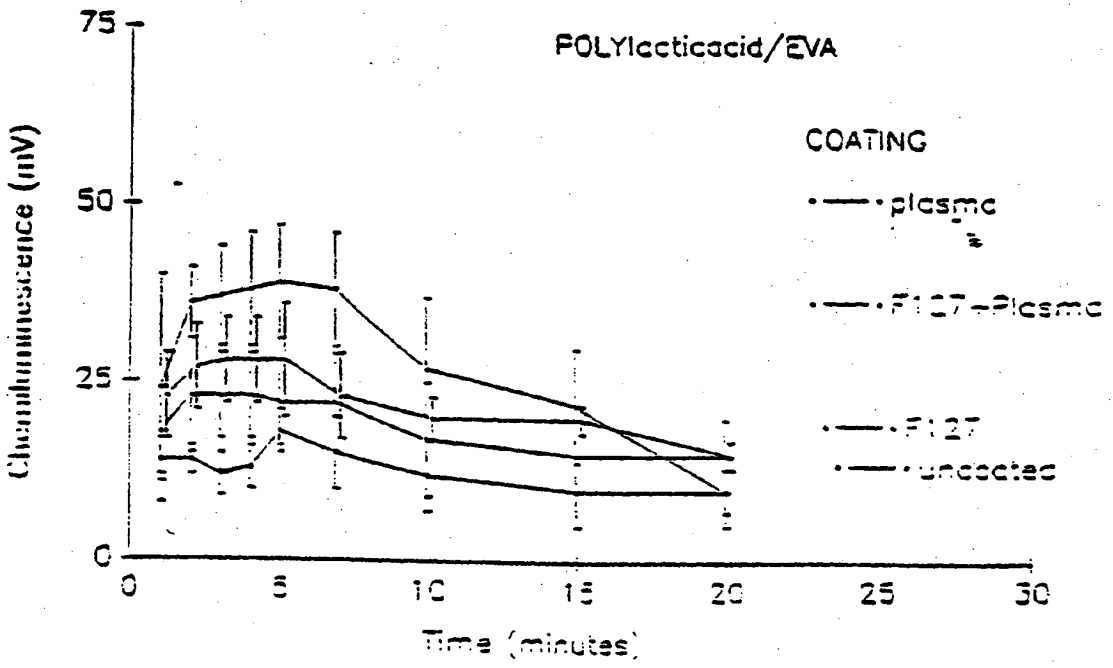
POLYlcctlcacid/EVA
COATING
plasmc
F127-Plasmc
F127
uncoatec
Chemiluminescence (mV)
75
50
25
0
0
5
10
15
20
25
30
Time (minutes)

FIGURE 49

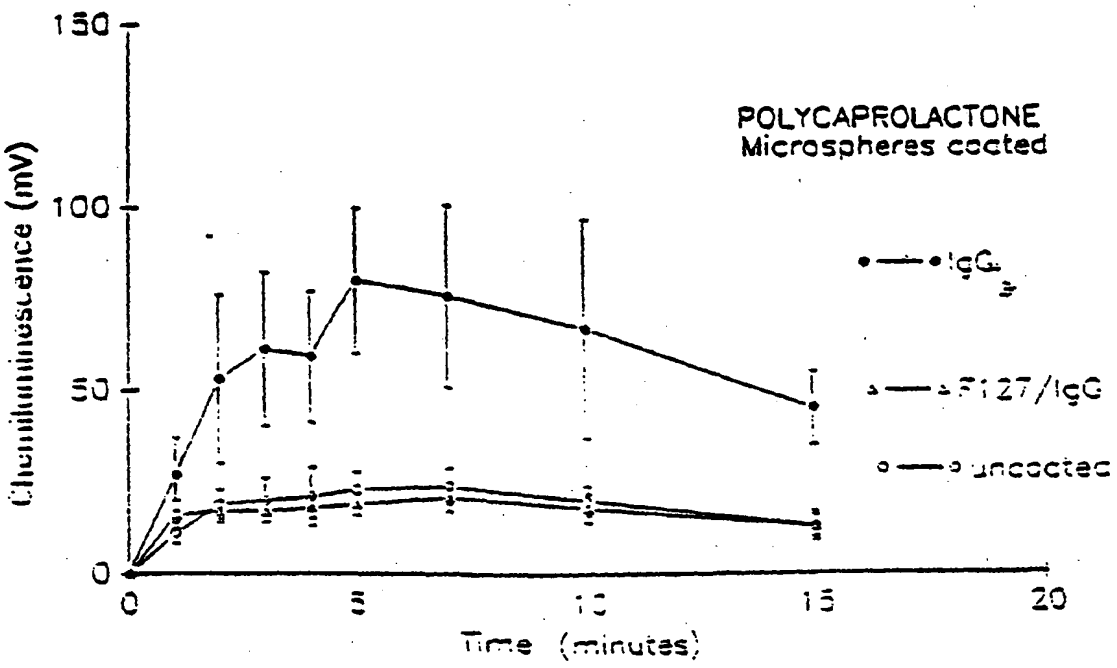
150
100
50
0
Chemiluminescence (mV)
0
5
10
15
20
Time (minutes)
POLYCAPROLACTONE
Microspheres coated
IgG
F127/IgG
uncoated

FIGURE 50

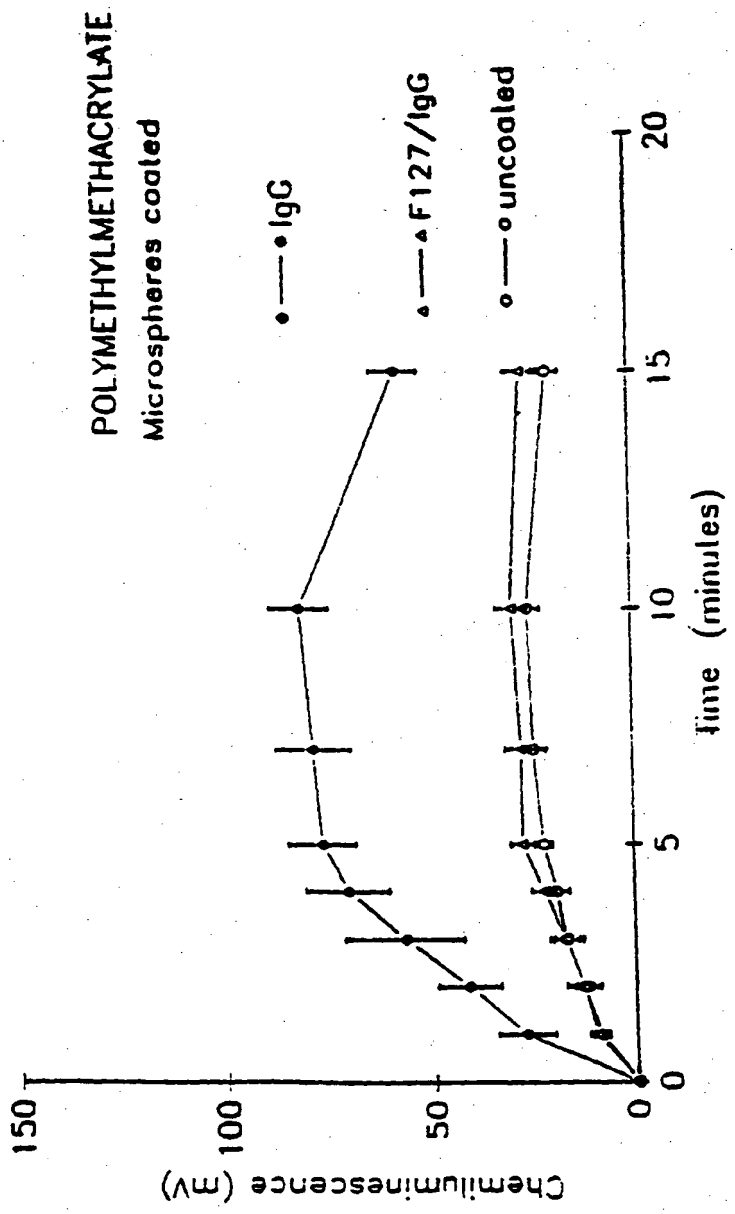
POLYMETHYLMETHACRYLATE
Microspheres coated
•—• IgG
▲—▲ F127/IgG
o—o uncoated
Chemiluminescence (mV)
150
100
50
0
0
5
10
15
20
Time (minutes)

FIGURE 51

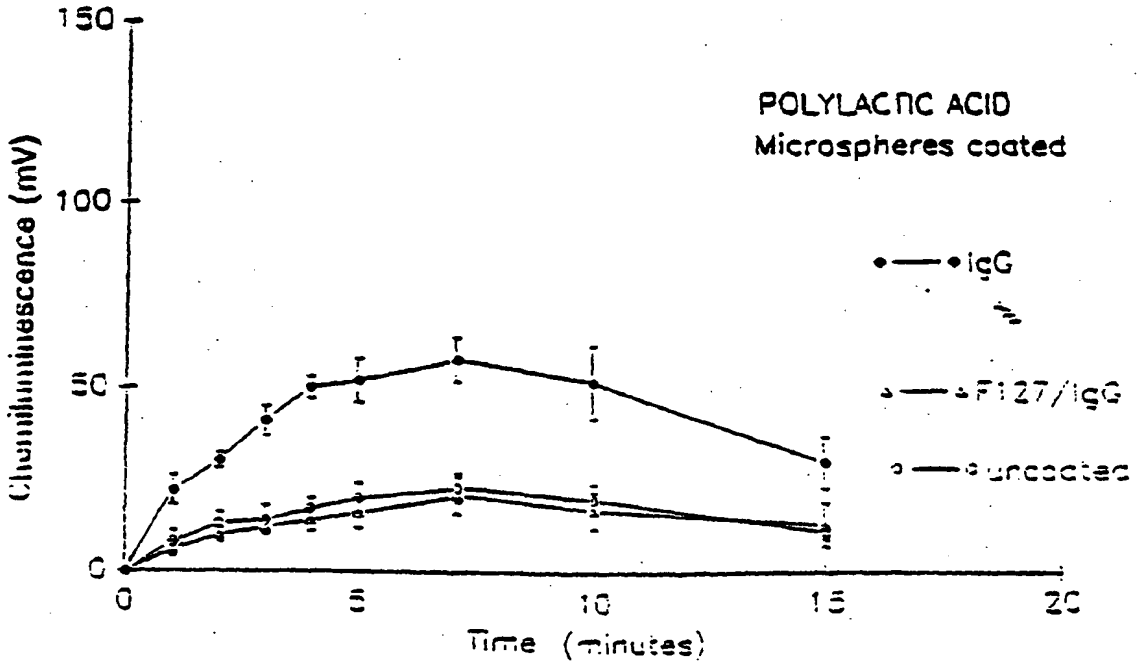
150
100
50
0
Chemiluminescence (mV)
POLYLACTIC ACID
Microspheres coated
IgG
F127/IgG
uncoated
0
5
10
15
20
Time (minutes)

FIGURE 52

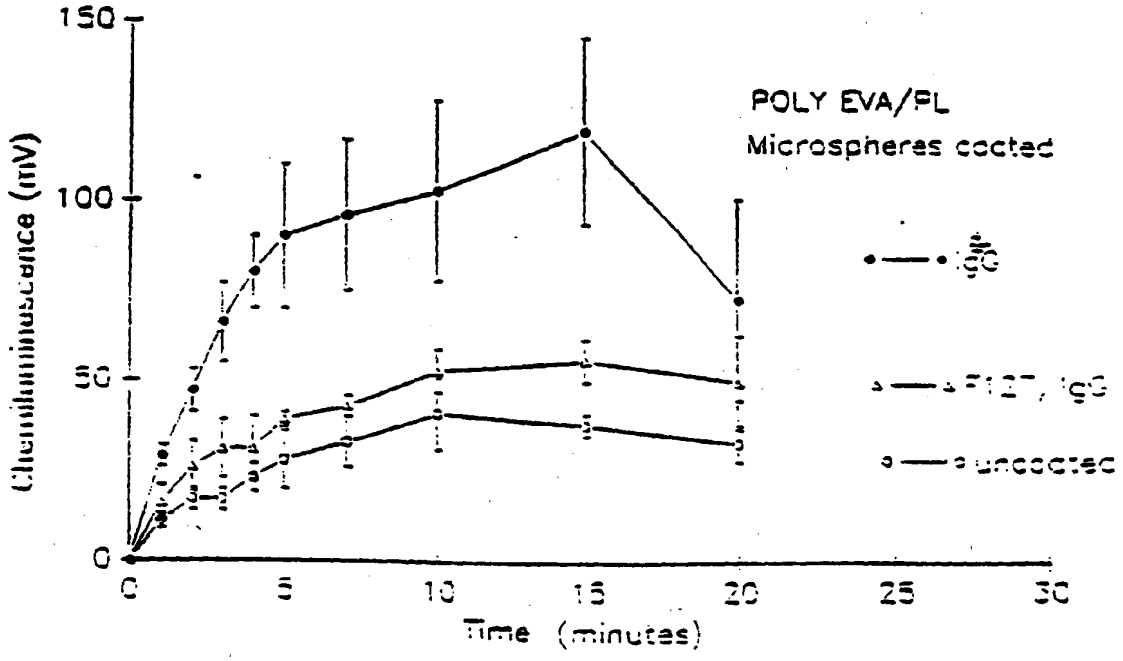
150
100
50
0
Chemiluminescence (mV)
0
5
10
15
20
25
30
Time (minutes)
POLY EVA/PL
Microspheres coated
IgG
F127, IgG
uncoated

FIGURE 53A

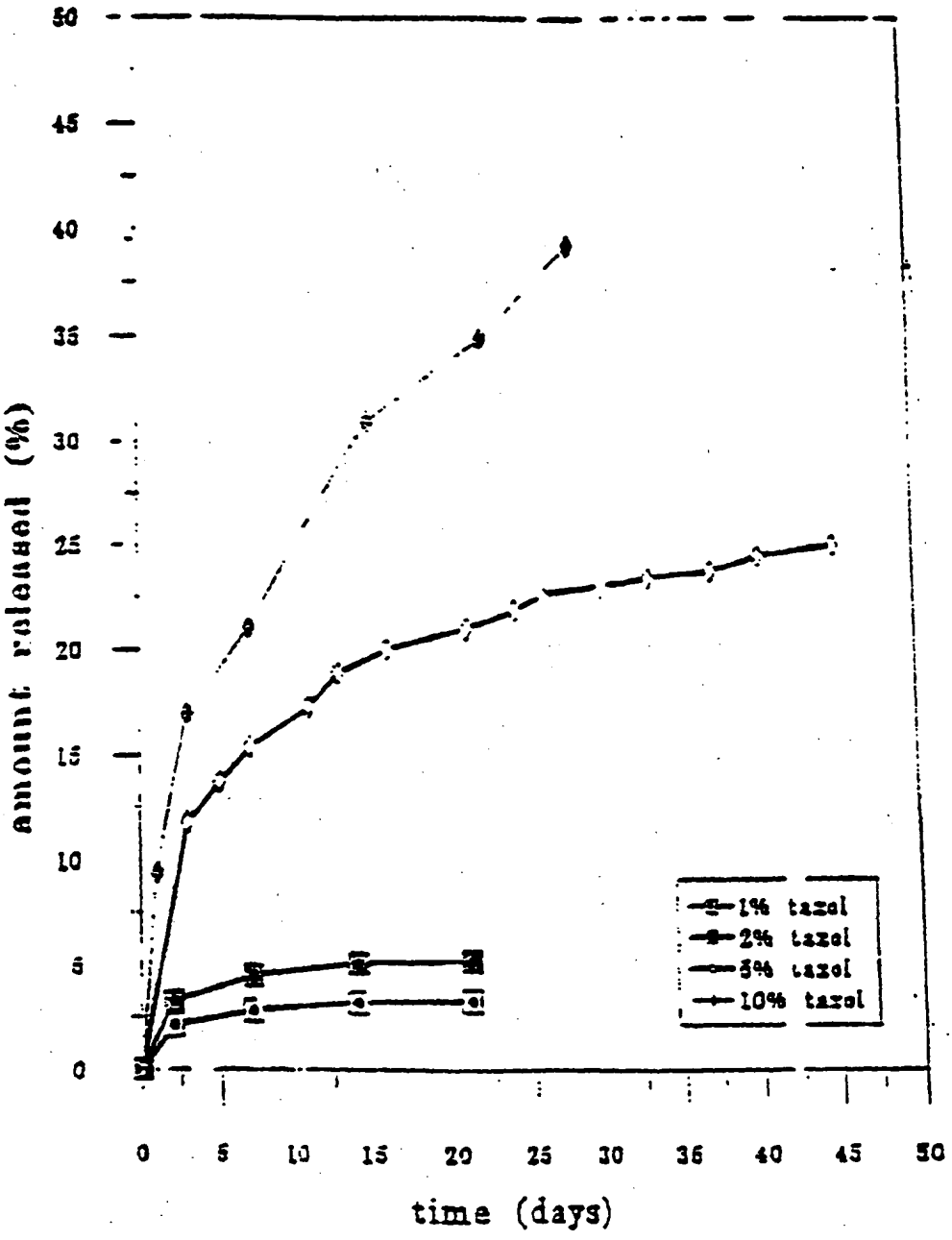

FIGURE 53B

FIGURE 53C

FIGURE 54

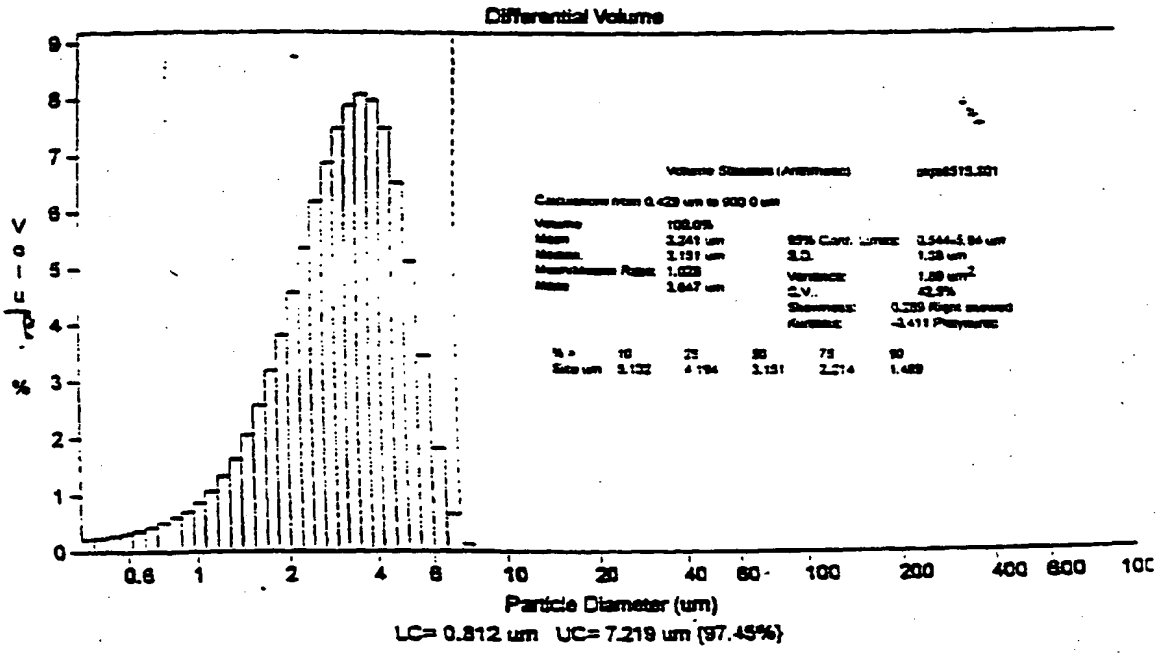
Differential Volume
%
0
1
2
3
4
5
6
7
8
9
0.6
1
2
4
6
10
20
40
60
100
200
400
600
Particle Diameter (um)
LC= 0.812 um UC= 7.219 um (97.45%)

FIGURE 55

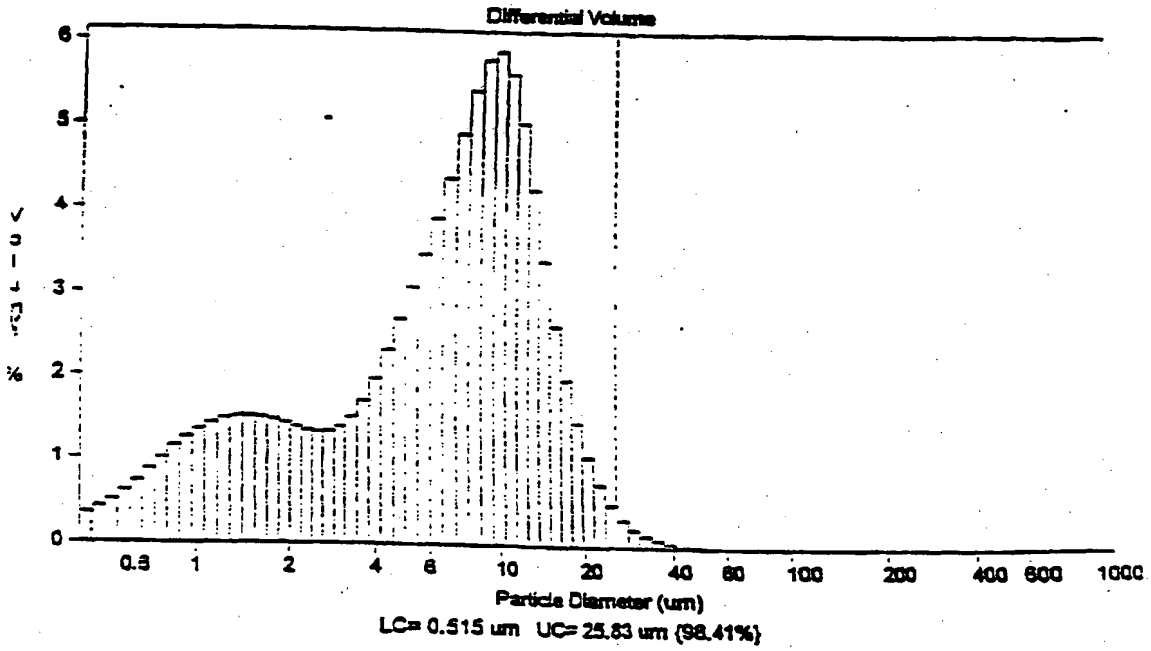
Differential Volume
%
0
1
2
3
4
5
6
0.5
1
2
4
6
10
20
40
60
100
200
400
600
1000
Particle Diameter (um)
LC= 0.515 um UC= 25.83 um (98.41%)

FIGURE 56

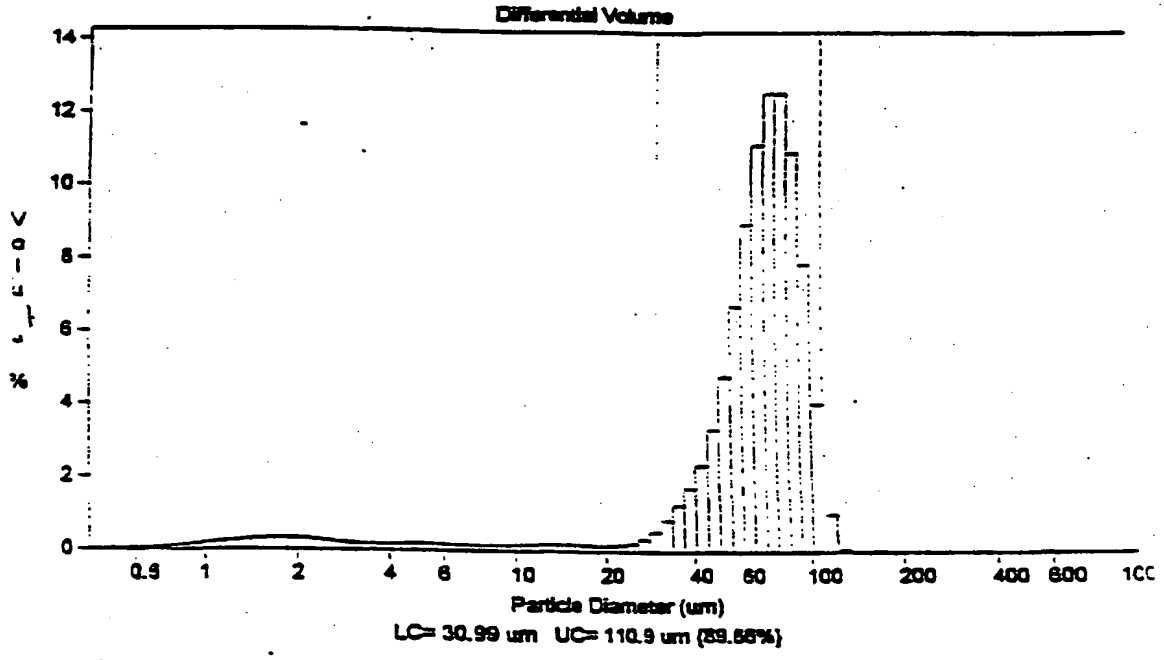
Differential Volume
14
12
10
8
6
4
2
0
0.9
1
2
4
6
10
20
40
60
100
200
400
800
Particle Diameter (um)
LC= 30.99 um UC= 110.9 um (89.66%)

FIGURE 57

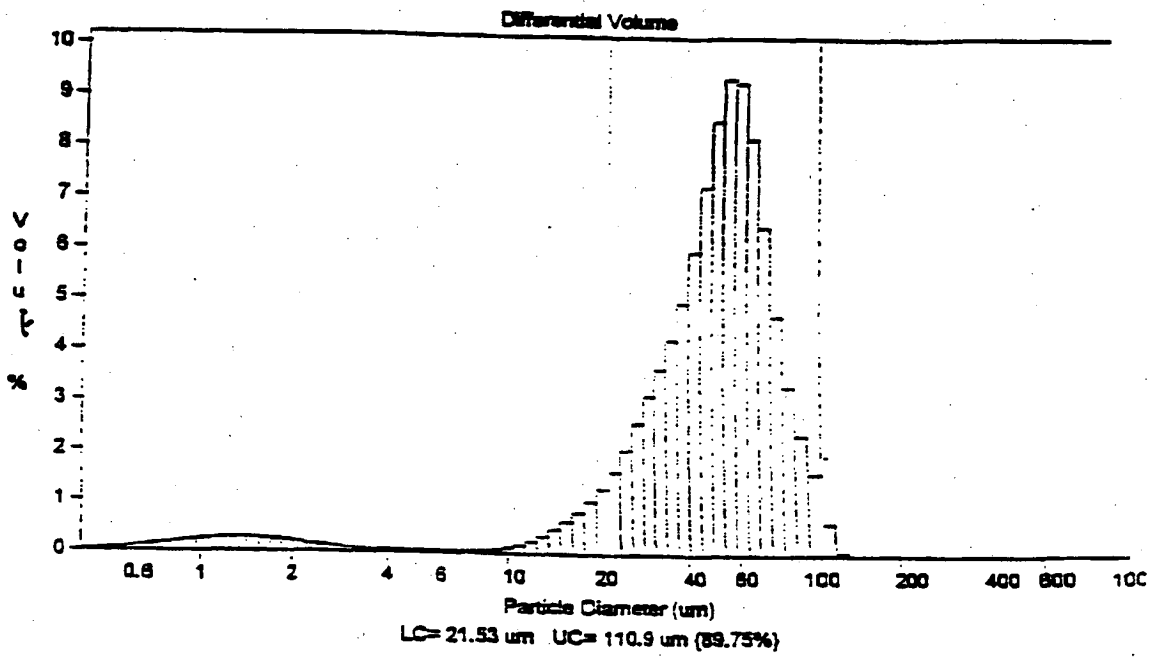
Differential Volume
% Volume
10
9
8
7
6
5
4
3
2
1
0
0.6
1
2
4
6
10
20
40
60
100
200
400
800
1000
Particle Diameter (um)
LC= 21.53 um UC= 110.9 um (89.75%)

FIGURE 58A-58C

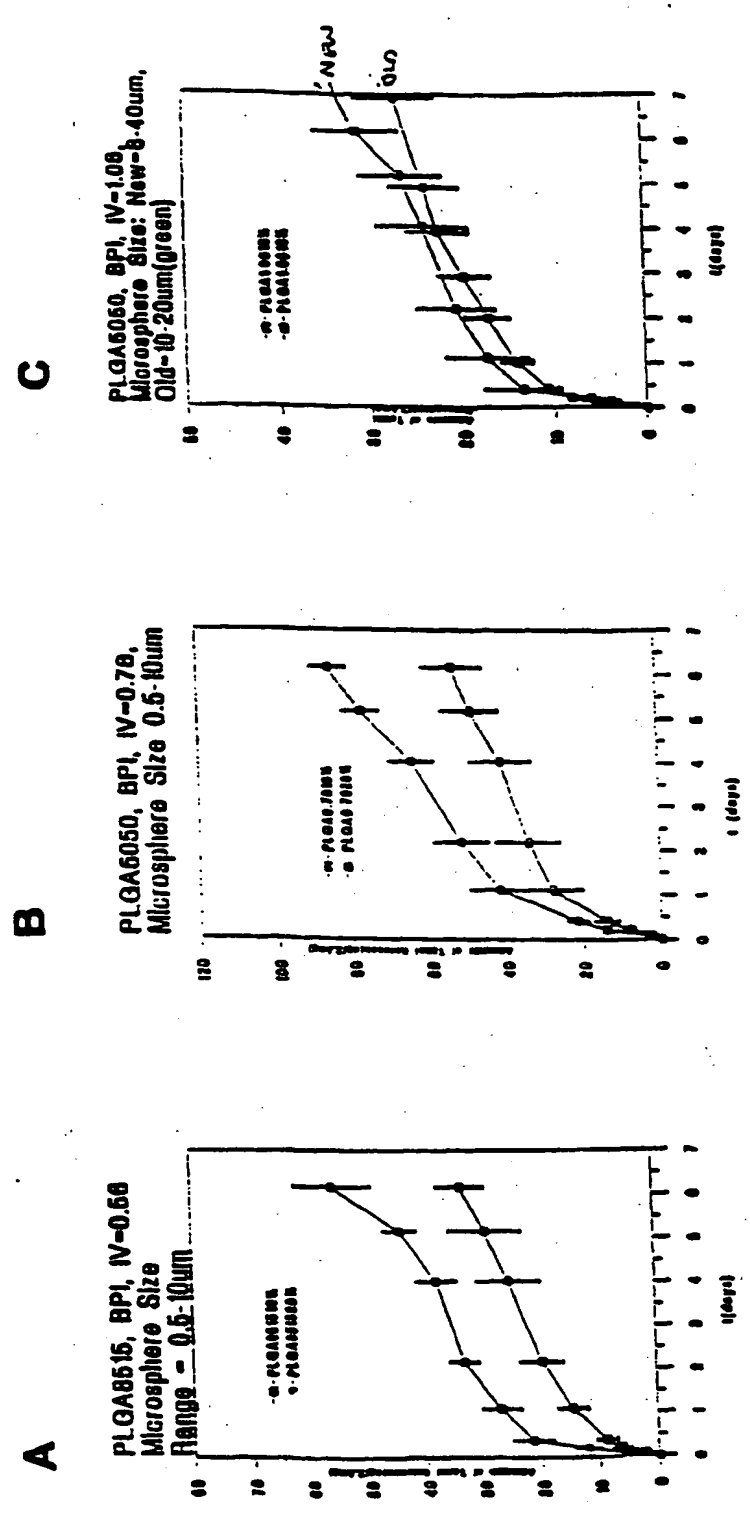

FIGURE 59A-59B

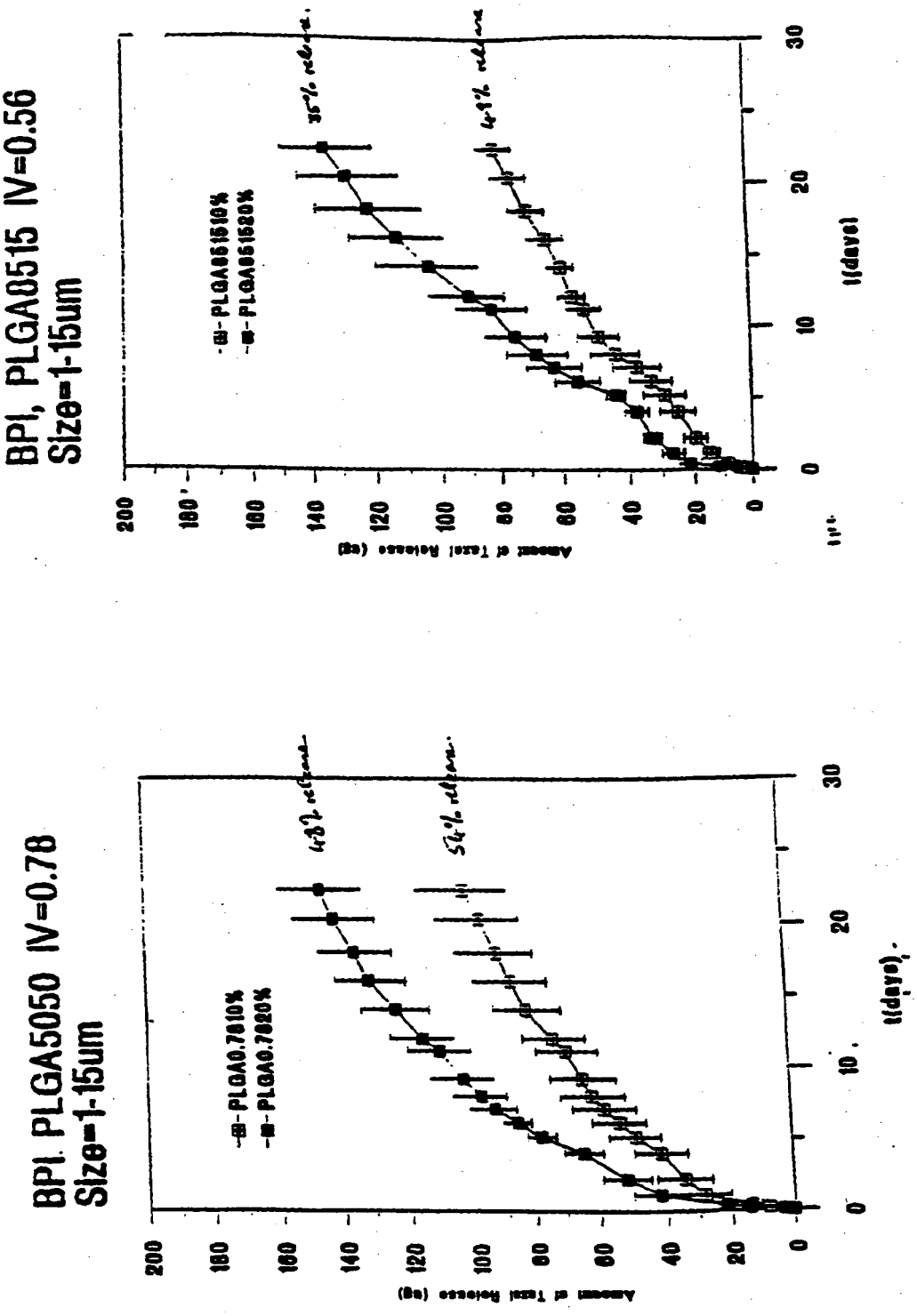

FIGURE 60A

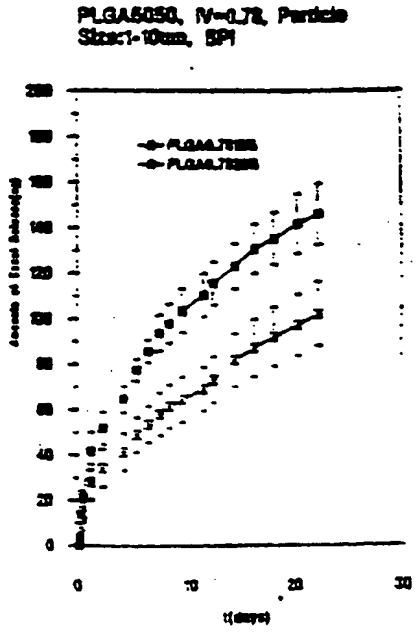

FIGURE 60B

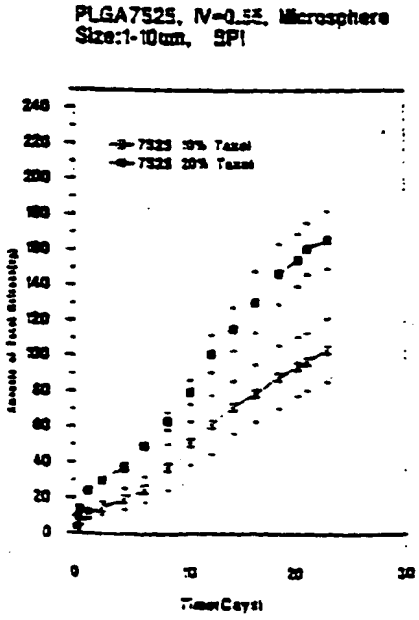

FIGURE 61A

A

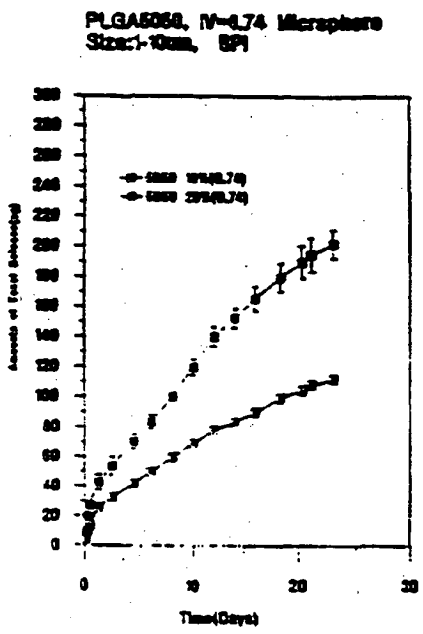

FIGURE 61B

B

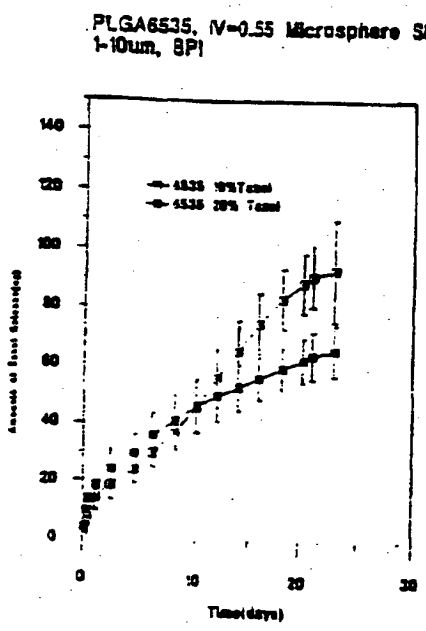

FIGURE 61C

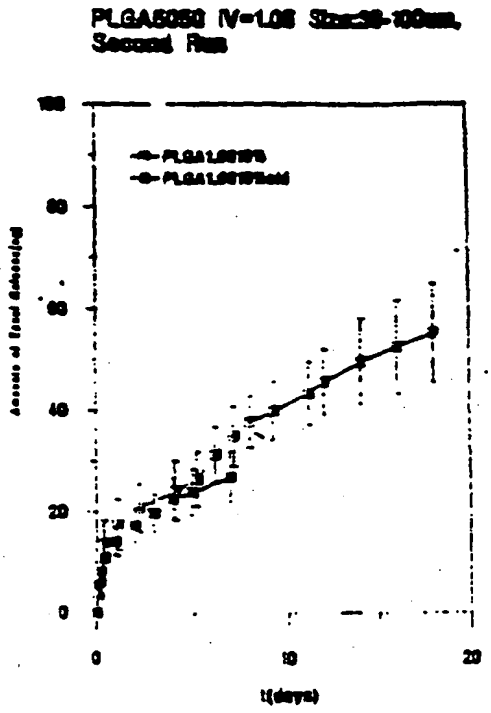

FIGURE 62

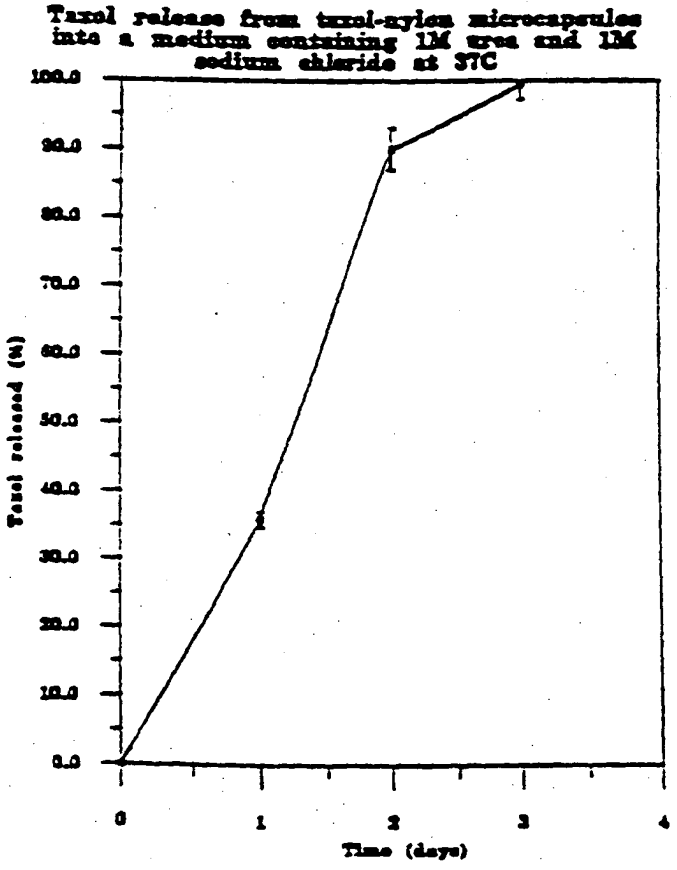
Taxol release from taxol-nylon microcapsules into a medium containing 1M urea and 1M sodium chloride at 37C
Taxol released (%)
100.0
90.0
80.0
70.0
60.0
50.0
40.0
30.0
20.0
10.0
0.0
0
1
2
3
4
Time (days)

FIGURE 63A

Fibronectin coated PLLA microspheres on bladder tissue

FIGURE 63B

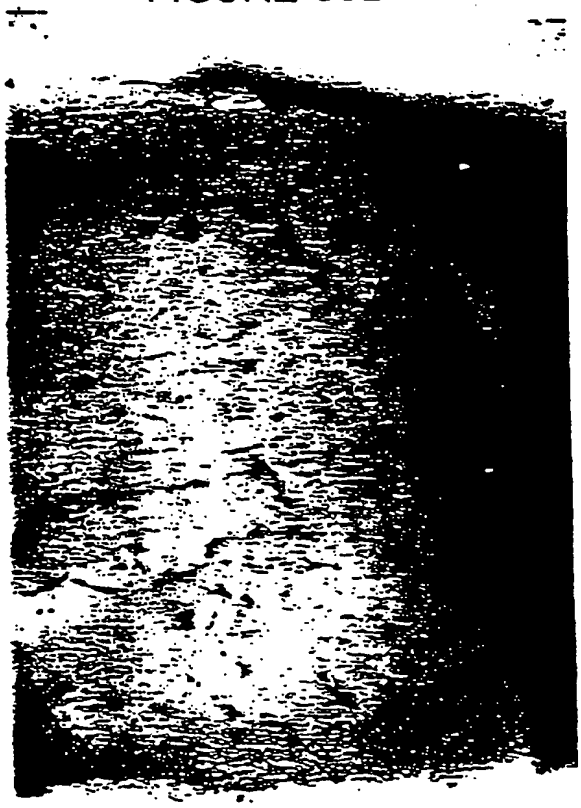

poly(L-lysine) microspheres on bladder tissue.

FIGURE 64

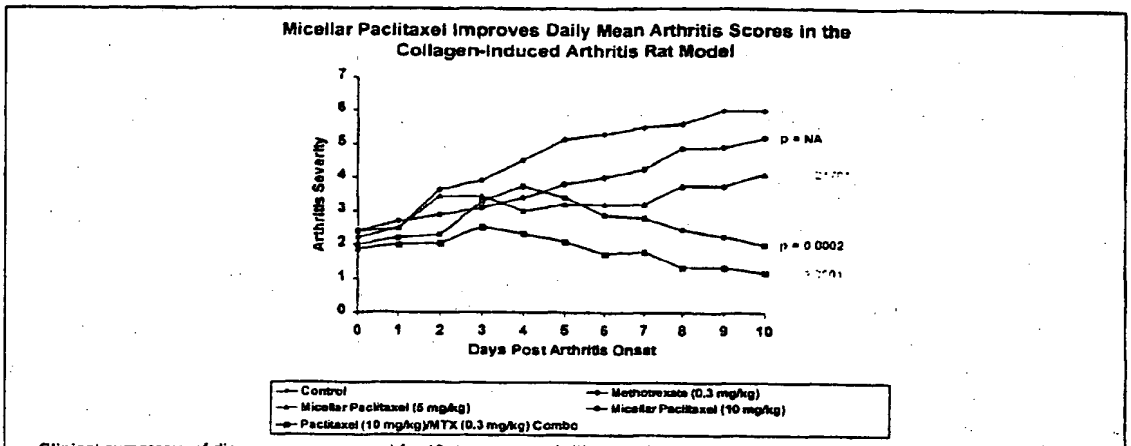

- Clinical symptoms of disease were assessed for 10 days post-arthritis onset in the collagen-induced arthritis (CIA) rat model.
- Both control and methotrexate animals had a progressive increase in clinical symptoms of disease, whereas animals receiving micellar paclitaxel at 10 mg/kg demonstrated a significant clinical improvement at day 10.
- At the end of the study paclitaxel at 10 mg/kg showed, by means of a t-test, a significant reduction in arthritic symptoms in the CIA model when compared to methotrexate (MTX)-treated and CIA control rats.

FIGURE 65

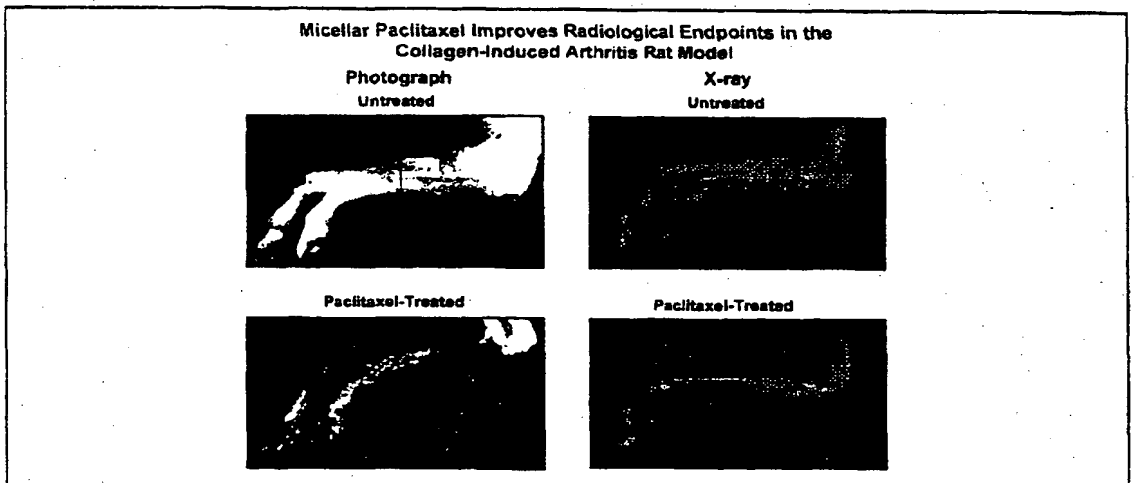

- Radiographs were taken 28 days after immunization with type II collagen. Control groups received vehicle alone, while paclitaxel-treated groups received 1 mg/kg of micellar paclitaxel every second day, beginning on the day of arthritis onset (day 9) to day 19.
- Animals in the control group displayed evidence of soft tissue swelling, joint space narrowing, bone destruction and periosteal new bone formation, whereas paclitaxel-treated animals had almost normal joint features on x-ray.

FIGURE 66

A.

Scanning Electron Micrographs of the Normal Rat Ankle Joint

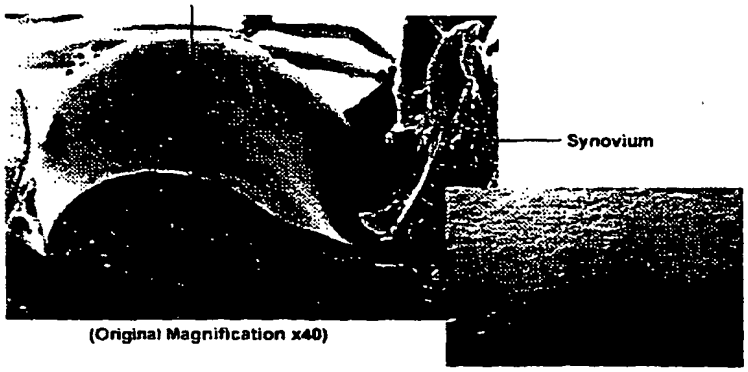

- The cartilage surface of normal animals were processed for scanning electron microscopy.
- Scanning electron micrographs illustrate the normal articular surface as being characterized by a smooth intact cartilage matrix surrounded by a thin synovial lining.

B.

Scanning Electron Micrographs of a Rat Ankle Joint in the Collagen-Induced Arthritis Model of Arthritis

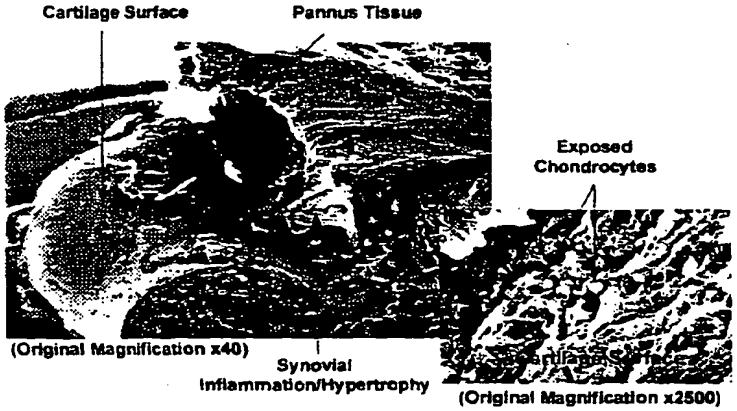

- Scanning electron micrographs of collagen-induced arthritis joints were characterized by an eroded cartilage surface and inflamed synovium. The superficial cartilage matrix is digested, exposing chondrocytes or the empty lacunae they once occupied (inset).

FIGURE 66

C.

Scanning Electron Micrographs of a Rat Ankle Joint in the Micellar Paclitaxel-Treated Collagen-Induced Arthritis Model

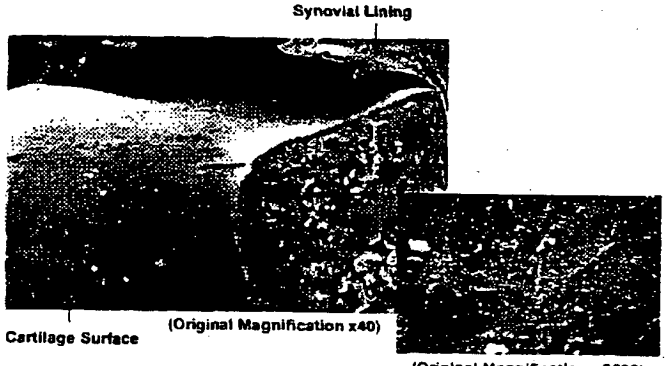

- The joint surface of collagen-induced arthritis animals treated with paclitaxel remained intact and the cartilage matrix appeared largely normal, even at high magnifications (inset). Pannus tissue formation and synovial hypertrophy were not seen in the paclitaxel-treated group (10 mg/kg).

FIGURE 67

Micellar Paclitaxel Improves the Histopathology of the Collagen-Induced Arthritis Rat Model

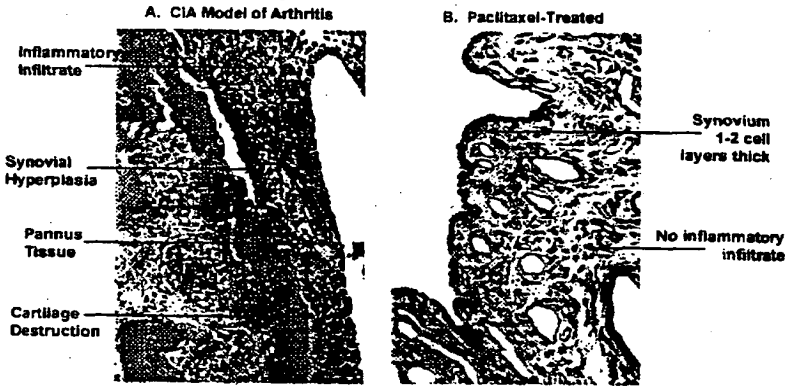

- Collagen-induced arthritis (CIA) is characterized histologically by marked synovial hypertrophy, inflammatory cell infiltration of the synovium and pannus tissue, as well as cartilage destruction (A).
- In paclitaxel-treated animals, the synovium appeared normal, with only 1 to 2 layers of synovial lining cells and no inflammatory cell infiltrate (B).

FIGURE 68

A.

Synovial Angiogenesis in the Collagen-Induced Arthritis Rat Model of Rheumatoid Arthritis

Corrosion Casts of Synovial Vasculature

(Original Magnification x160)

(Original Magnification x640)

- Corrosion casts of the synovial vasculature were prepared by infusing Mercox polymer into the femoral artery of collagen-induced arthritis (CIA) rats and then digesting the surrounding tissues after *in situ* polymerization of the polymer.
- Scanning electron microscopy of CIA corrosion casts revealed blind-ended capillary sprouts (characteristic to angiogenesis stimulation) projecting inwards towards the joint space.

B.

Inhibition of Synovial Angiogenesis by Paclitaxel in the Collagen-Induced Arthritis Rat Model

Corrosion Casts of Synovial Vasculature

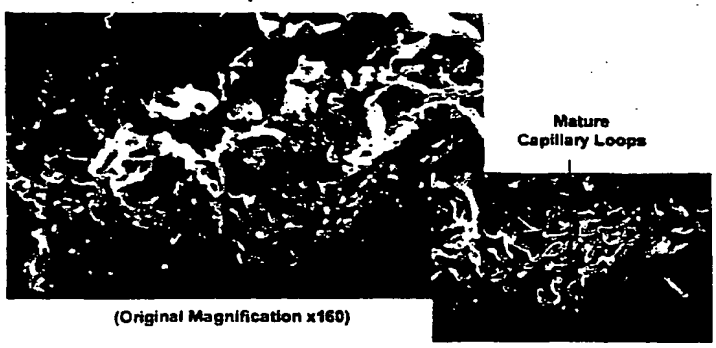

(Original Magnification x160)

(Original Magnification x320)

- Corrosion casts of paclitaxel-treated collagen-induced arthritis animals show synovial vessels arranged in mature capillary loops, characteristic of a quiescent state.

FIGURE 69

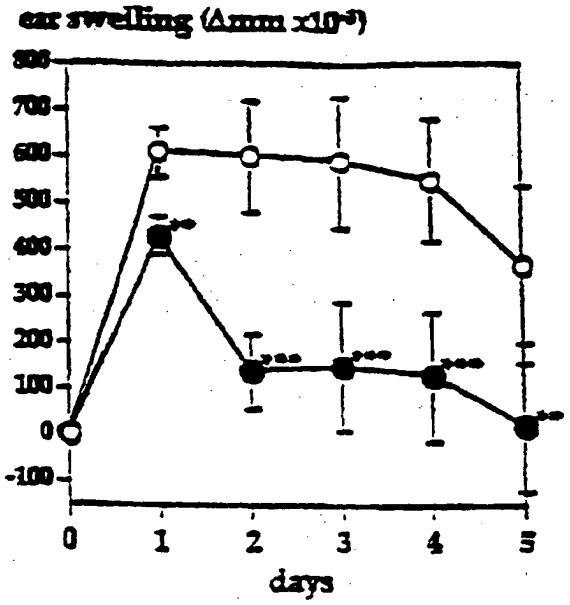

FIGURE 70

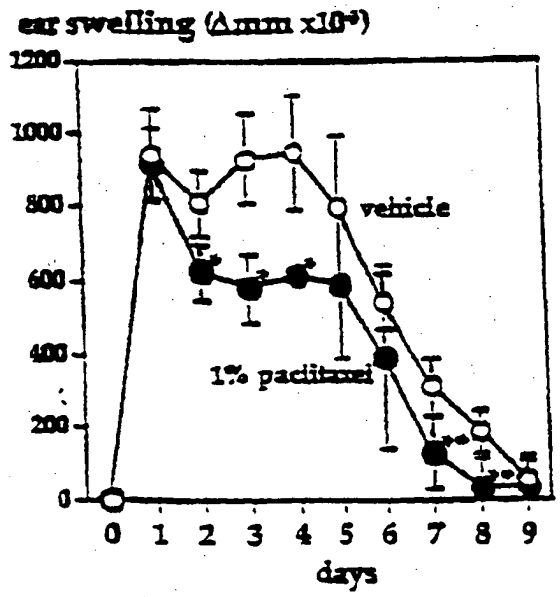

FIGURE 71

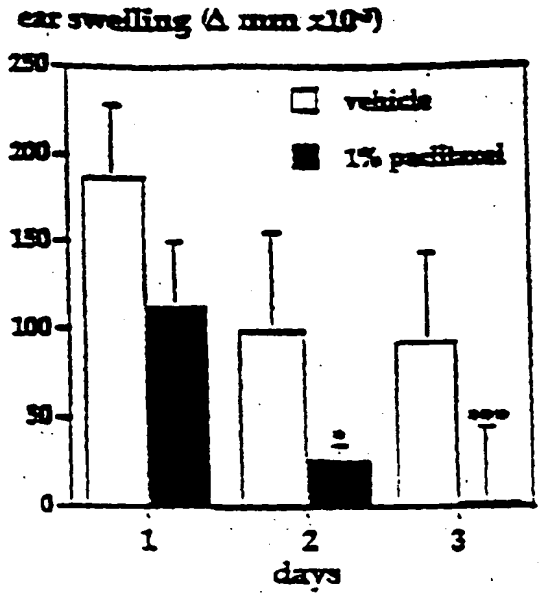

FIGURE 72

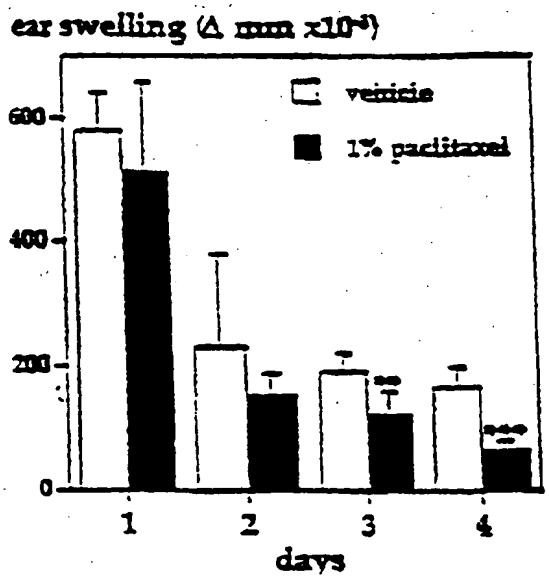

FIGURE 73


Right Ear: Pre-Treated with 1% topical paclitaxel formulation
Left Ear: Topical treatment with vehicle alone

FIGURE 74

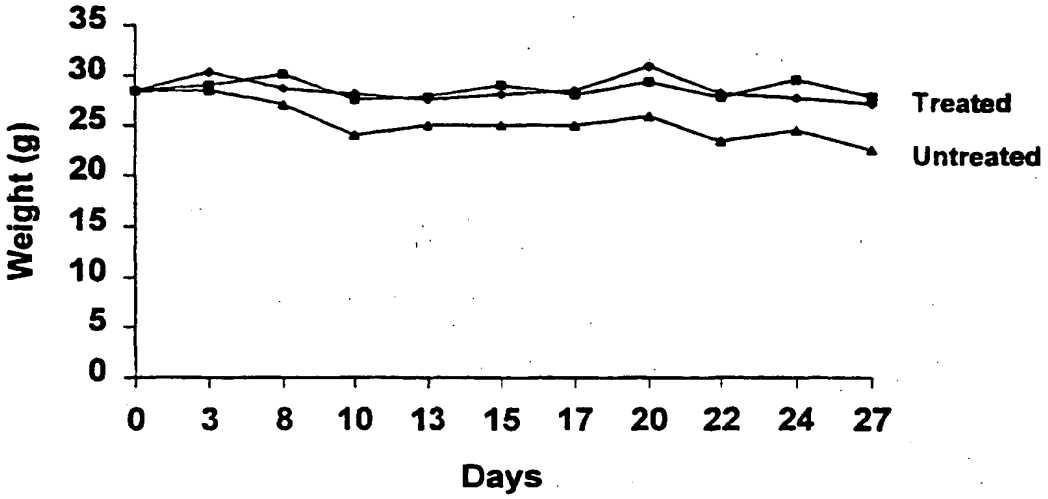

FIGURE 75

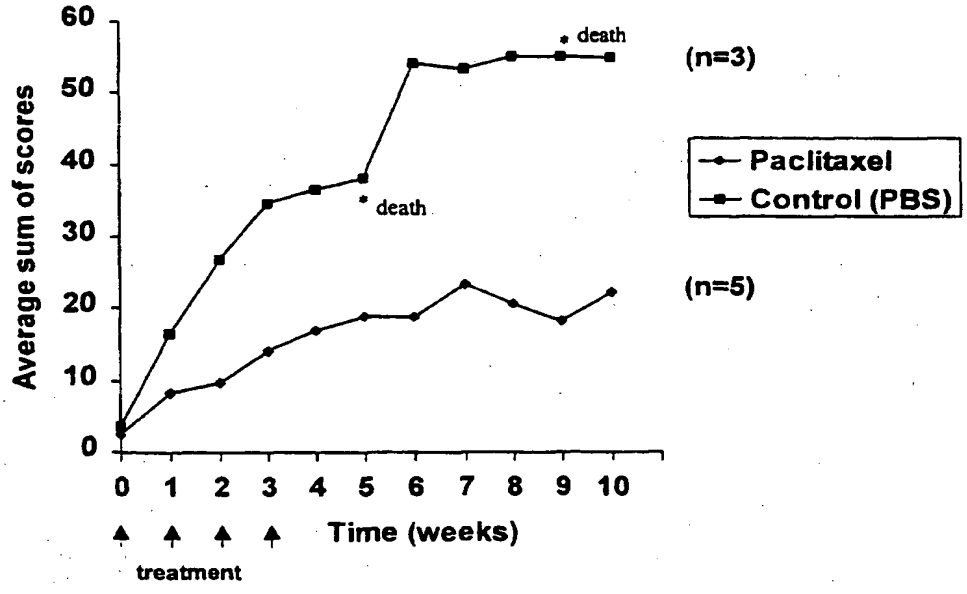

FIGURE 76

A. Untreated

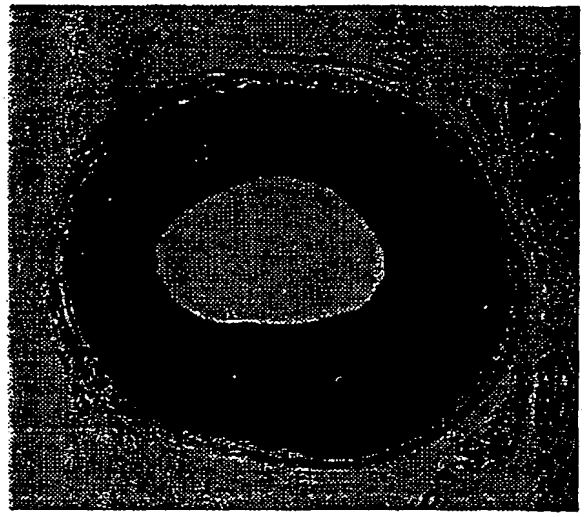

Neointimal Hyperplasia
(14 days post-injury)

B. Paclitaxel-Loaded Paste

Paste applied to the Adventitia
(14 days post-injury)

FIGURE 77

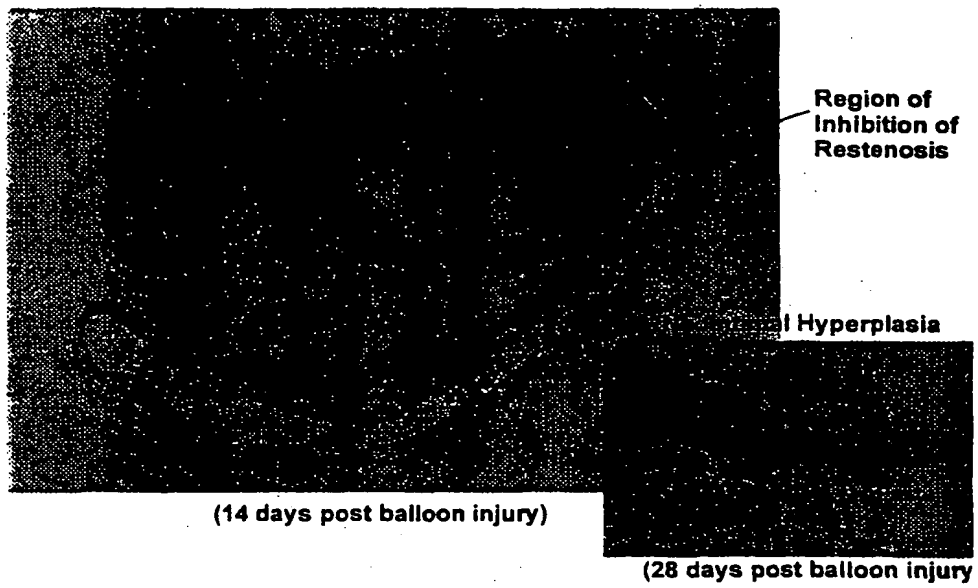
Region of
Inhibition of
Restenosis
l Hyperplasia
(14 days post balloon injury)
(28 days post balloon injury

FIGURE 78

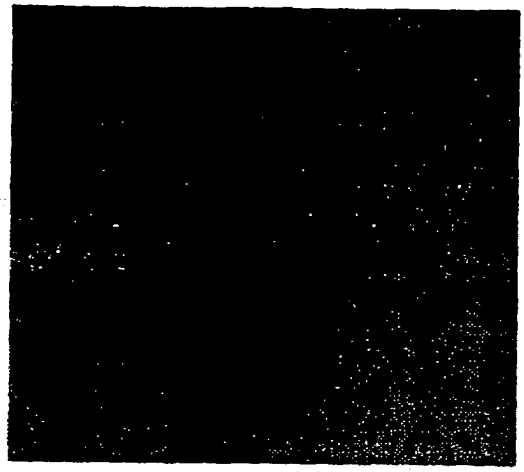

Normal Mice

Transgenic
Control

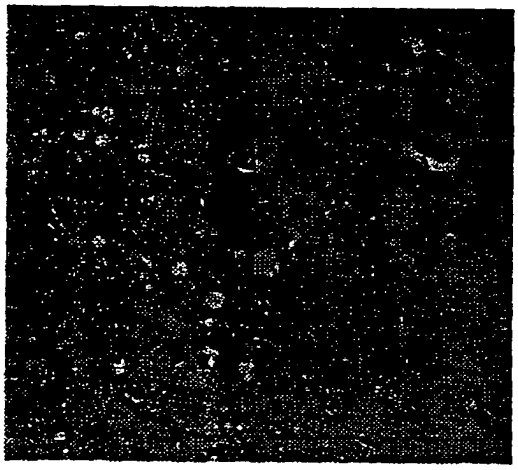

Transgenic
Paclitaxel Treated

FIGURE 79

A. RT-1 + GP68-88

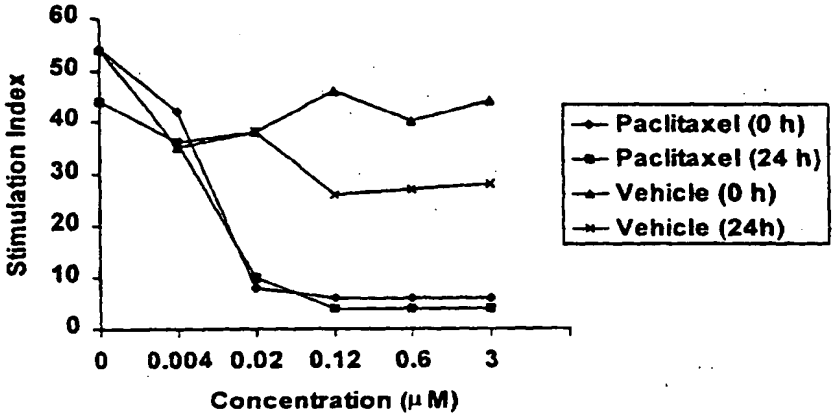

B. RT-1 + ConA

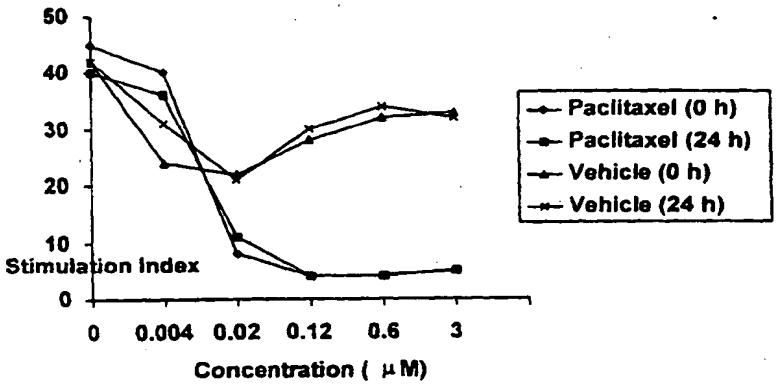

FIGURE 80

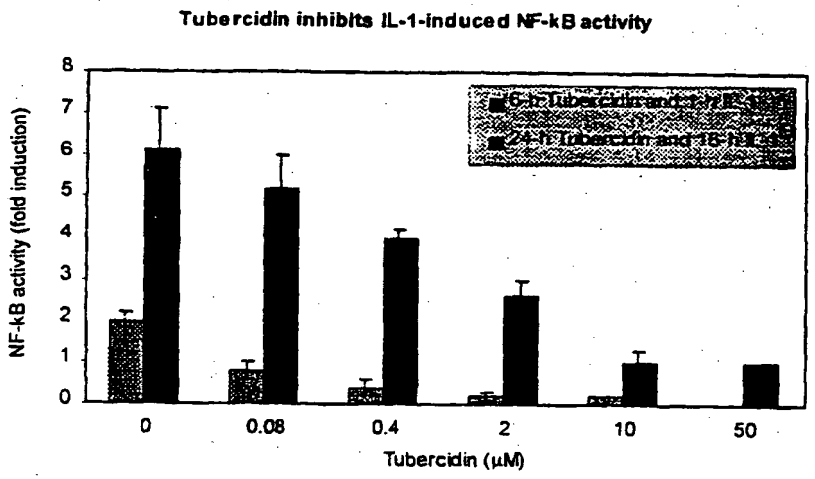
Tubercidin inhibits IL-1-induced NF-kB activity
NF-kB activity (fold induction)
0
1
2
3
4
5
6
7
8
0
0.08
0.4
2
10
50
Tubercidin (μM)

A.

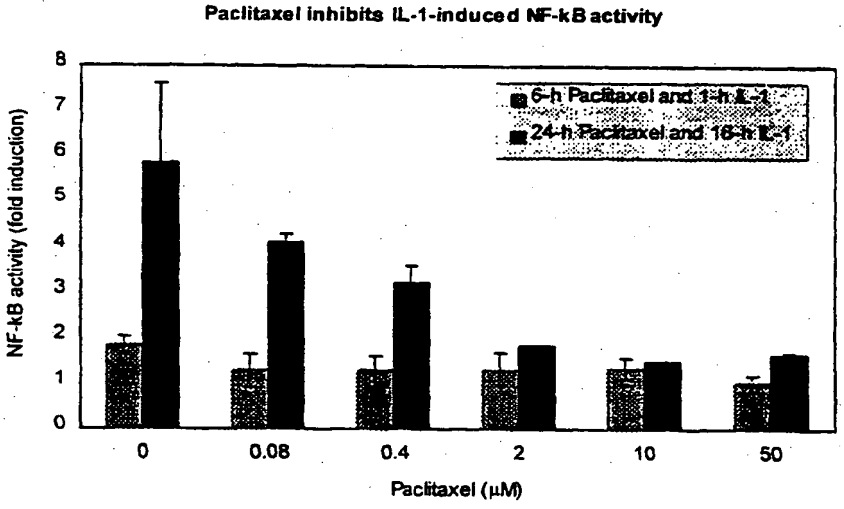
Paclitaxel inhibits IL-1-induced NF-kB activity
6-h Paclitaxel and 1-h IL-1
24-h Paclitaxel and 16-h IL-1
NF-kB activity (fold induction)
0
1
2
3
4
5
6
7
8
0
0.08
0.4
2
10
50
Paclitaxel (μM)

B.

FIGURE 80

C.

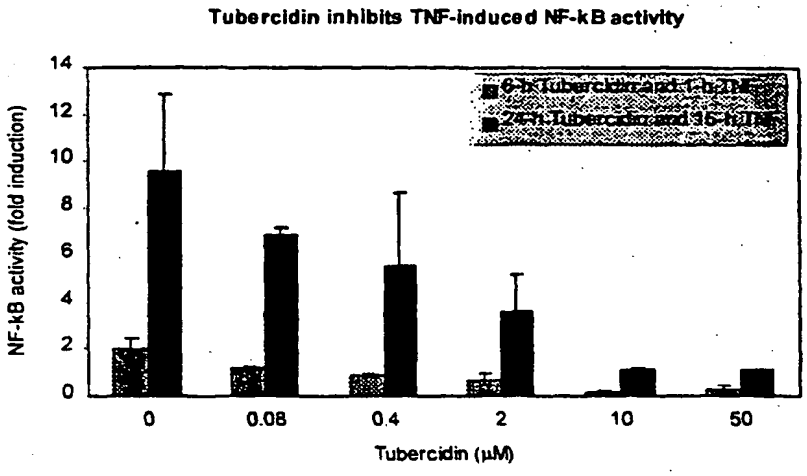
Tubercidin inhibits TNF-induced NF-kB activity
NF-kB activity (fold induction)
14
12
10
8
6
4
2
0
6-h Tubercidin and 1-h TNF
24-h Tubercidin and 18-h TNF
0
0.08
0.4
2
10
50
Tubercidin (μM)

D.

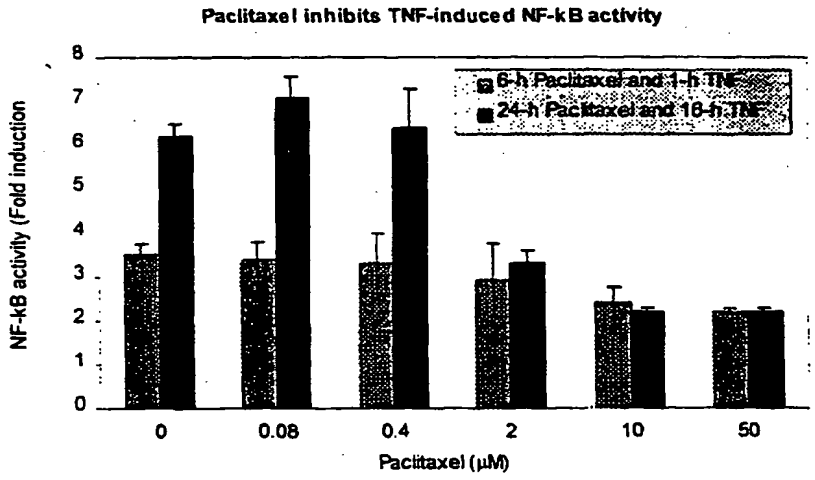
Paclitaxel inhibits TNF-induced NF-kB activity
NF-kB activity (Fold induction
8
7
6
5
4
3
2
1
0
6-h Paclitaxel and 1-h TNF
24-h Paclitaxel and 18-h TNF
0
0.08
0.4
2
10
50
Paclitaxel (μM)

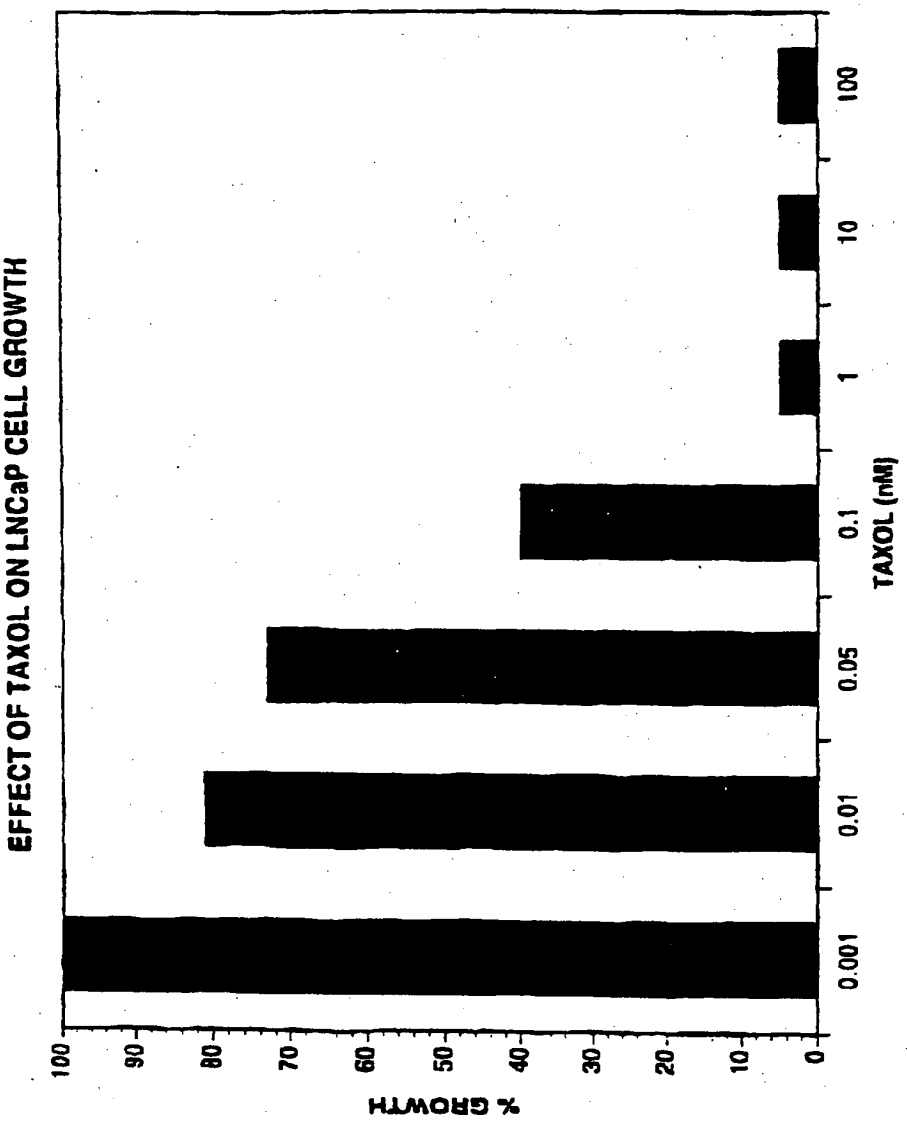
EFFECT OF TAXOL ON LNCaP CELL GROWTH
% GROWTH
100
90
80
70
60
50
40
30
20
10
0
0.001
0.01
0.05
0.1
1
10
100
TAXOL (nM)

FIGURE 81A

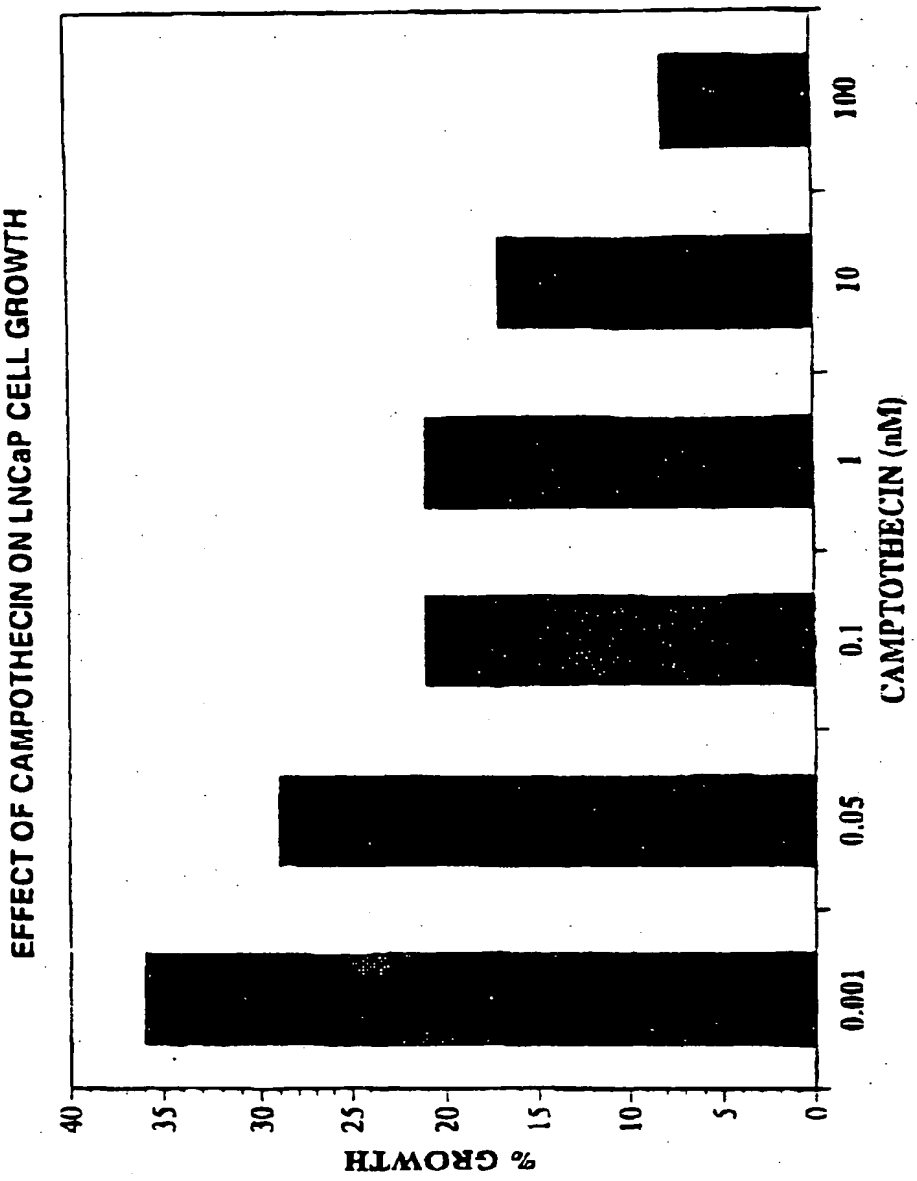
EFFECT OF CAMPOTHECIN ON LNCaP CELL GROWTH
% GROWTH
0
5
10
15
20
25
30
35
40
0.001
0.05
0.1
1
10
100
CAMPTOTHECIN (nM)

FIGURE 81B